DIRECT NON-LINEAR ACOUSTIC AND ELASTIC INVERSION: TOWARDS FUNDAMENTALLY NEW COMPREHENSIVE AND REALISTIC TARGET IDENTIFICATION

A Dissertation

Presented to

the Faculty of the Department of Physics

University of Houston

In Partial Fulfillment

of the Requirements for the Degree

Doctor of Philosophy

By

Haiyan Zhang

December 2006

DIRECT NON-LINEAR ACOUSTIC AND ELASTIC INVERSION: TOWARDS FUNDAMENTALLY NEW COMPREHENSIVE AND REALISTIC TARGET IDENTIFICATION

Haiyan Zhang

APPROVED:

Dr. Arthur B. Weglein, Chairman

Dr. Lowell Wood

Dr. Kristopher A. Innanen

Dr. David J. Francis

Dr. Robert G. Keys

Dr. Douglas J. Foster

Dr. Lawrence Pinsky

Dean, College of Natural Sciences and Mathematics

ACKNOWLEDGEMENTS

time-lapse seismic data project and permitting me to include the results in my dissertation. I would also like to thank Baishali Roy (ConocoPhillips) for kindly providing the schematic of synthetic well log A-52 and well log data.

Special thanks go to Chris Weglein for her invaluable help and encouragement in taking care of my baby daughter which is a very important part of my life directly affecting my research work.

Finally, it is barely adequate to say that I am deeply indebted to my parents, my parents-in law and my husband, Jingfeng Zhang, for their support and dedication.

DIRECT NON-LINEAR ACOUSTIC AND ELASTIC INVERSION: TOWARDS FUNDAMENTALLY NEW COMPREHENSIVE AND REALISTIC TARGET IDENTIFICATION

_____

An Abstract of a Dissertation

Presented to

the Faculty of the Department of Physics

University of Houston

_____

In Partial Fulfillment

of the Requirements for the Degree

Doctor of Philosophy

_____

By

Haiyan Zhang

December 2006

ABSTRACT

The objective of seismic exploration is to determine the location (imaging) and mechanical properties (inversion) of hydrocarbon resources in the earth using recorded data. The recorded data have a non-linear relationship with the property changes across a reflector. Current inversion methods either assume small property changes and solve a linear approximate form, or assume a non-linear relationship but use an indirect method to invert. The assumptions of the former methods are often violated in practice and can cause erroneous predictions; the latter category usually involves a significant computational effort (especially in multi-dimensional case) and/or has ambiguity issues in the predicted result.

In this dissertation, a more comprehensive multi-parameter multi-dimensional direct non-linear inversion framework is developed based on the inverse scattering task-specific sub-series (see, e.g., Weglein *et al.*, 2003). The procedure is direct and non-linear without global searching and small-change assumptions; hence, it has the potential to provide more accurate and reliable earth property predictions for large contrast and complex targets.

As an initial part of the more general multi-dimensional direct non-linear inversion project, this dissertation focuses on the inversion for 1D media and 2D experiments. Explicit direct non-linear inversion equations are derived for one and two parameter acoustic and three parameter elastic cases. The terms for imaging are separated from inversion-only terms.

Numerical tests show that non-linear inversion results provide improved estimates in comparison with the standard linear inversion. In this dissertation, we demonstrate that the direct non-linear *elastic* inversion in 2D requires all four components of data. However, we

introduce an approach which only uses pressure measurements and approximately synthe-sizes the other three required components of data. Added value beyond the corresponding conventional linear results can still be achieved from pressure-only acquisition. This permits us to derive value from direct non-linear elastic inversion, when only pressure measurements are available. We anticipate further improvement when all four components of data are used.

Finally, the method is applied to time-lapse seismic data to distinguish pressure changes from reservoir fluid changes, a situation in which conventional methods have difficulty. Initial tests provide encouraging results.

CONTENTS

1. INTRODUCTION AND BACKGROUND

This chapter provides some basic information about seismic exploration, pressing seismic challenges, the inverse scattering series as a part of the strategy to respond to those challenges, and the goal and structure of this dissertation. It includes the following three sections.

- **Section 1.1: General seismic exploration background.** In this section, we give a brief introduction of the objective of seismic exploration, current seismic processing procedures and their assumptions, the current most pressing seismic challenges and a strategy to address those challenges, and the specific goals of this dissertation.

- **Section 1.2: The inverse scattering task-specific subseries.** In this section, we briefly describe inverse scattering theory; then, we introduce the task-specific subseries including its history and where this dissertation's work fits in with previous work. We also provide a detailed explanation of technical terminology (e.g., linear/non-linear and direct/indirect) which helps to understand the difference between current inversion methods and the procedure developed in this dissertation.

- **Section 1.3: An overview of this dissertation.** This section describes the position of the inversion in the seismic data processing sequence. The work documented in this dissertation is placed as the initial part of a more general, multi-dimensional (multi-D) heterogeneous direct non-linear inversion project using the inverse scattering task-specific subseries.

1.1   General seismic exploration background

The objective of seismic exploration is to find hydrocarbon reservoirs in the earth using seismic waves. Seismic surveys for the purposes of exploration can be conducted on land (on-shore) and marine (off-shore) environments. However, the experiment is in essence the same: A man-made source generates seismic waves, and receivers record those that reflect back to the surface: this constitutes the data, D. Then, through analysis of the recorded data, (1) a structural map of the earth is estimated, in a procedure called imaging, or migration, and (2) the mechanical properties of the target are estimated in a procedure called inversion, target identification, or parameter estimation. This dissertation concentrates on the marine case, although some algorithms can also be applied to land data. An example of marine seismic exploration geometry is shown in Fig. 1.1.
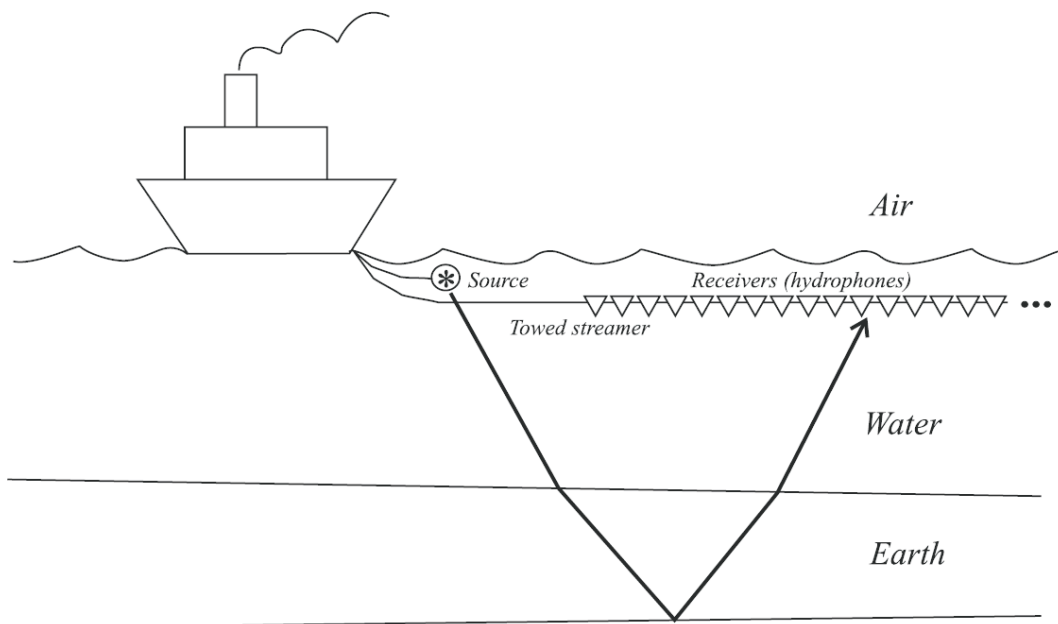
Fig. 1.1: *Marine seismic exploration geometry: $*$ and $\bigtriangledown$ indicate the source and receiver, respectively. The boat moves through the water towing the source and receiver arrays and the experiment is repeated at a multitude of surface locations. The collection of the different source-receiver wavefield measurements defines the seismic reflection data.* (Weglein et al., *2003*)

After the data are collected, we next consider means by which to produce a structure or parameter map of the subsurface. As a first thought, one might consider building an algorithm which would input the totality of the recorded data, and would output the structural map and mechanical properties of the target in one step. However, historically this brute force approach has proven unsuccessful due to the complexity of recorded data.

The recorded data contain many kinds of distinct arrivals of seismic energy, each having a different propagation history from the source to the receiver. Such a distinct arrival of the seismic energy is called a seismic event. It is useful to catalog and separate these events based on the type and complexity of the interactions they have experienced.

Basically, seismic reflection events are catalogued as primary or multiple depending on whether the energy arriving at the receiver has experienced one or more upward reflections, respectively (see Fig. 1.2). Multiples can be further classified as free-surface multiples and internal multiples according to whether or not they have been reflected by the free surface (air-water interface).
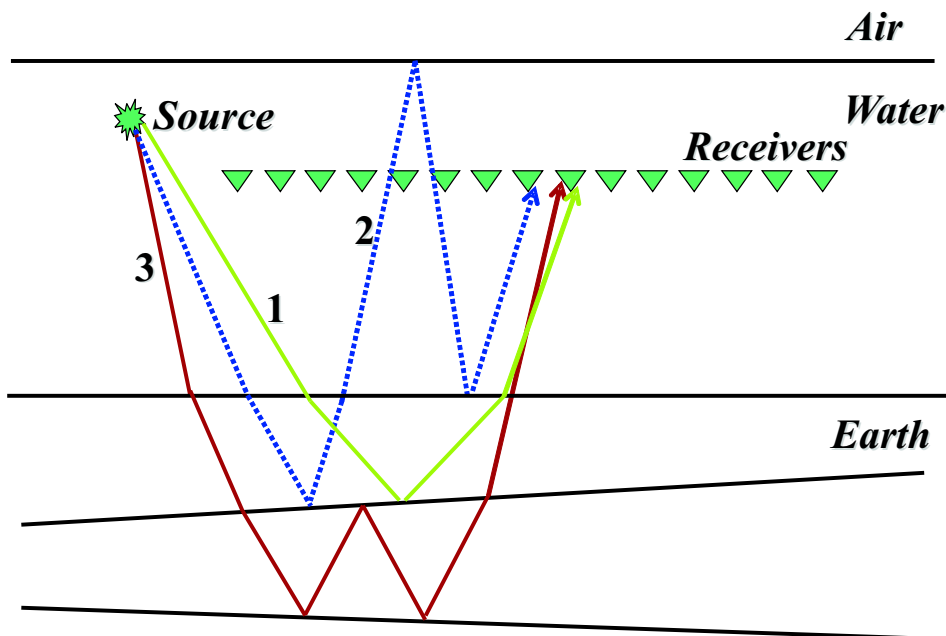
Fig. 1.2: *Marine primaries and multiples: 1, 2 and 3 are examples of primaries, free-surface multiples and internal multiples, respectively. (Weglein* et al., *2003)*

Methods for extracting subsurface information (imaging and inversion) from seismic data typically assume that the data consist exclusively of primaries. In other words, for most current imaging and inversion algorithms, only primaries are considered as signal and all other seismic events are considered noise, to be removed before imaging and inversion. The reason is that the relationship between primaries and the earth is simpler than the relationship between multiples and the earth. Put simply, multiples have more than one upward reflection; and, hence, involve the cumulative effect of more than one reflection interaction.

The primary-only assumption simplifies the processing of seismic data for determining the spatial locations of reflectors and mechanical property changes across a reflector. Hence, to satisfy this assumption, removal of the noise becomes a requisite precursor to seismic primary processing. Specific algorithms have been (and/or are still being) derived to remove free-surface multiples and internal multiples (e.g., Carvalho, 1992; Verschuur *et al.*, 1992; Araújo, 1994; Weglein *et al.*, 1997; Matson, 1997; Weglein, 1999; Ramírez and Weglein, 2005). A comprehensive list of the references can be found in Weglein and Dragoset (2005).

After the removal of the multiples, the objective of the seismic processing is to use primaries to find *where* rapid changes in medium properties (reflectors) are located (imaging), and *what* the medium changes across a reflector are (inversion). Examples of current imaging methods are finite difference (Claerbout, 1971), F-K (Stolt, 1978) and phase shift (Gazdag, 1978). Behind all current methods there resides the explicit algorithmic assumption and requirement for an adequate velocity model to produce an accurate depth image. However, under many circumstances, especially in complex geological environments, current best-practice velocity estimation techniques are inadequate for estimating the velocity model with a high-enough degree of accuracy (e.g., Herron, 2000; Gray *et al.*, 2001; Paffenholz *et al.*, 2002; Glogovsky *et al.*, 2002).

For inversion, current methods include: (1) the linear approximation (e.g., Clayton and

Stolt, 1981; Weglein and Stolt, 1992) which is often useful, especially in the presence of small earth property changes across the boundary and/or small angle reflections, and (2) indirect model matching methods with global searching (e.g., Tarantola *et al.*, 1984; Sen and Stoffa, 1995) which define an objective function assumed to be minimized when the best fitting model is obtained. The assumptions of the former methods (like the small contrast assumptions) are often violated in practice and can cause erroneous predictions; the latter category usually involves a significant and often daunting computation effort (especially in multi-D cases) and/or sometimes have reported erroneous or ambiguous results. Furthermore, most of the traditional inversion methods use a plane wave reflection coefficient form and have the need for overburden (medium above the target) information.

The above mentioned current imaging and inversion methods can give useful results when their assumptions are satisfied. However, under some circumstances, especially in deep water and in highly heterogeneous media and/or with a rapidly varying and corrugated boundaries, the assumptions and prerequisites (e.g., multiple removal) behind those algorithms cannot be adequately satisfied; and, hence, those methods for processing primaries can have difficulty and may become ineffective or fail. That processing failure is the origin of seismic exploration and production challenges.

In particular, the challenges associated with processing primaries are: (1) for imaging: locating structure beneath rapidly varying multi-D (e.g., 2D or 3D) heterogeneity within layers, or rapid variations at boundaries between layers, or at the target itself, and (2) for inversion: large contrast mechanical property changes at a 1D or multi-D target with or without a known multi-D overburden.

To address the challenges above, we seek to develop a fundamentally new procedure that avoids the assumptions behind current methods for processing primaries. The inverse scattering series is a direct multi-D inversion method that can perform the tasks associated with multiple removal, imaging and inversion, without *a priori* knowledge of the earth's

material properties. Hence, the inverse scattering based task-specific subseries strategy [1] is a direct response to all of the challenges listed above for depth imaging and inversion (and has already been successfully applied to multiple removal). It has the capability to directly determine where the spatial locations of earth mechanical property changes are, and what the values of the material property changes are across a reflector for either simple or complex targets, e.g., (a) a large contrast and/or (b) a multi-D corrugated target, and (c) a target with or without knowing the overburden (Weglein *et al.*, 2003; Weglein, 2006b).

In actuality, the overburden and target geometries can both be multi-D (i.e., non-horizontal). While the current methods for imaging assume the overburden is *multi-D*, current methods for target identification typically assume the target geometry is essentially *1D* (horizontal). In addition, for the latter target identification methods, changes in material properties are assumed to be small. This small-contrast assumption can often be violated in practice, especially when the target relates to hydrocarbons. Hence, removing the small-contrast assumption would be a major step in advancing target identification capability towards more realism, and that increased realism will have an associated increase in reliability for target identification and reduction in risk of drilling a dry hole.

Following the statement of the problem above, one important question is, "how does one develop a method for target identification that does not assume small contrasts?" It is worth reminding ourselves that the inverse scattering task-specific subseries has the potential to perform multiple removal, direct depth imaging and inversion for a large contrast and a multi-dimensional corrugated target with or without knowing the overburden. In this dissertation, based on the task-specific inverse scattering subseries strategy, we develop a direct multi-parameter [2] non-linear inversion [3] framework and algorithm. The method is direct and non-linear without making a small contrast assumption. Hence, it has the potential

---

[1] Details about the inverse scattering series and the inverse scattering task-speciˉc subseries will be discussed in next section.

[2] More than one mechanical property changes across a re°ector.

[3] Details will be presented in next section.

to provide more accurate target identification beyond the current inversion capability. As a general framework, the method developed in this dissertation has the following further advantages: (1) it determines data requirements for non-linear direct parameter estimation, and (2) it involves explicit algorithms which directly provide improved estimates for medium properties without recourse to highly non-linear optimization procedures.

The 1D elastic inversion model [4] is regarded as an acceptable level of realism for target identification by seismic exploration and target identification (Keys and Foster, 2006). Therefore, we are motivated to develop a 1D elastic inverse scattering task-specific subseries algorithm which has the capability to accurately perform *large contrast target identification* for a 1D elastic earth. The specific procedures are described below.

In this dissertation, we progress and develop direct non-linear parameter estimation concepts and algorithms in stages of increasing difficulty and complexity. Rather than starting directly with the 1D elastic inversion, we begin with the 1D acoustic one parameter (P-wave velocity) model, and look to *identify* task-specific imaging and inversion terms, generalizing the pioneering work on normal incidence case (e.g., Weglein *et al.*, 2001; Shaw, 2001; Shaw *et al.*, 2001; Shaw *et al.*, 2002; Weglein *et al.*, 2003; Shaw and Weglein, 2003; Shaw and Weglein, 2004) to the non-normal incidence case. We then move on to multi-parameter non-linear inversion models, starting each time with the basic equations, and deriving linear and low order but non-linear terms. First, the two parameter (P-wave velocity and density) acoustic case is considered, followed by the three parameter (P-wave velocity, S-wave velocity and density) elastic case.

At each stage of complexity and realism, from (1) one parameter acoustic to (2) two parameter acoustic, and finally to (3) three parameter elastic media, there are new sets of inverse issues and goals. The lessons gleaned in a simpler world can be useful to help decipher the

---

[4] *Elastic medium* is a material that supports both P- and S-wave travel. In contrast, *acoustic* implies that the shear modulus (an elastic constant) is zero and sometimes is restricted to P-waves in °uids (liquids and gases). In a \P-wave", the particles oscillate in the direction the wave propagates; while in a \S-wave", the particles oscillate perpendicular to the direction the wave propagates.

actions of the inverse series in the next step of added complexity and realism. For example, in 1D acoustic media, when the *one parameter* case is extended to the *two parameter* case, more terms (e.g., terms that address 'leakage', details of which are presented in Chapter 3) arise that have no analog in the one parameter case. Again, when the *two parameter acoustic* model is extended to the *three parameter elastic* model, yet more terms are obtained that have no analog in the two parameter acoustic case, especially for imaging terms. Our reasoning is that in the first case, the acoustic medium only supports P-waves, and hence only one reference velocity (P-wave velocity) is involved. Therefore, when only one velocity is incorrect (i.e., poorly estimated), there exists only one "mislocation" for each parameter, and the imaging terms only need to correct this one mislocation. In contrast, the elastic medium supports both P- and S-wave propagation, and hence two reference velocities (P-wave velocity and S-wave velocity) are involved. When both of these velocities are incorrect, generally, there exist four mislocations due to each of four different combinations [5] of the two wrong velocities. Therefore, in non-linear elastic imaging-inversion, the imaging terms need to correct the four mislocations arising from linear inversion of any single mechanical property, such that a single correct location for the corresponding actual change in that property is determined.

In addition, in progressing our work for the above mentioned three models, we have provided an important message and suggestion for the overall strategy of depth imaging. When *one parameter acoustic* is extended to *two parameter acoustic*, we observe similar mathematical mechanisms acting towards correction of reflector location — the first non-linear (beyond linear) imaging terms in both cases involve only velocity differences between the actual and reference media. In other words, velocity appears to be the only parameter that governs imaging, i.e., the location of reflectors. Also, in the *three parameter elastic* case, we observe similar imaging-only terms involving only velocity differences. This common theme obtained

---

[5] The \four combinations" refers to PP, PS, SP and SS, where, for instance, PP means P-wave incidence, and P-wave re°ection. Since P-waves non-normal incidence on an elastic interface can produce S-waves, or vice versa, which in those cases are known as converted waves (Aki and Richards, 2002), the elastic data generally contain four components: PP, PS, SP and SS.

from the three (1D) models — one parameter acoustic, two parameter acoustic and three parameter elastic, is a suggestion of possible generalization to multi-D media, also of possible model-type independent [6] imaging. The apparent lesson is that such algorithms will be driven entirely by velocity discrepancies between reference/actual media.

In this dissertation, we proceed as follows. In each of the three models (i.e., one parameter acoustic; two parameter acoustic; and three parameter elastic media), we first derive explicit equations for the non-linear terms in the inverse scattering series that correspond to that model. These equations provide a set of terms allowing the first step towards non-linear objectives associated with primaries to be taken (i.e., reflector location without the velocity and direct non-linear parameter estimation at the imaged reflector), with or without prior knowledge of the overburden. The terms for imaging the location with an inadequate velocity are next separated from non-linear inversion-only terms.

After the separation of inversion-only terms from location-only terms is accomplished, we then focus on the inversion-only terms assuming a known overburden [7]. However, the contrast in properties across an interface is no longer assumed to be small. We reduce the more general multi-D and multi-parameter framework to this narrowly specific objective to both assure that this dissertation addresses the current pressing challenge for inversion — *the direct inversion of large contrast elastic medium property changes at a 1D target with a known overburden* — but concurrently to create an algorithm that is manageable, in the sense of computation and complexity.

To determine the value of the new direct non-linear multi-parameter estimation method compared with the current inversion methods, we perform a suite of numerical tests on 1D one-interface examples. In the acoustic case, the non-linear inversion with P data (pressure measurements) shows significant improved estimates beyond the current linear inversion. In the elastic case, although in principle the direct non-linear inversion approach requires

---

[6] Model-type independent algorithms do not depend on e.g., acoustic, elastic or anelastic.

[7] The assumed known overburden means the non-linear imaging terms (that will only activate when the overburden velocity is incorrect) have the right velocity and will be zero.

all four components of elastic data (PP, PS, SP and SS data), in this dissertation we introduce an approach which only uses pressure measurements and approximately synthesizes the other required components of data. We show that added value is achieved in comparison to conventional linear inversion results for all tested models from this compromised pressure-only acquisition. We anticipate that significant further improvement will derive from actually measuring all four components of data, and utilizing the corresponding consistent and complete non-linear estimation equations.

The work presented in this dissertation is the first step into exploring the more comprehensive multi-parameter multi-D direct non-linear inversion framework, and represents both a conceptual advance and a practical addition to the algorithmic toolbox for target identification.

1.2 The inverse scattering task-specific subseries

In this section, details about the inverse scattering task-specific subseries and the task-specific subseries based direct non-linear inversion method are introduced.

Scattering theory relates the perturbation (the difference between the reference and actual medium properties) to the scattered wave field (the difference between the reference medium's and the actual medium's wave field). It is therefore reasonable that in discussing scattering theory, we begin with the basic wave equations governing the wave propagation in the actual and reference medium, respectively [8],

$$LG = \delta, \tag{1.1}$$

$$L_0 G_0 = \delta, \tag{1.2}$$

---

[8] In this introductory math development, we follow closely Weglein *et al.* (1997); Weglein *et al.* (2002); Weglein *et al.* (2003).

where L and L_0 are respectively the differential operators that describe wave propagation in the actual and reference medium, and G and G_0 are the corresponding Green's operators. The δ on the right hand side of both equations is a Dirac delta operator and represents an impulsive source.

The perturbation is defined as $V = L_0 - L$. The Lippmann- Schwinger equation,

$$G = G_0 + G_0 V G, \tag{1.3}$$

relates G, G_0 and V (see, e.g., Taylor, 1972). Iterating this equation back into itself generates the forward scattering series

$$G = G_0 + G_0 V G_0 + G_0 V G_0 V G_0 + \cdots . \tag{1.4}$$

Then the scattered field $\psi_s \equiv G - G_0$ can be written as

$$
\begin{aligned}
\psi_s &= G_0 V G_0 + G_0 V G_0 V G_0 + \cdots \\
&= (\psi_s)_1 + (\psi_s)_2 + \cdots ,
\end{aligned}
\tag{1.5}
$$

where $(\psi_s)_n$ is the portion of ψ_s that is n^{th} order in V. The measured values of ψ_s are the data, D, where

$$D = (\psi_s)_{ms} = (\psi_s)_{\text{on the measurement surface}}.$$

In the inverse scattering series, expanding V as a series in orders of D,

$$V = V_1 + V_2 + V_3 + \cdots , \tag{1.6}$$

then substituting Eq. (1.6) into Eq. (1.5), and evaluating Eq. (1.5) on the measurement

11

surface yields

$$D = [G_0(V_1 + V_2 + \cdots)G_0]_{ms} + [G_0(V_1 + V_2 + \cdots)G_0(V_1 + V_2 + \cdots)G_0]_{ms} + \cdots . \quad (1.7)$$

Setting terms of equal order in the data equal, leads to the equations that determine V_1, V_2, ... directly from D and G_0.

$$D = [G_0 V_1 G_0]_{ms}, \quad (1.8)$$

$$0 = [G_0 V_2 G_0]_{ms} + [G_0 V_1 G_0 V_1 G_0]_{ms}, \quad (1.9)$$

$$0 = [G_0 V_3 G_0]_{ms} + [G_0 V_1 G_0 V_2 G_0]_{ms} + [G_0 V_2 G_0 V_1 G_0]_{ms}$$
$$+ [G_0 V_1 G_0 V_1 G_0 V_1 G_0]_{ms}, \quad (1.10)$$

etc. Equations (1.8) $\sim$ (1.10) permit the sequential calculation of V_1, V_2, ..., and, hence, achieve full inversion for V (see Eq. 1.6) from the recorded data D and the reference wave field (i.e., the Green's operator of the reference medium) G_0. Therefore, the inverse scattering series is a multi-D inversion procedure that directly determines physical properties using only reflection data and reference medium information.

Therefore, in the *forward* problem (Eq. 1.4), given G_0 and the perturbation V, the forward series constructs the total field G by adding an infinite number of terms corresponding to propagations in a reference medium and interactions with the perturbation V. Meanwhile, in the *inverse* problem (Eqs. 1.8 $\sim$ 1.10), given reference medium G_0 and the measured scattered wave field, D, the inverse series determines the perturbation V order by order in the data.

Noting that the inverse scattering series needs an infinite number of terms to construct the unknown perturbation V, Prosser (1964; 1969; 1976; 1980; 1982; 1992) and Carvalho *et al.* (1992) studied/tested its convergence and found that the full series diverges for all but a

small range of earth models. Fortunately, convergent subseries have been identified which perform free-surface multiple removal and internal multiple suppression (Carvalho, 1992; Araújo, 1994; Weglein *et al.*, 1997). These efforts build and provide fundamentally new insights and capabilities that derive from the inverse scattering series (Weglein *et al.*, 2000). That is, instead of using the whole inverse scattering series to perform multiple removal, imaging and inversion all together, a specific subset of the series is isolated to accomplish only one task at a time. After each task has been finished, the problem is restarted, and it is assumed that the former task does not exist at all. A new subset series is then pursued to address the following problem. This is referred to as the inverse scattering task-specific subseries strategy (Weglein *et al.*, 2003). The order of the tasks is: (1) free-surface multiple removal, (2) internal multiple removal, (3) depth imaging without velocity, and (4) inversion or target identification. Since the entire process requires only reflection data and reference medium information, it is reasonable to assume that these intermediate steps, i.e., all of the derived subseries which are associated with achieving that objective, would also be attainable with only the reference medium and reflection data and no subsurface medium information is required.

After the above mentioned successful application of the inverse scattering task-specific subseries to free-surface and internal multiple removal (Carvalho, 1992; Araújo, 1994; Weglein *et al.*, 1997; Matson, 1997), further progress has been made, including: (1) terms have been identified which extend the internal multiple attenuation algorithm to an elimination algorithm (Ramírez and Weglein, 2005); (2) imaging without the velocity for one parameter 1D and then 2D acoustic media (Weglein *et al.*, 2002; Shaw and Weglein, 2003; Shaw *et al.*, 2003a; Shaw *et al.*, 2003b; Shaw *et al.*, 2004; Shaw and Weglein, 2004; Liu and Weglein, 2003; Liu *et al.*, 2004; Liu *et al.*, 2005), and (3) direct non-linear inversion for multi-parameter 1D acoustic and then elastic media (Zhang *et al.*, 2005; Zhang and Weglein, 2005). Also, recent work (Innanen and Weglein, 2004; Innanen and Weglein, 2005) suggests that some well-known seismic processing tasks associated with resolution enhancement (i.e.,

"Q-compensation") can be accomplished within the task-separated inverse scattering series framework. In this dissertation, we focus on item (3) above.

1.2.1 Linear and non-linear operations on the data

In this section, the direct non-linear inversion procedure is discussed in greater detail. In particular, we draw distinctions between: linear and non-linear operations on the data, and direct and indirect methods. By doing so, we better understand the difference between current inversion methods and the procedure developed in this dissertation.

We define an operation to be non-linear in the data D (regarded as a variable), if it involves multiplications of data, and/or multiplications of linear operations on the data, by themselves (e.g. D^2, D^3 etc.). Otherwise, it is called a linear operation. The above mentioned inverse scattering task-specific subseries related algorithms are non-linear operations on the data.

Examples of linear algorithms in seismic exploration are conventional migration/inversion methods (e.g., Claerbout, 1971; Stolt, 1978; Clayton and Stolt, 1981; Stolt and Weglein, 1985). Another alternative approach, e.g., iterative linear inversion (e.g., Verschuur and Berkhout, 1997; Berkhout and Verschuur, 1997) iterates the linear step (Eq. 1.8), each time updating the reference medium. In contrast, the inverse scattering series Eqs. (1.8) $\sim$ (1.10) inverts the same (original) input operator, G_0, at each step, and the reference medium is never updated.

In this dissertation, we refer to two kinds of non-linearities. One is called a "circumstantial non-linearity" which means that the degree of non-linearity depends on prior information, and given enough information, the operation becomes linear. In other words, the non-linearity is avoidable. For example, depth imaging is a linear process, if the medium velocity information is provided. Otherwise, non-linear operations on the data are required to obtain the correct image.

The other kind of non-linearity is called "intrinsic non-linearity" which means that it can not be avoided through provision of prior information. For inversion, the non-linearity is intrinsic in the above sense. This can be shown through a very simple example — involving a plane wave normally incident on a one-interface model (as shown in Fig. 1.3).
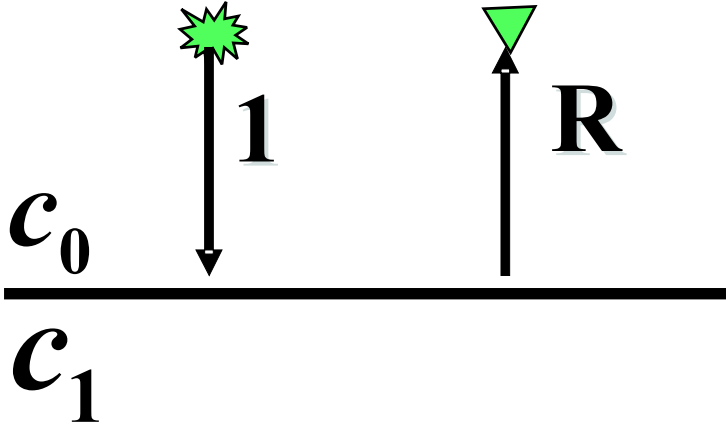
Fig. 1.3: 1D plane wave normal incidence acoustic example.

In this example, the velocity changes across the interface. Above the interface we have the reference medium with a constant velocity c_0, and below we have the actual medium with a constant velocity c. Assuming unit amplitude of the incident pulse, the data amplitude is equal to the reflection coefficient R:

$$R = \frac{c_1 - c_0}{c_1 + c_0}.$$
(1.11)

The velocity change across the interface can be characterized by α (details will be provided in Chapter 2), where

$$\alpha = 1 - \left(\frac{c_0}{c_1}\right)^2.$$
(1.12)

Therefore, R can be written in terms of α or α in terms of R, respectively as,

$$R = \frac{1}{4}\alpha + \frac{1}{8}\alpha^2 + O(\alpha^3),$$
(1.13)

and

$$\alpha = 4R - 8R^2 + 12R^3 + \cdots .\tag{1.14}$$

Both the forward expression for R as a function of α and the inverse expression for α as a function of R are non-linear in α and R, respectively. Knowledge of α and c_0, Eq. (1.12) allows the solution for c_1. Linear inversion, which in this simple case amounts to truncating Eq. (1.14) beyond the first term, is an approximation, only providing accurate estimates when the medium changes are small; and, hence, the higher order terms in Eq. (1.14) are negligible. For larger contrasts the error due to the linear approximation increases.

1.2.2 Direct and indirect methods

We next consider inverse approaches that honor the intrinsic non-linearity of the data/medium

direct methods. Indirect methods can provide value and benefit, but as with all methods, there are pitfalls and limitations that need to be recognized. Indirect methods are typically conceptually simple and accessible, understandable, and broadly accepted because the idea of minimizing a functional is not difficult or complicated to understand and visualize, if not always easy to realize. The latter simplicity combined with a lack of direct capability helps to explain the wide acceptance and use of indirect methods. Indirect inversion also often represents the definition of inversion for its practitioners. Direct methods have the benefit of providing the precise framework and explicit data requirements needed for the explicit direct sought after solution to the problem. The new inverse scattering series based imaging, non-linear parameter inversion techniques of this dissertation represent new direct inverse capability and methodology and it provides a framework for more reliable and more accurate target identification, and thus, it is more advantageous.

In the above, we discussed two important terms: direct and non-linear. The inverse scattering series is the only direct multi-D method which deals with both intrinsic and circumstantial non-linearity, separately or in combination, concurrently operating without the traditional need for subsurface information. It provides a framework for direct multi-D inversion which can be formulated for a 2D or 3D acoustic or elastic heterogeneous subsurface. Historically, direct methods e.g., Clayton and Stolt (1981) on 2D acoustic, and Weglein and Stolt (1992) on 2D elastic, focused on linear formulations, and hence assume that property changes across each boundary are small, giving erroneous predictions for larger contrast and more complex targets.

To summarize, the research documented in this dissertation presents the first direct non-linear multi-parameter estimation of acoustic or elastic properties from the comprehensive multi-D inverse scattering series framework. The inversion method is direct and non-linear without global searching or small-change assumptions; hence, it has the potential to provide more accurate and reliable earth property predictions for larger contrast and more complex targets.

1.3   An overview of this dissertation

The order of the seismic data processing using the task-specific inverse scattering subseries acts like a chain of operations. In deriving these processing algorithms, the first step was to identify the subseries that removes the free-surface multiples only, and then, restart the problem and assume the free-surface never existed. The second step was to remove the internal multiples by isolating another specific subseries. After the removal of multiples, the third step is to identify another series which only tries to locate the reflectors without determining the changes in parameters at those reflectors. The fourth and last step/subseries is the one discussed in this dissertation — to identify the mechanical properties of the medium assuming that there are no multiples in the data, and that the reflectors have already been located at the right depths.

The work presented in this dissertation on 1D acoustic and then elastic media is an initial part of the more general multi-D heterogeneous direct non-linear inversion project. We start with the one parameter case, generalizing the normal incidence case to the non-normal incidence case, and then, extend the discussion to the multi-parameter cases: two parameter acoustic case and three parameter elastic. We take the steps in 1D, to allow the use of analytic data for numerical tests, and to prime the next step: extension to a multi-parameter and multi-D medium.

In Chapter 2, for a 1D medium embedded in a 2D space, we derive the first direct non-linear inversion solutions with separated imaging-only and inversion-only terms. We start with the one parameter case, generalizing the normal incidence case to the non-normal incidence case or 1.5D [9] and solving the first three Eqs. (1.8) $\sim$ (1.10).

We then, in Chapters 3 and 4, respectively, extend the discussion to the multi-parameter cases: two parameter acoustic case and three parameter elastic and solve the first two

---

[9] An experiment performed in 2D while the medium is 1D (e.g., the velocity varies only in the vertical direction).

Eqs. (1.8) and (1.9). For the acoustic case, it is analytically shown that the imaging term will automatically shut down when the correct velocity is provided. Numerical tests on a one-interface model show that non-linear terms provide improved values compared with the conventional linear inversion results. For the elastic case, it is shown that in order to perform the direct non-linear elastic inversion in 2D, all four components of data ($\hat{D}^{PP}$, $\hat{D}^{PS}$, $\hat{D}^{SP}$ and $\hat{D}^{SS}$) are required. A major theme here is to show how $\hat{D}^{PP}$ can be used to approximately synthesize the $\hat{D}^{PS}$, $\hat{D}^{SP}$ and $\hat{D}^{SS}$ such that high quality inversion results can still be achieved with the measurement of only one data type. This permits us to perform elastic non-linear inversion in some situations with only pressure measurements available, i.e., towed streamer data. For the case when all four components of data are available, we give one consistent method to solve for all of the second terms (the first terms beyond linear). In the last part we apply the newly derived method to the case of seismic time-lapse or 4D data (details are in Section 4.4). The goal is to use the inverse scattering subseries algorithm to distinguish pressure changes from reservoir fluid changes in cases when conventional seismic methods have difficulties interpreting the data. The numerical tests show very useful results. In Chapter 5, an overall summary is presented.

2. ONE PARAMETER ACOUSTIC INVERSION

We start this chapter by extending the work of, e.g., Weglein *et al.* (2001); Shaw (2001); Shaw *et al.* (2001); Shaw *et al.* (2002); Weglein *et al.* (2003); Shaw and Weglein (2003); Shaw and Weglein (2004), from 1D acoustic normal incidence to non-normal incidence case. We look to calculate the first three terms in the inverse scattering series and to identify task-specific imaging and inversion terms. We assume that the acoustic medium only varies in one parameter (velocity) — assumption which will be generalized to two parameter (velocity and density) in the following chapter.

This chapter has the following structure. Sections 2.1, 2.2 and 2.3 give the solutions of the first, second and third terms, respectively. In section 2.4, we present some numerical results tested on three models. The last section includes some conclusions.

2.1 Derivation of α_1

Equations (1.1) and (1.2), for 1D acoustic and constant density media, can be written in the following forms respectively

$$\left[\frac{d^2}{dz^2} + \frac{\omega^2}{c^2(z)} \right] G\left(z, z_s; \omega\right) = \delta\left(z - z_s\right), \tag{2.1}$$

$$\left[\frac{d^2}{dz^2} + \frac{\omega^2}{c_0^2} \right] G_0\left(z, z_s; \omega\right) = \delta\left(z - z_s\right), \tag{2.2}$$

where z_s is the depth of the source, ω is the temporal frequency, and $c(z)$ and c_0 are the P-wave velocities in the actual media and reference media, respectively.

In this case, the perturbation can be written as

$$V(z) = \frac{\omega^2}{c_0^2} - \frac{\omega^2}{c^2(z)} = k^2 \alpha(z), \tag{2.3}$$

where $k = \frac{\omega}{c_0}$, and

$$\alpha(z) = 1 - \frac{c_0^2}{c^2(z)}, \tag{2.4}$$

is the parameter we choose to do the inversion. Similar to Eq. (1.6), $\alpha(z)$ can be expanded as

$$\alpha(z) = \alpha_1(z) + \alpha_2(z) + \alpha_3(z) + \cdots.$$

Then we have

$$V_1(z) = k^2 \alpha_1(z),$$

$$V_2(z) = k^2 \alpha_2(z),$$

$$V_3(z) = k^2 \alpha_3(z).$$

From the first equation of the inverse scattering series, Eq. (1.8), we have

$$D = G_0 k^2 \alpha_1 G_0, \tag{2.5}$$

then, in space domain, for 1D acoustic media and 2D experiment, it can be written as

$$D(x_g, z_g; x_s, z_s; \omega) = \int_{-\infty}^{+\infty} dx' \int_{-\infty}^{+\infty} dz' G_0(x_g, z_g; x', z'; \omega) k^2 \alpha_1(z') G_0(x', z'; x_s, z_s; \omega), \tag{2.6}$$

21

where x_g, z_g and x_s, z_s are respectively the positions of the receiver and source, and

$$G_0(x_g, z_g; x', z'; \omega) = \frac{1}{(2\pi)^2} \int\limits_{-\infty}^{+\infty} dk'_x \int\limits_{-\infty}^{+\infty} dk'_z \frac{e^{ik'_x(x_g-x')} e^{ik'_z(z_g-z')}}{k^2 - k'^2_x - k'^2_z}, \qquad (2.7)$$

$$G_0(x', z'; x_s, z_s; \omega) = \frac{1}{(2\pi)^2} \int\limits_{-\infty}^{+\infty} dk''_x \int\limits_{-\infty}^{+\infty} dk''_z \frac{e^{ik''_x(x'-x_s)} e^{ik''_z(z'-z_s)}}{k^2 - k''^2_x - k''^2_z}. \qquad (2.8)$$

Next we Fourier transform Eq. (2.6) over x_g and x_s on both sides and use the following convention

$$f(x) = \int\limits_{-\infty}^{+\infty} dk \widetilde{f}(k) e^{ikx};$$

$$\widetilde{f}(k) = \frac{1}{2\pi} \int\limits_{-\infty}^{+\infty} dx f(x) e^{-ikx}.$$

Then the left side becomes

$$\frac{1}{(2\pi)^2} \int\limits_{-\infty}^{+\infty} dx_g \int\limits_{-\infty}^{+\infty} dx_s e^{-ik_g x_g} D(x_g, z_g; x_s, z_s; \omega) e^{ik_s x_s} = \widetilde{D}(k_g, z_g; -k_s, z_s; \omega),$$

and the right side becomes

$$\int\limits_{-\infty}^{+\infty} dx' \int\limits_{-\infty}^{+\infty} dz' \widetilde{G_0}(k_g, z_g; x', z'; \omega) k^2 \alpha_1(z') \widetilde{G_0}(x', z'; -k_s, z_s; \omega)$$

$$= \int\limits_{-\infty}^{+\infty} dx' \int\limits_{-\infty}^{+\infty} dz' e^{-i(k_g-k_s)x'} \frac{e^{iq_g(z'-z_g)}}{4\pi i q_g} k^2 \alpha_1(z') \frac{e^{iq_s(z'-z_s)}}{4\pi i q_s},$$

where (it is assumed that the perturbation α and, hence, all the terms in the inverse scattering series, $\alpha_1, \alpha_2, \cdots$, are non-zero only below the source and receiver, i.e., for $z' > z_g$

22

and $z' > z_s$)

$$
\begin{aligned}
\widetilde{G}_0(k_g, z_g; x', z'; \omega) &= \frac{1}{2\pi} \int\limits_{-\infty}^{+\infty} dx_g e^{-ik_g x_g} G_0(x_g, z_g; x', z'; \omega) \\
&= e^{-ik_g x'} \frac{e^{iq_g(z'-z_g)}}{4\pi i q_g},
\end{aligned} \tag{2.9}
$$

$$
\begin{aligned}
\widetilde{G}_0(x', z'; -k_s, z_s; \omega) &= \frac{1}{2\pi} \int\limits_{-\infty}^{+\infty} dx_s G_0(x', z'; x_s, z_g; \omega) e^{ik_s x_s} \\
&= e^{ik_s x'} \frac{e^{iq_s(z'-z_s)}}{4\pi i q_s},
\end{aligned} \tag{2.10}
$$

and

$$
k^2 - k_g^2 = q_g^2, \; k^2 - k_s^2 = q_s^2.
$$

Letting left side = right side leads to

$$
\widetilde{D}(k_g, z_g; -k_s, z_s; \omega) = -\frac{k^2}{4q_g q_s} \left(\frac{1}{2\pi}\right)^2 e^{-i(q_g z_g + q_s z_s)} \int\limits_{-\infty}^{+\infty} dx' \int\limits_{-\infty}^{+\infty} dz' e^{-i(k_g - k_s)x'} \alpha_1(z') e^{i(q_g + q_s)z'}. \tag{2.11}
$$

Then, we have

$$
\widetilde{D}(q_g; z_g, z_s; \omega) = -\frac{k^2}{4q_g^2} e^{-iq_g(z_g + z_s)} \widetilde{\alpha_1}(-2q_g). \tag{2.12}
$$

Using the relation $q_g = k \cos\theta$, and choosing θ (the incident angle shown in Fig. 2.1) as the free parameter, Eq. (2.12) becomes

$$
\widetilde{D}(q_g, \theta; z_g, z_s) = -\frac{1}{4\cos^2\theta} e^{-iq_g(z_g + z_s)} \widetilde{\alpha_1}(-2q_g). \tag{2.13}
$$

This is the linear (first order) solution for α_1 in frequency domain. In the next section, we will give the derivation of the first non-linear (second order) solution for α_2.

23
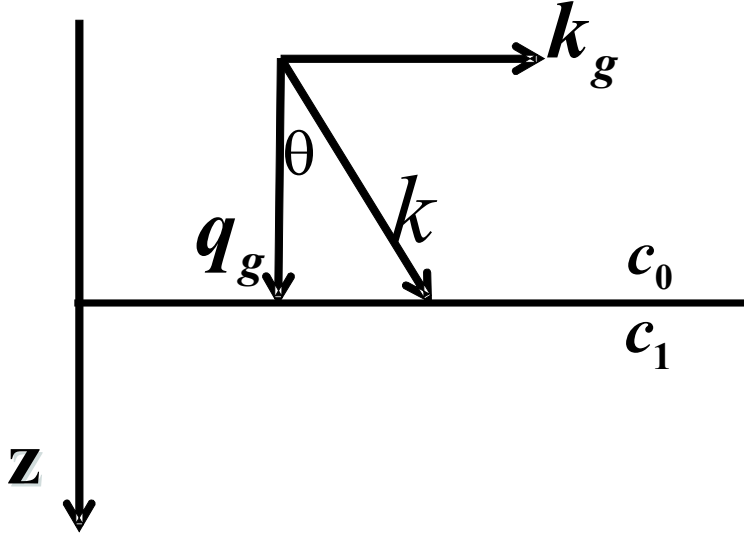
Fig. 2.1: The relationship between q_g, k_g and θ.

2.2 Derivation of α_2

From the second equation of the inverse scattering series, Eq. (1.9), we have

$$G_0 k^2 \alpha_2 G_0 = -G_0 k^2 \alpha_1 G_0 k^2 \alpha_1 G_0, \tag{2.14}$$

which can be written in space domain (for 2D experiment) as

$$\int\limits_{-\infty}^{+\infty} dx' \int\limits_{-\infty}^{+\infty} dz' G_0(x_g, z_g; x', z'; \omega) k^2 \alpha_2(z') G_0(x', z'; x_s, z_s; \omega)$$

$$= -\int\limits_{-\infty}^{+\infty} dx' \int\limits_{-\infty}^{+\infty} dz' \int\limits_{-\infty}^{+\infty} dx'' \int\limits_{-\infty}^{+\infty} dz'' G_0(x_g, z_g; x', z'; \omega) k^2 \alpha_1(z') G_0(x', z'; x'', z''; \omega)$$

$$\times k^2 \alpha_1(z'') G_0(x'', z''; x_s, z_s; \omega). \tag{2.15}$$

Similar to the derivation of α_1, after Fourier transforming Eq. (2.15) over x_g and x_s, the left side becomes

$$-\frac{1}{(8\pi)} k^2 \frac{e^{-iq_g(z_g+z_s)}}{q_g^2} \int\limits_{-\infty}^{+\infty} dz' \alpha_2(z') e^{2iq_g z'}.$$

The right side becomes (we use the same assumption that the perturbation α and its series components α_i for $i \geq 1$ are non-zero only below the source-receiver surface, i.e. for $z' > z_g$ and $z'' > z_s$)

$$
= -\frac{1}{(4\pi i)^3}(2\pi)^2 \int\limits_{-\infty}^{+\infty} dz' \int\limits_{-\infty}^{+\infty} dz'' \frac{e^{iq_g(z'-z_g)}}{q_g} k^2 \alpha_1(z') \frac{e^{iq_g|z'-z''|}}{q_g} k^2 \alpha_1(z'') \frac{e^{iq_g(z''-z_s)}}{q_g}
$$

$$
= -\frac{i}{16\pi} k^4 \frac{e^{-iq_g(z_g+z_s)}}{q_g^3} \int\limits_{-\infty}^{+\infty} dz' \int\limits_{-\infty}^{+\infty} dz'' \alpha_1(z')\alpha_1(z'') e^{iq_g(z'+z'')} e^{iq_g|z'-z''|}
$$

$$
= -\frac{i}{(8\pi)} k^4 \frac{e^{-iq_g(z_g+z_s)}}{q_g^3} \int\limits_{-\infty}^{+\infty} dz' \int\limits_{-\infty}^{+\infty} dz'' \alpha_1(z')\alpha_1(z'') e^{2iq_g z'} H(z'-z'').
$$

Imposing Left side = Right side, we get

$$
\int\limits_{-\infty}^{+\infty} dz'\alpha_2(z')e^{2iq_g z'} = \frac{ik^2}{q_g} \int\limits_{-\infty}^{+\infty} dz' \int\limits_{-\infty}^{+\infty} dz''\alpha_1(z')\alpha_1(z'') e^{2iq_g z'} H(z'-z''). \qquad (2.16)
$$

Using $q_g = k\cos\theta$, and Fourier transforming Eq. (2.16) over $2q_g$, we get

$$
\int\limits_{-\infty}^{+\infty} dz'\alpha_2(z') \int\limits_{-\infty}^{+\infty} dq_g e^{-2iq_g(z-z')} = \frac{1}{\cos^2\theta} \int\limits_{-\infty}^{+\infty} dz' \int\limits_{-\infty}^{+\infty} dz''\alpha_1(z')\alpha_1(z'') H(z'-z'')
$$

$$
\times \int\limits_{-\infty}^{+\infty} dq_g (iq_g) e^{-2iq_g(z-z')}. \qquad (2.17)
$$

Then we have

$$
\alpha_2(z) = -\frac{1}{2\cos^2\theta} \frac{d}{dz}\left[\alpha_1(z) \int\limits_{-\infty}^{+\infty} dz''\alpha_1(z'') H(z-z'')\right], \qquad (2.18)
$$

and finally, we get the following non-linear (in α_1 and hence in the data) solution for α_2

$$\alpha_2(z) = -\frac{1}{2\cos^2\theta}\left[\alpha_1^2(z) + \alpha_1'(z)\int\limits_{-\infty}^{z}dz'\alpha_1(z')\right], \qquad (2.19)$$

where $\alpha_1'(z) = \frac{d\alpha_1(z)}{dz}$. This is the first one parameter non-linear inversion of 1D acoustic media for a 2D experiment in which the imaging-only term(s) and inversion-only term(s) are isolated. The term $-\frac{1}{2\cos^2\theta}\alpha_1^2(z)$ represents the inversion-only, and $-\frac{1}{2\cos^2\theta}\alpha_1'(z)\int\limits_{-\infty}^{z}dz'\alpha_1(z')$ with an integral represents the imaging term. For $\theta = 0$, this solution reduces to the non-linear solution for 1D normal incidence case (e.g., Shaw, 2005)

$$\alpha_2(z) = -\frac{1}{2}\left[\alpha_1^2(z) + \alpha_1'(z)\int\limits_{-\infty}^{z}dz'\alpha_1(z')\right]. \qquad (2.20)$$

If another choice of free parameter other than θ (e.g., ω or k_h) is selected, then the functional form between the data and the first order perturbation Eq. (2.13) would change. Furthermore, the relationship between the first and second order perturbation Eq. (2.19) would, then, also be different, and new analysis would be required for the purpose of identifying specific task separated terms. Empirically, the choice of θ as free parameter (for a 1D medium) is particularly well suited for allowing a task separated identification of terms in the inverse series. The numerical tests shown in section 2.4, will indicate how the first non-linear term α_2 contributes to the parameter prediction on α.

2.3   Derivation of α_3

Similarly, from the third equation of the inverse scattering series, Eq. (1.10), we have

$$G_0k^2\alpha_3G_0 = -G_0k^2\alpha_1G_0k^2\alpha_2G_0 - G_0k^2\alpha_2G_0k^2\alpha_1G_0 - G_0k^2\alpha_1G_0k^2\alpha_1G_0k^2\alpha_1G_0, \quad (2.21)$$

then, in space domain and for 2D experiment, we have

$$
\int\limits_{-\infty}^{+\infty} dx' \int\limits_{-\infty}^{+\infty} dz' G_0(x_g, z_g; x', z'; \omega) k^2 \alpha_3(z') G_0(x', z'; x_s, z_s; \omega)
$$

$$
= - \int\limits_{-\infty}^{+\infty} dx' \int\limits_{-\infty}^{+\infty} dz' \int\limits_{-\infty}^{+\infty} dx'' \int\limits_{-\infty}^{+\infty} dz'' G_0(x_g, z_g; x', z'; \omega) k^2 \alpha_1(z') G_0(x', z'; x'', z''; \omega)
$$

$$
\times k^2 \alpha_2(z'') G_0(x'', z''; x_s, z_s; \omega)
$$

$$
- \int\limits_{-\infty}^{+\infty} dx' \int\limits_{-\infty}^{+\infty} dz' \int\limits_{-\infty}^{+\infty} dx'' \int\limits_{-\infty}^{+\infty} dz'' G_0(x_g, z_g; x', z'; \omega) k^2 \alpha_2(z') G_0(x', z'; x'', z''; \omega)
$$

$$
\times k^2 \alpha_1(z'') G_0(x'', z''; x_s, z_s; \omega)
$$

$$
- \int\limits_{-\infty}^{+\infty} dx' \int\limits_{-\infty}^{+\infty} dz' \int\limits_{-\infty}^{+\infty} dx'' \int\limits_{-\infty}^{+\infty} dz'' \int\limits_{-\infty}^{+\infty} dx''' \int\limits_{-\infty}^{+\infty} dz''' G_0(x_g, z_g; x', z'; \omega) k^2 \alpha_1(z')
$$

$$
\times G_0(x', z'; x'', z''; \omega) k^2 \alpha_1(z'') G_0(x'', z''; x''', z'''; \omega) k^2 \alpha_1(z''')
$$

$$
\times G_0(x''', z'''; x_s, z_s; \omega). \tag{2.22}
$$

Similar to the derivation of α_1 and α_2, after Fourier transforming Eq. (2.22) over x_g and x_s, the left side becomes

$$
= -\frac{1}{(8\pi)} k^2 \frac{e^{-iq_g(z_g+z_s)}}{q_g^2} \int\limits_{-\infty}^{+\infty} dz' \alpha_3(z') e^{2iq_g z'}.
$$

The right side (with the same assumption that α_1 is non-zero only below the source and receiver, i.e., for $z' > z_g$ and $z''' > z_s$) becomes

$$
= -\frac{i}{(8\pi)} k^4 \frac{e^{-iq_g(z_g+z_s)}}{q_g^3} \int\limits_{-\infty}^{+\infty} dz' \int\limits_{-\infty}^{+\infty} dz'' \alpha_1(z') \alpha_2(z'') e^{2iq_g z'} H(z' - z'')
$$

$$
- \frac{i}{(8\pi)} k^4 \frac{e^{-iq_g(z_g+z_s)}}{q_g^3} \int\limits_{-\infty}^{+\infty} dz' \int\limits_{-\infty}^{+\infty} dz'' \alpha_2(z') \alpha_1(z'') e^{2iq_g z'} H(z' - z'')
$$

$$-\frac{1}{(32\pi)}k^6\frac{e^{-iq_g(z_g+z_s)}}{q_g^4}\int\limits_{-\infty}^{+\infty}dz'\int\limits_{-\infty}^{+\infty}dz''\int\limits_{-\infty}^{+\infty}dz'''\alpha_1(z')\alpha_1(z'')\alpha_1(z''')e^{iq_g(z'+z''')}e^{iq_g|z'-z''|}$$
$$\times e^{iq_g|z''-z'''|}.$$

Again, imposing Left side = Right side, and using $q_g = k\cos\theta$, we get (for fixed θ)

$$\int\limits_{-\infty}^{+\infty}dz'\alpha_3(z')e^{2iq_gz'}$$
$$=\frac{1}{\cos^2\theta}iq_g\int\limits_{-\infty}^{+\infty}dz'\int\limits_{-\infty}^{+\infty}dz''\alpha_1(z')\alpha_2(z'')e^{2iq_gz'}H(z'-z'')$$
$$+\frac{1}{\cos^2\theta}iq_g\int\limits_{-\infty}^{+\infty}dz'\int\limits_{-\infty}^{+\infty}dz''\alpha_2(z')\alpha_1(z'')e^{2iq_gz'}H(z'-z'')$$
$$+\frac{1}{\cos^4\theta}\frac{q_g^2}{4}\int\limits_{-\infty}^{+\infty}dz'\int\limits_{-\infty}^{+\infty}dz''\int\limits_{-\infty}^{+\infty}dz'''\alpha_1(z')\alpha_1(z'')\alpha_1(z''')$$
$$\times e^{iq_g(z'+z''')}e^{iq_g|z'-z''|}e^{iq_g|z''-z'''|}. \tag{2.23}$$

Fourier transforming Eq. (2.23) over $2q_g$, we get (detailed derivations of the integrations on the right side of Eq. 2.23 are presented in Shaw *et al.*, 2003b)

$$\alpha_3(z)=\frac{1}{\cos^4\theta}\left[\frac{3}{16}\alpha_1^3(z)\right.$$
$$+\frac{1}{8}\alpha_1''(z)\left(\int\limits_{-\infty}^{z}dz'\alpha_1(z')\right)^2$$
$$+\frac{3}{4}\alpha_1(z)\alpha_1'(z)\int\limits_{-\infty}^{z}dz'\alpha_1(z')$$
$$-\frac{1}{8}\alpha_1'(z)\int\limits_{-\infty}^{z}dz'\alpha_1^2(z')$$
$$\left.-\frac{1}{16}\int\limits_{-\infty}^{z}dz'\int\limits_{-\infty}^{z}dz''\frac{d\alpha_1(z')}{dz'}\frac{d\alpha_1(z'')}{dz''}\alpha_1(z'+z''-z)\right]. \tag{2.24}$$

In this equation, the first term on the right hand side $\frac{3}{16\cos^4\theta}\alpha_1^3(z)$ represents the inversion-only term, and the second term $\frac{1}{8\cos^4\theta}\alpha_1''(z)\left(\int\limits_{-\infty}^{z}dz'\alpha_1(z')\right)^2$ represents the imaging-only term. The last term contributes to the removal of the internal multiples which begins in the third term in the inverse series (Weglein et $al.$, 1997).

In the following section, we will see how α_3 contributes to the parameter prediction on α.

2.4 Numerical tests

Consider a one-interface example, (shown in Fig. 2.2), the interface surface is at $z = a$, above the interface is the reference medium, and below is the actual medium. Suppose $z_s = z_g = 0$. In this case, the reflection coefficient has the following form

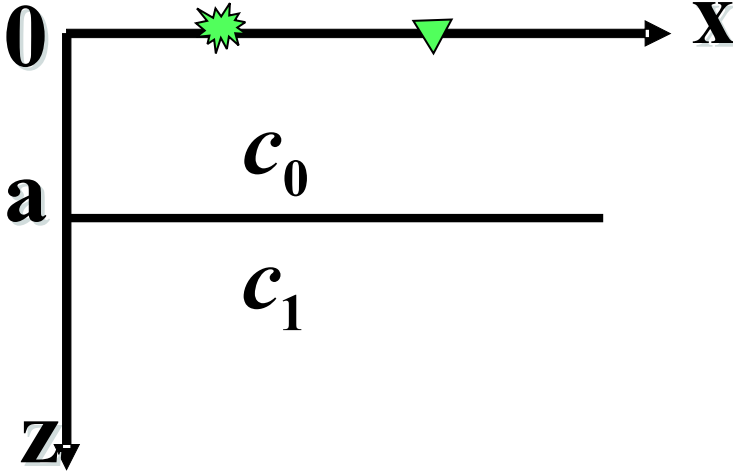Fig. 2.2: One-interface example.

$$R(\theta) = \frac{(c_1/c_0)\sqrt{1-\sin^2\theta} - \sqrt{1-(c_1^2/c_0^2)\sin^2\theta}}{(c_1/c_0)\sqrt{1-\sin^2\theta} + \sqrt{1-(c_1^2/c_0^2)\sin^2\theta}}. \tag{2.25}$$

With this coefficient, data may be expressed analytically (Clayton and Stolt, 1981; Weglein et $al.$, 1986) as:

$$\widetilde{D}(q_g,\theta) = R(\theta)\frac{e^{2iq_g a}}{4\pi i q_g}. \tag{2.26}$$

Substituting Eq. (2.26) into Eq. (2.13) and Fourier transforming Eq. (2.13) over $2q_g$, we have

$$\int_{-\infty}^{+\infty} dq_g e^{-2iq_g z} R(\theta) \frac{e^{2iq_g a}}{2iq_g} = -\frac{1}{4\cos^2\theta} \int_{-\infty}^{+\infty} dz' \int_{-\infty}^{+\infty} dq_g e^{-2iq_g z} \alpha_1(z') e^{2iq_g z'}. \qquad (2.27)$$

Then, for fixed θ, we have

$$\alpha_1(z) = 4R(\theta)\cos^2\theta H(z-a). \qquad (2.28)$$

Hence, given one angle θ, we can get the corresponding α_1.

After substituting Eq. (2.28) into Eqs. (2.19) and (2.24), respectively, we obtain

$$\alpha_2(z) = -8R^2(\theta)\cos^2\theta H(z-a), \qquad (2.29)$$

and

$$\alpha_3(z) = 12R^3(\theta)\cos^2\theta H(z-a). \qquad (2.30)$$

From Eqs. (2.29) and (2.30), we can see that only inversion terms are kept on the right side of the equations and the other terms with integrals in Eqs. (2.19) and (2.24) are automatically gone. The reason is that, for this one-interface model, we have the right velocity (reference velocity) and hence the interface is located at the right depth so it does not need to be corrected any more. Furthermore, there are no internal multiples in this one-interface model. Therefore, the task-specific subseries will automatically shut down when there is no such kind of task that needs to be performed, which is called purposeful perturbation.

The numerical tests are based on the following three specific models:

Model 1: $c_0 = 2000m/s, c_1 = 2200m/s$;

Model 2: $c_0 = 1500m/s, c_1 = 1800m/s$;

Model 3: $c_0 = 1800m/s, c_1 = 1500m/s$.

Model 2 has a bigger contrast than Model 1, and in Model 3, the velocity of the actual medium is less than the reference medium so the sign of α becomes negative.

As shown in Figs. 2.4, 2.3 and 2.5, for all three models presented in the numerical tests, including the non-linear terms α_2 and α_3 produces significant improvement.
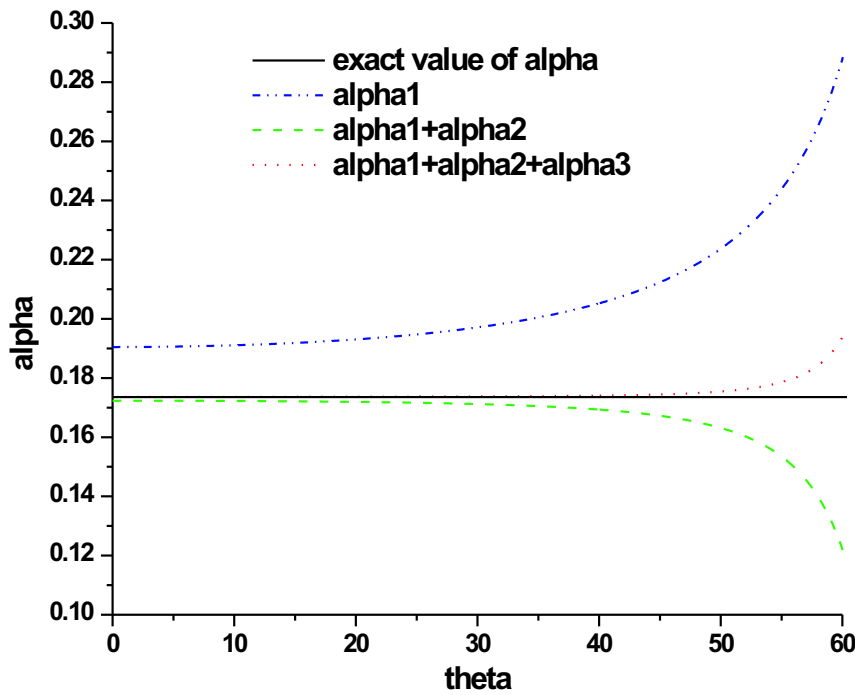
Fig. 2.3: *Model 1: $c_0 = 2000m/s, c_1 = 2200m/s$, exact value of α for this example is 0.174, the critical angle is 65.4^0.*

2.5 Conclusion

This chapter represents the first analysis of the direct non-linear target identification for a 1D acoustic medium and 2D experiment and provides a user guide and useful lessons
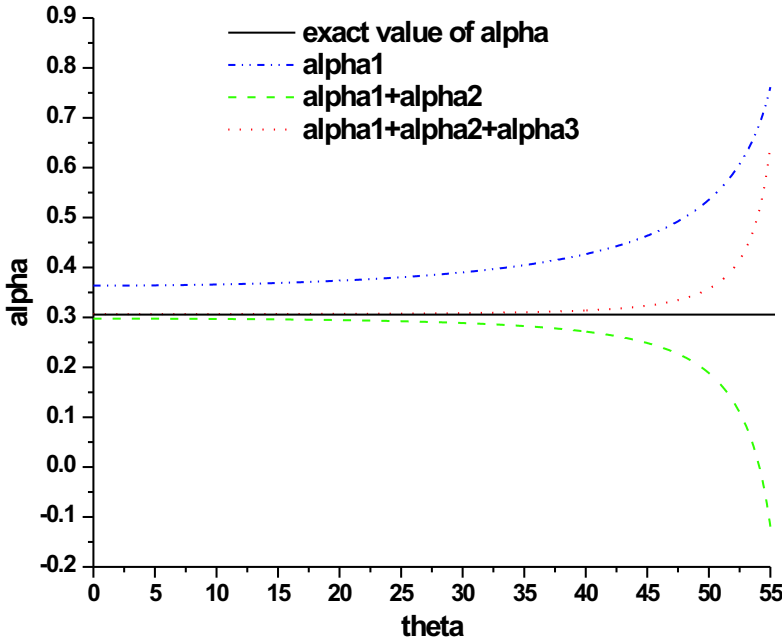
Fig. 2.4: Model 2: $c_0 = 1500m/s, c_1 = 1800m/s$, exact value of α for this example is 0.306, the critical angle is 56.4^0.

for its generalization to a more complex and realistic model. In particular, for all of the three models tested, the first and second non-linear terms in the inverse scattering inversion subseries provide added value and improved capability for target identification beyond the conventional linear inversion. Although the tested models involve only one interface, the solutions can be applied to multi-interface models too.

The work on the one parameter case has progressed further and Simon Shaw generalized this one parameter case to 3D acoustic data in, e.g., Shaw (2005).

In this one parameter case, we assume that the acoustic medium only varies in velocity and analytical tests show very good results. So what if both velocity and density change in an acoustic medium? In the next chapter, the algorithm will be generalized to more realistic models — two parameter 1D acoustic model. This is a major step for target identification towards realism — a multi-parameter world.
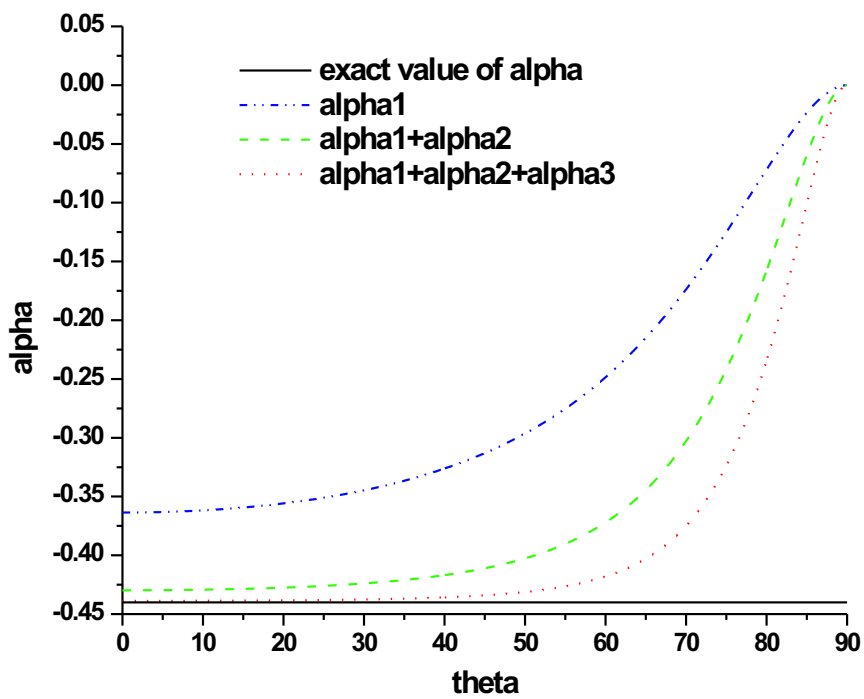
Fig. 2.5: *Model 3: $c_0 = 1800m/s, c_1 = 1500m/s$, exact value of α for this example is -0.44.*

3. **TWO PARAMETER ACOUSTIC INVERSION**

In this chapter, the direct non-linear inversion for the one parameter case is generalized to a multi-parameter case — two parameter acoustic inversion. For the first time, a two parameter direct non-linear inversion solution is obtained for 1D acoustic media (velocity and density vary vertically in depth) 2D experiment. Clayton and Stolt (1981) gave a two parameter *linear* inversion solution for *2D* acoustic media (velocity and density vary both vertically and laterally). In this chapter, we use the same parameters but concentrate on *1D* acoustic media to derive the direct *non-linear* inversion solution. In the application of the direct *non-linear* inverse algorithm, we move one step each time (e.g., from one parameter 1D acoustic case to two parameter 1D acoustic case, or to one parameter 2D acoustic case, instead of 'jumping' directly to two parameter 2D acoustic case) so that we can solve the problem step by step and learn lessons from each step which would guide us to step further towards greater realism. For one parameter 2D acoustic media, some work on direct non-linear imaging with reference velocity is presented by Liu *et al.* (2005).

For the direct non-linear inversion solution obtained in this chapter, the tasks for imaging-only and inversion-only terms are separated. Tests with analytic data indicate significant added value for parameter predictions, beyond linear estimates, in terms of both the proximity to actual value and the increased range of angles over which the improved estimates are useful.

A closed form of the inversion terms for one-interface case is also obtained. This closed form might be useful in predicting the precritical data using the postcritical data.

A special parameter Δc ($\Delta c = c - c_0$) (P-wave velocity change across an interface) is also found. Its Born inversion $(\Delta c)_1$ always has the right sign. That is, the sign of $(\Delta c)_1$ is always the same as that of Δc. In practice, it could be very useful to know whether the velocity increases or decreases across the interface. After changing parameters, from α (relative changes in P-wave bulk modulus) and β (relative changes in density) to velocity and β, another form of the non-linear solution is obtained. There is no leakage correction (please see details in Section 3.3) in this solution. This new form clearly indicates that the imaging terms care only about velocity errors. The mislocation is due to the wrong velocity. This is suggestive of possible generalization to multi-D medium, also of possible model-type independent imaging which only depends on velocity changes.

This chapter has the following structure. Section 3.1 gives the solutions of the first and second terms. In section 3.2, we derive the closed form and this is followed by numerical tests. The last section contains further discussions about the special parameters and conclusions.

3.1 Derivation of α_1, β_1 and α_2, β_2

In this section, we will consider a 1D acoustic two parameter earth model (e.g. bulk modulus and density or velocity and density). We start with the 3D acoustic wave equations in the actual and reference medium (Clayton and Stolt, 1981; Weglein *et al.*, 1997)

$$\left[\frac{\omega^2}{K(\mathbf{r})} + \nabla \cdot \frac{1}{\rho(\mathbf{r})}\nabla\right] G(\mathbf{r}, \mathbf{r}_s; \omega) = \delta(\mathbf{r} - \mathbf{r}_s), \tag{3.1}$$

$$\left[\frac{\omega^2}{K_0(\mathbf{r})} + \nabla \cdot \frac{1}{\rho_0(\mathbf{r})}\nabla\right] G_0(\mathbf{r}, \mathbf{r}_s; \omega) = \delta(\mathbf{r} - \mathbf{r}_s), \tag{3.2}$$

where $G(\mathbf{r}, \mathbf{r}_s; \omega)$ and $G_0(\mathbf{r}, \mathbf{r}_s; \omega)$ are respectively the free-space causal Green's functions that describe wave propagation in the actual and reference medium. $K = c^2\rho$, is P-wave bulk modulus, c is P-wave velocity and ρ is the density. The quantities with subscript "0" are for the reference medium, and those without the subscript are for the actual medium.

The perturbation is

$$V = L_0 - L = \frac{\omega^2 \alpha}{K_0} + \nabla \cdot \frac{\beta}{\rho_0} \nabla, \tag{3.3}$$

where $\alpha = 1 - \frac{K_0}{K}$ and $\beta = 1 - \frac{\rho_0}{\rho}$ are the two parameters we choose to do the inversion. Assuming both ρ_0 and c_0 are constants, Eq. (3.2) becomes

$$\left(\frac{\omega^2}{c_0^2} + \nabla^2 \right) G_0(\mathbf{r}, \mathbf{r}_s; \omega) = \rho_0 \delta(\mathbf{r} - \mathbf{r}_s). \tag{3.4}$$

For the 1-D case, the perturbation V has the following form

$$V(z, \nabla) = \frac{\omega^2 \alpha(z)}{K_0} + \frac{1}{\rho_0} \beta(z) \frac{\partial^2}{\partial x^2} + \frac{1}{\rho_0} \frac{\partial}{\partial z} \beta(z) \frac{\partial}{\partial z}. \tag{3.5}$$

$V(z, \nabla)$, $\alpha(z)$ and $\beta(z)$ can be expanded respectively as

$$V(z, \nabla) = V_1(z, \nabla) + V_2(z, \nabla) + \cdots, \tag{3.6}$$

$$\alpha(z) = \alpha_1(z) + \alpha_2(z) + \cdots, \tag{3.7}$$

$$\beta(z) = \beta_1(z) + \beta_2(z) + \cdots. \tag{3.8}$$

Then we have

$$V_1(z, \nabla) = \frac{\omega^2 \alpha_1(z)}{K_0} + \frac{1}{\rho_0} \beta_1(z) \frac{\partial^2}{\partial x^2} + \frac{1}{\rho_0} \frac{\partial}{\partial z} \beta_1(z) \frac{\partial}{\partial z}, \tag{3.9}$$

$$V_2(z, \nabla) = \frac{\omega^2 \alpha_2(z)}{K_0} + \frac{1}{\rho_0} \beta_2(z) \frac{\partial^2}{\partial x^2} + \frac{1}{\rho_0} \frac{\partial}{\partial z} \beta_2(z) \frac{\partial}{\partial z}, \tag{3.10}$$

$$\vdots$$

Substituting Eq. (3.9) into Eq. (1.8), we can get the linear solution for α_1 and β_1 in frequency domain

$$\widetilde{D}(q_g, \theta, z_g, z_s) = -\frac{\rho_0}{4} e^{-iq_g(z_s + z_g)} \left[\frac{1}{\cos^2 \theta} \widetilde{\alpha_1}(-2q_g) + (1 - \tan^2 \theta) \widetilde{\beta_1}(-2q_g) \right], \tag{3.11}$$

where the subscripts s and g denote source and receiver quantities respectively, and q_g, θ and $k = \omega/c_0$ shown in Fig. 3.1, have the following relations (Matson, 1997)

$$q_g = q_s = k\cos\theta,$$

$$k_g = k_s = k\sin\theta.$$

Similarly, substituting Eq. (3.10) into Eq. (1.9), we can get the solution for $\alpha_2(z)$ and
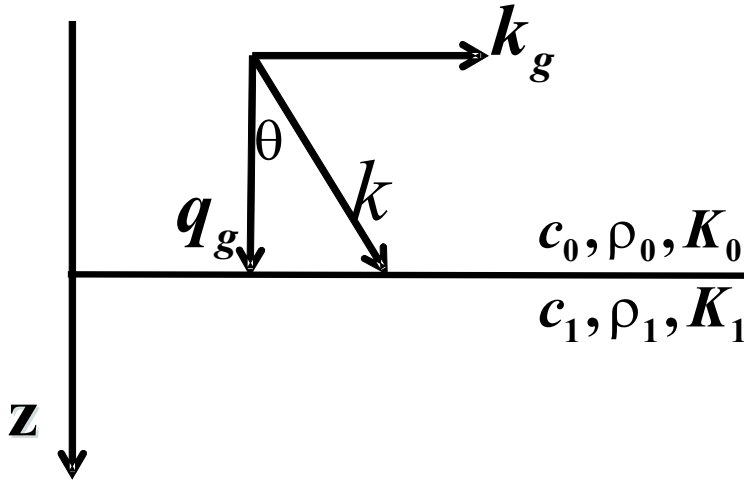
Fig. 3.1: *The relationship between q_g, k_g and θ.*

$\beta_2(z)$ as a function of $\alpha_1(z)$ and $\beta_1(z)$ (Detail derivation in Appendix A)

$$\frac{1}{\cos^2\theta}\alpha_2(z) + (1 - \tan^2\theta)\beta_2(z) = -\frac{1}{2\cos^4\theta}\alpha_1^2(z) - \frac{1}{2}(1 + \tan^4\theta)\beta_1^2(z) + \frac{\tan^2\theta}{\cos^2\theta}\alpha_1(z)\beta_1(z)$$

$$- \frac{1}{2\cos^4\theta}\alpha_1'(z)\int_0^z dz'[\alpha_1(z') - \beta_1(z')]$$

$$+ \frac{1}{2}(\tan^4\theta - 1)\beta_1'(z)\int_0^z dz'[\alpha_1(z') - \beta_1(z')], \qquad (3.12)$$

where $\alpha_1'(z) = \frac{d\alpha_1(z)}{dz}$, $\beta_1'(z) = \frac{d\beta_1(z)}{dz}$.

The first two parameter direct non-linear inversion of 1D acoustic media for a 2D experiment has been obtained. As shown in Eq. (3.11) and Eq. (3.12), given two different angles θ, we

can determine α_1, β_1 and then α_2, β_2. For a single-interface example, it can be shown that only the first three terms on the right hand side contribute to parameter predictions, while the last two terms perform imaging in depth since they will be zero after the integration across the interface (see Section 3.2). Therefore, in this solution, the tasks for imaging-only and inversion-only terms are separated. Details about the significance of this solution will be presented in the following sections.

3.2   A special case: one-interface model

In this section, we derive a closed form for the inversion-only terms. From this closed form, we can easily get the same inversion terms as those in Eqs. (3.11) and (3.12). We also show some numerical tests using analytic data. From the numerical results, we see how the corresponding non-linear terms contribute to the parameter predictions such as the relative changes in the P-wave bulk modulus $\left(\alpha = \frac{\Delta K}{K}\right)$, density $\left(\beta = \frac{\Delta \rho}{\rho}\right)$, impedance $\left(\frac{\Delta I}{I}\right)$ and velocity $\left(\frac{\Delta c}{c}\right)$.

3.2.1   Closed form for the inversion terms

1. Incident angle not greater than critical angle, i.e. $\theta \leq \theta_c$

For a single interface example, the reflection coefficient has the following form (Keys, 1989)

$$R(\theta) = \frac{(\rho_1/\rho_0)(c_1/c_0)\sqrt{1 - \sin^2\theta} - \sqrt{1 - (c_1^2/c_0^2)\sin^2\theta}}{(\rho_1/\rho_0)(c_1/c_0)\sqrt{1 - \sin^2\theta} + \sqrt{1 - (c_1^2/c_0^2)\sin^2\theta}}. \tag{3.13}$$

After adding 1 on both sides of Eq. (3.13), we can get

$$1 + R(\theta) = \frac{2\cos\theta}{\cos\theta + (\rho_0/\rho_1)\sqrt{(c_0^2/c_1^2) - \sin^2\theta}}. \tag{3.14}$$

Then, using the definitions of $\alpha = 1 - \frac{K_0}{K_1} = 1 - \frac{\rho_0 c_0^2}{\rho_1 c_1^2}$ and $\beta = 1 - \frac{\rho_0}{\rho_1}$, Eq. (3.14) becomes

$$\frac{4R(\theta)}{(1 + R(\theta))^2} = \frac{\alpha}{\cos^2 \theta} + (1 - \tan^2 \theta)\beta - \frac{\alpha\beta}{\cos^2 \theta} + \beta^2 \tan^2 \theta, \tag{3.15}$$

which is the closed form we derived for one interface two parameter acoustic inversion-only terms.

2. Incident angle greater than critical angle, i.e. $\theta > \theta_c$

For $\theta > \theta_c$, Eq. (3.13) becomes

$$R(\theta) = \frac{(\rho_1/\rho_0)(c_1/c_0)\sqrt{1 - \sin^2 \theta} - i\sqrt{(c_1^2/c_0^2)\sin^2 \theta - 1}}{(\rho_1/\rho_0)(c_1/c_0)\sqrt{1 - \sin^2 \theta} + i\sqrt{(c_1^2/c_0^2)\sin^2 \theta - 1}}. \tag{3.16}$$

Then, Eq. (3.14) becomes

$$1 + R(\theta) = \frac{2\cos\theta}{\cos\theta + i\,(\rho_0/\rho_1)\,\sqrt{\sin^2\theta - (c_0^2/c_1^2)}}, \tag{3.17}$$

which leads to the same closed form as Eq. (3.15)

$$\frac{4R(\theta)}{(1 + R(\theta))^2} = \frac{\alpha}{\cos^2 \theta} + (1 - \tan^2 \theta)\beta - \frac{\alpha\beta}{\cos^2 \theta} + \beta^2 \tan^2 \theta.$$

As we see, this closed form is valid for all incident angles.

In addition, for normal incidence $(\theta = 0)$ and constant density $(\beta = 0)$ media, the closed form Eq. (3.15) will be reduced to

$$\alpha = \frac{4R}{(1 + R)^2}. \tag{3.18}$$

This represents the relationship between α and R for one parameter 1D acoustic constant density medium and 1D normal incidence obtained in Innanen (2003). In this case, α becomes $1 - c_0^2/c_1^2$ and R becomes $(c_1 - c_0)/(c_1 + c_0)$.

3. Derivation of the inversion terms from the closed form

From the closed form Eq. (3.15), using Taylor expansion on the left hand side

$$\frac{1}{(1 + R(\theta))^2} = \left[1 - R(\theta) + R^2(\theta) - \ldots\right]^2,$$

and setting the terms of equal order in the data equal, we have

$$\frac{\alpha_1}{\cos^2 \theta} + (1 - \tan^2 \theta)\beta_1 = 4R(\theta), \tag{3.19}$$

$$\frac{\alpha_2}{\cos^2 \theta} + (1 - \tan^2 \theta)\beta_2 = -\frac{1}{2}\frac{\alpha_1^2}{\cos^4 \theta} - \frac{1}{2}(1 + \tan^4 \theta)\beta_1^2 + \frac{\tan^2 \theta}{\cos^2 \theta}\alpha_1\beta_1. \tag{3.20}$$

For a one-interface example (in Fig. 3.2), Eqs. (3.11) and (3.12) will respectively reduce to the same form as Eqs. (3.19) and (3.20), which is shown below.

Assume the interface surface is at depth $z = a$, and suppose $z_s = z_g = 0$. Using the similar
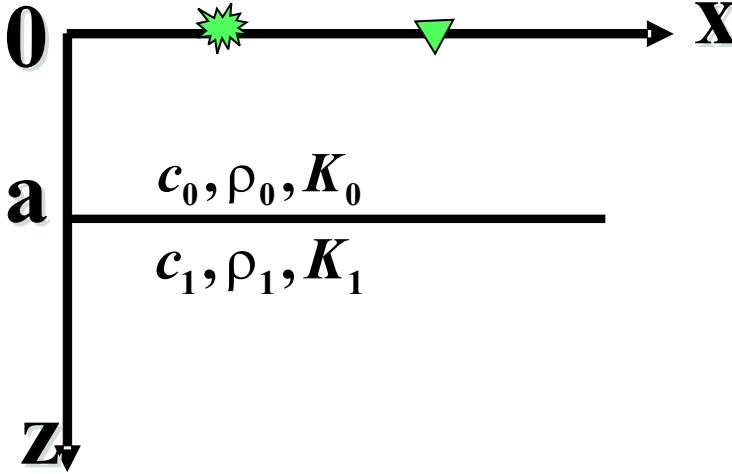

Fig. 3.2: *1D one-interface acoustic model.*

analytic data (Clayton and Stolt, 1981; Weglein *et al.*, 1986) as in Chapter 2,

$$\widetilde{D}(q_g, \theta) = \rho_0 R(\theta)\frac{e^{2iq_g a}}{4\pi i q_g}, \tag{3.21}$$

and substituting Eq. (3.21) into Eq. (3.11), after Fourier transformation over $2q_g$, for $z > a$ and fixed θ, we get

$$\frac{1}{\cos^2 \theta}\alpha_1(z) + (1 - \tan^2 \theta)\beta_1(z) = 4R(\theta)H(z - a). \tag{3.22}$$

Also, the non-linear solution Eq. (3.12) will reduce to

$$\frac{1}{\cos^2 \theta}\alpha_2(z) + (1 - \tan^2 \theta)\beta_2(z) = -\frac{1}{2\cos^4 \theta}\alpha_1^2(z) - \frac{1}{2}(1 + \tan^4 \theta)\beta_1^2(z)$$
$$+ \frac{\tan^2 \theta}{\cos^2 \theta}\alpha_1(z)\beta_1(z), \tag{3.23}$$

The two equations Eqs. (3.22) and (3.23) agree with Eqs. (3.19) and (3.20), respectively.

3.2.2   Numerical tests

From Eq. (3.22), choosing two different angles to solve for α_1 and β_1

$$\beta_1(\theta_1, \theta_2) = 4\frac{R(\theta_1)\cos^2 \theta_1 - R(\theta_2)\cos^2 \theta_2}{\cos(2\theta_1) - \cos(2\theta_2)}, \tag{3.24}$$

$$\alpha_1(\theta_1, \theta_2) = \beta_1(\theta_1, \theta_2) + 4\frac{R(\theta_1) - R(\theta_2)}{\tan^2 \theta_1 - \tan^2 \theta_2}. \tag{3.25}$$

Similarly, from Eq. (3.23), given two different angles we can solve for α_2 and β_2 in terms of α_1 and β_1

$$\beta_2(\theta_1, \theta_2) = \left[-\frac{1}{2}\alpha_1^2\left(\frac{1}{\cos^2 \theta_1} - \frac{1}{\cos^2 \theta_2}\right) + \alpha_1\beta_1\left(\tan^2 \theta_1 - \tan^2 \theta_2\right) - \frac{1}{2}\beta_1^2\right.$$
$$\left.\times \left(\cos^2 \theta_1 - \cos^2 \theta_2 + \frac{\sin^4 \theta_1}{\cos^2 \theta_1} - \frac{\sin^4 \theta_2}{\cos^2 \theta_2}\right)\right] / \left[\cos(2\theta_1) - \cos(2\theta_2)\right], \tag{3.26}$$

$$\alpha_2(\theta_1, \theta_2) = \beta_2(\theta_1, \theta_2) + \left[-\frac{1}{2}\alpha_1^2\left(\frac{1}{\cos^4 \theta_1} - \frac{1}{\cos^4 \theta_2}\right) + \alpha_1\beta_1\left(\frac{\tan^2 \theta_1}{\cos^2 \theta_1} - \frac{\tan^2 \theta_2}{\cos^2 \theta_2}\right)\right.$$

$$-\frac{1}{2}\beta_1^2 \left(\tan^4 \theta_1 - \tan^4 \theta_2\right)\Bigg] / \left(\tan^2 \theta_1 - \tan^2 \theta_2\right);\qquad(3.27)$$

where α_1 and β_1 in Eqs. (3.26) and (3.27) denote $\alpha_1(\theta_1, \theta_2)$ and $\beta_1(\theta_1, \theta_2)$, respectively.

For a specific model, $\rho_0 = 1.0g/cm^3$, $\rho_1 = 1.1g/cm^3$, $c_0 = 1500m/s$ and $c_1 = 1700m/s$. In the following figures, we give the results for the relative changes in the P-wave bulk modulus $\left(\alpha = \frac{\Delta K}{K}\right)$, density $\left(\beta = \frac{\Delta \rho}{\rho}\right)$, impedance $\left(\frac{\Delta I}{I}\right)$ and velocity $\left(\frac{\Delta c}{c}\right)$ corresponding to different pairs of θ_1 and θ_2.

From Fig. 3.3, we can see that when we add α_2 to α_1, the result is much closer to the exact value of α. Furthermore, the result is better behaved; i.e., the plot surface becomes flatter, over a larger range of precritical angles. Similarly, as shown in Fig. 3.4, the results of $\beta_1 + \beta_2$ are much better than those of β_1. In addition, the sign of β_1 is wrong at some angles, while, the results for $\beta_1 + \beta_2$ always have the right sign. So after including β_2, the sign of the density is corrected, which is very important in the earth identification, and also the results of $\frac{\Delta I}{I}$ (see Fig. 3.5) and $\frac{\Delta c}{c}$ (see Fig. 3.6) are much closer to their exact values respectively compared to the linear results.

Especially, the values of $\left(\frac{\Delta c}{c}\right)_1$ are always greater than zero, that is, the sign of $(\Delta c)_1$ is always positive, which is the same as that of the exact value Δc. We will further discuss this in the next section.

3.3   A Special parameter for linear inversion

As mentioned before, in general, since the relationship between data and target property changes is non-linear, linear inversion will produce errors in target property prediction. When one actual property change is zero, the linear prediction of the change can be non-zero. Also, when the actual change is positive, the predicted linear approximation can be negative. There is a special parameter for linear inversion of acoustic media, that never suffers the latter problem.

From Eq. (3.13) we can see when $c_0 = c_1$, the reflection coefficient is independent of θ, then from the linear form Eq. (3.25), we have

$$\left(\frac{\Delta c}{c}\right)_1 = \frac{1}{2}(\alpha_1 - \beta_1) = 0 \text{ when } \Delta c = 0,$$

i.e., when $\Delta c = 0$, $(\Delta c)_1 = 0$. This generalizes to when $\Delta c > 0$, then $(\Delta c)_1 > 0$, or when $\Delta c < 0$, then $(\Delta c)_1 < 0$, as well. This can be shown mathematically (See Appendix A for details).

Therefore, we can, first, get the right sign of the relative change in P-wave velocity from the linear inversion $(\Delta c)_1$, then, get more accurate values by including non-linear terms.

Another interesting point is that the image does not move when the velocity does not change across an interface, i.e., $c_0 = c_1$, since, in this situation, the integrands of imaging terms $\alpha_1 - \beta_1$ in Eq. (3.12) are zero. We can see this more explicitly when we change the two parameters α and β to $\frac{\Delta c}{c}$ and β. Using the two relationships below (See details in Appendix A)

$$\left(\frac{\Delta c}{c}\right)_1 = \frac{1}{2}(\alpha_1 - \beta_1),$$

and

$$\left(\frac{\Delta c}{c}\right)_2 = \frac{1}{2}\left[\frac{1}{4}(\alpha_1 + \beta_1)^2 - \beta_1^2 + (\alpha_2 - \beta_2)\right],$$

rewriting Eq. (3.12) as

$$\frac{1}{\cos^2\theta}\left(\frac{\Delta c}{c}\right)_2(z) + \beta_2(z) = \frac{\cos^2\theta - 2}{2\cos^4\theta}\left(\frac{\Delta c}{c}\right)_1^2(z) - \frac{1}{2}\beta_1^2(z)$$
$$-\frac{1}{\cos^4\theta}\left(\frac{\Delta c}{c}\right)_1'(z)\int_0^z dz'\left(\frac{\Delta c}{c}\right)_1$$
$$-\frac{1}{\cos^2\theta}\beta_1'(z)\int_0^z dz'\left(\frac{\Delta c}{c}\right)_1. \tag{3.28}$$

This equation indicates two important concepts. One is leakage: there is no leakage correc-

tion at all in this expression. Here the leakage means that, if the actual value of α (relative changes in P-wave bulk modulus) is zero, its linear approximation α_1 could be non-zero since α and β are coupled together (like the coupled term $\alpha_1\beta_1$ in Eq. 3.12) and α_1 could get leakage values from β_1. While in Eq. (3.28), no such coupled term is present at all and thus, if the actual changes in the velocity are zero, then its linear inversion $\left(\frac{\Delta c}{c}\right)_1$ would be zero and there would be no leakage from β_1. This leakage issue or coupled term has no analogue in the 1D one parameter acoustic case (Eq. 2.19) since in this case we only have one parameter and there is no other parameter to leak into. Or in other words, in the one parameter (velocity) case, each 'jump' in the amplitude of the data (primaries only) corresponds to each wrong location with a wrong amplitude for the parameter predicted in the linear inverse step; while in the two parameter case of this chapter, each 'jump' in the data no longer has the simple one-to-one relationship with the amplitude and location of the two parameters.

The other concept is purposeful perturbation which is mentioned in Chapter 2. The integrand $\left(\frac{\Delta c}{c}\right)_1$ of the imaging terms clearly tells that if we have the right velocity, the imaging terms will automatically be zero even without doing any integration; otherwise, if we do not have the right velocity, these imaging terms would be used to move the interface closer to the right location from the wrong location. The conclusion from this equation is that the depth imaging terms depend only on the velocity errors.

3.4 Conclusion

In this chapter, we derive the first two parameter direct non-linear inversion solution for 1D acoustic media with 2D experiment. Numerical tests show that the terms beyond linear in earth property identification subseries provide added value. Although the models we used in the numerical tests are simple (for some readers), Eqs. (3.11) and (3.12) also work for more complex models since the inverse scattering series is a direct inversion procedure

which inverts data directly without knowing the specific properties of the target.

The work presented in this chapter is an important step for target identification towards more realism. The encouraging numerical results motivated us to move one step further — extension of our work to the elastic case (see, e.g., Boyse and Keller, 1986) using three parameters in the next chapter.
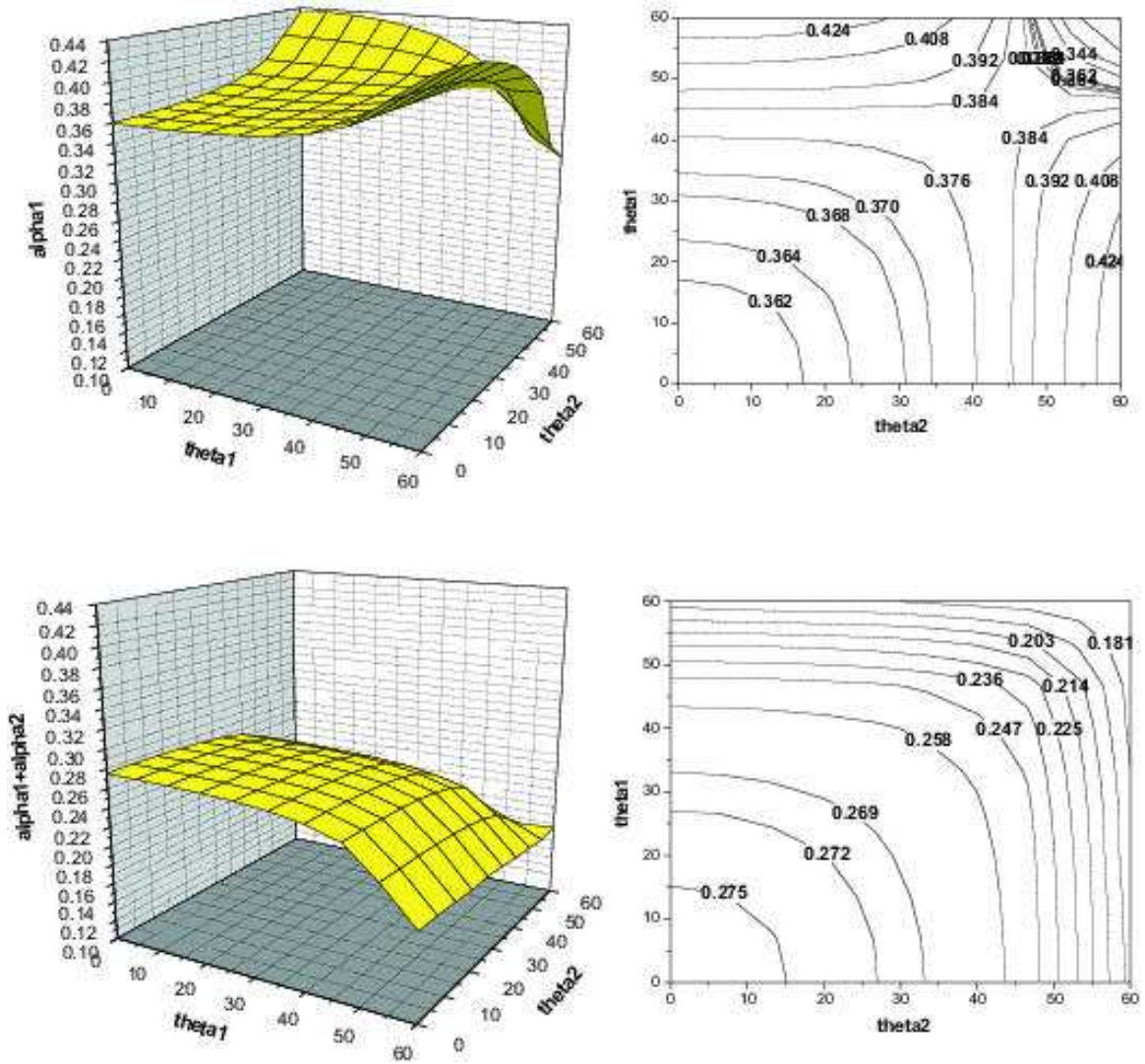
Fig. 3.3: α_1 (top) and $\alpha_1 + \alpha_2$ (bottom) displayed as a function of two different angles. The graphs on the right are the corresponding contour plots of the graphs on the left. In this example, the exact value of α is 0.292.
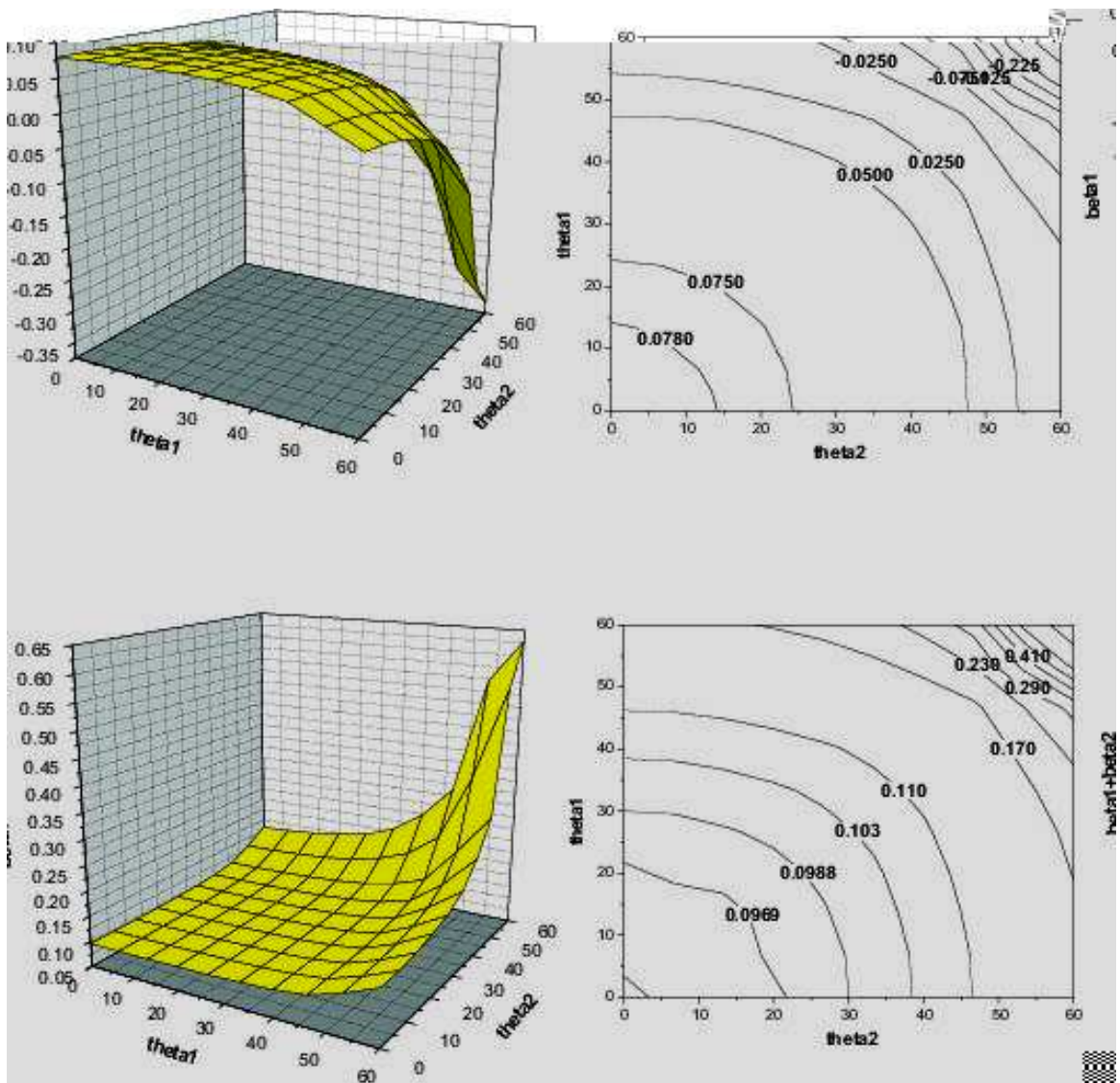
Fig. 3.4: β_1 (top) and $\beta_1 + \beta_2$ (bottom). In this example, the exact value of β is 0.09.
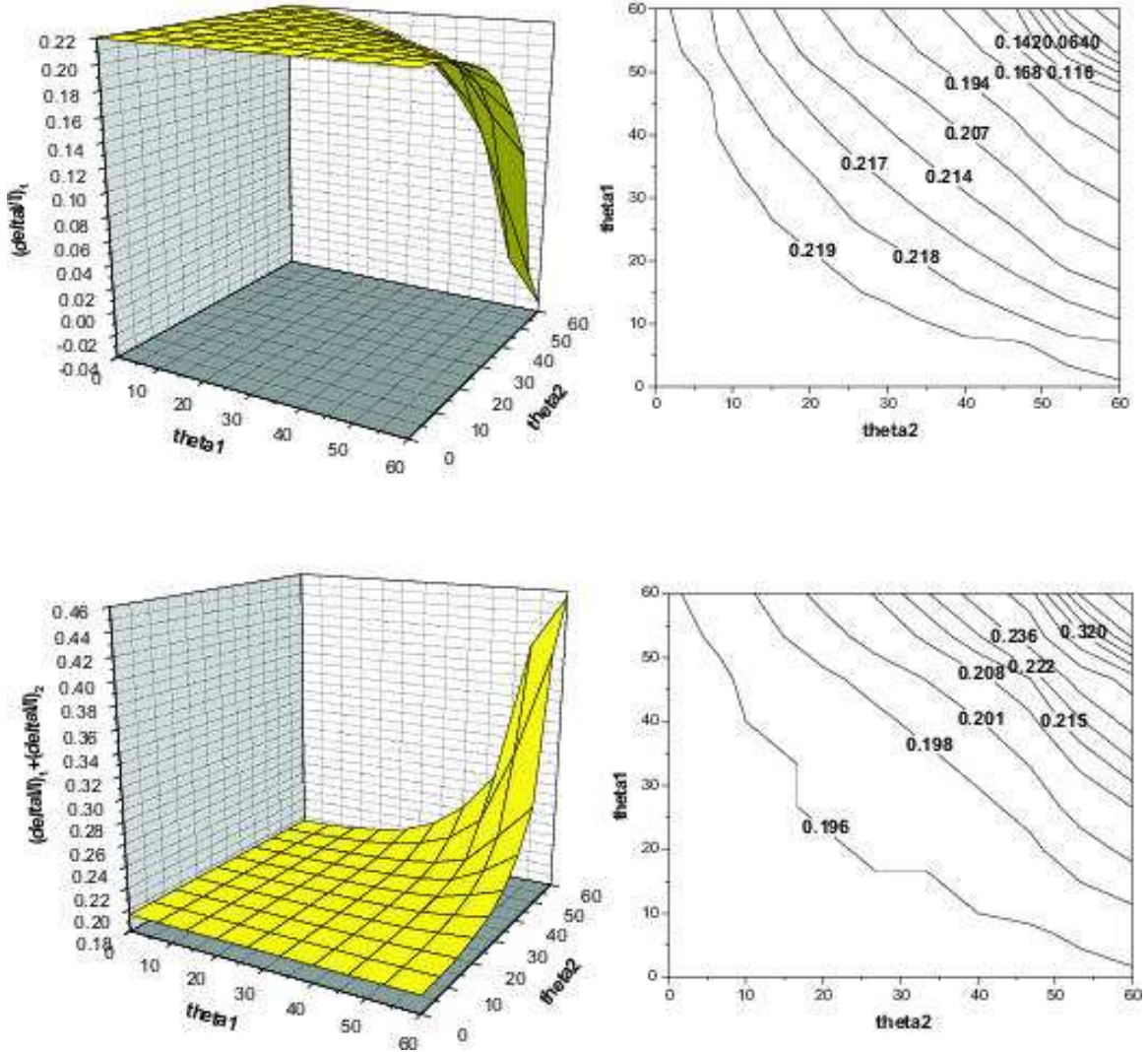
Fig. 3.5: *Linear approximation to relative change in impedance (see details in Appendix A)* $\left(\frac{\Delta I}{I}\right)_1 = \frac{1}{2}(\alpha_1 + \beta_1)$ *(top). Sum of linear and first non-linear terms* $\left(\frac{\Delta I}{I}\right)_1 + \left(\frac{\Delta I}{I}\right)_2 = \left(\frac{\Delta I}{I}\right)_1 + \frac{1}{2}\left[\frac{1}{4}(\alpha_1 - \beta_1)^2 + (\alpha_2 + \beta_2)\right]$ *(bottom). In this example, the exact value of* $\frac{\Delta I}{I}$ *is 0.198.*
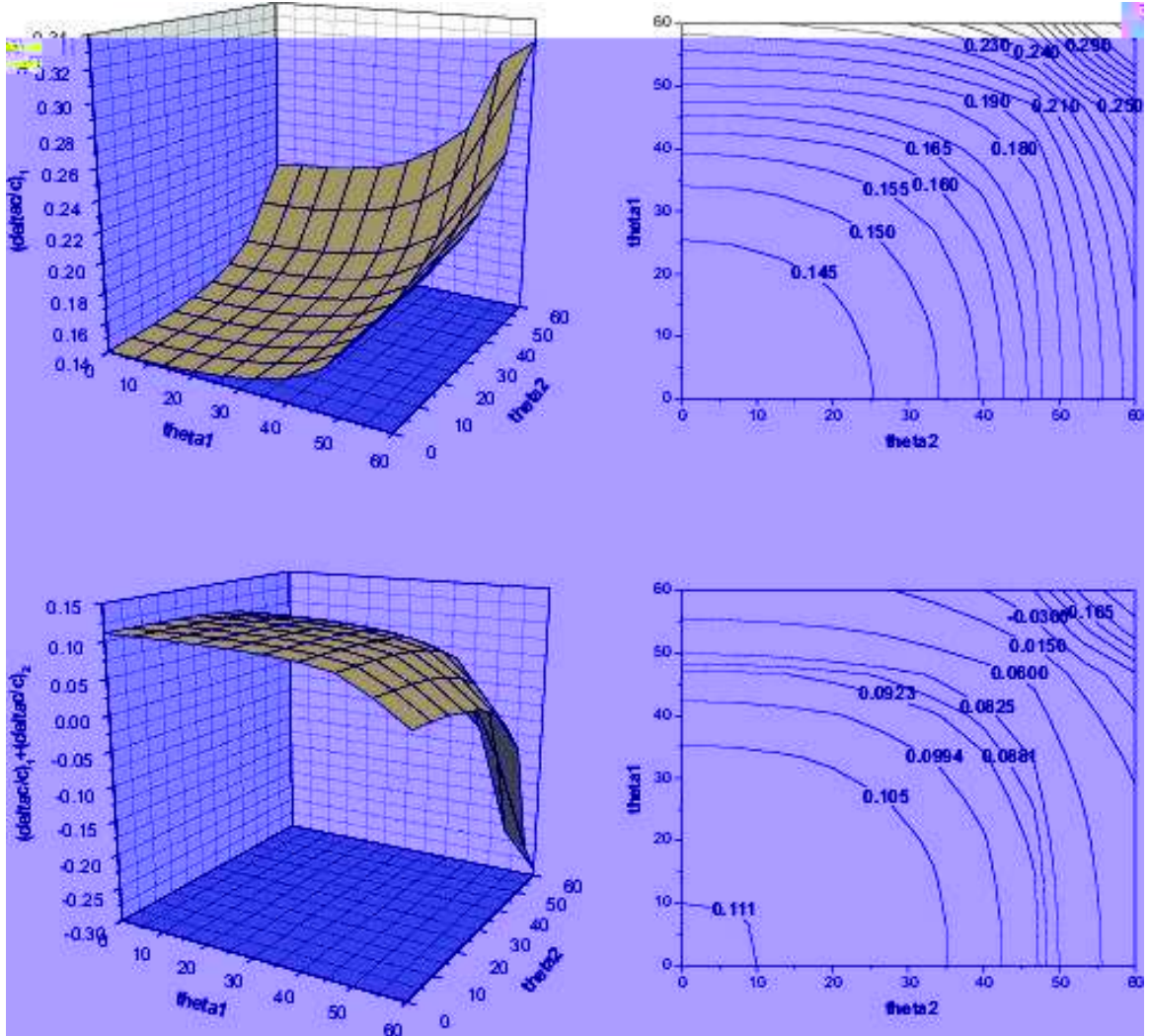
Fig. 3.6: *Linear approximation to relative change in velocity (see details in Appendix A)* $\left(\frac{\Delta c}{c}\right)_1 = \frac{1}{2}(\alpha_1 - \beta_1)$ *(top). Sum of linear and first non-linear terms* $\left(\frac{\Delta c}{c}\right)_1 + \left(\frac{\Delta c}{c}\right)_2 = \left(\frac{\Delta c}{c}\right)_1 + \frac{1}{2}\left[\frac{1}{4}(\alpha_1 + \beta_1)^2 - \beta_1^2 + (\alpha_2 - \beta_2)\right]$ *(bottom). In this example, the exact value of* $\frac{\Delta c}{c}$ *is 0.118.*

4. THREE PARAMETER ELASTIC INVERSION

In this chapter, we extend our work on direct non-linear inversion for 1D two parameter acoustic media (Chapter 3) to the three parameter elastic case. Weglein and Stolt (1992) presented the Born approximation inversion solutions for 2D elastic media (P-wave velocity, S-wave velocity and density vary vertically and laterally) using three parameters. Recently, R. H. Stolt extended the earlier elastic results to 3D. But that work mainly focuses on linear elastic formulations. In this chapter, we use the same parameters and derive the first set of direct non-linear inversion equations for 1D elastic media (i.e., depth/vertically varying P-wave velocity, S-wave velocity and density).

The terms for moving mislocated reflectors are separated from inversion-only terms. Although in principle this direct non-linear inversion approach requires all four components of elastic data, synthetic tests indicate that consistent value-added results may be achieved given only $\hat{D}^{PP}$ (PP data) measurements. This means that we can perform direct elastic non-linear inversion only using pressure measurements, i.e. towed streamer data. For the case that all four components of data are available, a consistent method is provided.

Finally, we present the application to the time-lapse seismic data to distinguish pressure changes from reservoir fluid changes while the conventional seismic time-lapse attributes has difficulty. Initial tests give very useful results.

4.1 Background for 2D elastic inversion

In this section we consider the inversion problem in two dimensions for an elastic medium. We start with the displacement space, and then, for convenience (see e.g., Weglein and Stolt, 1992; Aki and Richards, 2002), we change the basis and transform the equations to PS space. Finally, we do the elastic inversion in the PS domain.

4.1.1 In the displacement space

We begin with some basic equations in the displacement space (Matson, 1997):

$$L\mathbf{u} = \mathbf{f}, \tag{4.1}$$

$$L_0\mathbf{u} = \mathbf{f}, \tag{4.2}$$

$$LG = \delta, \tag{4.3}$$

$$L_0G_0 = \delta, \tag{4.4}$$

where L and L_0 are the differential operators that describe the wave propagation in the actual and reference medium, respectively, $\mathbf{u}$ and $\mathbf{f}$ are the corresponding displacement and source terms, respectively, and G and G_0 are the corresponding Green's operators for the actual and reference medium.

Similar to Chapter 1, defining the perturbation $V = L_0 - L$, the Lippmann- Schwinger equation for the elastic media in the displacement space is

$$G = G_0 + G_0VG. \tag{4.5}$$

Iterating this equation back into itself generates the Born series

$$G = G_0 + G_0 V G_0 + G_0 V G_0 V G_0 + \cdots . \tag{4.6}$$

We define the data D as the measured values of the scattered wave field. Then, on the measurement surface, we have

$$D = G_0 V G_0 + G_0 V G_0 V G_0 + \cdots . \tag{4.7}$$

Expanding V as a series in orders of D we have

$$V = V_1 + V_2 + V_3 + \cdots . \tag{4.8}$$

Substituting Eq. (4.8) into Eq. (4.7), evaluating Eq. (4.7), and setting terms of equal order in the data equal, the equations that determine V_1, V_2, ... from D and G_0 would be obtained.

$$D = G_0 V_1 G_0, \tag{4.9}$$

$$0 = G_0 V_2 G_0 + G_0 V_1 G_0 V_1 G_0, \tag{4.10}$$

$$\vdots$$

In the actual medium, the 2-D elastic wave equation is (Weglein and Stolt, 1992)

$$L\mathbf{u} \equiv \left[\rho\omega^2 \begin{pmatrix} 1 & 0 \\ 0 & 1 \end{pmatrix} + \begin{pmatrix} \partial_1\gamma\partial_1 + \partial_2\mu\partial_2 & \partial_1(\gamma - 2\mu)\partial_2 + \partial_2\mu\partial_1 \\ \partial_2(\gamma - 2\mu)\partial_1 + \partial_1\mu\partial_2 & \partial_2\gamma\partial_2 + \partial_1\mu\partial_1 \end{pmatrix} \right] \begin{bmatrix} u_1 \\ u_2 \end{bmatrix} = \mathbf{f}, \tag{4.11}$$

where

$$\mathbf{u} = \begin{bmatrix} u_1 \\ u_2 \end{bmatrix} = \text{displacement},$$

ρ = density,

γ = bulk modulus ($\equiv \rho\alpha^2$ where α = P-wave velocity),

μ = shear modulus ($\equiv \rho\beta^2$ where β = S-wave velocity),

ω = temporal frequency (angular), ∂_1 and ∂_2 denote the derivative over x and z, respectively, and

$\mathbf{f}$ is the source term.

For constant $(\rho, \gamma, \mu) = (\rho_0, \gamma_0, \mu_0)$, $(\alpha, \beta) = (\alpha_0, \beta_0)$, the operator L becomes

$$L_0 \equiv \left[\rho_0\omega^2 \begin{pmatrix} 1 & 0 \\ 0 & 1 \end{pmatrix} + \begin{pmatrix} \gamma_0\partial_1^2 + \mu_0\partial_2^2 & (\gamma_0 - \mu_0)\partial_1\partial_2 \\ (\gamma_0 - \mu_0)\partial_1\partial_2 & \mu_0\partial_1^2 + \gamma_0\partial_2^2 \end{pmatrix} \right]. \tag{4.12}$$

Then,

$$\begin{aligned} V \equiv & L_0 - L \\ = & -\rho_0 \begin{bmatrix} a_\rho\omega^2 + \alpha_0^2\partial_1 a_\gamma\partial_1 + \beta_0^2\partial_2 a_\mu\partial_2 & \partial_1(\alpha_0^2 a_\gamma - 2\beta_0^2 a_\mu)\partial_2 + \beta_0^2\partial_2 a_\mu\partial_1 \\ \partial_2(\alpha_0^2 a_\gamma - 2\beta_0^2 a_\mu)\partial_1 + \beta_0^2\partial_1 a_\mu\partial_2 & a_\rho\omega^2 + \alpha_0^2\partial_2 a_\gamma\partial_2 + \beta_0^2\partial_1 a_\mu\partial_1 \end{bmatrix}, \end{aligned} \tag{4.13}$$

where $a_\rho \equiv \frac{\rho}{\rho_0} - 1$, $a_\gamma \equiv \frac{\gamma}{\gamma_0} - 1$ and $a_\mu \equiv \frac{\mu}{\mu_0} - 1$ are the three parameters we choose to do the elastic inversion. For a 1D earth (i.e. a_ρ, a_γ and a_μ are only functions of depth z), the expression above for V becomes

$$V = -\rho_0 \begin{bmatrix} a_\rho\omega^2 + \alpha_0^2 a_\gamma\partial_1^2 + \beta_0^2\partial_2 a_\mu\partial_2 & (\alpha_0^2 a_\gamma - 2\beta_0^2 a_\mu)\partial_1\partial_2 + \beta_0^2\partial_2 a_\mu\partial_1 \\ \partial_2(\alpha_0^2 a_\gamma - 2\beta_0^2 a_\mu)\partial_1 + \beta_0^2 a_\mu\partial_1\partial_2 & a_\rho\omega^2 + \alpha_0^2\partial_2 a_\gamma\partial_2 + \beta_0^2 a_\mu\partial_1^2 \end{bmatrix}. \tag{4.14}$$

4.1.2 Transforming to PS space

For convenience, we can change the basis from $\mathbf{u} = \begin{bmatrix} u_1 \\ u_2 \end{bmatrix}$ to $\begin{pmatrix} \phi^P \\ \phi^S \end{pmatrix}$ to allow L_0 to be diagonal,

$$\boldsymbol{\Phi} = \begin{pmatrix} \phi^P \\ \phi^S \end{pmatrix} = \begin{bmatrix} \gamma_0(\partial_1 u_1 + \partial_2 u_2) \\ \mu_0(\partial_1 u_2 - \partial_2 u_1) \end{bmatrix}, \tag{4.15}$$

also, we have

$$\begin{pmatrix} \phi^P \\ \phi^S \end{pmatrix} = \Gamma_0 \Pi \mathbf{u} = \begin{bmatrix} \gamma_0(\partial_1 u_1 + \partial_2 u_2) \\ \mu_0(\partial_1 u_2 - \partial_2 u_1) \end{bmatrix}, \tag{4.16}$$

where $\Pi = \begin{pmatrix} \partial_1 & \partial_2 \\ -\partial_2 & \partial_1 \end{pmatrix}$, $\Gamma_0 = \begin{pmatrix} \gamma_0 & 0 \\ 0 & \mu_0 \end{pmatrix}$. In the reference medium, the operator L_0 will transform in the new basis via a transformation

$$\hat{L}_0 \equiv \Pi L_0 \Pi^{-1} \Gamma_0^{-1} = \begin{pmatrix} \hat{L}_0^P & 0 \\ 0 & \hat{L}_0^S \end{pmatrix},$$

where $\hat{L}_0$ is L_0 transformed to PS space, $\Pi^{-1} = \begin{pmatrix} \partial_1 & -\partial_2 \\ \partial_2 & \partial_1 \end{pmatrix} \nabla^{-2}$ is the inverse matrix of Π, $\hat{L}_0^P = \omega^2/\alpha_0^2 + \nabla^2$, $\hat{L}_0^S = \omega^2/\beta_0^2 + \nabla^2$, and

$$\mathbf{F} = \Pi \mathbf{f} = \begin{pmatrix} F^P \\ F^S \end{pmatrix}. \tag{4.17}$$

Then, in PS domain, Eq. (4.2) becomes,

$$\begin{pmatrix} \hat{L}_0^P & 0 \\ 0 & \hat{L}_0^S \end{pmatrix} \begin{pmatrix} \phi^P \\ \phi^S \end{pmatrix} = \begin{pmatrix} F^P \\ F^S \end{pmatrix}. \tag{4.18}$$

Since $G_0 \equiv L_0^{-1}$, let $\hat{G}_0^P = \left(\hat{L}_0^P\right)^{-1}$ and $\hat{G}_0^S = \left(\hat{L}_0^S\right)^{-1}$, then the displacement G_0 in PS domain becomes

$$\hat{G}_0 = \Gamma_0 \Pi G_0 \Pi^{-1} = \begin{pmatrix} \hat{G}_0^P & 0 \\ 0 & \hat{G}_0^S \end{pmatrix}. \tag{4.19}$$

So, in the reference medium, after transforming from the displacement domain to PS domain, both L_0 and G_0 become diagonal.

Multiplying Eq. (4.5) from the left by the operator $\Gamma_0 \Pi$ and from the right by the operator Π^{-1}, and using Eq. (4.19),

$$\Gamma_0 \Pi G \Pi^{-1} = \hat{G}_0 + \hat{G}_0 \left(\Pi V \Pi^{-1} \Gamma_0^{-1} \right) \Gamma_0 \Pi G \Pi^{-1}$$

$$= \hat{G}_0 + \hat{G}_0 \hat{V} \hat{G}, \tag{4.20}$$

where the displacement Green's operator G is transformed to the PS domain as

$$\hat{G} = \Gamma_0 \Pi G \Pi^{-1} = \begin{pmatrix} \hat{G}^{PP} & \hat{G}^{PS} \\ \hat{G}^{SP} & \hat{G}^{SS} \end{pmatrix}. \tag{4.21}$$

The perturbation V in the PS domain becomes

$$\hat{V} = \Pi V \Pi^{-1} \Gamma_0^{-1} = \begin{pmatrix} \hat{V}^{PP} & \hat{V}^{PS} \\ \hat{V}^{SP} & \hat{V}^{SS} \end{pmatrix}, \tag{4.22}$$

where the left superscripts of the matrix elements represent the type of measurement and the right ones are the source type.

Similarly, applying the PS transformation to the entire inverse series gives

$$\hat{V} = \hat{V}_1 + \hat{V}_2 + \hat{V}_3 + \cdots . \tag{4.23}$$

It follows, from Eqs. (4.20) and (4.23) that

$$\hat{D} = \hat{G}_0 \hat{V}_1 \hat{G}_0, \tag{4.24}$$

$$\hat{G}_0 \hat{V}_2 \hat{G}_0 = -\hat{G}_0 \hat{V}_1 \hat{G}_0 \hat{V}_1 \hat{G}_0, \tag{4.25}$$

$$\vdots$$

where $\hat{D} = \begin{pmatrix} \hat{D}^{PP} & \hat{D}^{PS} \\ \hat{D}^{SP} & \hat{D}^{SS} \end{pmatrix}$ are the data in the PS domain.

In the displacement space we have, for Eq. (4.1),

$$\mathbf{u} = G\mathbf{f}. \tag{4.26}$$

Then, in the PS domain, Eq. (4.26) becomes

$$\mathbf{\Phi} = \hat{G}\mathbf{F}. \tag{4.27}$$

On the measurement surface, we have

$$\hat{G} = \hat{G}_0 + \hat{G}_0 \hat{V}_1 \hat{G}_0. \tag{4.28}$$

Substituting Eq. (4.28) into Eq. (4.27), and rewriting Eq. (4.27) in matrix form:

$$\begin{pmatrix} \phi^P \\ \phi^S \end{pmatrix} = \begin{pmatrix} \hat{G}_0^P & 0 \\ 0 & \hat{G}_0^S \end{pmatrix} \begin{pmatrix} F^P \\ F^S \end{pmatrix} + \begin{pmatrix} \hat{G}_0^P & 0 \\ 0 & \hat{G}_0^S \end{pmatrix} \begin{pmatrix} \hat{V}_1^{PP} & \hat{V}_1^{PS} \\ \hat{V}_1^{SP} & \hat{V}_1^{SS} \end{pmatrix} \begin{pmatrix} \hat{G}_0^P & 0 \\ 0 & \hat{G}_0^S \end{pmatrix} \begin{pmatrix} F^P \\ F^S \end{pmatrix}. \tag{4.29}$$

This can be written as the following two equations

$$\phi^P = \hat{G}_0^P F^P + \hat{G}_0^P \hat{V}_1^{PP} \hat{G}_0^P F^P + \hat{G}_0^P \hat{V}_1^{PS} \hat{G}_0^S F^S, \tag{4.30}$$

$$\phi^S = \hat{G}_0^S F^S + \hat{G}_0^S \hat{V}_1^{SP} \hat{G}_0^P F^P + \hat{G}_0^S \hat{V}_1^{SS} \hat{G}_0^S F^S. \tag{4.31}$$

We can see, from the two equations above, that for homogeneous media, (no perturbation, $\hat{V}_1 = 0$), there are only direct P and S waves and that the two kind of waves are separated. However, for inhomogeneous media, these two kinds of waves will be mixed together. If only the P wave is incident, $F^P = 1$, $F^S = 0$, then the two Eqs. (4.30) and (4.31) above are respectively reduced to

$$\phi^P = \hat{G}_0^P + \hat{G}_0^P \hat{V}_1^{PP} \hat{G}_0^P, \tag{4.32}$$

$$\phi^S = \hat{G}_0^S \hat{V}_1^{SP} \hat{G}_0^P. \tag{4.33}$$

Hence, in this case, there is only the direct P wave $\hat{G}_0^P$, and no direct wave S. But there are two kinds of scattered waves: one is the P-to-P wave $\hat{G}_0^P \hat{V}_1^{PP} \hat{G}_0^P$, and the other is the P-to-S wave $\hat{G}_0^S \hat{V}_1^{SP} \hat{G}_0^P$. For the acoustic case, only the P wave exists, and hence we only have one equation $\phi^P = \hat{G}_0^P + \hat{G}_0^P \hat{V}_1^{PP} \hat{G}_0^P$.

Similarly, if only the S wave is incident, $F^P = 0$, $F^S = 1$, and the two Eqs. (4.30) and (4.31) are, respectively, reduced to

$$\phi^P = \hat{G}_0^P \hat{V}_1^{PS} \hat{G}_0^S, \tag{4.34}$$

$$\phi^S = \hat{G}_0^S + \hat{G}_0^S \hat{V}_1^{SS} \hat{G}_0^S. \tag{4.35}$$

In this case, there is only the direct S wave $\hat{G}_0^S$, and no direct P wave. There are also two kinds of scattered waves: one is the S-to-P wave $\hat{G}_0^P \hat{V}_1^{PS} \hat{G}_0^S$, the other is the S-to-S wave $\hat{G}_0^S \hat{V}_1^{SS} \hat{G}_0^S$.

4.2   Linear inversion of a 1D elastic medium

Writing Eq. (4.24) in matrix form

$$
\begin{pmatrix} \hat{D}^{PP} & \hat{D}^{PS} \\ \hat{D}^{SP} & \hat{D}^{SS} \end{pmatrix} = \begin{pmatrix} \hat{G}_0^P & 0 \\ 0 & \hat{G}_0^S \end{pmatrix} \begin{pmatrix} \hat{V}_1^{PP} & \hat{V}_1^{PS} \\ \hat{V}_1^{SP} & \hat{V}_1^{SS} \end{pmatrix} \begin{pmatrix} \hat{G}_0^P & 0 \\ 0 & \hat{G}_0^S \end{pmatrix},
\tag{4.36}
$$

leads to four equations

$$
\hat{D}^{PP} = \hat{G}_0^P \hat{V}_1^{PP} \hat{G}_0^P,
\tag{4.37}
$$

$$
\hat{D}^{PS} = \hat{G}_0^P \hat{V}_1^{PS} \hat{G}_0^S,
\tag{4.38}
$$

$$
\hat{D}^{SP} = \hat{G}_0^S \hat{V}_1^{SP} \hat{G}_0^P,
\tag{4.39}
$$

$$
\hat{D}^{SS} = \hat{G}_0^S \hat{V}_1^{SS} \hat{G}_0^S.
\tag{4.40}
$$

For $z_s = z_g = 0$, in the $(k_s, z_s; k_g, z_g; \omega)$ domain, we get the following four equations relating the linear components of the three elastic parameters and the four data types:

$$
\widetilde{D}^{PP}(k_g, 0; -k_g, 0; \omega) = -\frac{1}{4}\left(1 - \frac{k_g^2}{\nu_g^2}\right)\widetilde{a}_\rho^{(1)}(-2\nu_g) - \frac{1}{4}\left(1 + \frac{k_g^2}{\nu_g^2}\right)\widetilde{a}_\gamma^{(1)}(-2\nu_g)
$$
$$
+ \frac{2k_g^2\beta_0^2}{(\nu_g^2 + k_g^2)\alpha_0^2}\widetilde{a}_\mu^{(1)}(-2\nu_g),
\tag{4.41}
$$

$$
\widetilde{D}^{PS}(\nu_g, \eta_g) = -\frac{1}{4}\left(\frac{k_g}{\nu_g} + \frac{k_g}{\eta_g}\right)\widetilde{a}_\rho^{(1)}(-\nu_g - \eta_g) - \frac{\beta_0^2}{2\omega^2}k_g(\nu_g + \eta_g)\left(1 - \frac{k_g^2}{\nu_g\eta_g}\right)\widetilde{a}_\mu^{(1)}(-\nu_g - \eta_g),
\tag{4.42}
$$

$$
\widetilde{D}^{SP}(\nu_g, \eta_g) = \frac{1}{4}\left(\frac{k_g}{\nu_g} + \frac{k_g}{\eta_g}\right)\widetilde{a}_\rho^{(1)}(-\nu_g - \eta_g) + \frac{\beta_0^2}{2\omega^2}k_g(\nu_g + \eta_g)\left(1 - \frac{k_g^2}{\nu_g\eta_g}\right)\widetilde{a}_\mu^{(1)}(-\nu_g - \eta_g),
\tag{4.43}
$$

$$\widetilde{D}^{SS}(k_g, \eta_g) = -\frac{1}{4}\left(1 - \frac{k_g^2}{\eta_g^2}\right)\widetilde{a}_\rho^{(1)}(-2\eta_g) - \left[\frac{\eta_g^2 + k_g^2}{4\eta_g^2} - \frac{2k_g^2}{\eta_g^2 + k_g^2}\right]\widetilde{a}_\mu^{(1)}(-2\eta_g), \qquad (4.44)$$

where

$$\nu_g^2 + k_g^2 = \frac{\omega^2}{\alpha_0^2},$$

$$\eta_g^2 + k_g^2 = \frac{\omega^2}{\beta_0^2}.$$

For the P-wave incidence case (see Fig. 4.1), using $k_g^2/\nu_g^2 = \tan^2\theta$ and $k_g^2/(\nu_g^2 + k_g^2) = \sin^2\theta$, where θ is the P-wave incident angle, Eq. (4.41) becomes

$$\widetilde{D}^{PP}(\nu_g, \theta) = -\frac{1}{4}(1 - \tan^2\theta)\widetilde{a}_\rho^{(1)}(-2\nu_g) - \frac{1}{4}(1 + \tan^2\theta)\widetilde{a}_\gamma^{(1)}(-2\nu_g) + \frac{2\beta_0^2\sin^2\theta}{\alpha_0^2}\widetilde{a}_\mu^{(1)}(-2\nu_g).$$

$$(4.45)$$

In this case, when $\beta_0 = \beta_1 = 0$, Eq. (4.45) reduces to the acoustic two parameter case Eq. (3.11) for $z_g = z_s = 0$.

4.3   Direct non-linear inversion of 1D elastic medium

Writing Eq. (4.25) in matrix form:

$$\begin{pmatrix} \hat{G}_0^P & 0 \\ 0 & \hat{G}_0^S \end{pmatrix}\begin{pmatrix} \hat{V}_2^{PP} & \hat{V}_2^{PS} \\ \hat{V}_2^{SP} & \hat{V}_2^{SS} \end{pmatrix}\begin{pmatrix} \hat{G}_0^P & 0 \\ 0 & \hat{G}_0^S \end{pmatrix}$$

$$= -\begin{pmatrix} \hat{G}_0^P & 0 \\ 0 & \hat{G}_0^S \end{pmatrix}\begin{pmatrix} \hat{V}_1^{PP} & \hat{V}_1^{PS} \\ \hat{V}_1^{SP} & \hat{V}_1^{SS} \end{pmatrix}\begin{pmatrix} \hat{G}_0^P & 0 \\ 0 & \hat{G}_0^S \end{pmatrix}\begin{pmatrix} \hat{V}_1^{PP} & \hat{V}_1^{PS} \\ \hat{V}_1^{SP} & \hat{V}_1^{SS} \end{pmatrix}\begin{pmatrix} \hat{G}_0^P & 0 \\ 0 & \hat{G}_0^S \end{pmatrix}, \qquad (4.46)$$

leads to four equations

$$\hat{G}_0^P\hat{V}_2^{PP}\hat{G}_0^P = -\hat{G}_0^P\hat{V}_1^{PP}\hat{G}_0^P\hat{V}_1^{PP}\hat{G}_0^P - \hat{G}_0^P\hat{V}_1^{PS}\hat{G}_0^S\hat{V}_1^{SP}\hat{G}_0^P, \qquad (4.47)$$
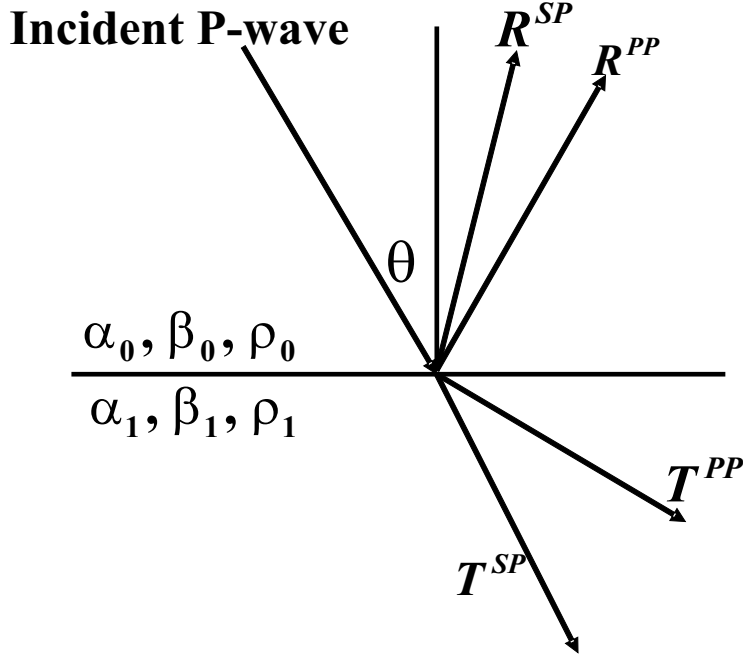
Fig. 4.1: *Response of incident compressional wave on a planar elastic interface. α_0, β_0 and ρ_0 are the compressional wave velocity, shear wave velocity and density of the upper layer, respectively; α_1, β_1 and ρ_1 denote the compressional wave velocity, shear wave velocity and density of the lower layer. R^{PP}, R^{SP}, T^{PP} and T^{SP} denote the coefficients of the reflected compressional wave, the reflected shear wave, the transmitted compressional wave and the transmitted shear wave, respectively. (Foster* et al.*, 1997)*

$$\hat{G}_0^P \hat{V}_2^{PS} \hat{G}_0^S = -\hat{G}_0^P \hat{V}_1^{PP} \hat{G}_0^P \hat{V}_1^{PS} \hat{G}_0^S - \hat{G}_0^P \hat{V}_1^{PS} \hat{G}_0^S \hat{V}_1^{SS} \hat{G}_0^S, \tag{4.48}$$

$$\hat{G}_0^S \hat{V}_2^{SP} \hat{G}_0^P = -\hat{G}_0^S \hat{V}_1^{SP} \hat{G}_0^P \hat{V}_1^{PP} \hat{G}_0^P - \hat{G}_0^S \hat{V}_1^{SS} \hat{G}_0^S \hat{V}_1^{SP} \hat{G}_0^P, \tag{4.49}$$

$$\hat{G}_0^S \hat{V}_2^{SS} \hat{G}_0^S = -\hat{G}_0^S \hat{V}_1^{SP} \hat{G}_0^P \hat{V}_1^{PS} \hat{G}_0^S - \hat{G}_0^S \hat{V}_1^{SS} \hat{G}_0^S \hat{V}_1^{SS} \hat{G}_0^S. \tag{4.50}$$

Since $\hat{V}_1^{PP}$ relates to $\hat{D}^{PP}$, $\hat{V}_1^{PS}$ relates to $\hat{D}^{PS}$, and so on, the four components of the data will be coupled in the non-linear elastic inversion. We cannot perform the direct non-linear inversion without knowing all components of the data. As shown in Chapter 3 and this chapter, when the work on the two parameter acoustic case is extended to the present three parameter elastic case, it is not just simply adding one more parameter, but there are more issues involved. Even for the linear case, the linear solutions found in (4.41) $\sim$ (4.44) are

much more complicated than those of the acoustic case. For instance, four different sets of linear parameter estimates are produced from each component of the data. Also, generally four distinct reflector mislocations arise from the two reference velocities (P-wave velocity and S-wave velocity).

However, in some situations like the towed streamer case, we do not have all components of data available. A particular non-linear approach to be presented in the next section, has been chosen to side-step a portion of this complexity and address our typical lack of four components of elastic data: using $\hat{D}^{PP}$ as the fundamental data input, and perform a reduced form of non-linear elastic inversion, concurrently asking: what beyond-linear value does this simpler framework add? We will see from the numerical tests presented in the following section.

4.3.1 Only using $\hat{D}^{PP}$ — a particular non-linear approach and the numerical tests

When assuming only $\hat{D}^{PP}$ are available, first, we compute the linear solution for $a_\rho^{(1)}$, $a_\gamma^{(1)}$ and $a_\mu^{(1)}$ from Eq. (4.41). Then, substituting the solution into the other three equations (4.42), (4.43) and (4.44), we synthesize the other components of data — $\hat{D}^{PS}$, $\hat{D}^{SP}$ and $\hat{D}^{SS}$. Finally, using the given $\hat{D}^{PP}$ and the synthesized data, we perform the non-linear elastic inversion, getting the following second order (first term beyond linear) elastic inversion solution from Eq. (4.47),

$$
\left(1 - \tan^2\theta\right) a_\rho^{(2)}(z) + \left(1 + \tan^2\theta\right) a_\gamma^{(2)}(z) - 8b^2 \sin^2\theta a_\mu^{(2)}(z)
$$

$$
= -\frac{1}{2}\left(\tan^4\theta - 1\right)\left[a_\gamma^{(1)}(z)\right]^2 + \frac{\tan^2\theta}{\cos^2\theta} a_\gamma^{(1)}(z) a_\rho^{(1)}(z)
$$

$$
+ \frac{1}{2}\left[\left(1 - \tan^4\theta\right) - \frac{2}{C+1}\left(\frac{1}{C}\right)\left(\frac{\alpha_0^2}{\beta_0^2} - 1\right)\frac{\tan^2\theta}{\cos^2\theta}\right]\left[a_\rho^{(1)}(z)\right]^2
$$

$$
- 4b^2\left[\tan^2\theta - \frac{2}{C+1}\left(\frac{1}{2C}\right)\left(\frac{\alpha_0^2}{\beta_0^2} - 1\right)\tan^4\theta\right] a_\rho^{(1)}(z) a_\mu^{(1)}(z)
$$

$$
+ 2b^4\left(\tan^2\theta - \frac{\alpha_0^2}{\beta_0^2}\right)\left[2\sin^2\theta - \frac{2}{C+1}\frac{1}{C}\left(\frac{\alpha_0^2}{\beta_0^2} - 1\right)\tan^2\theta\right]\left[a_\mu^{(1)}(z)\right]^2
$$

$$-\frac{1}{2}\left(\frac{1}{\cos^4\theta}\right)a_\gamma^{(1)\prime}(z)\int_0^z dz'\left[a_\gamma^{(1)}(z')-a_\rho^{(1)}(z')\right]$$

$$-\frac{1}{2}\left(1-\tan^4\theta\right)a_\rho^{(1)\prime}(z)\int_0^z dz'\left[a_\gamma^{(1)}(z')-a_\rho^{(1)}(z')\right]$$

$$+4b^2\tan^2\theta a_\mu^{(1)\prime}(z)\int_0^z dz'\left[a_\gamma^{(1)}(z')-a_\rho^{(1)}(z')\right]$$

$$+\frac{2}{C+1}\frac{1}{C}\left(\frac{\alpha_0^2}{\beta_0^2}-1\right)\tan^2\theta\left(\tan^2\theta-C\right)b^2\int_0^z dz'a_{\mu\ z}^{(1)}\left(\frac{(C-1)z'+2z}{(C+1)}\right)a_\rho^{(1)}(z')$$

$$-\frac{2}{C+1}\frac{2}{C}\left(\frac{\alpha_0^2}{\beta_0^2}-1\right)\tan^2\theta\left(\tan^2\theta-\frac{\alpha_0^2}{\beta_0^2}\right)b^4\int_0^z dz'a_{\mu\ z}^{(1)}\left(\frac{(C-1)z'+2z}{(C+1)}\right)a_\mu^{(1)}(z')$$

$$+\frac{2}{C+1}\frac{1}{C}\left(\frac{\alpha_0^2}{\beta_0^2}-1\right)\tan^2\theta\left(\tan^2\theta+C\right)b^2\int_0^z dz'a_\mu^{(1)}(z')a_{\rho\ z}^{(1)}\left(\frac{(C-1)z'+2z}{(C+1)}\right)$$

$$-\frac{2}{C+1}\frac{1}{2C}\left(\frac{\alpha_0^2}{\beta_0^2}-1\right)\tan^2\theta\left(\tan^2\theta+1\right)\int_0^z dz'a_\rho^{(1)}(z')a_{\rho\ z}^{(1)}\left(\frac{(C-1)z'+2z}{(C+1)}\right),$$

$$(4.51)$$

where $a_{\rho\ z}^{(1)}\left(\frac{(C-1)z'+2z}{(C+1)}\right)=d\left[a_\rho^{(1)}\left(\frac{(C-1)z'+2z}{(C+1)}\right)\right]/dz$, $b=\frac{\beta_0}{\alpha_0}$ and $C=\frac{\eta_g}{\nu_g}=\frac{\sqrt{1-b^2\sin^2\theta}}{b\sqrt{1-\sin^2\theta}}$.

The first five terms on the right side of Eq. (4.51) are inversion terms; i.e., they contribute to parameter predictions. The other terms on the right side of the equation are imaging terms. The arguments for the remarks above are the same as in the acoustic case in Chapter 2. For one interface model, there is no imaging task. The only task is inversion. In this case, all of the integration terms on the right side of Eq. (4.51) are zero, and only the first five terms can be non-zero. Thus, we conclude that the integration terms (which care about duration) are imaging terms, and the first five terms are inversion terms. Both the inversion and imaging terms (especially the imaging terms) become much more complicated after the extension of acoustic case (Chapter 2 and 3) to elastic case. The integrand of the first three integral terms is the first order approximation of the relative change in P-wave velocity. The derivatives $a_\gamma^{(1)\prime}$, $a_\rho^{(1)\prime}$ and $a_\mu^{(1)\prime}$ in front of those integrals are acting to correct the wrong locations caused by the inaccurate reference P-wave velocity. The other four terms with integrals will be zero as $\beta_0\to0$ since in this case $C\to\infty$.

In the following, we test this approach numerically.

For a single interface 1D elastic medium case, as shown in Fig. 4.1, the reflection coefficient R^{PP} has the following form (Foster *et al.*, 1997; Appendix B)

$$R^{PP} = \frac{N}{D},$$ (4.52)

where

$$\begin{aligned}
N = &-(1+2kx^2)^2 b\sqrt{1-c^2x^2}\sqrt{1-d^2x^2} - (1-a+2kx^2)^2 bcdx^2 \\
&+(a-2kx^2)^2 cd\sqrt{1-x^2}\sqrt{1-b^2x^2} \\
&+4k^2x^2\sqrt{1-x^2}\sqrt{1-b^2x^2}\sqrt{1-c^2x^2}\sqrt{1-d^2x^2} - ad\sqrt{1-b^2x^2}\sqrt{1-c^2x^2} \\
&+abc\sqrt{1-x^2}\sqrt{1-d^2x^2},
\end{aligned}$$ (4.53)

$$\begin{aligned}
D = &(1+2kx^2)^2 b\sqrt{1-c^2x^2}\sqrt{1-d^2x^2} + (1-a+2kx^2)^2 bcdx^2 \\
&+(a-2kx^2)^2 cd\sqrt{1-x^2}\sqrt{1-b^2x^2} \\
&+4k^2x^2\sqrt{1-x^2}\sqrt{1-b^2x^2}\sqrt{1-c^2x^2}\sqrt{1-d^2x^2} + ad\sqrt{1-b^2x^2}\sqrt{1-c^2x^2} \\
&+abc\sqrt{1-x^2}\sqrt{1-d^2x^2},
\end{aligned}$$ (4.54)

where $a = \rho_1/\rho_0$, $b = \beta_0/\alpha_0$, $c = \alpha_1/\alpha_0$, $d = \beta_1/\alpha_0$, $k = ad^2 - b^2$ and $x = \sin\theta$, and the subscripts "0" and "1" denote the reference medium and actual medium respectively. Similar to the acoustic case, using the analytic data (Clayton and Stolt, 1981; Weglein *et al.*, 1986)

$$\widetilde{D}^{PP}(\nu_g, \theta) = R^{PP}(\theta)\frac{e^{2i\nu_g a}}{4\pi i\nu_g},$$ (4.55)

where a is the depth of the interface. Substituting Eq.(4.55) into Eq.(4.45), Fourier transforming Eq.(4.45) over $2\nu_g$, and fixing $z > a$ and θ, we have

$$(1-\tan^2\theta)a_\rho^{(1)}(z) + (1+\tan^2\theta)a_\gamma^{(1)}(z) - 8\frac{\beta_0^2}{\alpha_0^2}\sin^2\theta a_\mu^{(1)}(z) = 4R^{PP}(\theta)H(z-a).$$ (4.56)

In this section, we numerically test the direct inversion approach on the following four models:

Model 1: shale (0.20 porosity) over oil sand (0.10 porosity). $\rho_0 = 2.32 g/cm^3$, $\rho_1 = 2.46 g/cm^3$; $\alpha_0 = 2627 m/s$, $\alpha_1 = 4423 m/s$; $\beta_0 = 1245 m/s$, $\beta_1 = 2939 m/s$.

Model 2: shale over oil sand, 0.20 porosity. $\rho_0 = 2.32 g/cm^3$, $\rho_1 = 2.27 g/cm^3$; $\alpha_0 = 2627 m/s$, $\alpha_1 = 3251 m/s$; $\beta_0 = 1245 m/s$, $\beta_1 = 2138 m/s$.

Model 3: shale (0.20 porosity) over oil sand (0.30 porosity). $\rho_0 = 2.32 g/cm^3$, $\rho_1 = 2.08 g/cm^3$; $\alpha_0 = 2627 m/s$, $\alpha_1 = 2330 m/s$; $\beta_0 = 1245 m/s$, $\beta_1 = 1488 m/s$.

Model 4: oil sand over wet sand, 0.20 porosity. $\rho_0 = 2.27 g/cm^3$, $\rho_1 = 2.32 g/cm^3$; $\alpha_0 = 3251 m/s$, $\alpha_1 = 3507 m/s$; $\beta_0 = 2138 m/s$, $\beta_1 = 2116 m/s$.

To test and compare methods, the top of sand reflection was modeled for oil sands with porosities of 10, 20, and 30%. The three models used the same shale overburden. An oil/water contact model was also constructed for the 20% porosity sand.

The low porosity model (10%) represents a deep, consolidated reservoir sand. Pore fluids have little effect on the seismic response of the reservoir sand. It is difficult to distinguish oil sands from brine sands on the basis of seismic response. Impedance of the sand is higher than impedance of the shale.

The moderate porosity model (20%) represents deeper, compacted reservoirs. Pore fluids have a large impact on seismic response, but the fluid effect is less than that of the high porosity case. The overlying shale has high density compared to the reservoir sand, but the P-wave velocity of the oil sand exceeds that of the shale. As a result, impedance contrast is reduced, and shear wave information becomes more important for detecting the reservoir.

The high porosity model (30%) is typical of a weakly consolidated, shallow reservoir sand. Pore fluids have a large impact on the seismic response. Density, P-wave velocity, and the α/β ratio of the oil sand are lower than the density, P-wave velocity, and α/β ratio of the

overlying shale. Consequently, there is a significant decrease in density and P-wave bulk modulus and an increase in shear modulus at the shale/oil sand interface.

The fourth model denotes an oil/water contact in a 20% porosity sand. At a fluid contact, both density and P-wave velocity increase in going from the oil zone into the wet zone. Because pore fluids have no affect on shear modulus, there is no change in shear modulus.

Using these four models, we can find the corresponding R^{PP} from Eq. (4.52). Then, choosing three different angles θ_1, θ_2 and θ_3, we can get the linear solutions for $a_\rho^{(1)}$, $a_\gamma^{(1)}$ and $a_\mu^{(1)}$ from Eq. (4.56) , and then get the solutions for $a_\rho^{(2)}$, $a_\gamma^{(2)}$ and $a_\mu^{(2)}$ from Eq. (4.51).

There are two plots in each figure. The left ones are the results for the first order, while the right ones are the results for the first order plus the second order. The red lines denote the corresponding actual values. In the figures, we illustrate the results corresponding to different sets of angles θ_1 and θ_2. The third angle θ_3 is fixed at zero.

Fig. 4.2: *Model 1: shale (0.20 porosity) over oil sand (0.10 porosity). $\rho_0 = 2.32 g/cm^3, \rho_1 = 2.46 g/cm^3; \alpha_0 = 2627 m/s, \alpha_1 = 4423 m/s; \beta_0 = 1245 m/s, \beta_1 = 2939 m/s$. For this model, the exact value of a_ρ is 0.06. The linear approximation $a_\rho^{(1)}$ (left) and the sum of linear and first non-linear $a_\rho^{(1)} + a_\rho^{(2)}$ (right).*

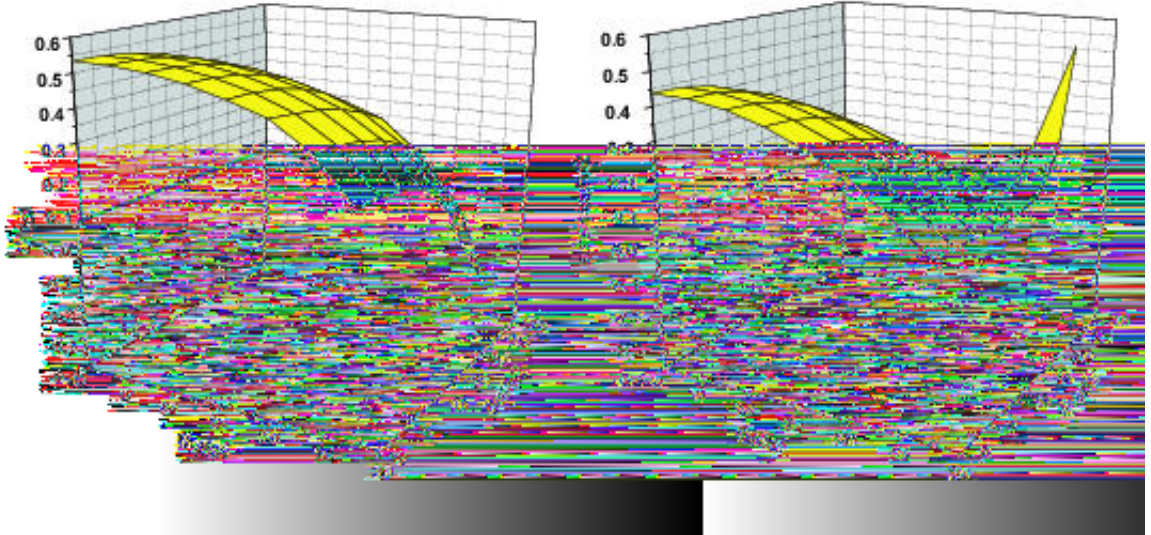The numerical results indicate that all the second order solutions provide improvements
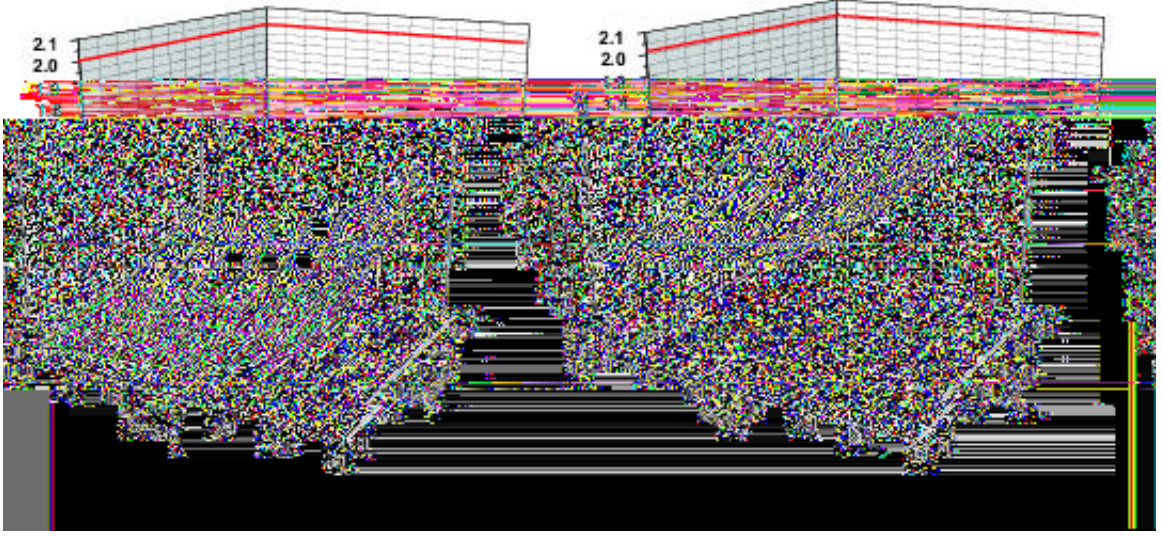
Fig. 4.3: *Model 1: shale (0.20 porosity) over oil sand (0.10 porosity). $\rho_0 = 2.32 g/cm^3, \rho_1 = 2.46 g/cm^3; \alpha_0 = 2627 m/s, \alpha_1 = 4423 m/s; \beta_0 = 1245 m/s, \beta_1 = 2939 m/s$. For this model, the exact value of a_γ is 2.01. The linear approximation $a_\gamma^{(1)}$ (left) and the sum of linear and first non-linear $a_\gamma^{(1)} + a_\gamma^{(2)}$ (right).*

over the linear solutions for all of the four models. When the second term is added to linear order, the results become much closer to the corresponding exact values and the surfaces become flatter in a larger range of angles. But the degrees of those improvements are different for different models. How accurately $\hat{D}^{PP}$ effectively synthesize $\hat{D}^{PS}$ and $\hat{D}^{SP}$ (as shown in Figs. 4.14 $\sim$ 4.17) determined the degree of benefit provided by the non-linear elastic approach. All of the "predicted" values in the figures are predicted using the linear results from $\hat{D}^{PP}$. And the "actual" values are calculated from the Zoeppritz' equations (Appendix B).

In principle, the elastic non-linear direct inversion in 2D requires all four components of data. However, in this section we introduce an approach which requires only $\hat{D}^{PP}$ and approximately synthesizes the other required components. Based on this approach, the first direct non-linear elastic inversion solution is derived. Value-added results are obtained from the non-linear inversion terms beyond linear. Although $\hat{D}^{PP}$ can itself provide useful non-linear direct inversion results, the implication of this research is that further value would

66

Fig. 4.4: *Model 1: shale (0.20 porosity) over oil sand (0.10 porosity). $\rho_0 = 2.32 g/cm^3, \rho_1 = 2.46 g/cm^3; \alpha_0 = 2627 m/s, \alpha_1 = 4423 m/s; \beta_0 = 1245 m/s, \beta_1 = 2939 m/s$. For this model, the exact value of a_μ is 4.91. The linear approximation $a_\mu^{(1)}$ (left) and the sum of linear and first non-linear $a_\mu^{(1)} + a_\mu^{(2)}$ (right).*

derive from actually measuring $\hat{D}^{PP}$, $\hat{D}^{PS}$, $\hat{D}^{SP}$ and $\hat{D}^{SS}$, as the method requires. In the following section, we give a consistent method and solve all of the second order Eqs. (4.47), (4.48), (4.49) and (4.50) with all four components of data available.

Fig. 4.5: *Model 2: shale over oil sand, 0.20 porosity.* $\rho_0 = 2.32g/cm^3, \rho_1 = 2.27g/cm^3; \alpha_0 = 2627m/s, \alpha_1 = 3251m/s; \beta_0 = 1245m/s, \beta_1 = 2138m/s$. *For this model, the exact value of a_ρ is -0.022. The linear approximation $a_\rho^{(1)}$ (left) and the sum of linear and first non-linear $a_\rho^{(1)} + a_\rho^{(2)}$ (right).*
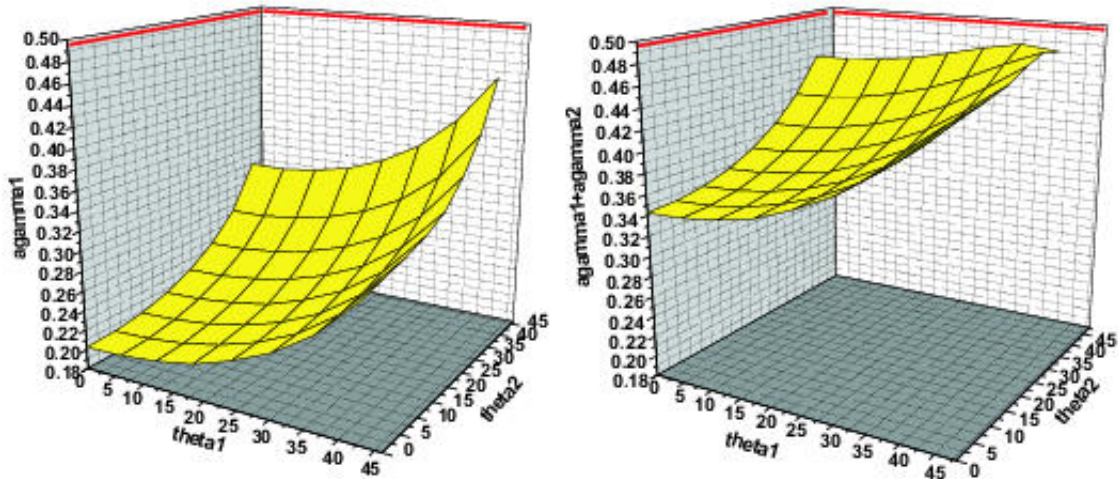
Fig. 4.6: *Model 2: shale over oil sand, 0.20 porosity.* $\rho_0 = 2.32g/cm^3, \rho_1 = 2.27g/cm^3; \alpha_0 = 2627m/s, \alpha_1 = 3251m/s; \beta_0 = 1245m/s, \beta_1 = 2138m/s$. *For this model, the exact value of a_γ is 0.498. The linear approximation $a_\gamma^{(1)}$ (left) and the sum of linear and first non-linear $a_\gamma^{(1)} + a_\gamma^{(2)}$ (right).*
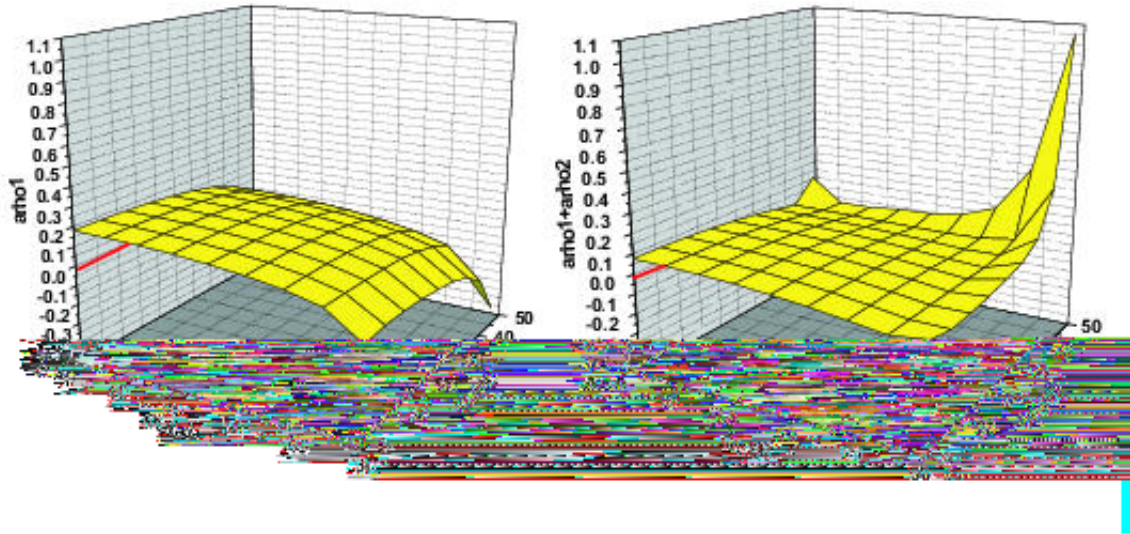
Fig. 4.7: *Model 2: shale over oil sand, 0.20 porosity.* $\rho_0 = 2.32g/cm^3, \rho_1 = 2.27g/cm^3; \alpha_0 = 2627m/s, \alpha_1 = 3251m/s; \beta_0 = 1245m/s, \beta_1 = 2138m/s$. *For this model, the exact value of a_μ is 1.89. The linear approximation $a_\mu^{(1)}$ (left) and the sum of linear and first non-linear $a_\mu^{(1)} + a_\mu^{(2)}$ (right).*
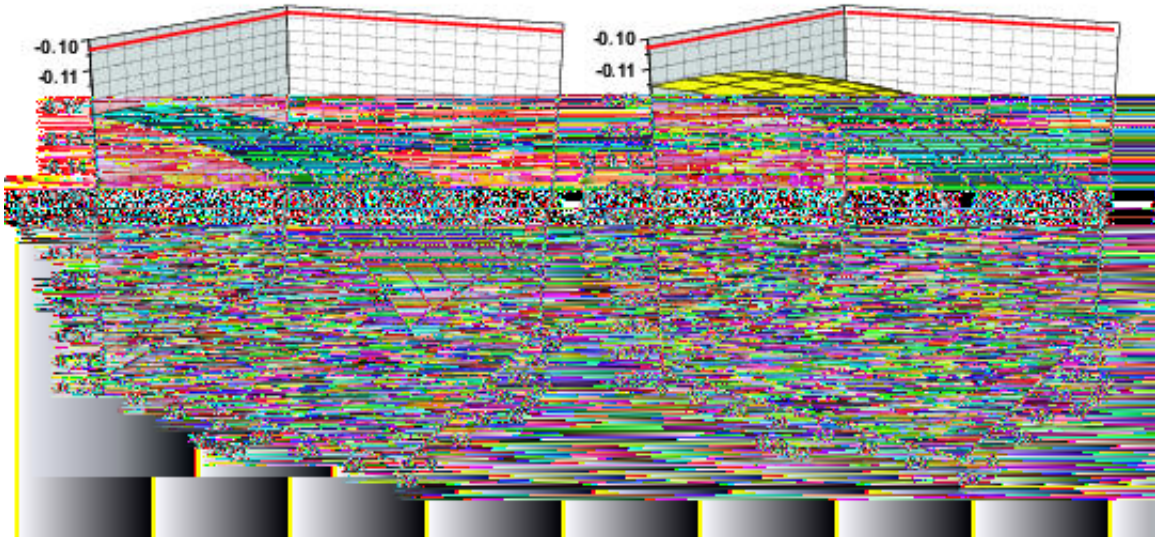
Fig. 4.8: *Model 3: shale (0.20 porosity) over oil sand (0.30 porosity).* $\rho_0 = 2.32g/cm^3, \rho_1 = 2.08g/cm^3; \alpha_0 = 2627m/s, \alpha_1 = 2330m/s; \beta_0 = 1245m/s, \beta_1 = 1488m/s$. *For this model, the exact value of a_ρ is -0.103. The linear approximation $a_\rho^{(1)}$ (left) and the sum of linear and first non-linear $a_\rho^{(1)} + a_\rho^{(2)}$ (right).*
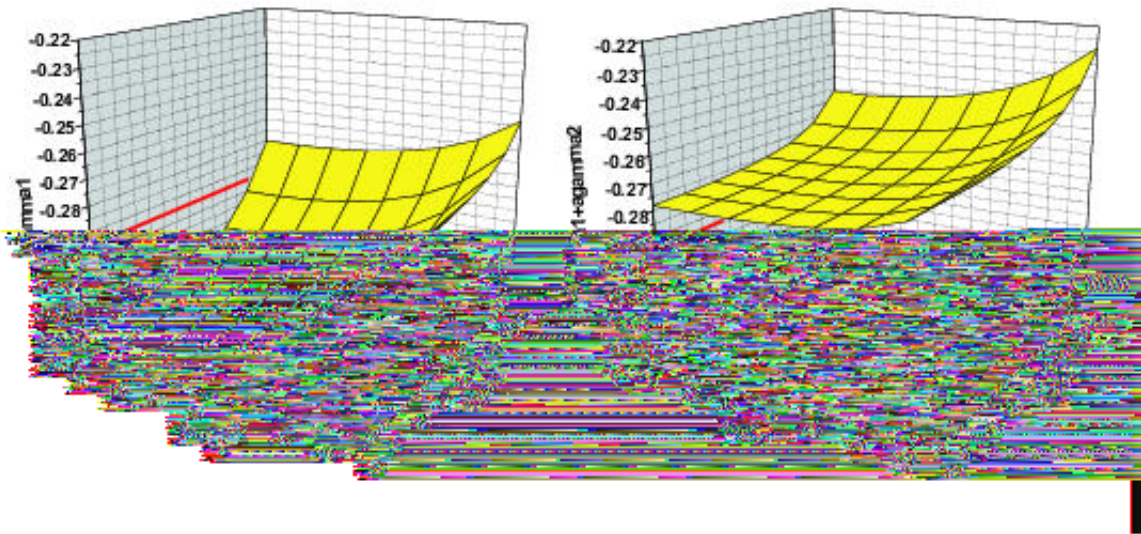
Fig. 4.9: *Model 3: shale (0.20 porosity) over oil sand (0.30 porosity). $\rho_0 = 2.32g/cm^3, \rho_1 = 2.08g/cm^3; \alpha_0 = 2627m/s, \alpha_1 = 2330m/s; \beta_0 = 1245m/s, \beta_1 = 1488m/s$. For this model, the exact value of a_γ is -0.295. The linear approximation $a_\gamma^{(1)}$ (left) and the sum of linear and first non-linear $a_\gamma^{(1)} + a_\gamma^{(2)}$ (right).*
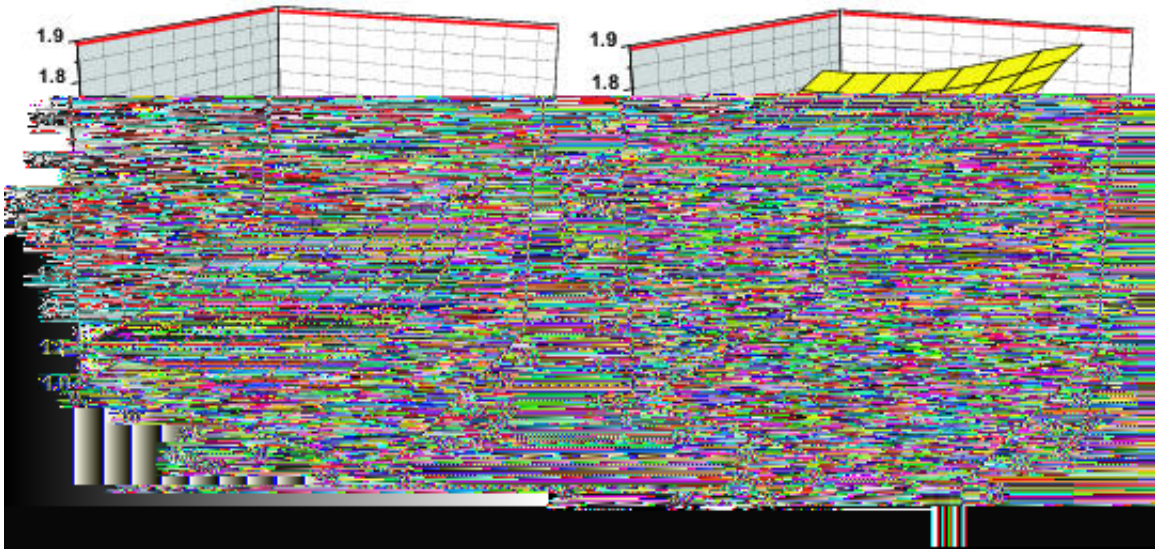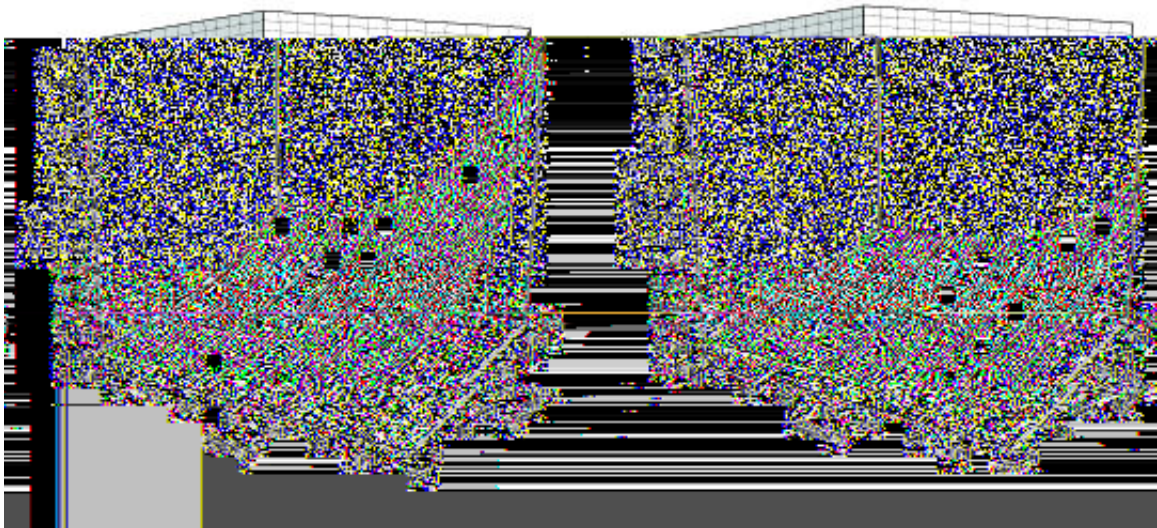

Fig. 4.10: *Model 3: shale (0.20 porosity) over oil sand (0.30 porosity). $\rho_0 = 2.32g/cm^3, \rho_1 = 2.08g/cm^3; \alpha_0 = 2627m/s, \alpha_1 = 2330m/s; \beta_0 = 1245m/s, \beta_1 = 1488m/s$. For this model, the exact value of a_μ is 0.281. The linear approximation $a_\mu^{(1)}$ (left) and the sum of linear and first non-linear $a_\mu^{(1)} + a_\mu^{(2)}$ (right).*
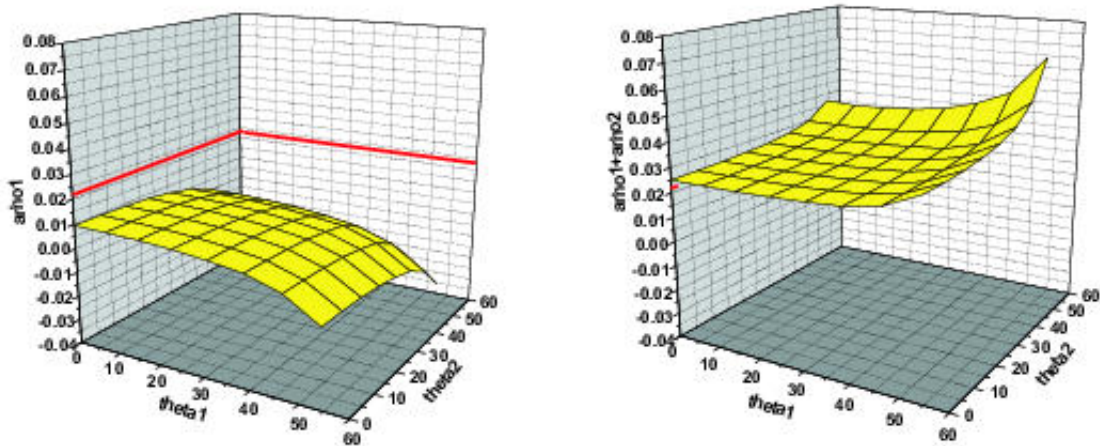
Fig. 4.11: *Model 4: oil sand over wet sand, 0.20 porosity. $\rho_0 = 2.27g/cm^3, \rho_1 = 2.32g/cm^3; \alpha_0 = 3251m/s, \alpha_1 = 3507m/s; \beta_0 = 2138m/s, \beta_1 = 2116m/s$. For this model, the exact value of a_ρ is 0.022. The linear approximation $a_\rho^{(1)}$ (left) and the sum of linear and first non-linear $a_\rho^{(1)} + a_\rho^{(2)}$ (right).*
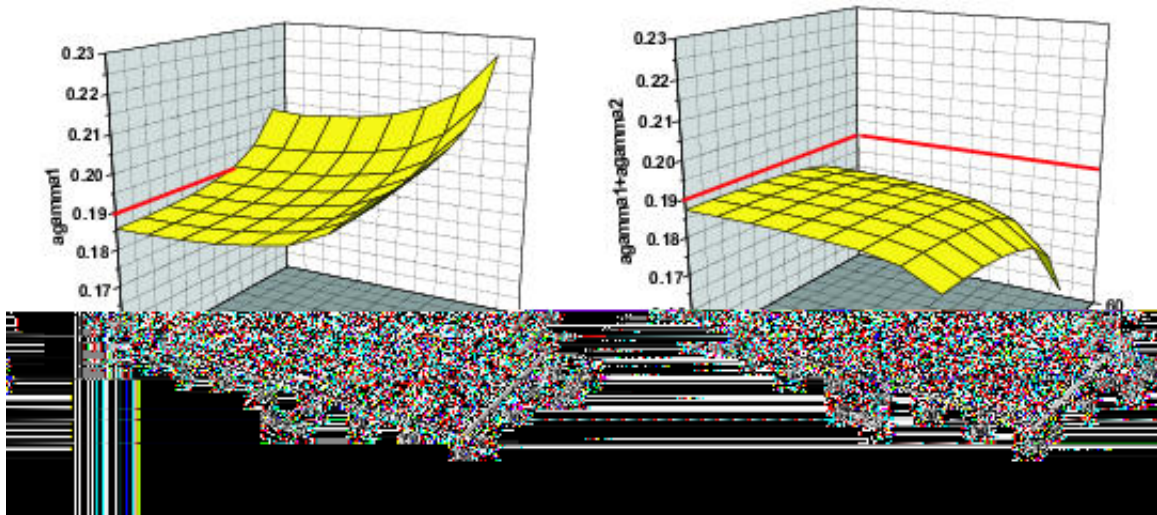
Fig. 4.12: *Model 4: oil sand over wet sand, 0.20 porosity. $\rho_0 = 2.27g/cm^3, \rho_1 = 2.32g/cm^3; \alpha_0 = 3251m/s, \alpha_1 = 3507m/s; \beta_0 = 2138m/s, \beta_1 = 2116m/s$. For this model, the exact value of a_γ is 0.19. The linear approximation $a_\gamma^{(1)}$ (left) and the sum of linear and first non-linear $a_\gamma^{(1)} + a_\gamma^{(2)}$ (right).*

71

Fig. 4.13: *Model 4: oil sand over wet sand, 0.20 porosity. $\rho_0 = 2.27g/cm^3, \rho_1 = 2.32g/cm^3; \alpha_0 = 3251m/s, \alpha_1 = 3507m/s; \beta_0 = 2138m/s, \beta_1 = 2116m/s$. For this model, the exact value of a_μ is 0.001. The linear approximation $a_\mu^{(1)}$ (left) and the sum of linear and first non-linear $a_\mu^{(1)} + a_\mu^{(2)}$ (right).*

Fig. 4.14: *The comparison between the synthesized values and the actual values of Rsp (top) and Rps (bottom) for Model 1: shale (0.20 porosity) over oil sand (0.10 porosity). $\rho_0 = 2.32g/cm^3, \rho_1 = 2.46g/cm^3; \alpha_0 = 2627m/s, \alpha_1 = 4423m/s; \beta_0 = 1245m/s, \beta_1 = 2939m/s.*

Fig. 4.15: *The comparison between the synthesized values and the actual values of Rsp (top) and Rps (bottom) for Model 2: shale over oil sand, 0.20 porosity. $\rho_0 = 2.32g/cm^3, \rho_1 = 2.27g/cm^3; \alpha_0 = 2627m/s, \alpha_1 = 3251m/s; \beta_0 = 1245m/s, \beta_1 = 2138m/s$.*
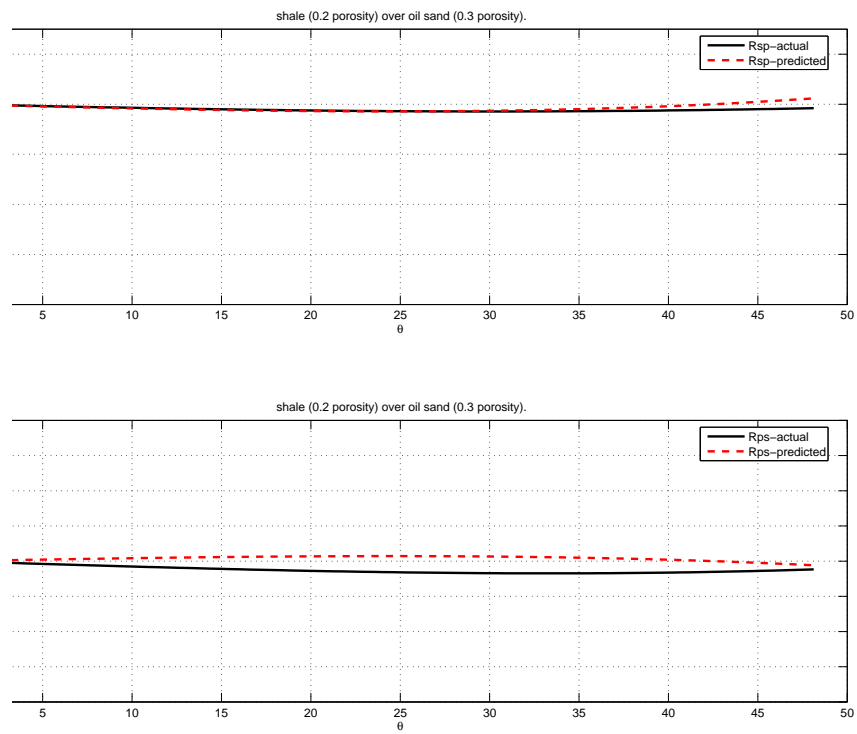
Fig. 4.16: *The comparison between the synthesized values and the actual values of Rsp (top) and Rps (bottom) for Model 3: shale (0.20 porosity) over oil sand (0.30 porosity).* $\rho_0 = 2.32 g/cm^3, \rho_1 = 2.08 g/cm^3; \alpha_0 = 2627 m/s, \alpha_1 = 2330 m/s; \beta_0 = 1245 m/s, \beta_1 = 1488 m/s.$

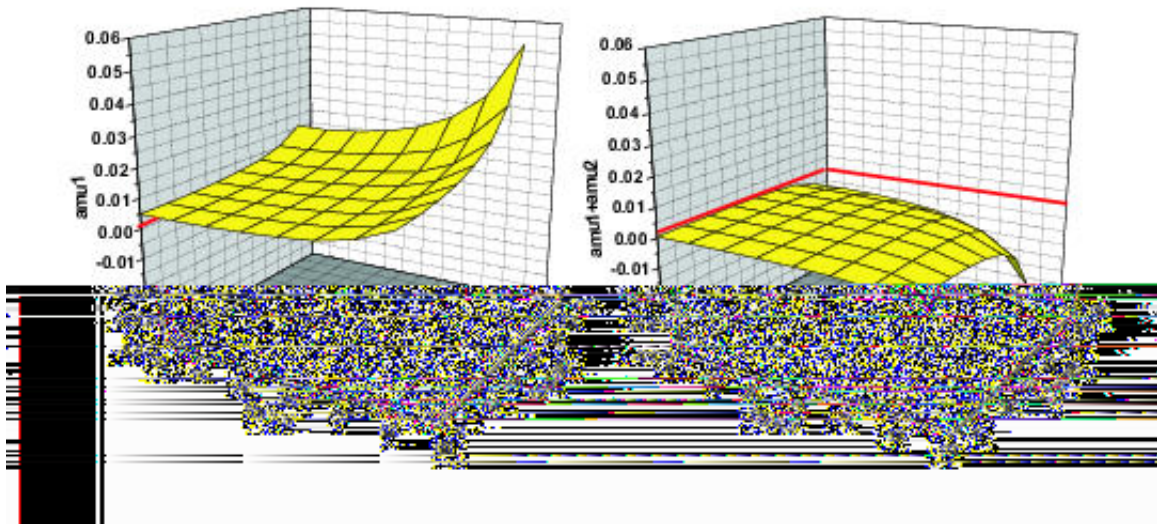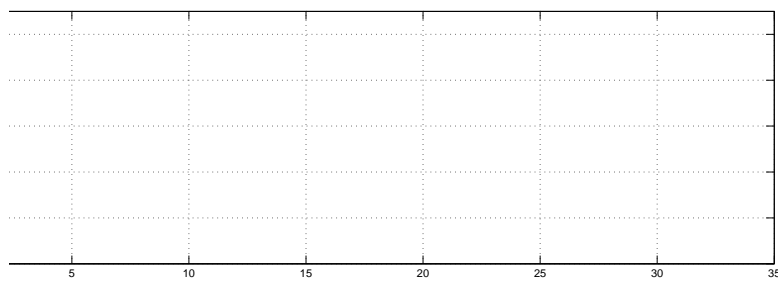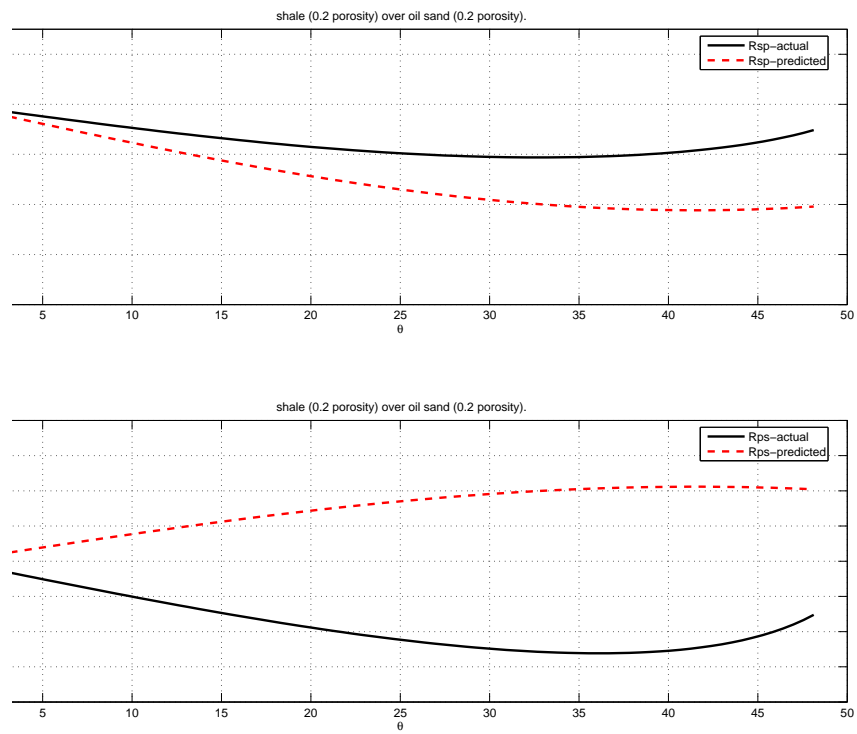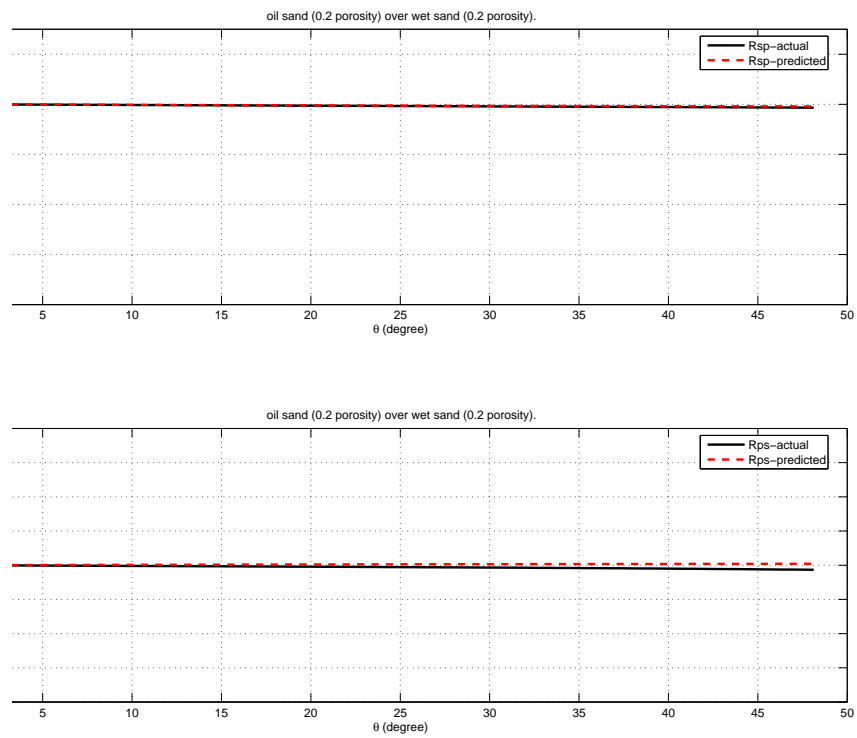Fig. 4.17: *The comparison between the synthesized values and the actual values of Rsp (top) and Rps (bottom) for Model 4: oil sand over wet sand, 0.20 porosity.* $\rho_0 = 2.27g/cm^3, \rho_1 = 2.32g/cm^3; \alpha_0 = 3251m/s, \alpha_1 = 3507m/s; \beta_0 = 2138m/s, \beta_1 = 2116m/s.$

4.3.2 Using all four components of data — full direct non-linear elastic inversion

Using four components of data, one consistent method to solve for the second terms is, first, using the linear solutions as shown in Eqs. (4.41), (4.42), (4.43) and (4.44), we can get the linear solution for $a_\rho^{(1)}$, $a_\gamma^{(1)}$ and $a_\mu^{(1)}$ in terms of $\hat{D}^{PP}, \hat{D}^{PS}, \hat{D}^{SP}$ and $\hat{D}^{SS}$ through the following way

$$\begin{pmatrix} a_\rho^{(1)} \\ a_\gamma^{(1)} \\ a_\mu^{(1)} \end{pmatrix} = (O^T O)^{-1} O^T \begin{pmatrix} \hat{D}^{PP} \\ \hat{D}^{PS} \\ \hat{D}^{SP} \\ \hat{D}^{SS} \end{pmatrix}, \tag{4.57}$$

where the matrix O is

$$\begin{pmatrix} -\frac{1}{4}\left(1 - \frac{k_g^{PP2}}{\nu_g^{PP2}}\right) & -\frac{1}{4}\left(1 + \frac{k_g^{PP2}}{\nu_g^{PP2}}\right) & \frac{2\beta_0^2 k_g^{PP2}}{\alpha_0^2\left(\nu_g^{PP2}+k_g^{PP2}\right)} \\ -\frac{1}{4}\left(\frac{k_g^{PS}}{\nu_g^{PS}} + \frac{k_g^{PS}}{\eta_g^{PS}}\right) & 0 & -\frac{\beta_0^2}{2\omega^2}k_g^{PS}\left(\nu_g^{PS} + \eta_g^{PS}\right)\left(1 - \frac{k_g^{PS2}}{\nu_g^{PS}\eta_g^{PS}}\right) \\ \frac{1}{4}\left(\frac{k_g^{SP}}{\nu_g^{SP}} + \frac{k_g^{SP}}{\eta_g^{SP}}\right) & 0 & \frac{\beta_0^2}{2\omega^2}k_g^{SP}\left(\nu_g^{SP} + \eta_g^{SP}\right)\left(1 - \frac{k_g^{SP2}}{\nu_g^{SP}\eta_g^{SP}}\right) \\ -\frac{1}{4}\left(1 - \frac{k_g^{SS2}}{\eta_g^{SS2}}\right) & 0 & -\left[\frac{k_g^{SS2}+\eta_g^{SS2}}{4\eta_g^{SS2}} - \frac{2k_g^{SS2}}{k_g^{SS2}+\eta_g^{SS2}}\right] \end{pmatrix}, \tag{4.58}$$

and O^T is the transpose of matrix O, the superscript -1 denotes the inverse of the matrix $O^T O$.

Let the arguments of $a_\rho^{(1)}$ and $a_\mu^{(1)}$ in Eqs. (4.41), (4.42), (4.43) and (4.44) equal, we need

$$-2\nu_g^{PP} = -\nu_g^{PS} - \eta_g^{PS} = -\nu_g^{SP} - \eta_g^{SP} = -2\eta_g^{SS},$$

which leads to (please see details in Appendix B)

$$2\frac{\omega}{\alpha_0}\cos\theta^{PP} = \frac{\omega}{\alpha_0}\sqrt{1 - \frac{\alpha_0^2}{\beta_0^2}\sin^2\theta^{PS}} + \frac{\omega}{\beta_0}\cos\theta^{PS} = \frac{\omega}{\alpha_0}\cos\theta^{SP} + \frac{\omega}{\beta_0}\sqrt{1 - \frac{\beta_0^2}{\alpha_0^2}\sin^2\theta^{SP}}$$

$$= 2\frac{\omega}{\beta_0}\cos\theta^{SS}.$$

From the expression above, given θ^{PP}, as shown in Fig. 4.18, we can find the corresponding angles θ^{PS}, θ^{SP} and θ^{SS} which appear in matrix O

$$\theta^{PS} = \cos^{-1}\left[\frac{4b^2\cos^2\theta^{PP} + 1 - b^2}{4b\cos\theta^{PP}}\right],$$

$$\theta^{SP} = \cos^{-1}\left[\frac{4b^2\cos^2\theta^{PP} - 1 + b^2}{4b^2\cos\theta^{PP}}\right],$$

$$\theta^{SS} = \cos^{-1}\left(b\cos\theta^{PP}\right),$$

where $b = \frac{\beta_0}{\alpha_0}$.

Fig. 4.18: *Different incident angles.*

Then, through the similar way, we can get the solution for $a_\rho^{(2)}$, $a_\gamma^{(2)}$ and $a_\mu^{(2)}$ in terms of $a_\rho^{(1)}$, $a_\gamma^{(1)}$ and $a_\mu^{(1)}$
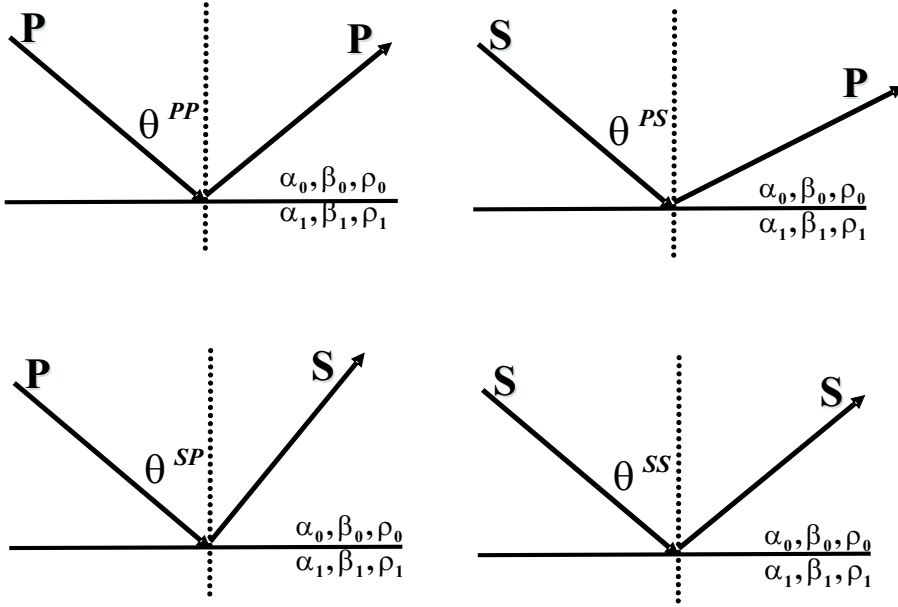
$$\begin{pmatrix} a_\rho^{(2)} \\ a_\gamma^{(2)} \\ a_\mu^{(2)} \end{pmatrix} = (O^T O)^{-1} O^T Q, \tag{4.59}$$

where the matrix Q is in terms of $a_\rho^{(1)}$, $a_\gamma^{(1)}$ and $a_\mu^{(1)}$.

Based on this idea, we get the following non-linear solutions for Eqs. (4.47), (4.48), (4.49) and (4.50) respectively.

The form of the solution for Eq. (4.47), i.e.,

$$\hat{G}_0^P \hat{V}_2^{PP} \hat{G}_0^P = -\hat{G}_0^P \hat{V}_1^{PP} \hat{G}_0^P \hat{V}_1^{PP} \hat{G}_0^P - \hat{G}_0^P \hat{V}_1^{PS} \hat{G}_0^S \hat{V}_1^{SP} \hat{G}_0^P,$$

is the same as Eq. (4.51). In the $(k_s, z_s; k_g, z_g; \omega)$ domain, we get the the other three solutions respectively, for Eqs. (4.48), (4.49) and (4.50).

The solution for Eq. (4.48), i.e.,

$$\hat{G}_0^P \hat{V}_2^{PS} \hat{G}_0^S = -\hat{G}_0^P \hat{V}_1^{PP} \hat{G}_0^P \hat{V}_1^{PS} \hat{G}_0^S - \hat{G}_0^P \hat{V}_1^{PS} \hat{G}_0^S \hat{V}_1^{SS} \hat{G}_0^S,$$

is

$$
-\frac{1}{4}\left(\frac{k_g}{\nu_g}+\frac{k_g}{\eta_g}\right)a_\rho^{(2)}(z) - \frac{\beta_0^2}{2\omega^2}k_g\left(\nu_g+\eta_g\right)\left(1-\frac{k_g^2}{\nu_g\eta_g}\right)a_\mu^{(2)}(z)
$$
$$
= -\left[\left(\frac{1}{2}+\frac{1}{C+1}\right)\frac{1}{\eta_g\nu_g^2}\left(\frac{\beta_0^4}{\alpha_0^4}Ck_g^3 - 3\frac{\beta_0^2}{\alpha_0^2}Ck_g^5\frac{\beta_0^2}{\omega^2} - k_g^3\nu_g^2\frac{\beta_0^2}{\omega^2} + 2k_g^5\nu_g^2\frac{\beta_0^4}{\omega^4} + 2Ck_g^7\frac{\beta_0^4}{\omega^4}\right)\right.
$$
$$
+\left(\frac{1}{2}-\frac{1}{C+1}\right)\frac{1}{\eta_g\nu_g^2}\left(\frac{\beta_0^2}{\alpha_0^2}Ck_g^3\nu_g^2\frac{\beta_0^2}{\omega^2} + 2\frac{\beta_0^2}{\alpha_0^2}k_g^5\frac{\beta_0^2}{\omega^2} - 2Ck_g^5\nu_g^2\frac{\beta_0^4}{\omega^4} - \frac{\beta_0^2}{\alpha_0^2}k_g^3 + k_g^5\frac{\beta_0^2}{\omega^2} - 2k_g^7\frac{\beta_0^4}{\omega^4}\right)
$$
$$
+\left(\frac{1}{2C}+\frac{1}{C+1}\right)\frac{1}{4\eta_g^2\nu_g}\left(6k_g^3 - 12k_g^5\frac{\beta_0^2}{\omega^2} - k_g\frac{\omega^2}{\beta_0^2} + 8k_g^7\frac{\beta_0^4}{\omega^4} + 8C^3\nu_g^2k_g^5\frac{\beta_0^4}{\omega^4}\right.
$$
$$
\left. -4\frac{\beta_0^2}{\alpha_0^2}C^3\nu_g^2k_g^3\frac{\beta_0^2}{\omega^2}\right)
$$
$$
-\left(\frac{1}{2C}-\frac{1}{C+1}\right)\frac{1}{4\eta_g\nu_g^2}\left(4\frac{\beta_0^2}{\alpha_0^2}k_g^3 - 8k_g^5\frac{\beta_0^2}{\omega^2} - k_g\frac{\omega^2}{\alpha_0^2} + 2k_g^3 - 4C\nu_g^2k_g^3\frac{\beta_0^2}{\omega^2} + 8C\nu_g^2k_g^5\frac{\beta_0^4}{\omega^4}\right.
$$
$$
\left.\left. -4\frac{\beta_0^2}{\alpha_0^2}k_g^5\frac{\beta_0^2}{\omega^2} + 8k_g^7\frac{\beta_0^4}{\omega^4}\right) - \frac{\beta_0^2}{\alpha_0^2}\frac{k_g^3}{\nu_g}\frac{\beta_0^2}{\omega^2} + \frac{k_g}{2\eta_g}\left(2k_g^2\frac{\beta_0^2}{\omega^2}-1\right)\right]a_\mu^{(1)}(z)a_\mu^{(1)}(z)
$$
$$
-\left[\left(\frac{1}{2}+\frac{1}{C+1}\right)\frac{k_g}{8\eta_g\nu_g^2}\left(Ck_g^2+\nu_g^2\right) - \left(\frac{1}{2}-\frac{1}{C+1}\right)\frac{k_g}{8\eta_g\nu_g^2}\left(k_g^2+C\nu_g^2\right)\right.
$$
$$
\left. +\left(\frac{1}{2C}+\frac{1}{C+1}\right)\frac{k_g}{8\eta_g^2\nu_g}\left(C^3\nu_g^2+k_g^2\right) - \left(\frac{1}{2C}-\frac{1}{C+1}\right)\frac{k_g}{8\eta_g\nu_g^2}\left(k_g^2+C\nu_g^2\right)\right]a_\rho^{(1)}(z)a_\rho^{(1)}(z)
$$

$$-\left[\left(\frac{1}{2}+\frac{1}{C+1}\right)\frac{\beta_0^2}{\alpha_0^2}\frac{1}{4\nu_g^3}k_g\left(k_g^2-\nu_g^2\right)+\left(\frac{1}{2}-\frac{1}{C+1}\right)\frac{1}{4\eta_g\nu_g^2}\left(k_g\frac{\omega^2}{\alpha_0^2}-2\frac{\beta_0^2}{\alpha_0^2}k_g^3\right)+\frac{\beta_0^2}{\alpha_0^2}\frac{k_g}{2\nu_g}\right]$$

$$\times\, a_\mu^{(1)}(z)a_\gamma^{(1)}(z)$$

$$+\left[\left(\frac{1}{2}+\frac{1}{C+1}\right)\frac{k_g\left(k_g^2+\nu_g^2\right)}{8\nu_g^3}-\left(\frac{1}{2}-\frac{1}{C+1}\right)\frac{k_g\left(k_g^2+\nu_g^2\right)}{8\eta_g\nu_g^2}\right]a_\rho^{(1)}(z)a_\gamma^{(1)}(z)$$

$$-\left[\left(\frac{1}{2}+\frac{1}{C+1}\right)\frac{1}{4\eta_g\nu_g^2}\left(3\frac{\beta_0^2}{\alpha_0^2}Ck_g^3+\nu_g^2k_g-4Ck_g^5\frac{\beta_0^2}{\omega^2}-4k_g^3\nu_g^2\frac{\beta_0^2}{\omega^2}\right)\right.$$

$$-\left(\frac{1}{2}-\frac{1}{C+1}\right)\frac{1}{4\eta_g\nu_g^2}\left(\frac{\beta_0^2}{\alpha_0^2}C\nu_g^2k_g+k_g^3-4k_g^5\frac{\beta_0^2}{\omega^2}-4Ck_g^3\nu_g^2\frac{\beta_0^2}{\omega^2}+2\frac{\beta_0^2}{\alpha_0^2}k_g^3\right)$$

$$+\left(\frac{1}{2C}+\frac{1}{C+1}\right)\frac{1}{4\eta_g^2\nu_g}\left(k_g^3-2k_g^5\frac{\beta_0^2}{\omega^2}+\frac{\beta_0^2}{\alpha_0^2}C^3\nu_g^2k_g-4C^3\nu_g^2k_g^3\frac{\beta_0^2}{\omega^2}-\frac{1}{2}k_g\frac{\omega^2}{\beta_0^2}\right.$$

$$+2C^2\nu_g^2k_g^3\frac{\beta_0^2}{\omega^2}\bigg)$$

$$-\left(\frac{1}{2C}-\frac{1}{C+1}\right)\frac{1}{4\eta_g\nu_g^2}\left(C\nu_g^2k_g-2C\nu_g^2k_g^3\frac{\beta_0^2}{\omega^2}+\frac{\beta_0^2}{\alpha_0^2}k_g^3-2k_g^5\frac{\beta_0^2}{\omega^2}+2C^2\nu_g^2k_g^3\frac{\beta_0^2}{\omega^2}\right.$$

$$\left.\left.-2C\nu_g^2k_g^3\frac{\beta_0^2}{\omega^2}-\frac{1}{2}k_g\frac{\omega^2}{\beta_0^2}\right)\right]\times a_\rho^{(1)}(z)a_\mu^{(1)}(z)$$

$$-\frac{1}{\eta_g\nu_g^2}\left(\frac{\beta_0^4}{\alpha_0^4}Ck_g^3-3\frac{\beta_0^2}{\alpha_0^2}Ck_g^5\frac{\beta_0^2}{\omega^2}-k_g^3\nu_g^2\frac{\beta_0^2}{\omega^2}+2k_g^5\nu_g^2\frac{\beta_0^4}{\omega^4}+2Ck_g^7\frac{\beta_0^4}{\omega^4}\right)$$

$$\times\left[\frac{1}{2}\int_0^z dz'a_\mu^{(1)}{}_z\left(\frac{(C+1)z-(C-1)z'}{2}\right)a_\mu^{(1)}\left(z'\right)+\frac{1}{C+1}a_\mu^{(1)\prime}(z)\int_0^z dz'a_\mu^{(1)}(z')\right]$$

$$-\frac{1}{\eta_g\nu_g^2}\left(\frac{\beta_0^2}{\alpha_0^2}Ck_g^3\nu_g^2\frac{\beta_0^2}{\omega^2}+2\frac{\beta_0^2}{\alpha_0^2}k_g^5\frac{\beta_0^2}{\omega^2}-2Ck_g^5\nu_g^2\frac{\beta_0^4}{\omega^4}-\frac{\beta_0^2}{\alpha_0^2}k_g^3+k_g^5\frac{\beta_0^2}{\omega^2}-2k_g^7\frac{\beta_0^4}{\omega^4}\right)$$

$$\times\left[\frac{1}{2}\int_0^z dz'a_\mu^{(1)}{}_z\left(\frac{(C+1)z-(C-1)z'}{2}\right)a_\mu^{(1)}\left(z'\right)-\frac{1}{C+1}a_\mu^{(1)\prime}(z)\int_0^z dz'a_\mu^{(1)}(z')\right]$$

$$-\frac{1}{4\eta_g^2\nu_g}\left(6k_g^3-12k_g^5\frac{\beta_0^2}{\omega^2}-k_g\frac{\omega^2}{\beta_0^2}+8k_g^7\frac{\beta_0^4}{\omega^4}+8C^3\nu_g^2k_g^5\frac{\beta_0^4}{\omega^4}-4\frac{\beta_0^2}{\alpha_0^2}C^3\nu_g^2k_g^3\frac{\beta_0^2}{\omega^2}\right)$$

$$\times\left[\frac{1}{2C}\int_0^z dz'a_\mu^{(1)}{}_z\left(\frac{(C+1)z+(C-1)z'}{2C}\right)a_\mu^{(1)}\left(z'\right)+\frac{1}{C+1}a_\mu^{(1)\prime}(z)\int_0^z dz'a_\mu^{(1)}(z')\right]$$

$$+\frac{1}{4\eta_g\nu_g^2}\left(4\frac{\beta_0^2}{\alpha_0^2}k_g^3-8k_g^5\frac{\beta_0^2}{\omega^2}-k_g\frac{\omega^2}{\alpha_0^2}+2k_g^3-4C\nu_g^2k_g^3\frac{\beta_0^2}{\omega^2}+8C\nu_g^2k_g^5\frac{\beta_0^4}{\omega^4}-4\frac{\beta_0^2}{\alpha_0^2}k_g^5\frac{\beta_0^2}{\omega^2}+8k_g^7\frac{\beta_0^4}{\omega^4}\right)$$

$$\times\left[\frac{1}{2C}\int_0^z dz'a_\mu^{(1)}{}_z\left(\frac{(C+1)z+(C-1)z'}{2C}\right)a_\mu^{(1)}\left(z'\right)-\frac{1}{C+1}a_\mu^{(1)\prime}(z)\int_0^z dz'a_\mu^{(1)}(z')\right]$$

$$-\frac{k_g\left(Ck_g^2+\nu_g^2\right)}{8\eta_g\nu_g^2}\left[\frac{1}{2}\int_0^z dz'a_\rho^{(1)}{}_z\left(\frac{(C+1)z-(C-1)z'}{2}\right)a_\rho^{(1)}\left(z'\right)\right.$$

$$\left.+\frac{1}{C+1}a_\rho^{(1)\prime}(z)\int_0^z dz'a_\rho^{(1)}(z')\right]$$

$$+ \frac{k_g \left(k_g^2 + C\nu_g^2\right)}{8\eta_g\nu_g^2} \left[\frac{1}{2} \int_0^z dz' a_\rho^{(1)}{}_z \left(\frac{(C+1)z - (C-1)z'}{2}\right) a_\rho^{(1)}(z')\right.$$

$$\left. - \frac{1}{C+1} a_\rho^{(1)'}(z) \int_0^z dz' a_\rho^{(1)}(z')\right]$$

$$- \frac{C^3 k_g \nu_g^2 + k_g^3}{8\eta_g^2\nu_g} \left[\frac{1}{2C} \int_0^z dz' a_\rho^{(1)}{}_z \left(\frac{(C+1)z + (C-1)z'}{2C}\right) a_\rho^{(1)}(z')\right.$$

$$\left. + \frac{1}{C+1} a_\rho^{(1)'}(z) \int_0^z dz' a_\rho^{(1)}(z')\right]$$

$$+ \frac{k_g \left(k_g^2 + C\nu_g^2\right)}{8\eta_g\nu_g^2} \left[\frac{1}{2C} \int_0^z dz' a_\rho^{(1)}{}_z \left(\frac{(C+1)z + (C-1)z'}{2C}\right) a_\rho^{(1)}(z')\right.$$

$$\left. - \frac{1}{C+1} a_\rho^{(1)'}(z) \int_0^z dz' a_\rho^{(1)}(z')\right]$$

$$- \frac{\beta_0^2}{\alpha_0^2} \frac{k_g \left(k_g^2 - \nu_g^2\right)}{4\nu_g^3} \left[\frac{1}{2} \int_0^z dz' a_\gamma^{(1)}{}_z \left(\frac{(C+1)z - (C-1)z'}{2}\right) a_\mu^{(1)}(z')\right.$$

$$\left. + \frac{1}{C+1} a_\mu^{(1)'}(z) \int_0^z dz' a_\gamma^{(1)}(z')\right]$$

$$- \frac{1}{4\eta_g\nu_g^2} \left(k_g \frac{\omega^2}{\alpha_0^2} - 2\frac{\beta_0^2}{\alpha_0^2} k_g^3\right) \left[\frac{1}{2} \int_0^z dz' a_\gamma^{(1)}{}_z \left(\frac{(C+1)z - (C-1)z'}{2}\right) a_\mu^{(1)}(z')\right.$$

$$\left. - \frac{1}{C+1} a_\mu^{(1)'}(z) \int_0^z dz' a_\gamma^{(1)}(z')\right]$$

$$+ \frac{k_g \left(k_g^2 + \nu_g^2\right)}{8\nu_g^3} \left[\frac{1}{2} \int_0^z dz' a_\gamma^{(1)}{}_z \left(\frac{(C+1)z - (C-1)z'}{2}\right) a_\rho^{(1)}(z')\right.$$

$$\left. + \frac{1}{C+1} a_\rho^{(1)'}(z) \int_0^z dz' a_\gamma^{(1)}(z')\right]$$

$$- \frac{k_g \left(k_g^2 + \nu_g^2\right)}{8\eta_g\nu_g^2} \left[\frac{1}{2} \int_0^z dz' a_\gamma^{(1)}{}_z \left(\frac{(C+1)z - (C-1)z'}{2}\right) a_\rho^{(1)}(z')\right.$$

$$\left. - \frac{1}{C+1} a_\rho^{(1)'}(z) \int_0^z dz' a_\gamma^{(1)}(z')\right]$$

$$- \frac{1}{4\eta_g\nu_g^2} \left(\frac{\beta_0^2}{\alpha_0^2} C k_g^3 + \nu_g^2 k_g - 2C k_g^5 \frac{\beta_0^2}{\omega^2} - 2k_g^3 \nu_g^2 \frac{\beta_0^2}{\omega^2}\right)$$

$$\times \left[\frac{1}{2} \int_0^z dz' a_\rho^{(1)}{}_z \left(\frac{(C+1)z - (C-1)z'}{2}\right) a_\mu^{(1)}(z') + \frac{1}{C+1} a_\mu^{(1)'}(z) \int_0^z dz' a_\rho^{(1)}(z')\right]$$

$$- \frac{1}{4\eta_g\nu_g^2} \left(2\frac{\beta_0^2}{\alpha_0^2} C k_g^3 - 2C k_g^5 \frac{\beta_0^2}{\omega^2} - 2k_g^3 \nu_g^2 \frac{\beta_0^2}{\omega^2}\right)$$

$$\times \left[\frac{1}{2} \int_0^z dz' a_\mu^{(1)}{}_z \left(\frac{(C+1)z - (C-1)z'}{2}\right) a_\rho^{(1)}(z') + \frac{1}{C+1} a_\rho^{(1)'}(z) \int_0^z dz' a_\mu^{(1)}(z')\right]$$

$$+ \frac{1}{4\eta_g\nu_g^2} \left(\frac{\beta_0^2}{\alpha_0^2} C \nu_g^2 k_g + k_g^3 - 2k_g^5 \frac{\beta_0^2}{\omega^2} - 2C k_g^3 \nu_g^2 \frac{\beta_0^2}{\omega^2}\right)$$

$$\times \left[\frac{1}{2} \int_0^z dz' a_\rho^{(1)}{}_z \left(\frac{(C+1)z - (C-1)z'}{2} \right) a_\mu^{(1)}(z') - \frac{1}{C+1} a_\mu^{(1)'}(z) \int_0^z dz' a_\rho^{(1)}(z') \right]$$

$$+ \frac{1}{4\eta_g \nu_g^2} \left(2\frac{\beta_0^2}{\alpha_0^2} k_g^3 - 2k_g^5 \frac{\beta_0^2}{\omega^2} - 2C k_g^3 \nu_g^2 \frac{\beta_0^2}{\omega^2} \right)$$

$$\times \left[\frac{1}{2} \int_0^z dz' a_\mu^{(1)}{}_z \left(\frac{(C+1)z - (C-1)z'}{2} \right) a_\rho^{(1)}(z') - \frac{1}{C+1} a_\rho^{(1)'}(z) \int_0^z dz' a_\mu^{(1)}(z') \right]$$

$$- \frac{1}{4\eta_g^2 \nu_g} \left(k_g^3 - 2k_g^5 \frac{\beta_0^2}{\omega^2} + \frac{\beta_0^2}{\alpha_0^2} C^3 \nu_g^2 k_g - 2C^3 \nu_g^2 k_g^3 \frac{\beta_0^2}{\omega^2} \right)$$

$$\times \left[\frac{1}{2C} \int_0^z dz' a_\rho^{(1)}{}_z \left(\frac{(C+1)z + (C-1)z'}{2C} \right) a_\mu^{(1)}(z') + \frac{1}{C+1} a_\mu^{(1)'}(z) \int_0^z dz' a_\rho^{(1)}(z') \right]$$

$$- \frac{1}{4\eta_g^2 \nu_g} \left(-2C^3 \nu_g^2 k_g^3 \frac{\beta_0^2}{\omega^2} - \frac{1}{2} k_g \frac{\omega^2}{\beta_0^2} + 2C^2 \nu_g^2 k_g^3 \frac{\beta_0^2}{\omega^2} \right)$$

$$\times \left[\frac{1}{2C} \int_0^z dz' a_\mu^{(1)}{}_z \left(\frac{(C+1)z + (C-1)z'}{2C} \right) a_\rho^{(1)}(z') + \frac{1}{C+1} a_\rho^{(1)'}(z) \int_0^z dz' a_\mu^{(1)}(z') \right]$$

$$+ \frac{1}{4\eta_g \nu_g^2} \left(C\nu_g^2 k_g - 2C\nu_g^2 k_g^3 \frac{\beta_0^2}{\omega^2} + \frac{\beta_0^2}{\alpha_0^2} k_g^3 - 2k_g^5 \frac{\beta_0^2}{\omega^2} \right)$$

$$\times \left[\frac{1}{2C} \int_0^z dz' a_\rho^{(1)}{}_z \left(\frac{(C+1)z + (C-1)z'}{2C} \right) a_\mu^{(1)}(z') - \frac{1}{C+1} a_\mu^{(1)'}(z) \int_0^z dz' a_\rho^{(1)}(z') \right]$$

$$+ \frac{1}{4\eta_g \nu_g^2} \left(2C^2 \nu_g^2 k_g^3 \frac{\beta_0^2}{\omega^2} - 2C\nu_g^2 k_g^3 \frac{\beta_0^2}{\omega^2} - \frac{1}{2} k_g \frac{\omega^2}{\beta_0^2} \right)$$

$$\times \left[\frac{1}{2C} \int_0^z dz' a_\mu^{(1)}{}_z \left(\frac{(C+1)z + (C-1)z'}{2C} \right) a_\rho^{(1)}(z') - \frac{1}{C+1} a_\rho^{(1)'}(z) \int_0^z dz' a_\mu^{(1)}(z') \right],$$

the solution for Eq. (4.49), i.e.,

$$\hat{G}_0^S \hat{V}_2^{SP} \hat{G}_0^P = -\hat{G}_0^S \hat{V}_1^{SP} \hat{G}_0^P \hat{V}_1^{PP} \hat{G}_0^P - \hat{G}_0^S \hat{V}_1^{SS} \hat{G}_0^S \hat{V}_1^{SP} \hat{G}_0^P,$$

is

$$\frac{1}{4} \left(\frac{k_g}{\nu_g} + \frac{k_g}{\eta_g} \right) a_\rho^{(2)}(z) + \frac{\beta_0^2}{2\omega^2} k_g (\nu_g + \eta_g) \left(1 - \frac{k_g^2}{\nu_g \eta_g} \right) a_\mu^{(2)}(z)$$

$$= \left\{ -\frac{1}{2\eta_g \nu_g^2} \left[2(C-1)\nu_g^2 k_g^5 \frac{\beta_0^4}{\omega^4} + \left(1 - \frac{\beta_0^2}{\alpha_0^2} C \right) \nu_g^2 k_g^3 \frac{\beta_0^2}{\omega^2} \right] - \frac{\beta_0^2}{\alpha_0^2} \frac{k_g^3}{\nu_g} \frac{\beta_0^2}{\omega^2} + \frac{k_g}{2\eta_g} \left(2k_g^2 \frac{\beta_0^2}{\omega^2} - 1 \right) \right.$$

$$+ \left(\frac{1}{2C} + \frac{1}{C+1} \right) \frac{1}{4\eta_g^2 \nu_g} \left(6k_g^3 - 12k_g^5 \frac{\beta_0^2}{\omega^2} - k_g \frac{\omega^2}{\beta_0^2} + 8k_g^7 \frac{\beta_0^4}{\omega^4} + 8C^3 \nu_g^2 k_g^5 \frac{\beta_0^4}{\omega^4} \right.$$

$$\left. -4\frac{\beta_0^2}{\alpha_0^2} C^3 \nu_g^2 k_g^3 \frac{\beta_0^2}{\omega^2} \right)$$

$$-\left(\frac{1}{2C}-\frac{1}{C+1}\right)\frac{1}{4\eta_g\nu_g^2}\left(4\frac{\beta_0^2}{\alpha_0^2}k_g^3-8k_g^5\frac{\beta_0^2}{\omega^2}-k_g\frac{\omega^2}{\alpha_0^2}+2k_g^3-4C\nu_g^2k_g^3\frac{\beta_0^2}{\omega^2}+8C\nu_g^2k_g^5\frac{\beta_0^4}{\omega^4}\right.$$

$$\left.\left.-4\frac{\beta_0^2}{\alpha_0^2}k_g^5\frac{\beta_0^2}{\omega^2}+8k_g^7\frac{\beta_0^4}{\omega^4}\right)\right\}a_\mu^{(1)}(z)a_\mu^{(1)}(z)$$

$$+\left[\left(\frac{1}{2}+\frac{1}{C+1}\right)\frac{k_g}{8\eta_g\nu_g^2}\left(Ck_g^2+\nu_g^2\right)-\left(\frac{1}{2}-\frac{1}{C+1}\right)\frac{k_g}{8\eta_g\nu_g^2}\left(k_g^2+C\nu_g^2\right)\right.$$

$$\left.+\left(\frac{1}{2C}+\frac{1}{C+1}\right)\frac{k_g}{8\eta_g^2\nu_g}\left(C^3\nu_g^2+k_g^2\right)-\left(\frac{1}{2C}-\frac{1}{C+1}\right)\frac{k_g}{8\eta_g\nu_g^2}\left(k_g^2+C\nu_g^2\right)\right]a_\rho^{(1)}(z)a_\rho^{(1)}(z)$$

$$+\left[\left(\frac{1}{2}+\frac{1}{C+1}\right)\frac{\beta_0^2}{\alpha_0^2}\frac{1}{4\nu_g^3}k_g\left(k_g^2-\nu_g^2\right)+\left(\frac{1}{2}-\frac{1}{C+1}\right)\frac{1}{4\eta_g\nu_g^2}\left(k_g\frac{\omega^2}{\alpha_0^2}-2\frac{\beta_0^2}{\alpha_0^2}k_g^3\right)\right.$$

$$\left.+\frac{\beta_0^2}{\alpha_0^2}\frac{k_g}{2\nu_g}\right]a_\mu^{(1)}(z)a_\gamma^{(1)}(z)$$

$$-\left[\left(\frac{1}{2}+\frac{1}{C+1}\right)\frac{k_g\left(k_g^2+\nu_g^2\right)}{8\nu_g^3}-\left(\frac{1}{2}-\frac{1}{C+1}\right)\frac{k_g\left(k_g^2+\nu_g^2\right)}{8\eta_g\nu_g^2}\right]a_\rho^{(1)}(z)a_\gamma^{(1)}(z)$$

$$-\left[\left(\frac{1}{2}+\frac{1}{C+1}\right)\frac{1}{4\eta_g\nu_g^2}\left(2\nu_g^2k_g^3\frac{\beta_0^2}{\omega^2}-\nu_g^2k_g+2Ck_g^5\frac{\beta_0^2}{\omega^2}-\frac{\beta_0^2}{\alpha_0^2}Ck_g^3\right)\right.$$

$$-\left(\frac{1}{2}-\frac{1}{C+1}\right)\frac{1}{4\eta_g\nu_g^2}\left(2C\nu_g^2k_g^3\frac{\beta_0^2}{\omega^2}-\frac{\beta_0^2}{\alpha_0^2}C\nu_g^2k_g+2k_g^5\frac{\beta_0^2}{\omega^2}-k_g^3\right)$$

$$-\left(\frac{1}{2C}+\frac{1}{C+1}\right)\frac{1}{4\eta_g^2\nu_g}\left(3k_g^3+\frac{\beta_0^2}{\alpha_0^2}C^3\nu_g^2k_g-4C^3\nu_g^2k_g^3\frac{\beta_0^2}{\omega^2}-4k_g^5\frac{\beta_0^2}{\omega^2}-\frac{1}{2}k_g\frac{\omega^2}{\beta_0^2}\right)$$

$$+\left(\frac{1}{2C}-\frac{1}{C+1}\right)\frac{1}{4\eta_g\nu_g^2}\left(C\nu_g^2k_g+2k_g^3+\frac{\beta_0^2}{\alpha_0^2}k_g^3-4k_g^5\frac{\beta_0^2}{\omega^2}-4C\nu_g^2k_g^3\frac{\beta_0^2}{\omega^2}-\frac{1}{2}k_g\frac{\omega^2}{\beta_0^2}\right)$$

$$\left.-(C-1)\frac{k_g^3}{2\eta_g}\frac{\beta_0^2}{\omega^2}\right]a_\rho^{(1)}(z)a_\mu^{(1)}(z)$$

$$-\frac{1}{2\eta_g\nu_g^2}\left[2(C-1)\nu_g^2k_g^5\frac{\beta_0^4}{\omega^4}+\left(1-\frac{\beta_0^2}{\alpha_0^2}C\right)\nu_g^2k_g^3\frac{\beta_0^2}{\omega^2}\right]$$

$$\times\int_0^z dz'a_\mu^{(1)}{}_z\left(\frac{(C+1)z-(C-1)z'}{2}\right)a_\mu^{(1)}\left(z'\right)$$

$$+\frac{1}{4\eta_g^2\nu_g}\left(6k_g^3-12k_g^5\frac{\beta_0^2}{\omega^2}-k_g\frac{\omega^2}{\beta_0^2}+8k_g^7\frac{\beta_0^4}{\omega^4}+8C^3\nu_g^2k_g^5\frac{\beta_0^4}{\omega^4}-4\frac{\beta_0^2}{\alpha_0^2}C^3\nu_g^2k_g^3\frac{\beta_0^2}{\omega^2}\right)$$

$$\times\left[\frac{1}{2C}\int_0^z dz'a_\mu^{(1)}{}_z\left(\frac{(C+1)z+(C-1)z'}{2C}\right)a_\mu^{(1)}\left(z'\right)+\frac{1}{C+1}a_\mu^{(1)'}(z)\int_0^z dz'a_\mu^{(1)}(z')\right]$$

$$-\frac{1}{4\eta_g\nu_g^2}\left(4\frac{\beta_0^2}{\alpha_0^2}k_g^3-8k_g^5\frac{\beta_0^2}{\omega^2}-k_g\frac{\omega^2}{\alpha_0^2}+2k_g^3-4C\nu_g^2k_g^3\frac{\beta_0^2}{\omega^2}+8C\nu_g^2k_g^5\frac{\beta_0^4}{\omega^4}-4\frac{\beta_0^2}{\alpha_0^2}k_g^5\frac{\beta_0^2}{\omega^2}+8k_g^7\frac{\beta_0^4}{\omega^4}\right)$$

$$\times\left[\frac{1}{2C}\int_0^z dz'a_\mu^{(1)}{}_z\left(\frac{(C+1)z+(C-1)z'}{2C}\right)a_\mu^{(1)}\left(z'\right)-\frac{1}{C+1}a_\mu^{(1)'}(z)\int_0^z dz'a_\mu^{(1)}(z')\right]$$

$$+\frac{k_g\left(Ck_g^2+\nu_g^2\right)}{8\eta_g\nu_g^2}\left[\frac{1}{2}\int_0^z dz'a_\rho^{(1)}{}_z\left(\frac{(C+1)z-(C-1)z'}{2}\right)a_\rho^{(1)}\left(z'\right)\right.$$

$$+\frac{1}{C+1}a_\rho^{(1)'}(z)\int_0^z dz' a_\rho^{(1)}(z')\Bigg]$$

$$-\frac{k_g\left(k_g^2+C\nu_g^2\right)}{8\eta_g\nu_g^2}\left[\frac{1}{2}\int_0^z dz' a_\rho^{(1)}{}_z\left(\frac{(C+1)z-(C-1)z'}{2}\right)a_\rho^{(1)}(z')\right.$$

$$\left.-\frac{1}{C+1}a_\rho^{(1)'}(z)\int_0^z dz' a_\rho^{(1)}(z')\right]$$

$$+\frac{C^3 k_g\nu_g^2+k_g^3}{8\eta_g^2\nu_g}\left[\frac{1}{2C}\int_0^z dz' a_\rho^{(1)}{}_z\left(\frac{(C+1)z+(C-1)z'}{2C}\right)a_\rho^{(1)}(z')\right.$$

$$\left.+\frac{1}{C+1}a_\rho^{(1)'}(z)\int_0^z dz' a_\rho^{(1)}(z')\right]$$

$$-\frac{k_g\left(k_g^2+C\nu_g^2\right)}{8\eta_g\nu_g^2}\left[\frac{1}{2C}\int_0^z dz' a_\rho^{(1)}{}_z\left(\frac{(C+1)z+(C-1)z'}{2C}\right)a_\rho^{(1)}(z')\right.$$

$$\left.-\frac{1}{C+1}a_\rho^{(1)'}(z)\int_0^z dz' a_\rho^{(1)}(z')\right]$$

$$+\frac{\beta_0^2}{\alpha_0^2}\frac{k_g\left(k_g^2-\nu_g^2\right)}{4\nu_g^3}\left[\frac{1}{2}\int_0^z dz' a_\gamma^{(1)}{}_z\left(\frac{(C+1)z-(C-1)z'}{2}\right)a_\mu^{(1)}(z')\right.$$

$$\left.+\frac{1}{C+1}a_\mu^{(1)'}(z)\int_0^z dz' a_\gamma^{(1)}(z')\right]$$

$$+\frac{1}{4\eta_g\nu_g^2}\left(k_g\frac{\omega^2}{\alpha_0^2}-2\frac{\beta_0^2}{\alpha_0^2}k_g^3\right)\left[\frac{1}{2}\int_0^z dz' a_\gamma^{(1)}{}_z\left(\frac{(C+1)z-(C-1)z'}{2}\right)a_\mu^{(1)}(z')\right.$$

$$\left.-\frac{1}{C+1}a_\mu^{(1)'}(z)\int_0^z dz' a_\gamma^{(1)}(z')\right]$$

$$-\frac{k_g\left(k_g^2+\nu_g^2\right)}{8\nu_g^3}\left[\frac{1}{2}\int_0^z dz' a_\gamma^{(1)}{}_z\left(\frac{(C+1)z-(C-1)z'}{2}\right)a_\rho^{(1)}(z')\right.$$

$$\left.+\frac{1}{C+1}a_\rho^{(1)'}(z)\int_0^z dz' a_\gamma^{(1)}(z')\right]$$

$$+\frac{k_g\left(k_g^2+\nu_g^2\right)}{8\eta_g\nu_g^2}\left[\frac{1}{2}\int_0^z dz' a_\gamma^{(1)}{}_z\left(\frac{(C+1)z-(C-1)z'}{2}\right)a_\rho^{(1)}(z')\right.$$

$$\left.-\frac{1}{C+1}a_\rho^{(1)'}(z)\int_0^z dz' a_\gamma^{(1)}(z')\right]$$

$$-\frac{1}{4\eta_g\nu_g^2}\left(2\nu_g^2 k_g^3\frac{\beta_0^2}{\omega^2}-\nu_g^2 k_g+2Ck_g^5\frac{\beta_0^2}{\omega^2}-\frac{\beta_0^2}{\alpha_0^2}Ck_g^3\right)$$

$$\times\left[\frac{1}{2}\int_0^z dz' a_\rho^{(1)}{}_z\left(\frac{(C+1)z-(C-1)z'}{2}\right)a_\mu^{(1)}(z')+\frac{1}{C+1}a_\mu^{(1)'}(z)\int_0^z dz' a_\rho^{(1)}(z')\right]$$

$$+\frac{1}{4\eta_g\nu_g^2}\left(2C\nu_g^2 k_g^3\frac{\beta_0^2}{\omega^2}-\frac{\beta_0^2}{\alpha_0^2}C\nu_g^2 k_g+2k_g^5\frac{\beta_0^2}{\omega^2}-k_g^3\right)$$

$$\times\left[\frac{1}{2}\int_0^z dz' a_\rho^{(1)}{}_z\left(\frac{(C+1)z-(C-1)z'}{2}\right)a_\mu^{(1)}(z')-\frac{1}{C+1}a_\mu^{(1)'}(z)\int_0^z dz' a_\rho^{(1)}(z')\right]$$

$$
+ (C-1)\frac{k_g^3}{2\eta_g}\frac{\beta_0^2}{\omega^2}\int_0^z dz' a_{\mu\ z}^{(1)}\left(\frac{(C+1)z - (C-1)z'}{2}\right)a_\rho^{(1)}(z')
$$

$$
- \frac{1}{4\eta_g^2\nu_g}\left(-2k_g^3 + 2C^3\nu_g^2k_g^3\frac{\beta_0^2}{\omega^2} + 2k_g^5\frac{\beta_0^2}{\omega^2} + \frac{1}{2}k_g\frac{\omega^2}{\beta_0^2}\right)
$$

$$
\times\left[\frac{1}{2C}\int_0^z dz' a_{\mu\ z}^{(1)}\left(\frac{(C+1)z + (C-1)z'}{2C}\right)a_\rho^{(1)}(z') + \frac{1}{C+1}a_\rho^{(1)'}(z)\int_0^z dz' a_\mu^{(1)}(z')\right]
$$

$$
- \frac{1}{4\eta_g^2\nu_g}\left(-k_g^3 - \frac{\beta_0^2}{\alpha_0^2}C^3\nu_g^2k_g + 2C^3\nu_g^2k_g^3\frac{\beta_0^2}{\omega^2} + 2k_g^5\frac{\beta_0^2}{\omega^2}\right)
$$

$$
\times\left[\frac{1}{2C}\int_0^z dz' a_{\rho\ z}^{(1)}\left(\frac{(C+1)z + (C-1)z'}{2C}\right)a_\mu^{(1)}(z') + \frac{1}{C+1}a_\mu^{(1)'}(z)\int_0^z dz' a_\rho^{(1)}(z')\right]
$$

$$
- \frac{1}{4\eta_g\nu_g^2}\left(2k_g^3 - 2k_g^5\frac{\beta_0^2}{\omega^2} - 2C\nu_g^2k_g^3\frac{\beta_0^2}{\omega^2} - \frac{1}{2}k_g\frac{\omega^2}{\beta_0^2}\right)
$$

$$
\times\left[\frac{1}{2C}\int_0^z dz' a_{\mu\ z}^{(1)}\left(\frac{(C+1)z + (C-1)z'}{2C}\right)a_\rho^{(1)}(z') - \frac{1}{C+1}a_\rho^{(1)'}(z)\int_0^z dz' a_\mu^{(1)}(z')\right]
$$

$$
- \frac{1}{4\eta_g\nu_g^2}\left(C\nu_g^2k_g + \frac{\beta_0^2}{\alpha_0^2}k_g^3 - 2k_g^5\frac{\beta_0^2}{\omega^2} - 2C\nu_g^2k_g^3\frac{\beta_0^2}{\omega^2}\right)
$$

$$
\times\left[\frac{1}{2C}\int_0^z dz' a_{\rho\ z}^{(1)}\left(\frac{(C+1)z + (C-1)z'}{2C}\right)a_\mu^{(1)}(z') - \frac{1}{C+1}a_\mu^{(1)'}(z)\int_0^z dz' a_\rho^{(1)}(z')\right],
$$

and the solution for Eq. (4.50), i.e.,

$$
\hat{G}_0^S\hat{V}_2^{SS}\hat{G}_0^S = -\hat{G}_0^S\hat{V}_1^{SP}\hat{G}_0^P\hat{V}_1^{PS}\hat{G}_0^S - \hat{G}_0^S\hat{V}_1^{SS}\hat{G}_0^S\hat{V}_1^{SS}\hat{G}_0^S,
$$

is

$$
-\frac{1}{4}\left(1 - \frac{k_g^2}{\eta_g^2}\right)a_\rho^{(2)}(z) - \left[\frac{k_g^2 + \eta_g^2}{4\eta_g^2} - \frac{2k_g^2}{k_g^2 + \eta_g^2}\right]a_\mu^{(2)}(z)
$$

$$
= -\left\{\frac{1}{8\eta_g^4}\left(8k_g^2\eta_g^2 - \frac{\omega^4}{\beta_0^4}\right) - \frac{1}{4\eta_g^2}\left(\frac{\omega^2}{\beta_0^2} - 4\frac{\beta_0^2}{\omega^2}\eta_g^2k_g^2\right) - \frac{\beta_0^2}{\alpha_0^2}k_g^2\frac{\beta_0^2}{\omega^2}\right.
$$

$$
\left. + \frac{1}{\eta_g^2(C+1)}\left[k_g^2\left(\frac{\beta_0^4}{\alpha_0^4}C^2 - 1\right) - 4k_g^4\frac{\beta_0^2}{\omega^2}\left(\frac{\beta_0^2}{\alpha_0^2}C^2 - 1\right) + 4k_g^6\frac{\beta_0^4}{\omega^4}(C^2 - 1)\right]\right\}a_\mu^{(1)}(z)a_\mu^{(1)}(z)
$$

$$
- \left[\frac{1}{8\eta_g^4}\left(\eta_g^4 - k_g^4\right) + \frac{1}{4\eta_g^2}k_g^2(C-1)\right]a_\rho^{(1)}(z)a_\rho^{(1)}(z)
$$

$$
+ \left\{\frac{k_g^2}{\eta_g^2} - \frac{1}{\eta_g^2(C+1)}\left[k_g^2\left(\frac{\beta_0^2}{\alpha_0^2}C^2 - 1\right) - 2\frac{\beta_0^2}{\omega^2}k_g^4\left(C^2 - 1\right)\right]\right\}a_\mu^{(1)}(z)a_\rho^{(1)}(z)
$$

$$
- \frac{1}{8\eta_g^4}\left(8k_g^2\eta_g^2 - \frac{\omega^4}{\beta_0^4}\right)a_\mu^{(1)'}(z)\int_0^z dz' a_\mu^{(1)}(z')
$$

$$-\frac{1}{8\eta_g^4}\left(\eta_g^4-k_g^4\right)a_\rho^{(1)'}(z)\int_0^z dz' a_\rho^{(1)}(z')$$

$$+\frac{k_g^2}{2\eta_g^2}\left[a_\mu^{(1)'}(z)\int_0^z dz' a_\rho^{(1)}(z')+a_\rho^{(1)'}(z)\int_0^z dz' a_\mu^{(1)}(z')\right]$$

$$-\frac{1}{8\eta_g^2}\left(\eta_g^2-3k_g^2\right)\left[a_\mu^{(1)'}(z)\int_0^z dz' a_\rho^{(1)}(z')-a_\rho^{(1)'}(z)\int_0^z dz' a_\mu^{(1)}(z')\right]$$

$$-\frac{1}{\eta_g^2(C+1)}\left[k_g^2\left(\frac{\beta_0^4}{\alpha_0^4}C^2-1\right)-4k_g^4\frac{\beta_0^2}{\omega^2}\left(\frac{\beta_0^2}{\alpha_0^2}C^2-1\right)+4k_g^6\frac{\beta_0^4}{\omega^4}(C^2-1)\right]$$

$$\times\int_0^z dz' a_\mu^{(1)}{}_z\left(\frac{2Cz-(C-1)z'}{(C+1)}\right)a_\mu^{(1)}(z')$$

$$-\frac{1}{4\eta_g^2}k_g^2(C-1)\int_0^z dz' a_\rho^{(1)}{}_z\left(\frac{2Cz-(C-1)z'}{(C+1)}\right)a_\rho^{(1)}(z')$$

$$-\frac{1}{2\eta_g^2(C+1)}\left[k_g^2\left(\frac{\beta_0^2}{\alpha_0^2}C^2-1\right)-2\frac{\beta_0^2}{\omega^2}k_g^4\left(C^2-1\right)\right]$$

$$\times\left[\int_0^z dz' a_\mu^{(1)}{}_z\left(\frac{2Cz-(C-1)z'}{(C+1)}\right)a_\rho^{(1)}(z')+\int_0^z dz' a_\rho^{(1)}{}_z\left(\frac{2Cz-(C-1)z'}{(C+1)}\right)a_\mu^{(1)}(z')\right]$$

$$+\frac{Ck_g^2}{2(C+1)\eta_g^2}\left(\frac{\beta_0^2}{\alpha_0^2}-1\right)$$

$$\times\left[\int_0^z dz' a_\mu^{(1)}{}_z\left(\frac{2Cz-(C-1)z'}{(C+1)}\right)a_\rho^{(1)}(z')-\int_0^z dz' a_\rho^{(1)}{}_z\left(\frac{2Cz-(C-1)z'}{(C+1)}\right)a_\mu^{(1)}(z')\right],$$

where $\eta_g=C\nu_g, k_g^2+\nu_g^2=\omega^2/\alpha_0^2$ and $k_g^2+\eta_g^2=\omega^2/\beta_0^2$. In Appendix B, we give some typical integrations which can be useful for the derivations, and Appendix C could help in both derivation of the solution and understanding the algorithm. The interpretation of these results are similar to those provided in Chapter 4.

After we solve all (four) of the second order equations, future research is to perform numerical tests with all four components of data available.

The next section is another application of the direct non-linear inversion method (with PP data only) to the time-lapse seismic data.

4.4 An application to time-lapse seismic data

The inverse scattering series based direct non-linear inversion method has shown positive results on its application to multi-parameter 1D acoustic and elastic media (see, e.g., Chapter 3 and previous sections of Chapter 4). In this section, we present another application of this method to time-lapse seismic data aiming to distinguish pressure changes from reservoir fluid changes. Two elastic parameters (Shear modulus and velocity ratio) are chosen to discriminate the two changes. Synthetic tests indicate that these two parameters are very useful in mapping the pressure and fluid changes; and, the direct non-linear inversion method gives closer and more reliable parameter predictions compared to conventional linear order approximation.

4.4.1 Introduction

Time-lapse seismic data can be defined as those seismic data acquired at different times over the same area to assess changes in the subsurface with time, such as fluid movement or the fraction of hydrocarbons that can be or has been produced from a well, reservoir or field. In the production field, it is very important to monitor the development of the reservoir, like timely information on changes in reservoir pressure and fluids. In order to do this, repeated experiments would be needed at different times over the same area. Since the changes in reservoir pressure and fluids could affect the seismic response very similarly, conventional seismic time-lapse attributes find difficulty in distinguishing pressure changes from reservoir fluid changes. Some works on studying the sensitivities and/or discrimination of these two changes have been presented by, e.g., Tura and Lumley (1999); Landrø (2001); Landrø *et al.* (2003); Landrø and Duffaut (2004); Stovas and Landrø (2005); Kvam and Landrø (2005).

In this section, as suggested by Robert G. Keys and Douglas J. Foster, we choose two parameters — relative changes in shear modulus and velocity ratio V_p/V_s (V_p is the acoustic P-wave velocity and V_s is the elastic S-wave velocity) which may be useful for separating

pressure changes from fluid changes. The reason for choosing these two parameters is that V_p/V_s is sensitive to changes in fluid/water saturation, but insensitive to changes in pressure; while, shear modulus is sensitive to changes in pore pressure but unaffected by changes in fluid. These two parameters can help to indicate either a pressure or a fluid changed in the reservoir. Hence, if these two parameters can be more accurately predicted/estimated using the direct non-linear inversion method, it would be easier to accomplish this goal.

The direct non-linear inversion method is based on the inverse scattering series, and it uses the measured scattered wave field, i.e., data D, to predict the earth property changes in space. Over here, the baseline survey is considered as the reference wave field G_0 in the inverse scattering series, and the monitor survey as the actual wave field G. The initial reservoir condition is considered as the background and the reservoir property changes in TIME are related to the earth property changes in SPACE in the inverse scattering series, and the monitor survey minus the baseline survey is related to the scattered field. The relationship between the inverse scattering series and the time-lapse seismic monitoring is illustrated in the following table:

Inverse scattering series	Time-lapse seismic monitoring
Reference medium L_0	Initial reservoir condition
Actual medium L	Current reservoir condition
Earth property changes in space $V = L_0 - L$	Reservoir property changes in time
Reference wave field G_0	Baseline survey
Actual wave field G	Monitor survey
Scattered wave field $D = G - G_0$	Monitor $-$ Baseline

In the following sections, we show the numerical tests of the first and second order algorithms to estimate shear modulus and V_p/V_s contrasts with only $\hat{D}^{PP}$ (PP data). The applications are on the core data (Gregory, 1976) and Heidrun well log data, respectively. The tests are similar to those numerical tests described in my previous work (e.g., Chapter 3 and

previous sections of Chapter 4) with reference medium over actual medium replaced by baseline over monitor; and the parameters require modification from a_γ, a_ρ and a_μ to a_R, a_ρ and a_μ, where a_R is the relative change in the velocity ratio V_p/V_s. The detailed derivations of writing $a_R^{(1)}$ and $a_R^{(2)}$ in terms of $a_\gamma^{(1)}$, $a_\gamma^{(2)}$, $a_\mu^{(1)}$ and $a_\mu^{(2)}$ are in Appendix B.

4.4.2   Core data tests

In this section, we numerically test the direct non-linear inversion approach and compare the effects of pressure and fluid changes on the elastic properties in the following two cases:

(1) Fixing the fluid as 100% water saturation, while the pressure changes from 1000 to 9000psi. The measurement at pressure = 5000psi presents the baseline and the measurements at the other different pressures are respectively considered as monitors (Gregory, 1976, Table 3).

(2) Fixing the pressure at 5000psi, while the fluid changes from 0 to 100 percent. The measurement at 100% saturation is the baseline and the other cases with different water saturations are monitors, respectively (Gregory, 1976, Table 4).

The numerical results are shown in the figures at the end of this chapter. As illustrated in Figs. 4.19 and 4.20, when pressure changes, shear modulus has the most variation and V_p/V_s has the least variation; while when only water saturation changes, shear modulus has the least variation and V_p/V_s has bigger variation. So shear modulus is very sensitive to pressure changes while relatively not sensitive to the fluid changes, and V_p/V_s is very sensitive to the fluid changes, but is relatively insensitive to the pressure changes. These two parameters would be very useful in indicating/mapping pressure and fluid changes. The P impedance has very big variation in both cases. So it is very sensitive to each of the two kinds of changes and cannot discriminate fluid changes from pressure changes.

Figures. 4.21 ∼ 4.24 show the comparison of first and second order approximation of the relative changes in shear modulus and V_p/V_s in the two cases as stated above. Among all of

the examples tested, because the contrast here is relatively small, both the first and second order approximation give good approximations, and the second order approximation does an even better job, especially for larger contrasts, the improvements are more obvious. Here, it is worth noting that the objective of the direct non-linear inversion method (e.g., Weglein *et al.*, 2003) is trying to predict more reliable property changes for more complex, larger contrast targets where the error coming from the linear approximation would be significant.

4.4.3 Heidrun well log data tests

In this section, well log data tests are performed on the Heidrun synthetic well log A-52 (Fig. 4.25). From the year 1986 to the year 2001, at the first layer of the reservoir, oil is replaced by gas, and at the second layer, oil is replaced by water. Throughout the interval, the pore pressure decreased. So the main change that happened in the reservoir is the fluid change. The baseline is the log data in 1986 and the monitor is the log data in 2001. In the numerical tests, the inputs are analytically calculated reflection coefficients $R_1, R_2, \cdots, R_i, \cdots$ and the corresponding actual changes are, respectively, $\frac{M_1}{B_1} - 1, \frac{M_2}{B_2} - 1, \cdots, \frac{M_i}{B_i} - 1, \cdots$ (as shown in Fig. 4.26), where M_i and B_i denote the ith layer mechanical properties of the monitor and baseline, respectively.

From Fig. 4.27, we can see that, in the interval from about $3150 \sim 3185$m, oil goes to gas, and V_p/V_s decreases; while in the interval from about $3200 \sim 3220$m, oil is replaced by water, and V_p/V_s increases. Throughout this area, the pore pressure decreases a little bit, so the shear modulus increases in a small amount. The numerical results agree with the given well log A-52, and also indicate that the shear modulus is not sensitive to fluid changes since it has very small changes throughout the interval because the pressure change is small. Figure 4.28 is the comparison of the first order and second order approximation for the relative changes in the shear modulus. In this case, the second order approximation provides significant improvements beyond the linear results. It is much closer to the actual

values. Figure 4.29 shows that both the first and second order approximation give very good results for the relative changes in V_p/V_s. The error from the first approximation is smaller and hence the first order approximation is more reliable compared with shear modulus (Fig. 4.28). But when we zoom in on Fig. 4.29, say from about $3150 \sim 3590$m, the results can be re-illustrated in Fig. 4.30, and we can see that the second order approximation does give better results compared with the first order approximation.

4.4.4 Conclusion

In this application of the direct non-linear inversion method to time-lapse seismic data, we perform numerical tests (with PP data only), respectively, on core data and well log data. In both cases, numerical results indicate that the second order approximation provides improvements in the earth property predictions compared to the conventional first order approximation. In addition, the numerical results (especially from the well log data tests) show that the second order approximation is more helpful for predicting shear modulus compared to V_p/V_s. This is a very important message since, in practice, the shear modulus is more difficult to be reliably predicted compared to V_p/V_s with conventional inversion methods. Future research is expected to apply this method to more realistic cases — synthetic data and then real seismic data.
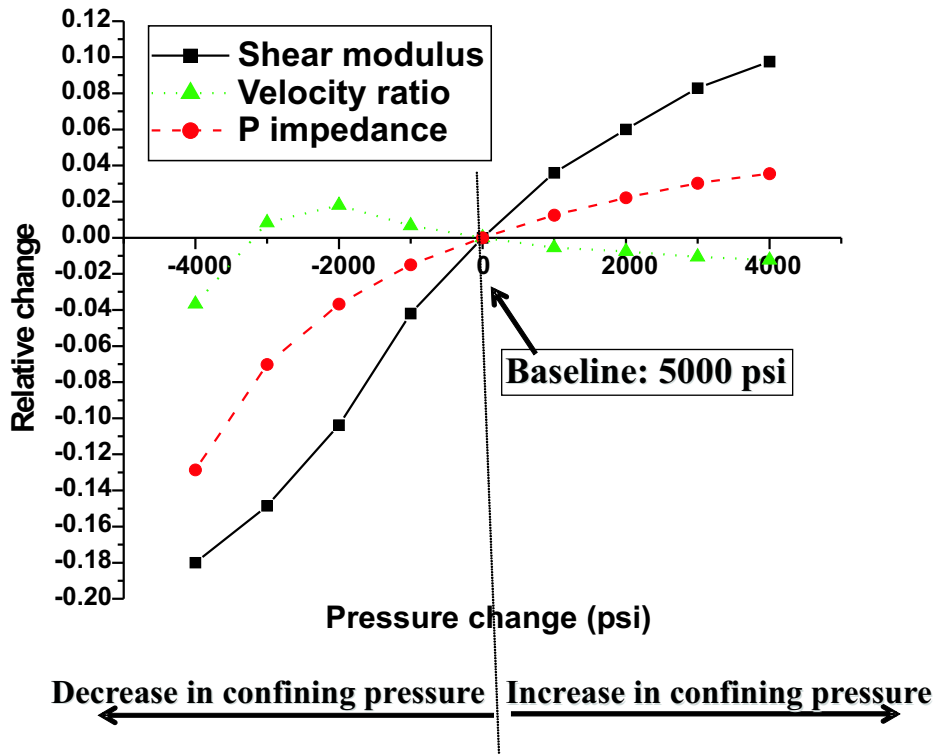
Fig. 4.19: *Comparison of attributes for pressure changes, fluid fixed (100% water saturation). Gregory (1976), Table 3.*
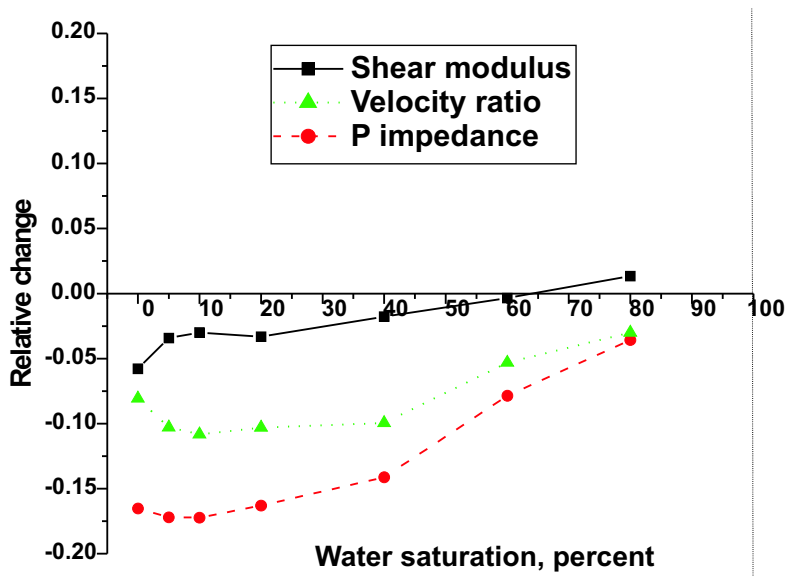
Fig. 4.20: *Comparison of attributes for fluid changes, pressure fixed (5000psi). Gregory (1976), Table 4.*
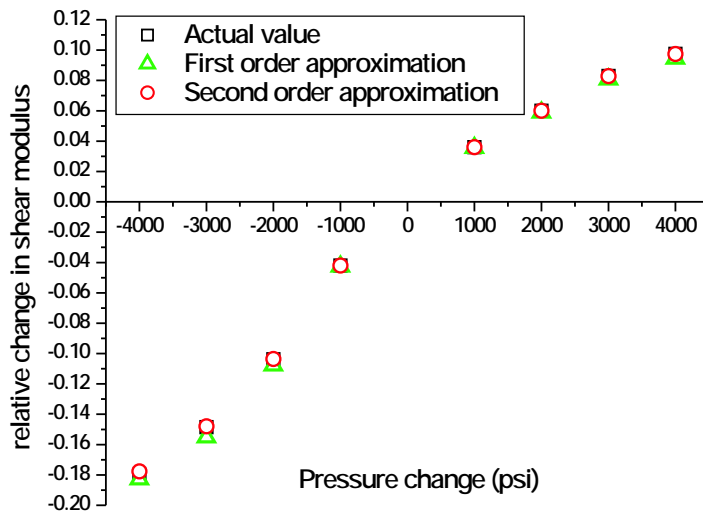
Fig. 4.21: *Comparison of first and second order approximation of relative change in shear modulus for pressure changes, fluid fixed (100% water saturation). Gregory (1976), Table 3.*
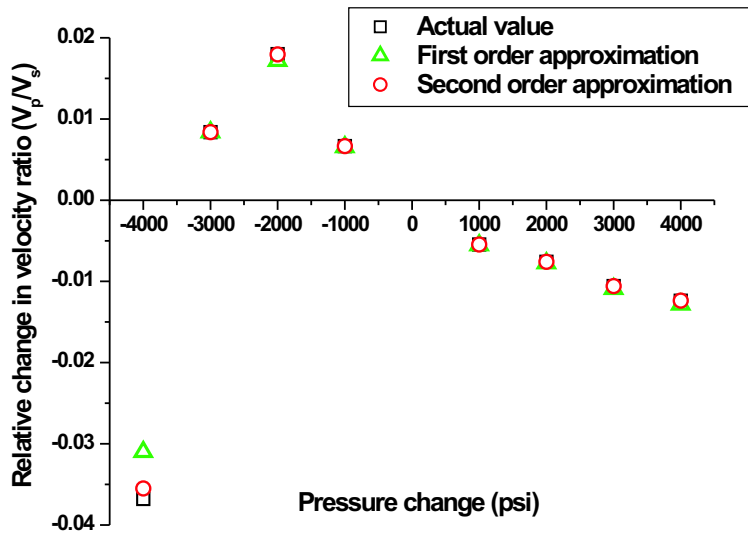
Fig. 4.22: *Comparison of first and second order approximation of relative change in V_p/V_s (See Appendix B) for pressure changes, fluid fixed (100% water saturation). Gregory (1976), Table 3.*
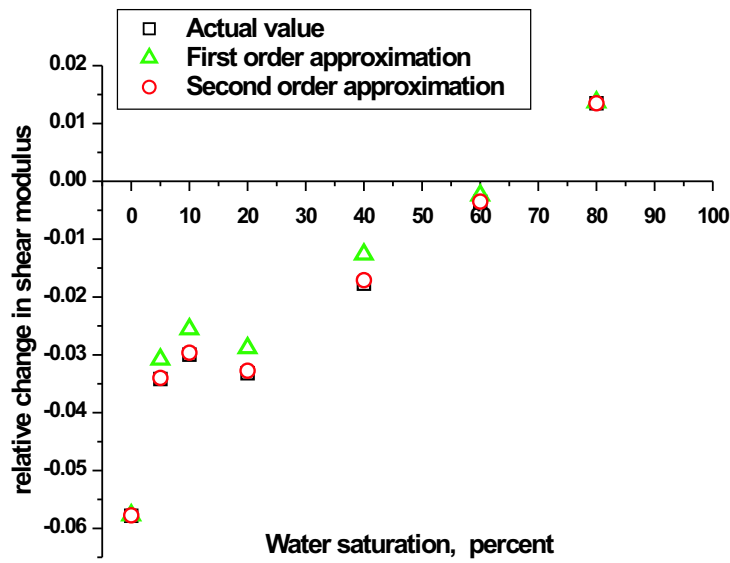
Fig. 4.23: *Comparison of first and second order approximation of relative change in shear modulus for fluid changes, pressure fixed (5000psi). Gregory (1976), Table 4.*
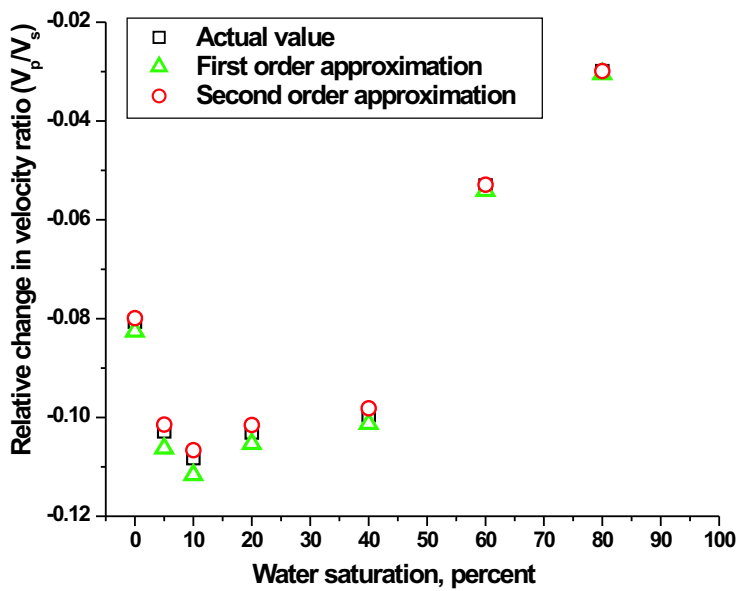
Fig. 4.24: *Comparison of first and second order approximation of relative change in V_p/V_s for fluid changes, pressure fixed (5000psi). Gregory (1976), Table 4.*

Depth (m)

3150

Garn

3185

| 90 % oil 10% water | 50 % gas 50% water | 100 % water |

Ile

| 90 % oil 10% water | 20 % oil 80% water | 100 % water |

Initial (1986)   2001   Wet
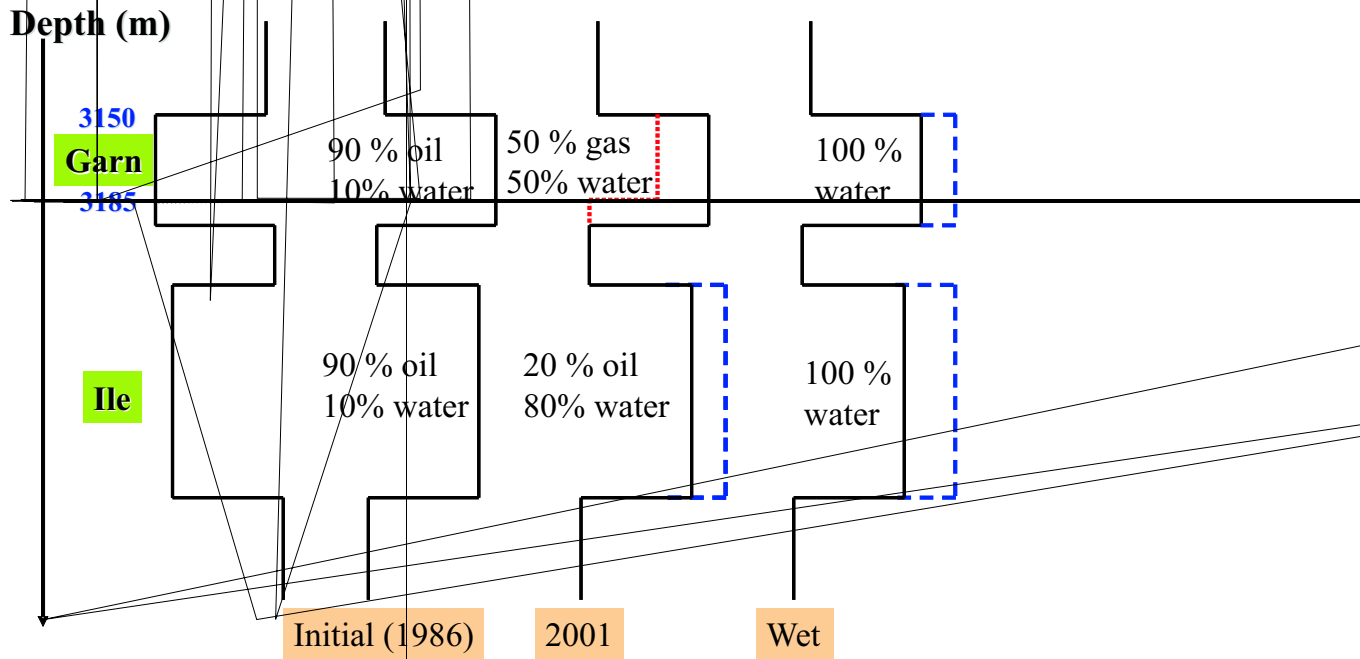
Fig. 4.25: *Schematic of the synthetic well log A-52.*

Shale
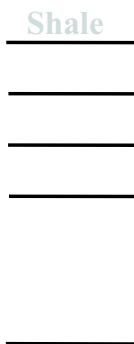
Fig. 4.26: *Schematic of the baseline, monitor and input reflection coefficients.*

95
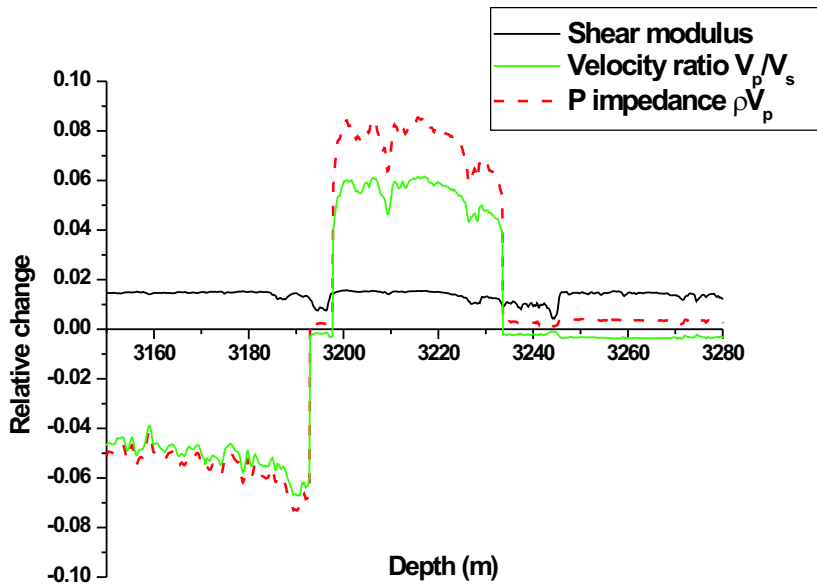
Fig. 4.27: *Comparison of actual changes in shear modulus, P-impedance and velocity ratio V_p/V_s. The baseline is the log data in 1986 and the monitor is the log data in 2001.*
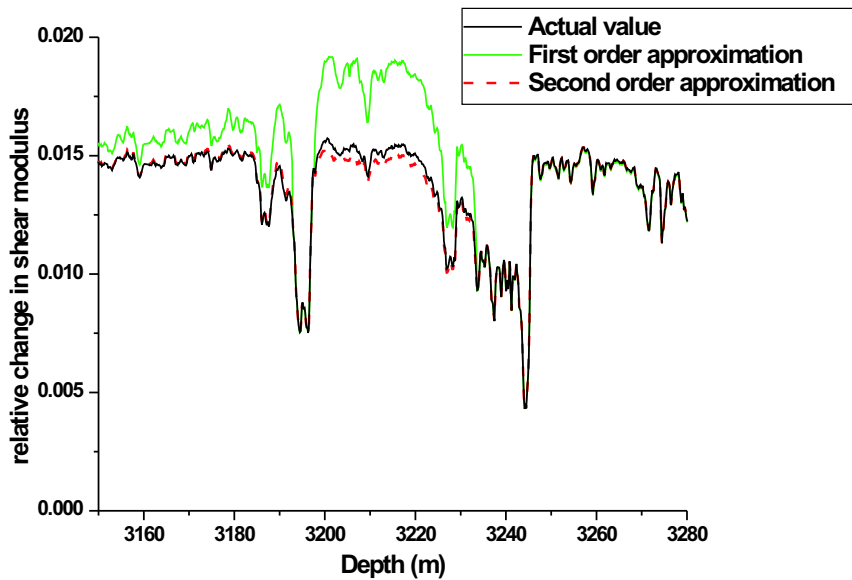
Fig. 4.28: *Comparison of first and second order approximation of relative change in shear modulus. The baseline is the log data in 1986 and the monitor is the log data in 2001.*
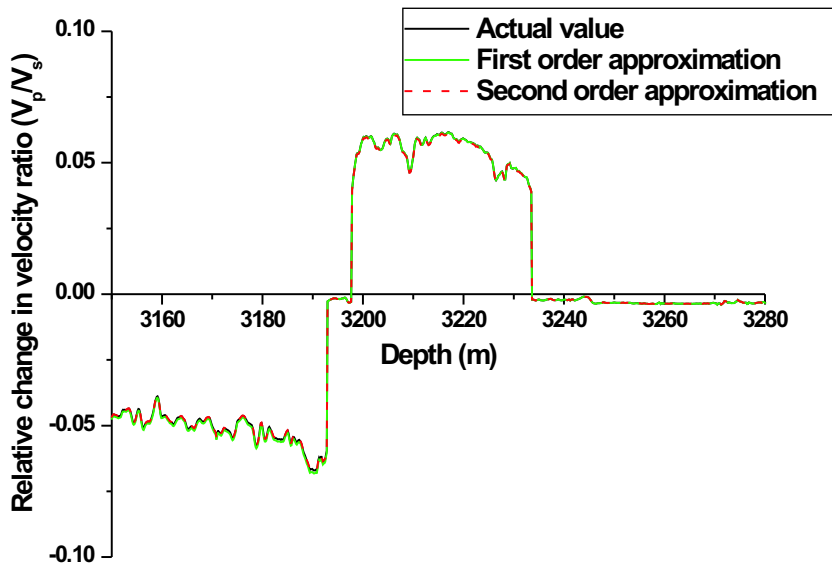
Fig. 4.29: *Comparison of first and second order approximation of relative change in V_p/V_s. The baseline is the log data in 1986 and the monitor is the log data in 2001.*
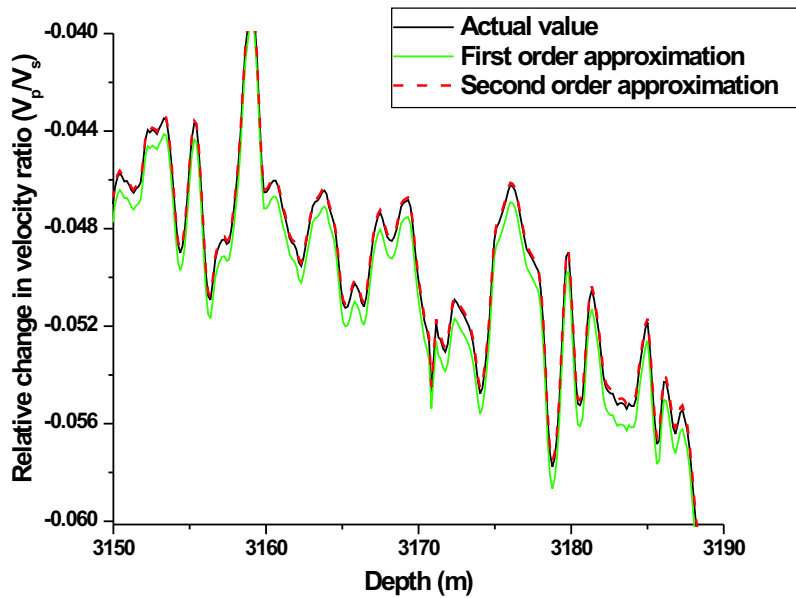
Fig. 4.30: *Zoomed in comparison of first and second order approximation of relative change in V_p/V_s. The baseline is the log data in 1986 and the monitor is the log data in 2001.*

97

5. **SUMMARY**

The current methods for removing multiples and processing primaries can give useful results when their assumptions are satisfied. However, under some circumstances, especially in deep water and in highly heterogeneous media and/or with a rapidly varying and corrugated boundary, the assumptions behind those algorithms cannot be adequately satisfied; and, hence, those methods can have difficulty and may become ineffective or fail. This technical difficulty combining with the increased interest and cost in exploring potential hydrocarbon targets under such circumstances as mentioned above, motivated the need for fundamentally new seismic concepts and capability (Weglein, 2006a).

To deal with the difficulties faced by current methods, one strategy is trying to develop a fundamentally new procedure which avoids those assumptions behind current methods. The inverse scattering series based task-specific subseries strategy has the potential to: (1) not only attenuate but eliminate internal multiples; (2) image and invert primaries under complex circumstances with large earth property changes. It provided a sequence of algorithms, respectively, for multiple removals (Carvalho, 1992; Araújo, 1994; Weglein *et al.*, 1997; Matson, 1997; Ramírez and Weglein, 2005), imaging without velocity (Shaw, 2005; Liu *et al.*, 2005) and direct non-linear inversion.

In this dissertation, we develop a framework and algorithm for more accurate target identification. We focus on the direct non-linear inversion of 1D acoustic or elastic properties. This is the first step into exploring the more comprehensive multi-parameter multi-D direct non-linear inversion framework.

Summary

Specifically, in Chapter 2, we extended the earlier work of, e.g., Weglein *et al.* (2001); Weglein *et al.* (2003); Shaw and Weglein (2003); Shaw and Weglein (2004), from one parameter (velocity) 1D normal incidence to non-normal incidence case. We calculated the first three terms in the inverse scattering series and identified task-specific imaging and inversion terms. Numerical tests on three different one-interface models show that including the first and second non-linear terms in the inverse scattering inversion subseries provides added value and improved capability for parameter estimation compared to the conventional linear results.

In Chapter 3, the direct non-linear inversion for the 1D one parameter case was generalized to a multi-parameter case — two parameter (velocity and density) acoustic inversion. For the first direct non-linear inversion solution obtained in this chapter, the tasks for imaging-only and inversion-only terms were separated. Tests with analytic data indicated significant added value, beyond linear estimates, in terms of both the proximity to actual value and the increased range of angles over which the improved estimates are useful.

A closed form of the inversion terms for one-interface case was also obtained. This closed form might be useful in predicting the precritical data using the postcritical data.

A special parameter Δc ($\Delta c = c - c_0$) (P-velocity change across an interface) was also found. Its Born inversion $(\Delta c)_1$ always has the right sign. That is, the sign of $(\Delta c)_1$ is the same as that of Δc. In practice, it could be very useful to know whether the velocity increases or decreases across the interface. After exchanging the parameters from α (relative changes in P-bulk modulus) and β (relative changes in density) to velocity and β, another form of the non-linear solution was obtained. There would be no leakage correction (please see details in Section 3.3) at all in this solution. This new form obviously indicates that the imaging terms care only about velocity errors. The mislocation is due to the wrong velocity. This is suggestive of possible generalization to multi-D medium, also of possible model type independent imaging which only depends on velocity changes.

Summary

In Chapter 4, the work on direct non-linear inversion for 1D two parameter (velocity and density) acoustic media was extended to the three parameter (P-wave velocity, S-wave velocity and density) elastic case. We presented the first set of direct non-linear inversion equations for 1D elastic media. The terms for moving mislocated reflectors were separated from inversion-only terms. Although in principle this elastic non-linear direct inversion in 2D requires all four components of data, the elastic non-linear inversion showed benefit in all the cases tested with $\hat{D}^{PP}$ (PP data) only. This means that we could perform elastic inversion in some situations with only pressure measurements available, i.e. towed streamer data. How accurately PP data effectively synthesize PS, SP and SS data determined the degree of benefit provided by the non-linear elastic inversion. For the case that all four components of data are available, a consistent method was provided. We anticipate collecting PP, PS, SP and SS would provide further benefit.

The direct non-linear elastic inversion method was also applied to the case of seismic time-lapse data (with PP data only), which was under the mentor and guidance of Robert Keys, Douglas Foster and Simon Shaw of ConocoPhillips. The goal is to distinguish pressure changes from reservoir fluid changes in cases when conventional seismic methods have difficulties. The numerical tests show excellent results.

Although the work presented in this dissertation is mainly focused on 1D media, the procedure can be generalized to multi-D. The objective of the direct non-linear inversion project is to provide more reliable and more accurate earth property predictions for more complex targets compared to current inversion methods. The future research will examine the multi-D generalizations and the practical data requirements when move to field data tests. The work presented in this dissertation is an initial part of the whole project. It would help to demonstrate how this fundamentally new method would work in a simple 1D acoustic and elastic world with perfect analytic data. Then, we could expect it to be useful in the real world and field data application.

REFERENCES

ACHENBACH, J. D. 1973. *Wave propagation in elastic solids.* Amsterdam : North-Holland; New York : American Elsevier.

AKI, K. AND RICHARDS, P. G. 2002. *Quantitative Seismology*, 2nd ed. University Science Books.

ARAÚJO, F. V. 1994. Linear and non-linear methods derived from scattering theory: backscattered tomography and internal multiple attenuation. Ph.D. thesis, Universidade Federal da Bahia.

BERKHOUT, A. J. AND VERSCHUUR, D. J. 1997. Estimation of multiple scattering by iterative inversion, part I: Theoretical considerations. *Geophysics 62*, 1586–1595.

BOYSE, W. E. AND KELLER, J. B. 1986. Inverse elastic scattering in three dimensions. *J. Acoust. Soc. Am. 79*, 215–218.

CARVALHO, P. M. 1992. Free-surface multiple reflection elimination method based on nonlinear inversion of seismic data. Ph.D. thesis, Universidade Federal da Bahia.

CARVALHO, P. M., WEGLEIN, A. B., AND STOLT, R. H. 1992. Nonlinear inverse scattering for multiple suppression: Application to real data. part I. In *62nd Ann. Internat. Mtg: Soc. of Expl. Geophys., Expanded Abstracts*. Soc. Expl. Geophys., 1093–1095.

CLAERBOUT, J. F. 1971. Toward a unified theory of reflector mapping. *Geophysics 36,* 3, 467–481.

References

CLAYTON, R. W. AND STOLT, R. H. 1981. A Born-WKBJ inversion method for acoustic reflection data. *Geophysics 46,* 11, 1559–1567.

EWING, W. M., JARDETZKY, W. S., AND PRESS, F. 1957. *Elastic waves in layered media.* McGraw-Hill Book Co.

FOSTER, D. J., KEYS, R. G., AND SCHMITT, D. P. 1997. *Detecting subsurface hydrocarbons with elastic wavefields.* Springer-In Inverse Problems in Wave Progagation, Volume 90 of The IMA Volumes in Mathematics and its Applications.

GAZDAG, J. 1978. Wave equation migration with the phase-shift method. *Geophysics 43,* 07, 1342–1351.

GLOGOVSKY, V., LANDA, E., AND PAFFENHOLZ, J. 2002. Integrated approach to subsalt depth imaging: Synthetic case study. *The Leading Edge 21,* 12, 1217–1226.

GRAY, S. H., ETGEN, J., DELLINGER, J., AND WHITMORE, D. 2001. Seismic migration problems and solutions. *Geophysics 66,* 5, 1622–1640.

GREGORY, A. R. 1976. Fluid saturation effects on dynamic elastic properties of sedimentary rocks. *Geophysics 41,* 5, 895–921.

HERRON, D. 2000. Pitfalls in seismic interpretation: Depth migration artifacts. *The Leading Edge 19*, 1016–1017.

INNANEN, K. A. 2003. Methods for the treatment of acoustic and absorptive/dispersive wave field measurements. Ph.D. thesis, University of British Columbia.

INNANEN, K. A. AND WEGLEIN, A. B. 2004. Linear inversion for absorptive/dispersive medium parameters. In *74th Annual Internat. Mtg., Soc. Expl. Geophys., Expanded Abstracts.* Soc. Expl. Geophys., 1834–1837.

References

INNANEN, K. A. AND WEGLEIN, A. B. 2005. Towards non-linear construction of a Q-compensation operator directly from measured seismic reflection data. In *75th Annual Internat. Mtg., Soc. Expl. Geophys., Expanded Abstracts*. Soc. Expl. Geophys., 1693–1696.

KEYS, R. G. 1989. Polarity reversals in reflections from layered media. *Geophysics 54,* 900–905.

KEYS, R. G. AND FOSTER, D. J. 2006. Personal Communication.

KVAM, O. AND LANDRØ, M. 2005. Pore-pressure detection sensitivities tested with time-lapse seismic data. *Geophysics 70,* 6, O39–O50.

LANDRØ, M. 2001. Discrimination between pressure and fluid saturation changes from time-lapse seismic data. *Geophysics 66,* 3, 836–844.

LANDRØ, M. AND DUFFAUT, K. 2004. Vp-vs ratio versus effective pressure and rock consolidation – a comparison between rock models and time-lapse avo studies. In *74th Annual Internat. Mtg., Soc. Expl. Geophys., Expanded Abstracts*. Soc. Expl. Geophys.

LANDRØ, M., VEIRE, H. H., DUFFAUT, K., AND NAJJAR, N. 2003. Discrimination between pressure and fluid saturation changes from marine multicomponent time-lapse seismic data. *Geophysics 68,* 5, 1592–1599.

LIU, F., INNANEN, A. B. W. K. A., AND NITA, B. G. 2005. Extension of the non-linear depth imaging capability of the inverse scattering series to multidimensional media: strategies and numerical results. In *9th Ann. Cong. SBGf, Expanded Abstracts*. SBGf.

LIU, F., NITA, B. G., WEGLEIN, A. B., AND INNANEN, K. A. 2004. Inverse scattering series in the presence of lateral variations. *M-OSRP Annual Report 3.*

LIU, F. AND WEGLEIN, A. B. 2003. Initial analysis of the inverse scattering series for a variable background. *M-OSRP Annual Report 2,* 210–225.

References

MATSON, K. H. 1997. An inverse-scattering series method for attenuating elastic multiples from multicomponent land and ocean bottom seismic data. Ph.D. thesis, University of British Columbia.

PAFFENHOLZ, J., McLAIN, W. H., ZASKE, J., AND KELIHER, P. 2002. Subsalt multiple attenuation and imaging: Observations from the sigsbee2b synthetic dataset. In *72nd Annual Internat. Mtg., Soc. Expl. Geophys., Expanded Abstracts*. Soc. Expl. Geophys., 2122–2125.

PROSSER, R. T. 1964. Convergent perturbation expansions for certain wave operators. *Journal of Mathematical Physics 5,* 6, 708–713.

PROSSER, R. T. 1969. Formal solutions of inverse scattering problems. *Journal of Mathematical Physics 10,* 10, 1819–1822.

PROSSER, R. T. 1976. Formal solutions of inverse scattering problems II. *Journal of Mathematical Physics 17,* 10, 1775–1779.

PROSSER, R. T. 1980. Formal solutions of inverse scattering problems III. *Journal of Mathematical Physics 21,* 11, 2648–2653.

PROSSER, R. T. 1982. Formal solutions of inverse scattering problems IV. Error estimates. *Journal of Mathematical Physics 23,* 11, 2127–2130.

PROSSER, R. T. 1992. Formal solutions of inverse scattering problems V. *Journal of Mathematical Physics 33,* 10, 3493–3496.

RAMÍREZ, A. C. AND WEGLEIN, A. B. 2005. An inverse scattering internal multiple elimination method: Beyond attenuation, a new algorithm and initial tests. In *75th Annual Internat. Mtg., Soc. Expl. Geophys., Expanded Abstracts*. Soc. Expl. Geophys., 2115–2118.

SEN, M. AND STOFFA, P. L. 1995. *Global Optimization Methods in Geophysical Inversion.* Amsterdam: Elsevier.

SHAW, S. A. 2001. An inverse-scattering sub-series for predicting the correct spacial location of reflectors: Initial analysis, testing and evaluation. In *7th International Congress of the Brazilian Geophysical Society.*

SHAW, S. A. 2005. An inverse scattering series algorithm for depth imaging of reflection data from a layered acoustic medium with an unknown velocity model. Ph.D. thesis, University of Houston.

SHAW, S. A. AND WEGLEIN, A. B. 2003. Imaging seismic reflection data at the correct depth without specifying an accurate velocity model: Initial examples of an inverse scattering subseries. In *Frontiers of remote sensing information processing*, C. H. Chen, Ed. World Scientific Publishing Company, Chapter 21, 469–484.

SHAW, S. A. AND WEGLEIN, A. B. 2004. A leading order imaging series for prestack data acquired over a laterally invariant acoustic medium. Part II: Analysis for data missing low frequencies. *M-OSRP Annual Report 3.*

SHAW, S. A., WEGLEIN, A. B., FOSTER, D. J., MATSON, K. H., AND KEYS, R. G. 2003a. Convergence properties of a leading order depth imaging series. In *73rd Annual Internat. Mtg., Soc. Expl. Geophys., Expanded Abstracts.* Soc. Expl. Geophys., 937–940.

SHAW, S. A., WEGLEIN, A. B., FOSTER, D. J., MATSON, K. H., AND KEYS, R. G. 2003b. Isolation of a leading order depth imaging series and analysis of its convergence properties. *M-OSRP Annual Report 2*, 157–195.

SHAW, S. A., WEGLEIN, A. B., FOSTER, D. J., MATSON, K. H., AND KEYS, R. G. 2004. Isolation of a leading order depth imaging series and analysis of its convergence properties. *Journal of Seismic Exploration 2*, 157–195.

SHAW, S. A., WEGLEIN, A. B., MATSON, K. H., AND FOSTER, D. J. 2001. Understanding coefficients in the 1-D inverse scattering sub-series for imaging — Notes. *M-OSRP Annual Report 1*.

SHAW, S. A., WEGLEIN, A. B., MATSON, K. H., AND FOSTER, D. J. 2002. Cooperation of the leading order terms in an inverse-scattering subseries for imaging: 1-D analysis and evaluation. In *72nd Annual Internat. Mtg., Soc. Expl. Geophys., Expanded Abstracts*. Soc. Expl. Geophys., 2277–2280.

SHERIFF, R. E. AND GELDART, L. P. 1994. *Exploration seismology*, 2nd ed. Cambridge ; New York : Cambridge University Press.

STOLT, R. H. 1978. Migration by Fourier transform. *Geophysics 43,* 1, 23–48.

STOLT, R. H. AND WEGLEIN, A. B. 1985. Migration and inversion of seismic data. *Geophysics 50,* 12, 2458–2472.

STOVAS, A. AND LANDRø, M. 2005. Fluid-pressure discrimination in anisotropic reservoir rocks — a sensitivity study. *Geophysics 70,* 3, O1–O11.

TARANTOLA, A., NERCESSIAN, A., AND GAUTHIER, O. 1984. Nonlinear inversion of seismic reflection data. In *54rd Annual Internat. Mtg., Soc. Expl. Geophys., Expanded Abstracts*. Soc. Expl. Geophys., 645–649.

TAYLOR, J. R. 1972. *Scattering theory: the quantum theory of nonrelativistic collisions*. John Wiley & Sons, Inc.

TURA, A. AND LUMLEY, D. E. 1999. Estimating pressure and saturation changes from time-lapse avo data. In *69th Annual Internat. Mtg., Soc. Expl. Geophys., Expanded Abstracts*. Soc. Expl. Geophys.

VERSCHUUR, D. J. AND BERKHOUT, A. J. 1997. Estimation of multiple scattering by iterative inversion, part II: Practical aspects and examples. *Geophysics 62*, 1596–1611.

VERSCHUUR, D. J., BERKHOUT, A. J., AND WAPENAAR, C. P. A. 1992. Adaptive surface-related multiple elimination. *Geophysics 57*, 1166–1177.

WEGLEIN, A. B. 1999. Multiple attenuation: an overview of recent advances and the road ahead. *The Leading Edge*, 40–44.

WEGLEIN, A. B. 2006a. Introduction and overview: Mosrp05. *M-OSRP Annual Report 5*.

WEGLEIN, A. B. 2006b. Removing multiples and imaging and inverting primaries beneath a complex ill-defined overburden: defining and addressing the pressing seismic challenge. In *76th Annual Internat. Mtg., Soc. Expl. Geophys., Expanded Abstracts*. Soc. Expl. Geophys., 2639–2643.

WEGLEIN, A. B., ARAÚJO, F. V., CARVALHO, P. M., STOLT, R. H., MATSON, K. H., COATES, R. T., CORRIGAN, D., FOSTER, D. J., SHAW, S. A., AND ZHANG, H. 2003. Inverse scattering series and seismic exploration. *Inverse Problems 19*, R27–R83.

WEGLEIN, A. B. AND DRAGOSET, W. H. 2005. *Multiple Attenuation, Geophysics reprint series, No. 23*. Society of Exploration Geophysicists.

WEGLEIN, A. B., FOSTER, D. J., MATSON, K. H., SHAW, S. A., CARVALHO, P. M., AND CORRIGAN, D. 2001. An inverse-scattering sub-series for predicting the spatial location of reflectors without the precise reference medium and wave velocity. In *71st Annual Internat. Mtg., Soc. Expl. Geophys., Expanded Abstracts*. Soc. Expl. Geophys., 2108–2111.

WEGLEIN, A. B., FOSTER, D. J., MATSON, K. H., SHAW, S. A., CARVALHO, P. M., AND CORRIGAN, D. 2002. Predicting the correct spatial location of reflectors without knowing or determining the precise medium and wave velocity: initial concept, algorithm and analytic and numerical example. *Journal of Seismic Exploration 10*, 4, 367–382.

References

WEGLEIN, A. B., GASPAROTTO, F. A., CARVALHO, P. M., AND STOLT, R. H. 1997. An inverse-scattering series method for attenuating multiples in seismic reflection data. *Geophysics 62,* 6, 1975–1989.

WEGLEIN, A. B., MATSON, K. H., FOSTER, D. J., CARVALHO, P. M., CORRIGAN, D., AND SHAW, S. A. 2000. Imaging and inversion at depth without a velocity model: Theory, concepts and initial evaluation. In *70th Annual Internat. Mtg., Soc. Expl. Geophys., Expanded Abstracts.* Soc. Expl. Geophys., 1016–1019.

WEGLEIN, A. B. AND STOLT, R. H. 1992. Approaches on linear and non-linear migration-inversion. Personal Communication.

WEGLEIN, A. B., VIOLETTE, P. B., AND KEHO, T. H. 1986. Using multiparameter born theory to obtain certain exact multiparameter inversion goals. *Geophysics 51,* 1069–1074.

ZHANG, H. AND WEGLEIN, A. B. 2005. The inverse scattering series for tasks associated with primaries: Depth imaging and direct non-linear inversion of 1d variable velocity and density acoustic media. In *75th Annual Internat. Mtg., Soc. Expl. Geophys., Expanded Abstracts.* Soc. Expl. Geophys., 1705–1708.

ZHANG, H., WEGLEIN, A. B., AND KEYS, R. G. 2005. Velocity independent depth imaging and non-linear direct target identification for 1D elastic media: testing and evaluation for application to non-linear AVO, using only PP data. *M-OSRP Annual Report 4.*

APPENDICES

A. ACOUSTIC CASE

1 Derivation of α_1, β_1 and α_2, β_2

1. α_1 and β_1

Since

$$
\begin{aligned}
V_1(z, \nabla) &= \frac{\omega^2 \alpha_1(z)}{K_0} + \frac{1}{\rho_0} \beta_1(z) \frac{\partial^2}{\partial x^2} + \frac{1}{\rho_0} \frac{\partial}{\partial z} \beta_1(z) \frac{\partial}{\partial z} \\
&= \frac{1}{\rho_0} \left[k^2 \alpha_1(z) + \beta_1(z) \frac{\partial^2}{\partial x^2} + \frac{\partial}{\partial z} \beta_1(z) \frac{\partial}{\partial z} \right],
\end{aligned}
\tag{A.1}
$$

and

$$
D = G_0 V_1 G_0,
\tag{A.2}
$$

then, we have

$$
\begin{aligned}
D(x_g, z_g; x_s, z_s; \omega) = \frac{1}{\rho_0} \int\limits_{-\infty}^{+\infty} dx' \int\limits_{-\infty}^{+\infty} dz' G_0(x_g, z_g; x', z'; \omega) \\
\times \left[k^2 \alpha_1(z') + \beta_1(z') \frac{\partial^2}{\partial x'^2} + \frac{\partial}{\partial z'} \beta_1(z') \frac{\partial}{\partial z'} \right] G_0(x', z'; x_s, z_s; \omega).
\end{aligned}
\tag{A.3}
$$

Similar to the one parameter case, after the Fourier transform over x_g and x_s, Eq. (A.3) becomes

$$
\widetilde{D}(k_g, z_g; -k_s, z_s; \omega) = \frac{1}{\rho_0} \int\limits_{-\infty}^{+\infty} dx' \int\limits_{-\infty}^{+\infty} dz' \widetilde{G_0}(k_g, z_g; x', z'; \omega)
$$

110

$$\times \left[k^2 \alpha_1(z') - k_s^2 \beta_1(z') + \frac{\partial}{\partial z'} \beta_1(z') \frac{\partial}{\partial z'} \right] \widetilde{G_0}(x', z'; -k_s, z_s; \omega), \quad \text{(A.4)}$$

where (Suppose α_1 and β_1 are not zero only under the source and receiver.)

$$\widetilde{G_0}(k_g, z_g; x', z'; \omega) = \rho_0 e^{-ik_g x'} \frac{e^{iq_g(z'-z_g)}}{4\pi i q_g}, \quad \text{(A.5)}$$

$$\widetilde{G_0}(x', z'; -k_s, z_s; \omega) = \rho_0 e^{ik_s x'} \frac{e^{iq_s(z'-z_s)}}{4\pi i q_s}. \quad \text{(A.6)}$$

Then, Eq. (A.4) becomes

$$\widetilde{D}(k_g, z_g; -k_s, z_s; \omega)$$

$$= -\frac{\rho_0}{4 q_g q_s} \left(\frac{1}{2\pi} \right)^2 e^{-i(q_g z_g + q_s z_s)} \int_{-\infty}^{+\infty} dx' \int_{-\infty}^{+\infty} dz' e^{-i(k_g - k_s)x'} \left[k^2 \alpha_1(z') - k_s^2 \beta_1(z') \right] e^{i(q_g+q_s)z'}$$

$$- \frac{\rho_0}{4 q_g q_s} \left(\frac{1}{2\pi} \right)^2 e^{-i(q_g z_g + q_s z_s)} \int_{-\infty}^{+\infty} dx' \int_{-\infty}^{+\infty} dz' e^{-i(k_g - k_s)x'} e^{iq_g z'} \frac{\partial}{\partial z'} \beta_1(z') \frac{\partial}{\partial z'} e^{iq_s z'}. \quad \text{(A.7)}$$

After partial integration, where

$$\int_{-\infty}^{+\infty} dz' e^{iq_g z'} \frac{\partial}{\partial z'} \beta_1(z') \frac{\partial}{\partial z'} e^{iq_s z'} = q_g q_s \int_{-\infty}^{+\infty} dz' \beta_1(z') e^{i(q_g+q_s)z'},$$

then, we have

$$\widetilde{D}(q_g; z_g, z_s; \omega) = -\frac{\rho_0}{4} e^{-iq_g(z_g+z_s)} \left[\frac{k^2}{q_g^2} \widetilde{\alpha_1}(-2q_g) - \frac{k_g^2}{q_g^2} \widetilde{\beta_1}(-2q_g) + \widetilde{\beta_1}(-2q_g) \right]. \quad \text{(A.8)}$$

Similarly, using the relation $q_g = k \cos\theta$, Eq. (A.8) becomes

$$\widetilde{D}(q_g, \theta; z_g, z_s) = -\frac{\rho_0}{4} e^{-iq_g(z_g+z_s)} \left[\frac{1}{\cos^2\theta} \widetilde{\alpha_1}(-2q_g) + (1 - \tan^2\theta)\widetilde{\beta_1}(-2q_g) \right]. \quad \text{(A.9)}$$

This is Eq. (3.11).

2. α_2 and β_2

Since

$$
\begin{aligned}
V_2(z, \nabla) &= \frac{\omega^2 \alpha_2(z)}{K_0} + \frac{1}{\rho_0} \beta_2(z) \frac{\partial^2}{\partial x^2} + \frac{1}{\rho_0} \frac{\partial}{\partial z} \beta_2(z) \frac{\partial}{\partial z} \\
&= \frac{1}{\rho_0} \left[k^2 \alpha_2(z) + \beta_2(z) \frac{\partial^2}{\partial x^2} + \frac{\partial}{\partial z} \beta_2(z) \frac{\partial}{\partial z} \right],
\end{aligned} \tag{A.10}
$$

and

$$
G_0 V_2 G_0 = -G_0 V_1 G_0 V_1 G_0, \tag{A.11}
$$

then, we have

$$
\begin{aligned}
&\int\limits_{-\infty}^{+\infty} dx' \int\limits_{-\infty}^{+\infty} dz' G_0(x_g, z_g; x', z'; \omega) \left[k^2 \alpha_2(z') + \beta_2(z') \frac{\partial^2}{\partial x'^2} + \frac{\partial}{\partial z'} \beta_2(z') \frac{\partial}{\partial z'} \right] G_0(x', z'; x_s, z_s; \omega) \\
&= -\int\limits_{-\infty}^{+\infty} dx' \int\limits_{-\infty}^{+\infty} dz' \int\limits_{-\infty}^{+\infty} dx'' \int\limits_{-\infty}^{+\infty} dz'' G_0(x_g, z_g; x', z'; \omega) \left[k^2 \alpha_1(z') + \beta_1(z') \frac{\partial^2}{\partial x'^2} + \frac{\partial}{\partial z'} \beta_1(z') \frac{\partial}{\partial z'} \right] \\
&\quad \times G_0(x', z'; x'', z''; \omega) \left[k^2 \alpha_1(z'') + \beta_1(z'') \frac{\partial^2}{\partial x''^2} + \frac{\partial}{\partial z''} \beta_1(z'') \frac{\partial}{\partial z''} \right] \\
&\quad \times G_0(x'', z''; x_s, z_s; \omega).
\end{aligned} \tag{A.12}
$$

After the Fourier transform over x_g and x_s, Eq. (A.12) becomes (Suppose α_1 and β_1 is not zero only under the source and receiver.)

$$
\begin{aligned}
&\int\limits_{-\infty}^{+\infty} dz' \left[\frac{k^2}{q_g^2} \alpha_2(z') + \left(1 - \frac{k_g^2}{q_g^2} \right) \beta_2(z') \right] e^{2iq_g z'} \\
&= \frac{i}{2} \int\limits_{-\infty}^{+\infty} dz' \int\limits_{-\infty}^{+\infty} dz'' \frac{e^{iq_g z'}}{q_g} \left[k^2 \alpha_1(z') - k_g^2 \beta_1(z') + \frac{\partial}{\partial z'} \beta_1(z') \frac{\partial}{\partial z'} \right] \\
&\quad \times \frac{e^{iq_g |z' - z''|}}{q_g} \left[k^2 \alpha_1(z'') - k_g^2 \beta_1(z'') + \frac{\partial}{\partial z''} \beta_1(z'') \frac{\partial}{\partial z''} \right] \frac{e^{iq_g z''}}{q_g}
\end{aligned}
$$

$$
=\frac{i}{2q_g^3}\int\limits_{-\infty}^{+\infty}dz'\int\limits_{-\infty}^{+\infty}dz''\left[k^2\alpha_1(z')-k_g^2\beta_1(z')\right]\left[k^2\alpha_1(z'')-k_g^2\beta_1(z'')\right]e^{iq_g(z'+z'')}e^{iq_g|z'-z''|}
$$

$$
+\frac{i}{2q_g^3}\int\limits_{-\infty}^{+\infty}dz'\int\limits_{-\infty}^{+\infty}dz''e^{iq_gz'}\left[k^2\alpha_1(z')-k_g^2\beta_1(z')\right]e^{iq_g|z'-z''|}\frac{\partial}{\partial z''}\beta_1(z'')\frac{\partial}{\partial z''}e^{iq_gz''}
$$

$$
+\frac{i}{2q_g^3}\int\limits_{-\infty}^{+\infty}dz'\int\limits_{-\infty}^{+\infty}dz''e^{iq_gz'}\frac{\partial}{\partial z'}\beta_1(z')\frac{\partial}{\partial z'}e^{iq_g|z'-z''|}\left[k^2\alpha_1(z'')-k_g^2\beta_1(z'')\right]e^{iq_gz''}
$$

$$
+\frac{i}{2q_g^3}\int\limits_{-\infty}^{+\infty}dz'\int\limits_{-\infty}^{+\infty}dz''e^{iq_gz'}\frac{\partial}{\partial z'}\beta_1(z')\frac{\partial}{\partial z'}e^{iq_g|z'-z''|}\frac{\partial}{\partial z''}\beta_1(z'')\frac{\partial}{\partial z''}e^{iq_gz''}
$$

$$
=I_1+I_2+I_3+I_4. \tag{A.13}
$$

Then, after the Fourier transformation over $2q_g$ on both sides of Eq. (A.13) and divided by π, the left side becomes

$$
\frac{1}{\cos^2\theta}\alpha_2(z)+(1-\tan^2\theta)\beta_2(z).
$$

On the right side, where

$$
I_1=\frac{i}{2q_g^3}\int\limits_{-\infty}^{+\infty}dz'\int\limits_{-\infty}^{+\infty}dz''\left[k^2\alpha_1(z')-k_g^2\beta_1(z')\right]\left[k^2\alpha_1(z'')-k_g^2\beta_1(z'')\right]e^{iq_g(z'+z'')}e^{iq_g|z'-z''|}
$$

$$
=\frac{i}{q_g^3}\int\limits_{-\infty}^{+\infty}dz'\int\limits_{-\infty}^{+\infty}dz''\left[k^2\alpha_1(z')-k_g^2\beta_1(z')\right]\left[k^2\alpha_1(z'')-k_g^2\beta_1(z'')\right]e^{2iq_gz'}H(z'-z'')
$$

$$
=iq_g\int\limits_{-\infty}^{+\infty}dz'\int\limits_{-\infty}^{+\infty}dz''\left[\frac{k^2}{q_g^2}\alpha_1(z')-\frac{k_g^2}{q_g^2}\beta_1(z')\right]\left[\frac{k^2}{q_g^2}\alpha_1(z'')-\frac{k_g^2}{q_g^2}\beta_1(z'')\right]e^{2iq_gz'}H(z'-z'')
$$

$$
=iq_g\int\limits_{-\infty}^{+\infty}dz'\int\limits_{-\infty}^{+\infty}dz''\left[\frac{1}{\cos^2\theta}\alpha_1(z')-\tan^2\theta\beta_1(z')\right]\left[\frac{1}{\cos^2\theta}\alpha_1(z'')-\tan^2\theta\beta_1(z'')\right]
$$

$$
\times e^{2iq_gz'}H(z'-z''),
$$

<div align="center">113</div>

then, after the Fourier transformation over $2q_g$ and divided by π, I_1 becomes

$$\widetilde{I_1} = -\frac{1}{2}\frac{\partial}{\partial z}\int\limits_{-\infty}^{+\infty}dz'\int\limits_{-\infty}^{+\infty}dz''\left[\frac{1}{\cos^2\theta}\alpha_1(z') - \tan^2\theta\beta_1(z')\right]\left[\frac{1}{\cos^2\theta}\alpha_1(z'') - \tan^2\theta\beta_1(z'')\right]$$

$$\times \delta(z-z')H(z'-z'')$$

$$= -\frac{1}{2}\frac{\partial}{\partial z}\left\{\left[\frac{1}{\cos^2\theta}\alpha_1(z) - \tan^2\theta\beta_1(z)\right]\int\limits_{-\infty}^{+\infty}dz''\left[\frac{1}{\cos^2\theta}\alpha_1(z'') - \tan^2\theta\beta_1(z'')\right]H(z-z'')\right\}$$

$$= -\frac{1}{2}\left[\frac{1}{\cos^2\theta}\alpha_1(z) - \tan^2\theta\beta_1(z)\right]^2$$

$$-\frac{1}{2}\left[\frac{1}{\cos^2\theta}\alpha_1'(z) - \tan^2\theta\beta_1'(z)\right]\int\limits_{-\infty}^{z}dz'\left[\frac{1}{\cos^2\theta}\alpha_1(z') - \tan^2\theta\beta_1(z')\right]$$

$$= -\frac{1}{2\cos^4\theta}\alpha_1^2(z) - \frac{\tan^4\theta}{2}\beta_1^2(z) + \frac{\tan^2\theta}{\cos^2\theta}\alpha_1(z)\beta_1(z)$$

$$-\frac{1}{2\cos^4\theta}\alpha_1'(z)\int\limits_{-\infty}^{z}dz'\alpha_1(z') - \frac{\tan^4\theta}{2}\beta_1'(z)\int\limits_{-\infty}^{z}dz'\beta_1(z')$$

$$+\frac{\tan^2\theta}{2\cos^2\theta}\alpha_1'(z)\int\limits_{-\infty}^{z}dz'\beta_1(z') + \frac{\tan^2\theta}{2\cos^2\theta}\beta_1'(z)\int\limits_{-\infty}^{z}dz'\alpha_1(z'),$$

and

$$I_2 = \frac{i}{2q_g^3}\int\limits_{-\infty}^{+\infty}dz'\int\limits_{-\infty}^{+\infty}dz''e^{iq_gz'}\left[k^2\alpha_1(z') - k_g^2\beta_1(z')\right]e^{iq_g|z'-z''|}\frac{\partial}{\partial z''}\beta_1(z'')\frac{\partial}{\partial z''}e^{iq_gz''}$$

$$= \frac{i}{2q_g^3}\int\limits_{-\infty}^{+\infty}dz'\int\limits_{-\infty}^{+\infty}dz''e^{iq_gz'}\left[k^2\alpha_1(z') - k_g^2\beta_1(z')\right]$$

$$\times e^{iq_g|z'-z''|}\left[(iq_g)^2\beta_1(z'')e^{iq_gz''} + iq_g\beta_1'(z'')e^{iq_gz''}\right]$$

$$= -\frac{iq_g}{2\cos^2\theta}\int\limits_{-\infty}^{+\infty}dz'\int\limits_{-\infty}^{+\infty}dz''\alpha_1(z')\beta_1(z'')\left[e^{2iq_gz'}H(z'-z'') + e^{2iq_gz''}H(z''-z')\right]$$

$$+ iq_g\tan^2\theta\int\limits_{-\infty}^{+\infty}dz'\int\limits_{-\infty}^{+\infty}dz''\beta_1(z')\beta_1(z'')e^{2iq_gz'}H(z'-z'')$$

114

$$
-\frac{1}{2\cos^2\theta}\int\limits_{-\infty}^{+\infty}dz'\int\limits_{-\infty}^{+\infty}dz''\alpha_1(z')\beta_1'(z'')\left[e^{2iq_gz'}H(z'-z'')+e^{2iq_gz''}H(z''-z')\right]
$$

$$
+\frac{\tan^2\theta}{2}\int\limits_{-\infty}^{+\infty}dz'\int\limits_{-\infty}^{+\infty}dz''\beta_1(z')\beta_1'(z'')\left[e^{2iq_gz'}H(z'-z'')+e^{2iq_gz''}H(z''-z')\right],
$$

then, after the Fourier transformation over $2q_g$ and divided by π, I_2 becomes

$$
\widetilde{I_2}=\frac{1}{4\cos^2\theta}\alpha_1'(z)\int\limits_{-\infty}^{z}dz'\beta_1(z')+\frac{1}{4\cos^2\theta}\beta_1'(z)\int\limits_{-\infty}^{z}dz'\alpha_1(z')+\frac{1}{2\cos^2\theta}\alpha_1(z)\beta_1(z)
$$

$$
-\frac{\tan^2\theta}{2}\beta_1^2(z)-\frac{\tan^2\theta}{2}\beta_1'(z)\int\limits_{-\infty}^{z}dz'\beta_1(z')
$$

$$
-\frac{1}{2\cos^2\theta}\alpha_1(z)\beta_1(z)-\frac{1}{2\cos^2\theta}\beta_1'(z)\int\limits_{-\infty}^{z}dz'\alpha_1(z')
$$

$$
+\frac{\tan^2\theta}{2}\beta_1^2(z)+\frac{\tan^2\theta}{2}\beta_1'(z)\int\limits_{-\infty}^{z}dz'\beta_1(z')
$$

$$
=\frac{1}{4\cos^2\theta}\alpha_1'(z)\int\limits_{-\infty}^{z}dz'\beta_1(z')-\frac{1}{4\cos^2\theta}\beta_1'(z)\int\limits_{-\infty}^{z}dz'\alpha_1(z'),
$$

and

$$
I_3=\frac{i}{2q_g^3}\int\limits_{-\infty}^{+\infty}dz'\int\limits_{-\infty}^{+\infty}dz''e^{iq_gz'}\frac{\partial}{\partial z'}\beta_1(z')\frac{\partial}{\partial z'}e^{iq_g|z'-z''|}\left[k^2\alpha_1(z'')-k_g^2\beta_1(z'')\right]e^{iq_gz''}
$$

$$
=\frac{i}{2q_g^3}\int\limits_{-\infty}^{+\infty}dz'\int\limits_{-\infty}^{+\infty}dz''e^{iq_gz'}\frac{\partial}{\partial z'}\left[\beta_1(z')iq_gsign(z'-z'')e^{iq_g|z'-z''|}\right]\left[k^2\alpha_1(z'')-k_g^2\beta_1(z'')\right]e^{iq_gz''}
$$

$$
=\frac{i}{2q_g^3}\int\limits_{-\infty}^{+\infty}dz'\int\limits_{-\infty}^{+\infty}dz''\left[\beta_1'(z')iq_gsign(z'-z'')e^{iq_g|z'-z''|}+\beta_1(z')2iq_g\delta(z'-z'')\right.
$$

$$
\left.+\beta_1(z')(iq_g)^2e^{iq_g|z'-z''|}\right]\left[k^2\alpha_1(z'')-k_g^2\beta_1(z'')\right]e^{iq_g(z'+z'')}
$$

$$
=-\frac{1}{2}\int\limits_{-\infty}^{+\infty}dz'\int\limits_{-\infty}^{+\infty}dz''\beta_1'(z')\left[\frac{1}{\cos^2\theta}\alpha_1(z'')-\tan^2\theta\beta_1(z'')\right]
$$

$$\times \left[e^{2iq_g z'} H(z' - z'') - e^{2iq_g z''} H(z'' - z') \right]$$

$$- \int\limits_{-\infty}^{+\infty} dz' \beta_1(z') \left[\frac{1}{\cos^2 \theta} \alpha_1(z') - \tan^2 \theta \beta_1(z') \right] e^{2iq_g z'}$$

$$- \frac{iq_g}{2} \int\limits_{-\infty}^{+\infty} dz' \int\limits_{-\infty}^{+\infty} dz'' \beta_1(z') \left[\frac{1}{\cos^2 \theta} \alpha_1(z'') - \tan^2 \theta \beta_1(z'') \right]$$

$$\times \left[e^{2iq_g z'} H(z' - z'') + e^{2iq_g z''} H(z'' - z') \right],$$

then, after the Fourier transformation over $2q_g$ and divided by π, I_3 becomes

$$\widetilde{I_3} = - \frac{1}{2 \cos^2 \theta} \beta_1'(z) \int\limits_{-\infty}^{z} dz' \alpha_1(z') + \frac{1}{2} \tan^2 \theta \beta_1'(z) \int\limits_{-\infty}^{z} dz' \beta_1(z') + \frac{1}{2 \cos^2 \theta} \alpha_1(z) \beta_1(z)$$

$$- \frac{1}{2} \tan^2 \theta \beta_1^2(z) - \frac{1}{\cos^2 \theta} \alpha_1(z) \beta_1(z) + \tan^2 \theta \beta_1^2(z)$$

$$+ \frac{1}{4 \cos^2 \theta} \beta_1'(z) \int\limits_{-\infty}^{z} dz' \alpha_1(z') + \frac{1}{4 \cos^2 \theta} \alpha_1'(z) \int\limits_{-\infty}^{z} dz' \beta_1(z') + \frac{1}{2 \cos^2 \theta} \alpha_1(z) \beta_1(z)$$

$$- \frac{1}{2} \tan^2 \theta \beta_1'(z) \int\limits_{-\infty}^{z} dz' \beta_1(z') - \frac{1}{2} \tan^2 \theta \beta_1^2(z)$$

$$= - \frac{1}{4 \cos^2 \theta} \beta_1'(z) \int\limits_{-\infty}^{z} dz' \alpha_1(z')$$

$$+ \frac{1}{4 \cos^2 \theta} \alpha_1'(z) \int\limits_{-\infty}^{z} dz' \beta_1(z'),$$

and

$$I_4 = \frac{i}{2q_g^3} \int\limits_{-\infty}^{+\infty} dz' \int\limits_{-\infty}^{+\infty} dz'' e^{iq_g z'} \frac{\partial}{\partial z'} \beta_1(z') \frac{\partial}{\partial z'} e^{iq_g |z' - z''|} \frac{\partial}{\partial z''} \beta_1(z'') \frac{\partial}{\partial z''} e^{iq_g z''}$$

$$= \frac{i}{2q_g^3} \int\limits_{-\infty}^{+\infty} dz' \int\limits_{-\infty}^{+\infty} dz'' e^{iq_g z'} \frac{\partial}{\partial z'} \beta_1(z') \frac{\partial}{\partial z'} e^{iq_g |z' - z''|} \left[(iq_g)^2 \beta_1(z'') e^{iq_g z''} + iq_g \beta_1'(z'') e^{iq_g z''} \right]$$

$$=\frac{i}{2q_g^3}\int\limits_{-\infty}^{+\infty}dz'\int\limits_{-\infty}^{+\infty}dz''e^{iq_gz'}\frac{\partial}{\partial z'}\beta_1(z')\left[iq_g sign(z'-z'')e^{iq_g|z'-z''|}\right]$$

$$\times\left[(iq_g)^2\beta_1(z'')e^{iq_gz''}+iq_g\beta_1'(z'')e^{iq_gz''}\right]$$

$$=\frac{i}{2q_g^3}\int\limits_{-\infty}^{+\infty}dz'\int\limits_{-\infty}^{+\infty}dz''e^{iq_g(z'+z'')}\beta_1(z')\left[(iq_g)^2e^{iq_g|z'-z''|}+2iq_g\delta(z'-z'')\right]$$

$$\times\left[(iq_g)^2\beta_1(z'')+iq_g\beta_1'(z'')\right]$$

$$+\frac{i}{2q_g^3}\int\limits_{-\infty}^{+\infty}dz'\int\limits_{-\infty}^{+\infty}dz''e^{iq_g(z'+z'')}\beta_1'(z')\left[iq_g sign(z'-z'')e^{iq_g|z'-z''|}\right]$$

$$\times\left[(iq_g)^2\beta_1(z'')+iq_g\beta_1'(z'')\right]$$

$$=iq_g\int\limits_{-\infty}^{+\infty}dz'\int\limits_{-\infty}^{+\infty}dz''\beta_1(z')\beta_1(z'')e^{2iq_gz'}H(z'-z'')$$

$$+\frac{1}{2}\int\limits_{-\infty}^{+\infty}dz'\int\limits_{-\infty}^{+\infty}dz''\beta_1(z')\beta_1'(z'')\left[e^{2iq_gz'}H(z'-z'')+e^{2iq_gz''}H(z''-z')\right]$$

$$+\int\limits_{-\infty}^{+\infty}dz'\beta_1^2(z')e^{2iq_gz'}$$

$$-\frac{i}{q_g}\int\limits_{-\infty}^{+\infty}dz'\beta_1'(z')\beta_1(z')e^{2iq_gz'}$$

$$+\frac{1}{2}\int\limits_{-\infty}^{+\infty}dz'\int\limits_{-\infty}^{+\infty}dz''\beta_1'(z')\beta_1(z'')\left[e^{2iq_gz'}H(z'-z'')-e^{2iq_gz''}H(z''-z')\right],$$

then, after the Fourier transformation over $2q_g$ and divided by π, I_4 becomes

$$\widetilde{I_4}=-\frac{1}{2}\beta_1^2(z)-\frac{1}{2}\beta_1'(z)\int\limits_{-\infty}^{z}dz'\beta_1(z')$$

$$+\frac{1}{2}\beta_1^2(z)+\frac{1}{2}\beta_1'(z)\int\limits_{-\infty}^{z}dz'\beta_1(z')$$

$$+\beta_1^2(z)$$

$$- \beta_1^2(z)$$

$$+ \frac{1}{2}\beta_1'(z) \int_{-\infty}^{z} dz'\beta_1(z') - \frac{1}{2}\beta_1^2(z)$$

$$= -\frac{1}{2}\beta_1^2(z) + \frac{1}{2}\beta_1'(z) \int_{-\infty}^{z} dz'\beta_1(z'),$$

where we use

$$\frac{1}{\pi} \int_{-\infty}^{+\infty} dz' \int_{-\infty}^{+\infty} dq_g \left(-\frac{i}{q_g}\right) \beta_1'(z')\beta_1(z')e^{2iq_g(z'-z)}$$

$$= -2 \int_{-\infty}^{z} dz'\beta_1'(z')\beta_1(z') = -\beta_1^2(z).$$

Then, the right side should be:

$$\widetilde{I}_1 + \widetilde{I}_2 + \widetilde{I}_3 + \widetilde{I}_4$$

$$= -\frac{1}{2\cos^4\theta}\alpha_1^2(z) - \frac{\tan^4\theta}{2}\beta_1^2(z) + \frac{\tan^2\theta}{\cos^2\theta}\alpha_1(z)\beta_1(z)$$

$$- \frac{1}{2\cos^4\theta}\alpha_1'(z) \int_{-\infty}^{z} dz'\alpha_1(z') - \frac{\tan^4\theta}{2}\beta_1'(z) \int_{-\infty}^{z} dz'\beta_1(z')$$

$$+ \frac{\tan^2\theta}{2\cos^2\theta}\alpha_1'(z) \int_{-\infty}^{z} dz'\beta_1(z') + \frac{\tan^2\theta}{2\cos^2\theta}\beta_1'(z) \int_{-\infty}^{z} dz'\alpha_1(z')$$

$$+ \frac{1}{4\cos^2\theta}\alpha_1'(z) \int_{-\infty}^{z} dz'\beta_1(z') - \frac{1}{4\cos^2\theta}\beta_1'(z) \int_{-\infty}^{z} dz'\alpha_1(z')$$

$$- \frac{1}{4\cos^2\theta}\beta_1'(z) \int_{-\infty}^{z} dz'\alpha_1(z') + \frac{1}{4\cos^2\theta}\alpha_1'(z) \int_{-\infty}^{z} dz'\beta_1(z')$$

$$- \frac{1}{2}\beta_1^2(z) + \frac{1}{2}\beta_1'(z) \int_{-\infty}^{z} dz'\beta_1(z')$$

$$= -\frac{1}{2\cos^4\theta}\alpha_1^2(z) - \frac{1}{2}(1 + \tan^4\theta)\beta_1^2(z) + \frac{\tan^2\theta}{\cos^2\theta}\alpha_1(z)\beta_1(z)$$

118

$$-\frac{1}{2\cos^4\theta}\alpha_1'(z)\int_{-\infty}^{z}dz'[\alpha_1(z')-\beta_1(z')]$$

$$+\frac{1}{2}(\tan^4\theta-1)\beta_1'(z)\int_{-\infty}^{z}dz'[\alpha_1(z')-\beta_1(z')].$$

After letting left side = right side, we have

$$\frac{1}{\cos^2\theta}\alpha_2(z)+(1-\tan^2\theta)\beta_2(z)$$

$$=-\frac{1}{2\cos^4\theta}\alpha_1^2(z)-\frac{1}{2}(1+\tan^4\theta)\beta_1^2(z)+\frac{\tan^2\theta}{\cos^2\theta}\alpha_1(z)\beta_1(z)$$

$$-\frac{1}{2\cos^4\theta}\alpha_1'(z)\int_{-\infty}^{z}dz'[\alpha_1(z')-\beta_1(z')]$$

$$+\frac{1}{2}(\tan^4\theta-1)\beta_1'(z)\int_{-\infty}^{z}dz'[\alpha_1(z')-\beta_1(z')]. \tag{A.14}$$

This is Eq. (3.12).

2 Expressing $\left(\frac{\Phi c}{c}\right)_1$, $\left(\frac{\Phi c}{c}\right)_2$, $\left(\frac{\Phi I}{I}\right)_1$ and $\left(\frac{\Phi I}{I}\right)_2$ in terms of α_1, β_1 and α_2, β_2

The following is the derivation of writing $\left(\frac{\Delta c}{c}\right)_1$, $\left(\frac{\Delta c}{c}\right)_2$, $\left(\frac{\Delta I}{I}\right)_1$ and $\left(\frac{\Delta I}{I}\right)_2$ in terms of α_1, β_1 and α_2, β_2. Define $\Delta c=c-c_0$, $\Delta I=I-I_0$, $\Delta K=K-K_0$ and $\Delta\rho=\rho-\rho_0$.

Since $K=c^2\rho$, then we have

$$(c-\Delta c)^2=\frac{K-\Delta K}{\rho-\Delta\rho}.$$

Divided by c^2, the equation above will become

$$2\left(\frac{\Delta c}{c}\right)-\left(\frac{\Delta c}{c}\right)^2=\frac{\frac{\Delta K}{K}-\frac{\Delta\rho}{\rho}}{1-\frac{\Delta\rho}{\rho}}.$$

Remember that $\alpha = \frac{\Delta K}{K}$ and $\beta = \frac{\Delta \rho}{\rho}$, the equation above can be rewritten as

$$2\left(\frac{\Delta c}{c}\right) - \left(\frac{\Delta c}{c}\right)^2 = \frac{\alpha - \beta}{1 - \beta}.$$

Then we have

$$2\left(\frac{\Delta c}{c}\right) - \left(\frac{\Delta c}{c}\right)^2 = (\alpha - \beta)(1 + \beta + \beta^2 + \cdots), \tag{A.15}$$

where the series expansion is valid for $|\beta| < 1$.

Similar to Eqs. (3.7) and (3.8), $\frac{\Delta c}{c}$ can be expanded as

$$\left(\frac{\Delta c}{c}\right) = \left(\frac{\Delta c}{c}\right)_1 + \left(\frac{\Delta c}{c}\right)_2 + \cdots. \tag{A.16}$$

Then substitute Eqs. (A.16), (3.7) and (3.8) into Eq. (A.15), and set those terms of equal order equal on both sides of Eq. (A.15), we can get

$$\left(\frac{\Delta c}{c}\right)_1 = \frac{1}{2}(\alpha_1 - \beta_1), \tag{A.17}$$

and

$$\left(\frac{\Delta c}{c}\right)_2 = \frac{1}{2}\left[\frac{1}{4}(\alpha_1 + \beta_1)^2 - \beta_1^2 + (\alpha_2 - \beta_2)\right]. \tag{A.18}$$

Similarly, using $I = c\rho$, we have

$$(I - \Delta I)^2 = (K - \Delta K)(\rho - \Delta \rho).$$

Divided by I^2, the equation above will become

$$2\left(\frac{\Delta I}{I}\right) - \left(\frac{\Delta I}{I}\right)^2 = \alpha + \beta - \alpha\beta. \tag{A.19}$$

120

Expanding $\frac{\Delta I}{I}$ as

$$\left(\frac{\Delta I}{I}\right) = \left(\frac{\Delta I}{I}\right)_1 + \left(\frac{\Delta I}{I}\right)_2 + \cdots , \qquad (A.20)$$

and substitute Eqs. (A.20), (3.7) and (3.8) into Eq. (A.19), setting those terms of equal order equal on both sides of Eq. (A.19), we can get

$$\left(\frac{\Delta I}{I}\right)_1 = \frac{1}{2}(\alpha_1 + \beta_1), \qquad (A.21)$$

and

$$\left(\frac{\Delta I}{I}\right)_2 = \frac{1}{2}\left[\frac{1}{4}(\alpha_1 - \beta_1)^2 + (\alpha_2 + \beta_2)\right]. \qquad (A.22)$$

3   Showing $\left(\frac{\Delta c}{c}\right)_1$ having the same sign as Δc

For the single interface example, from Eq. (3.25), we have

$$\left(\frac{\Delta c}{c}\right)_1 = 2\frac{R(\theta_1) - R(\theta_2)}{\tan^2 \theta_1 - \tan^2 \theta_2}.$$

The reflection coefficient is

$$R(\theta) = \frac{(\rho_1/\rho_0)(c_1/c_0)\sqrt{1 - \sin^2 \theta} - \sqrt{1 - (c_1^2/c_0^2)\sin^2 \theta}}{(\rho_1/\rho_0)(c_1/c_0)\sqrt{1 - \sin^2 \theta} + \sqrt{1 - (c_1^2/c_0^2)\sin^2 \theta}}.$$

Let

$$A(\theta) = (\rho_1/\rho_0)(c_1/c_0)\sqrt{1 - \sin^2 \theta},$$

$$B(\theta) = \sqrt{1 - (c_1^2/c_0^2)\sin^2 \theta}.$$

Then

$$R(\theta_1) - R(\theta_2) = 2\frac{A(\theta_1)B(\theta_2) - B(\theta_1)A(\theta_2)}{[A(\theta_1) + B(\theta_1)][A(\theta_2) + B(\theta_2)]},$$

where the denominator is greater than zero. The numerator is

$$2\left[A(\theta_1)B(\theta_2) - B(\theta_1)A(\theta_2)\right] = 2(\rho_1/\rho_0)(c_1/c_0)\left[\sqrt{1 - \sin^2\theta_1}\sqrt{1 - (c_1^2/c_0^2)\sin^2\theta_2}\right.$$
$$\left. - \sqrt{1 - \sin^2\theta_2}\sqrt{1 - (c_1^2/c_0^2)\sin^2\theta_1}\right].$$

Let

$$C = \sqrt{1 - \sin^2\theta_1}\sqrt{1 - (c_1^2/c_0^2)\sin^2\theta_2},$$

$$D = \sqrt{1 - \sin^2\theta_2}\sqrt{1 - (c_1^2/c_0^2)\sin^2\theta_1}.$$

Then,

$$C^2 - D^2 = \left(\frac{c_1^2}{c_0^2} - 1\right)(sin^2\theta_1 - sin^2\theta_2).$$

When $c_1 > c_0$ and $\theta_1 > \theta_2$, we have (Noticing that both C and D are positive.)

$$\left(\frac{c_1^2}{c_0^2} - 1\right)(sin^2\theta_1 - sin^2\theta_2) > 0,$$

so

$$R(\theta_1) - R(\theta_2) > 0;$$

Similarly, when $c_1 < c_0$ and $\theta_1 > \theta_2$, we have

$$\left(\frac{c_1^2}{c_0^2} - 1\right)(sin^2\theta_1 - sin^2\theta_2) < 0,$$

so

$$R(\theta_1) - R(\theta_2) < 0.$$

Remembering that $\left(\frac{\Delta c}{c}\right)_1 = 2\frac{R(\theta_1) - R(\theta_2)}{\tan^2\theta_1 - \tan^2\theta_2}$. So for $c_1 > c_0$, $(\Delta c)_1 > 0$ and for $c_1 < c_0$, $(\Delta c)_1 < 0$.

B. ELASTIC CASE

1 Background for elastic 2D wave equation

For an isotropic solid, the relations between stress and strain are (Sheriff and Geldart, 1994)

$$
\begin{pmatrix} \sigma_{xx} \\ \sigma_{yy} \\ \sigma_{zz} \\ \sigma_{xy} \\ \sigma_{yz} \\ \sigma_{zx} \end{pmatrix} = \begin{pmatrix} \lambda + 2\mu & \lambda & \lambda & 0 & 0 & 0 \\ \lambda & \lambda + 2\mu & \lambda & 0 & 0 & 0 \\ \lambda & \lambda & \lambda + 2\mu & 0 & 0 & 0 \\ 0 & 0 & 0 & \mu & 0 & 0 \\ 0 & 0 & 0 & 0 & \mu & 0 \\ 0 & 0 & 0 & 0 & 0 & \mu \end{pmatrix} \begin{pmatrix} \epsilon_{xx} \\ \epsilon_{yy} \\ \epsilon_{zz} \\ \epsilon_{xy} \\ \epsilon_{yz} \\ \epsilon_{zx} \end{pmatrix}
$$

The six components of strain, in terms of displacements, are $\epsilon_{xx} = \frac{\partial u_x}{\partial x}$, $\epsilon_{yy} = \frac{\partial u_y}{\partial y}$, $\epsilon_{zz} = \frac{\partial u_z}{\partial z}$, $\epsilon_{xy} = \epsilon_{yx} = \frac{\partial u_x}{\partial y} + \frac{\partial u_y}{\partial x}$, $\epsilon_{yz} = \epsilon_{zy} = \frac{\partial u_y}{\partial z} + \frac{\partial u_z}{\partial y}$, $\epsilon_{zx} = \epsilon_{xz} = \frac{\partial u_z}{\partial x} + \frac{\partial u_x}{\partial z}$. The equations of motion for an isotropic solid are (Body forces are set to zero.):

$$
\frac{\partial \sigma_{xx}}{\partial x} + \frac{\partial \sigma_{xy}}{\partial y} + \frac{\partial \sigma_{zx}}{\partial z} = \rho \frac{\partial^2 u_x}{\partial t^2},
$$

$$
\frac{\partial \sigma_{xy}}{\partial x} + \frac{\partial \sigma_{yy}}{\partial y} + \frac{\partial \sigma_{yz}}{\partial z} = \rho \frac{\partial^2 u_y}{\partial t^2},
$$

$$
\frac{\partial \sigma_{zx}}{\partial x} + \frac{\partial \sigma_{yz}}{\partial y} + \frac{\partial \sigma_{zz}}{\partial z} = \rho \frac{\partial^2 u_z}{\partial t^2},
$$

then, the 2D (x,z) equations of motion in terms of displacement are:

$$\rho\omega^2 u_x + \frac{\partial}{\partial x}(\lambda + 2\mu)\frac{\partial u_x}{\partial x} + \frac{\partial}{\partial z}\mu\frac{\partial u_x}{\partial z} + \frac{\partial}{\partial x}\lambda\frac{\partial u_z}{\partial z} + \frac{\partial}{\partial z}\mu\frac{\partial u_z}{\partial x} = 0,$$

$$\rho\omega^2 u_z + \frac{\partial}{\partial z}\lambda\frac{\partial u_x}{\partial x} + \frac{\partial}{\partial x}\mu\frac{\partial u_x}{\partial z} + \frac{\partial}{\partial z}(\lambda + 2\mu)\frac{\partial u_z}{\partial z} + \frac{\partial}{\partial x}\mu\frac{\partial u_z}{\partial x} = 0,$$

where $\lambda + 2\mu = \rho\alpha^2 = \gamma$, $\mu = \rho\beta^2$.

2 Derivation of $R_{pp}, R_{ps}, T_{pp}, T_{ps}, R_{sp}$ and R_{ss}

1. Derivation of R_{pp}, R_{ps}, T_{pp} and T_{ps}

Non-normal incidence of P-plane wave on a horizontal interface between two elastic solids will generate four independent propagating waves, the reflected P-wave (R_{pp}), the reflected shear wave (R_{ps}), the transmitted P-wave (T_{pp}) and the transmitted shear wave (T_{ps}). The incident P-wave and the resulting reflected and transmitted waves are shown in Fig. 4.1 of Chapter 4. The amplitudes (coefficients) of these waves are given by the conditions that the normal and tangential components of stress and displacement must be continuous across the boundary between the two elastic solids. From these boundary conditions, four equations are derived for the coefficients of the four plane waves (See e.g., Achenbach, 1973; Sheriff and Geldart, 1994; Foster $et\ al.$, 1997). In matrix form, the four equations are

$$M\begin{bmatrix} R_{pp} \\ R_{ps} \\ T_{pp} \\ T_{ps} \end{bmatrix} = \begin{bmatrix} x \\ \sqrt{1-x^2} \\ 2b^2 x\sqrt{1-x^2} \\ 1 - 2b^2 x^2 \end{bmatrix}, \tag{B.1}$$

where M is the matrix

$$
\begin{bmatrix}
-x & -\sqrt{1-b^2x^2} & cx & -\sqrt{1-d^2x^2} \\
\sqrt{1-x^2} & -bx & \sqrt{1-c^2x^2} & dx \\
2b^2x\sqrt{1-x^2} & b(1-2b^2x^2) & 2ad^2x\sqrt{1-c^2x^2} & -ad(1-2d^2x^2) \\
-(1-2b^2x^2) & 2b^2x\sqrt{1-b^2x^2} & ac(1-2d^2x^2) & 2ad^2x\sqrt{1-d^2x^2}
\end{bmatrix},
\tag{B.2}
$$

$$
a = \rho_2/\rho_1, \; b = \beta_1/\alpha_1, \; c = \alpha_2/\alpha_1, \; d = \beta_2/\alpha_1 \; and \; x = sin\theta.
$$

The angle θ is the angle of incidence measured counter-clockwise from the normal to the reflecting boundary.

Let D denote the determinant of M, and let N_{Rpp} be the determinant of the matrix obtained by replacing the first column of M with the vector on the right hand side of Eq. (B.1). The compressional wave reflection coefficient is given by $R_{pp} = N_{Rpp}/D$, where

$$
\begin{aligned}
N_{Rpp} = &- (1+2kx^2)^2 b\sqrt{1-c^2x^2}\sqrt{1-d^2x^2} - (1-a+2kx^2)^2 bcdx^2 \\
&+ (a-2kx^2)^2 cd\sqrt{1-x^2}\sqrt{1-b^2x^2} \\
&+ 4k^2x^2\sqrt{1-x^2}\sqrt{1-b^2x^2}\sqrt{1-c^2x^2}\sqrt{1-d^2x^2} - ad\sqrt{1-b^2x^2}\sqrt{1-c^2x^2} \\
&+ abc\sqrt{1-x^2}\sqrt{1-d^2x^2}.
\end{aligned}
\tag{B.3}
$$

$$
\begin{aligned}
D = &(1+2kx^2)^2 b\sqrt{1-c^2x^2}\sqrt{1-d^2x^2} + (1-a+2kx^2)^2 bcdx^2 \\
&+ (a-2kx^2)^2 cd\sqrt{1-x^2}\sqrt{1-b^2x^2} \\
&+ 4k^2x^2\sqrt{1-x^2}\sqrt{1-b^2x^2}\sqrt{1-c^2x^2}\sqrt{1-d^2x^2} + ad\sqrt{1-b^2x^2}\sqrt{1-c^2x^2} \\
&+ abc\sqrt{1-x^2}\sqrt{1-d^2x^2},
\end{aligned}
\tag{B.4}
$$

where $k = ad^2 - b^2$.

D is positive for all precritical angles of incidence; i.e., for all $|x|$ less than or equal to the

minimum of 1 and $1/c$. N is real over the same range of angles. Therefore, the compressional wave reflection coefficient is real and continuous for all precritical angles of incidence.

Let N_{Rps} be the determinant of the matrix obtained by replacing the second column of M with the vector on the right hand side of Eq. (B.1). The shear wave reflection coefficient is given by $R_{ps} = N_{Rps}/D$. Where

$$
\begin{aligned}
N_{Rps} = & -4kx(1+2kx^2)\sqrt{1-x^2}\sqrt{1-c^2x^2}\sqrt{1-d^2x^2} \\
& -2cdx(2kx^2-a)(2kx^2-a+1)\sqrt{1-x^2}.
\end{aligned}
\tag{B.5}
$$

Let N_{Tpp} be the determinant of the matrix obtained by replacing the third column of M with the vector on the right hand side of Eq. (B.1). The P wave transmission coefficient is given by $T_{pp} = N_{Tpp}/D$, where

$$
\begin{aligned}
N_{Tpp} = & 2b\left(1+2kx^2\right)\sqrt{1-x^2}\sqrt{1-d^2x^2} \\
& +2d\left(a-2kx^2\right)\sqrt{1-x^2}\sqrt{1-b^2x^2}.
\end{aligned}
\tag{B.6}
$$

Let N_{Tps} be the determinant of the matrix obtained by replacing the fourth column of M with the vector on the right hand side of Eq. (B.1). The shear wave transmission coefficient is given by $T_{ps} = N_{Tps}/D$. Where

$$
\begin{aligned}
N_{Tps} = & 4kx\sqrt{1-x^2}\sqrt{1-b^2x^2}\sqrt{1-c^2x^2} \\
& +2bcx\left(1-a+2kx^2\right)\sqrt{1-x^2}.
\end{aligned}
\tag{B.7}
$$

2. Derivation of R_{sp} and R_{SS}

For non-normal incidence of SV-plane wave on a horizontal interface between two elastic solids will generate four independent propagating waves, the reflected P-wave (R_{sp}), the reflected shear wave (R_{ss}), the transmitted P-wave (T_{sp}) and the transmitted shear wave

(T_{ss}).

The amplitudes (coefficients) of these waves are given by the conditions that the normal and tangential components of stress and displacement must be continuous across the boundary between the two elastic solids. From these boundary conditions, four equations are derived for the coefficients of the four plane waves. In matrix form, the four equations are

$$
M \begin{bmatrix} R_{sp} \\ R_{ss} \\ T_{sp} \\ T_{ss} \end{bmatrix} = \begin{bmatrix} \sqrt{1 - b^2 x^2} \\ -bx \\ b\left(1 - 2b^2 x^2\right) \\ -2b^2 x \sqrt{1 - b^2 x^2} \end{bmatrix},
\tag{B.8}
$$

where M is the same matrix as the P-wave incidence case,

$$
\begin{bmatrix}
-x & -\sqrt{1 - b^2 x^2} & cx & -\sqrt{1 - d^2 x^2} \\
\sqrt{1 - x^2} & -bx & \sqrt{1 - c^2 x^2} & dx \\
2b^2 x \sqrt{1 - x^2} & b(1 - 2b^2 x^2) & 2ad^2 x \sqrt{1 - c^2 x^2} & -ad(1 - 2d^2 x^2) \\
-(1 - 2b^2 x^2) & 2b^2 x \sqrt{1 - b^2 x^2} & ac(1 - 2d^2 x^2) & 2ad^2 x \sqrt{1 - d^2 x^2}
\end{bmatrix},
$$

$$
a = \rho_2/\rho_1, \ b = \beta_1/\alpha_1, \ c = \alpha_2/\alpha_1, \ d = \beta_2/\alpha_1 \ and \ x = sin\theta.
$$

The angle θ is the angle of P-wave reflection measured counter-clockwise from the normal to the reflecting boundary.

Let N_{Rsp} be the determinant of the matrix obtained by replacing the first column of M with the vector on the right hand side of Eq. (B.8). The P wave reflection coefficient is given by $R_{sp} = N_{Rsp}/D$, where

$$
N_{Rsp} = - 4kbx(1 + 2kx^2)\sqrt{1 - b^2 x^2}\sqrt{1 - c^2 x^2}\sqrt{1 - d^2 x^2}
$$

$$
- 2cdbx(2kx^2 - a)(2kx^2 - a + 1)\sqrt{1 - b^2 x^2}.
\tag{B.9}
$$

Let N_{Rss} be the determinant of the matrix obtained by replacing the second column of M with the vector on the right hand side of Eq. (B.8). The shear wave reflection coefficient is given by $R_{ss} = N_{Rss}/D$, where

$$
\begin{aligned}
N_{Rss} =& (1 + 2kx^2)^2 b\sqrt{1 - c^2x^2}\sqrt{1 - d^2x^2} + (1 - a + 2kx^2)^2 bcdx^2 \\
& - (a - 2kx^2)^2 cd\sqrt{1 - x^2}\sqrt{1 - b^2x^2} \\
& - 4k^2x^2\sqrt{1 - x^2}\sqrt{1 - b^2x^2}\sqrt{1 - c^2x^2}\sqrt{1 - d^2x^2} - ad\sqrt{1 - b^2x^2}\sqrt{1 - c^2x^2} \\
& + abc\sqrt{1 - x^2}\sqrt{1 - d^2x^2}.
\end{aligned}
\tag{B.10}
$$

2.2.1 Something more about the reflection and transmission coefficients and energy distribution

1. The reflection coefficients and transmission coefficients given by the Zoeppritz' equations are not the same as that from Knott's equations. Sheriff and Geldart (1994) use the Zoeppritz' equations to define the coefficients, while Ewing *et al.* (1957) use Knott's equations. The differences between those two groups of coefficients are some constants (the velocity ratios) respectively. So only those coefficients experiencing velocity changes are different.

For example, R_{pp} from both of the two kinds of equations are the same while T_{pp} are different. As $\theta = 0$ (normal incidence) and $\rho_1 = \rho_0$, using the Zoeppritz' equations (e.g., Eq. 3.15 in Sheriff and Geldart, 1994 or the matrix form from Foster *et al.*, 1997)

$$
T_{pp} = \frac{2c_0}{c_0 + c_1},
$$

and if using Knott's equations (e.g., Eq. 3-19 in Ewing *et al.*, 1957)

$$
T_{pp} = \frac{2c_1}{c_0 + c_1}.
$$

In summary, among the references, e.g., Ewing *et al.* (1957) use Knott's equations; while

Achenbach (1973), Aki and Richards (2002) and Foster *et al.* (1997) use Zoeppritz' equations. And Sheriff and Geldart (1994) give both methods.

2. Energy distribution equations:

Using Knott's equations, the corresponding energy distribution equation is:

$$R_{pp}^2 + \frac{\cot \delta_1}{\cot \theta_1} R_{ps}^2 + \frac{\rho_2}{\rho_1} \frac{\cot \theta_2}{\cot \theta_1} T_{pp}^2 + \frac{\rho_2}{\rho_1} \frac{\cot \delta_2}{\cot \theta_1} T_{ps}^2 = 1.$$

Using Zoeppritz' equations, we derived the corresponding energy distribution equation according to Sheriff and Geldart (1994) as

$$R_{pp}^2 + \frac{\cot \delta_1}{\cot \theta_1} \frac{\beta_1^2}{\alpha_1^2} R_{ps}^2 + \frac{\rho_2}{\rho_1} \frac{\cot \theta_2}{\cot \theta_1} \frac{\alpha_2^2}{\alpha_1^2} T_{pp}^2 + \frac{\rho_2}{\rho_1} \frac{\cot \delta_2}{\cot \theta_1} \frac{\beta_2^2}{\alpha_1^2} T_{ps}^2 = 1.$$

3   The form of perturbation $\hat{V}$

From Eq. (4.14), we have

$$V = -\rho_0 \begin{bmatrix} a_\rho \omega^2 + \alpha_0^2 a_\gamma \partial_1^2 + \beta_0^2 \partial_2 a_\mu \partial_2 & (\alpha_0^2 a_\gamma - 2\beta_0^2 a_\mu)\partial_1 \partial_2 + \beta_0^2 \partial_2 a_\mu \partial_1 \\ \partial_2(\alpha_0^2 a_\gamma - 2\beta_0^2 a_\mu)\partial_1 + \beta_0^2 a_\mu \partial_1 \partial_2 & a_\rho \omega^2 + \alpha_0^2 \partial_2 a_\gamma \partial_2 + \beta_0^2 a_\mu \partial_1^2 \end{bmatrix}. \quad \text{(B.11)}$$

Then, in PS domain, using the relation in Eq. (4.22), i.e.,

$$\hat{V} = \Pi V \Pi^{-1} \Gamma_0^{-1} = \begin{pmatrix} \hat{V}^{PP} & \hat{V}^{PS} \\ \hat{V}^{SP} & \hat{V}^{SS} \end{pmatrix}, \quad \text{(B.12)}$$

where, as before, the left superscripts of the matrix elements represent the type of measurement and the right ones are the source type. The form of $\hat{V}^{PP}, \hat{V}^{PS}, \hat{V}^{SP}$ and $\hat{V}^{SS}$ can be written, respectively, as

$$\hat{V}_1^{PP} = -\nabla^2 a_\gamma^{(1)} - \frac{\omega^2}{\alpha_0^2}\left(a_\rho^{(1)}\partial_1^2 + \partial_2 a_\rho^{(1)}\partial_2\right)\frac{1}{\nabla^2} - \left[-2\partial_2^2 a_{mu}^{(1)}\partial_1^2 - 2\partial_1^2 a_{mu}^{(1)}\partial_2^2 + 4\partial_1^2 \partial_2 a_{mu}^{(1)}\partial_2\right]\frac{1}{\nabla^2},$$

$$\hat{V}_1^{PS} = \frac{\alpha_0^2}{\beta_0^2}\left[\frac{\omega^2}{\alpha_0^2}\left(\partial_1 a_\rho^{(1)}\partial_2 - \partial_2 a_\rho^{(1)}\partial_1\right) + 2\partial_1\partial_2 a_{mu}^{(1)}\left(\partial_2^2 - \partial_1^2\right) - 2\left(\partial_2^2 - \partial_1^2\right)a_{mu}^{(1)}\partial_2\partial_1\right]\frac{1}{\nabla^2},$$

$$\hat{V}_1^{SP} = -\left[\frac{\omega^2}{\alpha_0^2}\left(\partial_1 a_\rho^{(1)}\partial_2 - \partial_2 a_\rho^{(1)}\partial_1\right) + 2\partial_1\partial_2 a_{mu}^{(1)}\left(\partial_2^2 - \partial_1^2\right) - 2\left(\partial_2^2 - \partial_1^2\right)a_{mu}^{(1)}\partial_2\partial_1\right]\frac{1}{\nabla^2},$$

$$\hat{V}_1^{SS} = -\frac{\alpha_0^2}{\beta_0^2}\left[\frac{\omega^2}{\alpha_0^2}\left(a_\rho^{(1)}\partial_1^2 + \partial_2 a_\rho^{(1)}\partial_2\right) + (\partial_2^2 - \partial_1^2)a_{mu}^{(1)}(\partial_2^2 - \partial_1^2) + 4\partial_1\partial_2 a_{mu}^{(1)}\partial_1\partial_2\right]\frac{1}{\nabla^2},$$

where $a_{mu} = \frac{\mu - \mu_0}{\gamma_0} = \frac{\beta_0^2}{\alpha_0^2}a_\mu$. We make this definition only for convenience, also we have $a_{mu} = 0$ as $\beta = \beta_0 = 0$. We can also rewrite the forms above as the following

$$\hat{V}_1^{PP} = -\nabla^2 a_\gamma^{(1)} - \frac{\omega^2}{\alpha_0^2}\left(a_\rho^{(1)}\partial_1^2 + \partial_2 a_\rho^{(1)}\partial_2\right)\frac{1}{\nabla^2} - \left[-2(\partial_1^2 + \partial_2^2)a_{mu}^{(1)}\partial_1^2 - 2\partial_1^2 a_{mu}^{(1)}(\partial_1^2 + \partial_2^2)\right.$$
$$\left. + 4\partial_1^2 a_{mu}^{(1)}\partial_1^2 + 4\partial_1^2\partial_2 a_{mu}^{(1)}\partial_2\right]\frac{1}{\nabla^2}$$
$$= -\nabla^2 a_\gamma^{(1)} - \frac{\omega^2}{\alpha_0^2}\left(a_\rho^{(1)}\partial_1^2 + \partial_2 a_\rho^{(1)}\partial_2\right)\frac{1}{\nabla^2} + 2\partial_1^2 a_{mu}^{(1)} + 2\partial_1^2\nabla^2 a_{mu}^{(1)}\frac{1}{\nabla^2}$$
$$- 4\partial_1^2\left(a_{mu}^{(1)}\partial_1^2 + \partial_2 a_{mu}^{(1)}\partial_2\right)\frac{1}{\nabla^2},$$

$$\hat{V}_1^{PS} = \frac{\alpha_0^2}{\beta_0^2}\left[\frac{\omega^2}{\alpha_0^2}\left(\partial_1 a_\rho^{(1)}\partial_2 - \partial_2 a_\rho^{(1)}\partial_1\right) + 2\partial_1\partial_2 a_{mu}^{(1)}\left(\partial_2^2 + \partial_1^2\right) - 4\partial_1\partial_2 a_{mu}^{(1)}\partial_1^2\right.$$
$$\left. - 2\left(\partial_2^2 + \partial_1^2\right)a_{mu}^{(1)}\partial_2\partial_1 + 4\partial_1^2 a_{mu}^{(1)}\partial_2\partial_1\right]\frac{1}{\nabla^2}$$
$$= \frac{\alpha_0^2}{\beta_0^2}2\partial_1\partial_2 a_{mu}^{(1)} + \frac{\alpha_0^2}{\beta_0^2}\left[\frac{\omega^2}{\alpha_0^2}\left(\partial_1 a_\rho^{(1)}\partial_2 - \partial_2 a_\rho^{(1)}\partial_1\right) - 4\partial_1\partial_2 a_{mu}^{(1)}\partial_1^2 - 2\nabla^2 a_{mu}^{(1)}\partial_2\partial_1\right.$$
$$\left. + 4\partial_1^2 a_{mu}^{(1)}\partial_2\partial_1\right]\frac{1}{\nabla^2}.$$

Similarly, $\hat{V}_1^{SP}$ can be written as

$$\hat{V}_1^{SP} = -2\partial_1\partial_2 a_{mu}^{(1)} - \left[\frac{\omega^2}{\alpha_0^2}\left(\partial_1 a_\rho^{(1)}\partial_2 - \partial_2 a_\rho^{(1)}\partial_1\right) - 4\partial_1\partial_2 a_{mu}^{(1)}\partial_1^2 - 2\nabla^2 a_{mu}^{(1)}\partial_2\partial_1\right.$$
$$\left. + 4\partial_1^2 a_{mu}^{(1)}\partial_2\partial_1\right]\frac{1}{\nabla^2},$$

and $\hat{V}_1^{SS}$ as

$$
\begin{aligned}
\hat{V}_1^{SS} =& \frac{\alpha_0^2}{\beta_0^2} \left[-\nabla^2 a_{mu}^{(1)} - \frac{\omega^2}{\alpha_0^2} \left(a_\rho^{(1)} \partial_1^2 + \partial_2 a_\rho^{(1)} \partial_2 \right) \frac{1}{\nabla^2} + 2\partial_1^2 a_{mu}^{(1)} + 2\partial_1^2 \nabla^2 a_{mu}^{(1)} \frac{1}{\nabla^2} \right. \\
& \left. -4\partial_1^2 \left(a_{mu}^{(1)} \partial_1^2 + \partial_2 a_{mu}^{(1)} \partial_2 \right) \frac{1}{\nabla^2} \right].
\end{aligned}
$$

4 $\frac{1}{\nabla^2}$ acting on the middle causal Green's function

Considering term

$$
\hat{G}_0^P a_\rho^{(1)} \frac{1}{\nabla^2} \hat{G}_0^P a_\rho^{(1)} \hat{G}_0^P, \tag{B.13}
$$

writing in the integral form

$$
\begin{aligned}
I =& \frac{1}{(2\pi)^6} \int \int \int \int dz' dz'' dx' dx'' \int \int dk_x' dk_z' \frac{e^{ik_x'(x_g-x')} e^{ik_z'(z_g-z')}}{k^2 - k_x'^2 - k_z'^2} a_\rho^{(1)}(z') \frac{1}{\nabla'^2} \\
& \times \int \int dk_x'' dk_z'' \frac{e^{ik_x''(x'-x'')} e^{ik_z''(z'-z'')}}{k^2 - k_x''^2 - k_z''^2} a_\rho^{(1)}(z'') \int \int dk_x''' dk_z''' \frac{e^{ik_x'''(x''-x_s)} e^{ik_z'''(z''-z_s)}}{k^2 - k_x'''^2 - k_z'''^2}.
\end{aligned}
$$

Fourier transform over x_s and x_g, multiply $\frac{1}{(2\pi)^2} \int \int dx_g dx_s e^{-ik_g x_g} e^{ik_s x_s}$ on both sides, we get (assume $z' > z_g$ and $z'' > z_s$)

$$
\begin{aligned}
\widetilde{I} =& \frac{1}{(2\pi)^6} \int \int \int \int dz' dz'' dx' dx'' e^{-ik_g x'} (-\pi i) \frac{e^{i\nu_g(z'-z_g)}}{\nu_g} a_\rho^{(1)}(z') \frac{1}{\nabla'^2} \\
& \times \int \int dk_x'' dk_z'' \frac{e^{ik_x''(x'-x'')} e^{ik_z''(z'-z'')}}{k^2 - k_x''^2 - k_z''^2} a_\rho^{(1)}(z'') e^{ik_s x''} (-\pi i) \frac{e^{i\nu_s(z''-z_s)}}{\nu_s},
\end{aligned}
$$

where $\nu_g^2 = k^2 - k_g^2$, $\nu_s^2 = k^2 - k_s^2$. After integration over x'', and then over k_x'', we get

$$
\begin{aligned}
\widetilde{I} =& -2\pi^3 \frac{1}{(2\pi)^6} \int \int dz' dz'' \frac{e^{i\nu_g(z'-z_g)}}{\nu_g} a_\rho^{(1)}(z') \int dx' e^{-ik_g x'} \frac{1}{\nabla'^2} \\
& \times \int dk_z'' \frac{e^{ik_s x'} e^{ik_z''(z'-z'')}}{\nu_s^2 - k_z''^2} a_\rho^{(1)}(z'') \frac{e^{i\nu_s(z''-z_s)}}{\nu_s}
\end{aligned}
$$

$$
\begin{aligned}
= & -2\pi^3 \frac{1}{(2\pi)^6} \int\int dz' dz'' \frac{e^{i\nu_g(z'-z_g)}}{\nu_g} a_\rho^{(1)}(z') \int dx' e^{-ik_g x'} \\
& \times \int dk_z'' \frac{e^{ik_s x'} e^{ik_z''(z'-z'')}}{(\nu_s^2 - k_z''^2)(-k_s^2 - k_z''^2)} a_\rho^{(1)}(z'') \frac{e^{i\nu_s(z''-z_s)}}{\nu_s},
\end{aligned}
$$

After the integration over x', we get

$$
\begin{aligned}
\widetilde{I} = & -4\pi^4 \frac{1}{(2\pi)^6} \int\int dz' dz'' \frac{e^{i\nu_g(z'-z_g)}}{\nu_g} a_\rho^{(1)}(z') \int dk_z'' \frac{e^{ik_z''(z'-z'')}}{(\nu_g^2 - k_z''^2)(-k_g^2 - k_z''^2)} a_\rho^{(1)}(z'') \frac{e^{i\nu_g(z''-z_s)}}{\nu_g} \\
= & -4\pi^4 \frac{1}{(2\pi)^6} \int\int dz' dz'' \frac{e^{i\nu_g(z'-z_g)}}{\nu_g} a_\rho^{(1)}(z') \int dk_z'' \frac{e^{ik_z''(z'-z'')}}{(k_z''^2 - \nu_g^2)(k_z''^2 + k_g^2)} a_\rho^{(1)}(z'') \frac{e^{i\nu_g(z''-z_s)}}{\nu_g},
\end{aligned}
$$

where

$$
\int dk_z'' \frac{e^{ik_z''(z'-z'')}}{(k_z''^2 - \nu_g^2)(k_z''^2 + k_g^2)},
$$

in the complex plane

$$
= \lim_{\epsilon \to 0^+} \int dk_z'' \frac{e^{ik_z''(z'-z'')}}{\left[k_z''^2 - (\nu_g + i\epsilon)^2\right](k_z''^2 + k_g^2)},
$$

For $\nu_g > 0$, $k_g > 0$ and $z' > z''$,

$$
\begin{aligned}
Res f(k_z'' = \nu_g + i\epsilon) = & \frac{e^{i(\nu_g+i\epsilon)(z'-z'')}}{\left[(\nu_g + i\epsilon) + (\nu_g + i\epsilon)\right]\left[(\nu_g + i\epsilon)^2 + k_g^2\right]} \\
= & \frac{e^{i(\nu_g+i\epsilon)(z'-z'')}}{(2\nu_g + 2i\epsilon)\left[(\nu_g + i\epsilon)^2 + k_g^2\right]},
\end{aligned}
$$

$$
\begin{aligned}
Res f(k_z'' = ik_g) = & \frac{e^{i(ik_g)(z'-z'')}}{\left[-k_g^2 - (\nu_g + i\epsilon)^2\right] 2ik_g} \\
= & \frac{e^{-k_g(z'-z'')}}{\left[-k_g^2 - (\nu_g + i\epsilon)^2\right] 2ik_g},
\end{aligned}
$$

Then,

$$\lim_{\epsilon \to 0}$$

We know that, for

$$\hat{G}_0^P a_\rho^{(1)} \hat{G}_0^P a_\rho^{(1)} \hat{G}_0^P, \tag{B.15}$$

written in the integral form

$$
\begin{aligned}
I' = &\frac{1}{(2\pi)^6} \int \int \int \int dz' dz'' dx' dx'' \int \int dk'_x dk'_z \frac{e^{ik'_x(x_g - x')} e^{ik'_z(z_g - z')}}{k^2 - k'^2_x - k'^2_z} a_\rho^{(1)}(z') \\
&\times \int \int dk''_x dk''_z \frac{e^{ik''_x(x' - x'')} e^{ik''_z(z' - z'')}}{k^2 - k''^2_x - k''^2_z} a_\rho^{(1)}(z'') \int \int dk'''_x dk'''_z \frac{e^{ik'''_x(x'' - x_s)} e^{ik'''_z(z'' - z_s)}}{k^2 - k'''^2_x - k'''^2_z},
\end{aligned}
$$

After fourier transform over x_s and x_g, multiply $\frac{1}{(2\pi)^2} \int \int dx_g dx_s e^{-ik_g x_g} e^{ik_s x_s}$ on both sides, we get

$$\widetilde{I'} = 4\pi^5 i \frac{1}{(2\pi)^6} \int \int dz' dz'' \frac{e^{i\nu_g(z' - z_g)}}{\nu_g} a_\rho^{(1)}(z') \frac{e^{i\nu_g|z' - z''|}}{\nu_g} a_\rho^{(1)}(z'') \frac{e^{i\nu_g(z'' - z_s)}}{\nu_g}, \tag{B.16}$$

Compare the result Eq. (B.14) of Eq. (B.13) with Eq. (B.16) of Eq. (B.15), we can know that

$$\frac{1}{\nabla'^2} \left[\frac{e^{i\nu_g|z' - z''|}}{\nu_g} e^{ik_g x'} \right] = -\frac{1}{\nu_g^2 + k_g^2} \left[\frac{e^{i\nu_g|z' - z''|}}{\nu_g} - \frac{e^{-k_g|z' - z''|}}{ik_g} \right] e^{ik_g x'}.$$

5 Typical integrations

For PPP case, considering

$$()\hat{G}_0^P a_\mu^{(1)} \hat{G}_0^P a_\rho^{(1)} \hat{G}_0^P,$$

134

where "()" is the coefficient in terms of k_g, q_g and some constants. After Fourier transform over x_s, x_g, i.e., multiply

$$\frac{1}{(2\pi)^2} \int\limits_{-\infty}^{+\infty} dx_g \int\limits_{-\infty}^{+\infty} dx_s e^{-ik_g x_g} e^{ik_s x_s},$$

and then Fourier transform over ν_g, i.e., multiply

$$2\pi \frac{1}{\pi} \int\limits_{-\infty}^{+\infty} d\nu_g e^{-2i\nu_g z},$$

$$= () \frac{1}{8\nu_g^4} \left[-a_\mu^{(1)}(z) a_\rho^{(1)}(z) - \frac{1}{2} a_\mu^{(1)\prime}(z) \int\limits_{-\infty}^{z} dz' a_\rho^{(1)}(z') - \frac{1}{2} a_\rho^{(1)\prime}(z) \int\limits_{-\infty}^{z} dz' a_\mu^{(1)}(z') \right],$$

and for

$$() \hat{G}_0^P a_\mu^{(1)} \hat{G}_0^P a_\rho^{(1)} sgn(z' - z'') \hat{G}_0^P,$$

after Fourier transform over x_s, x_g, and ν_g,

$$= () \frac{1}{8\nu_g^4} \left[-\frac{1}{2} a_\mu^{(1)\prime}(z) \int\limits_{-\infty}^{z} dz' a_\rho^{(1)}(z') + \frac{1}{2} a_\rho^{(1)\prime}(z) \int\limits_{-\infty}^{z} dz' a_\mu^{(1)}(z') \right],$$

and for

$$() \hat{G}_0^P a_\mu^{(1)} \hat{G}_0^P a_\rho^{(1)} \delta(z' - z'') \hat{G}_0^P,$$

after Fourier transform over x_s, x_g, and ν_g,

$$= () \frac{i}{8\nu_g^3} \left[a_\mu^{(1)}(z) a_\rho^{(1)}(z) \right],$$

135

For PSP case, considering

$$()\hat{G}_0^P a_\mu^{(1)} \hat{G}_0^S a_\rho^{(1)} \hat{G}_0^P,$$

where "()" is the coefficient in terms of k_g, q_g and some constants. After Fourier transform over x_s, x_g, and ν_g,

$$=() \left(\frac{1}{8\eta_g \nu_g^3}\right) \frac{2}{C+1} \left[-a_\mu^{(1)}(z)a_\rho^{(1)}(z) - \frac{1}{2} \int_{-\infty}^{z} dz' a_{\mu}^{(1)}{}_z \left(\frac{2z+(C-1)z'}{C+1}\right) a_\rho^{(1)}(z')\right.$$
$$\left. -\frac{1}{2} \int_{-\infty}^{z} dz' a_\mu^{(1)}(z')a_{\rho}^{(1)}{}_z \left(\frac{2z+(C-1)z'}{C+1}\right)\right],$$

where C satisfies $\eta_g = C\nu_g$. For

$$()\hat{G}_0^P a_\mu^{(1)} \hat{G}_0^S a_\rho^{(1)} sgn(z'-z'')\hat{G}_0^P,$$

after Fourier transform over x_s, x_g, and ν_g,

$$=() \left(\frac{1}{8\eta_g \nu_g^3}\right) \frac{2}{C+1} \left[-\frac{1}{2} \int_{-\infty}^{z} dz' a_{\mu}^{(1)}{}_z \left(\frac{2z+(C-1)z'}{C+1}\right) a_\rho^{(1)}(z')\right.$$
$$\left. +\frac{1}{2} \int_{-\infty}^{z} dz' a_\mu^{(1)}(z')a_{\rho}^{(1)}{}_z \left(\frac{2z+(C-1)z'}{C+1}\right)\right],$$

and for

$$()\hat{G}_0^P a_\mu^{(1)} \hat{G}_0^S a_\rho^{(1)} \delta(z'-z'')\hat{G}_0^P,$$

after Fourier transform over x_s, x_g, and ν_g,

$$= () \frac{i}{8\eta_g \nu_g^2} \left[a_\mu^{(1)}(z)a_\rho^{(1)}(z)\right],$$

136

For SSS case, considering

$$()\hat{G}_0^S a_\mu^{(1)} \hat{G}_0^S a_\rho^{(1)} \hat{G}_0^S,$$

where "()" is the coefficient in terms of k_g, q_g and some constants. After Fourier transform over x_s, x_g, and ν_g, where Fourier transform over ν_g is to multiply

$$2\pi \frac{1}{\pi} \int\limits_{-\infty}^{+\infty} d\eta_g e^{-2i\eta_g z},$$

$$=() \left(\frac{1}{8\eta_g^4}\right) \left[-a_\mu^{(1)}(z)a_\rho^{(1)}(z) - \frac{1}{2}a_\mu^{(1)\prime}(z) \int\limits_{-\infty}^{z} dz' a_\rho^{(1)}(z') - \frac{1}{2}a_\rho^{(1)\prime}(z) \int\limits_{-\infty}^{z} dz' a_\mu^{(1)}(z')\right],$$

and for

$$()\hat{G}_0^S a_\mu^{(1)} \hat{G}_0^S a_\rho^{(1)} sgn(z' - z'')\hat{G}_0^S,$$

after Fourier transform over x_s, x_g, and ν_g,

$$= () \frac{1}{8\eta_g^4} \left[-\frac{1}{2}a_\mu^{(1)\prime}(z) \int\limits_{-\infty}^{z} dz' a_\rho^{(1)}(z') + \frac{1}{2}a_\rho^{(1)\prime}(z) \int\limits_{-\infty}^{z} dz' a_\mu^{(1)}(z')\right],$$

and for

$$()\hat{G}_0^S a_\mu^{(1)} \hat{G}_0^S a_\rho^{(1)} \delta(z' - z'')\hat{G}_0^S,$$

after Fourier transform over x_s, x_g, and ν_g,

$$= () \frac{i}{8\eta_g^3} \left[a_\mu^{(1)}(z)a_\rho^{(1)}(z)\right],$$

For SPS case, considering

$$()\hat{G}_0^S a_\mu^{(1)} \hat{G}_0^P a_\rho^{(1)} \hat{G}_0^S,$$

where "()" is the coefficient in terms of k_g, q_g and some constants. After Fourier transform over x_s, x_g, and ν_g, where Fourier transform over ν_g is to multiply

$$2\pi \frac{1}{\pi} \int\limits_{-\infty}^{+\infty} d\eta_g e^{-2i\eta_g z},$$

$$=() \left(\frac{1}{8\eta_g^3 \nu_g}\right) \frac{2C}{C+1} \left[-a_\mu^{(1)}(z)a_\rho^{(1)}(z) - \frac{1}{2} \int\limits_{-\infty}^{z} dz' a_{\mu}^{(1)}{}_{,z} \left(\frac{2Cz - (C-1)z'}{C+1}\right) a_\rho^{(1)}(z') \right.$$

$$\left. -\frac{1}{2} \int\limits_{-\infty}^{z} dz' a_\mu^{(1)}(z') a_{\rho}^{(1)}{}_{,z} \left(\frac{2Cz - (C-1)z'}{C+1}\right) \right],$$

where C satisfies $\eta_g = C\nu_g$. For

$$()\hat{G}_0^S a_\mu^{(1)} \hat{G}_0^P a_\rho^{(1)} sgn(z' - z'') \hat{G}_0^S,$$

after Fourier transform over x_s, x_g, and ν_g,

$$=() \left(\frac{1}{8\eta_g^3 \nu_g}\right) \frac{2C}{C+1} \left[-\frac{1}{2} \int\limits_{-\infty}^{z} dz' a_{\mu}^{(1)}{}_{,z} \left(\frac{2Cz - (C-1)z'}{C+1}\right) a_\rho^{(1)}(z') \right.$$

$$\left. +\frac{1}{2} \int\limits_{-\infty}^{z} dz' a_\mu^{(1)}(z') a_{\rho}^{(1)}{}_{,z} \left(\frac{2Cz - (C-1)z'}{C+1}\right) \right],$$

and for

$$()\hat{G}_0^S a_\mu^{(1)} \hat{G}_0^P a_\rho^{(1)} \delta(z' - z'') \hat{G}_0^S,$$

138

after Fourier transform over x_s, x_g, and ν_g,

$$= ()\frac{i}{8\eta_g^2\nu_g}\left[a_\mu^{(1)}(z)a_\rho^{(1)}(z)\right],$$

For SPP case, considering

$$()\hat{G}_0^S a_\mu^{(1)}\hat{G}_0^P a_\rho^{(1)}\hat{G}_0^P,$$

where "()" is the coefficient in terms of k_g, q_g and some constants. After Fourier transform over x_s, x_g, and ν_g, where Fourier transform over ν_g is to multiply

$$2\pi\frac{1}{2\pi}\int\limits_{-\infty}^{+\infty}d(\nu_g+\eta_g)e^{-i(\nu_g+\eta_g)z},$$

$$\begin{aligned}=()\left(\frac{1}{8\eta_g\nu_g^3}\right)\Bigg[&-\frac{1}{C+1}a_\mu^{(1)}(z)a_\rho^{(1)}(z)-\frac{1}{C+1}a_\mu^{(1)\prime}(z)\int\limits_{-\infty}^{z}dz'a_\rho^{(1)}(z')\\&-\frac{1}{2}a_\mu^{(1)}(z)a_\rho^{(1)}(z)-\frac{1}{2}\int\limits_{-\infty}^{z}dz'a_\mu^{(1)}(z')a_{\rho\,z}^{(1)}\left(\frac{(C+1)z-(C-1)z'}{2}\right)\Bigg],\end{aligned}$$

where C satisfies $\eta_g=C\nu_g$. For

$$()\hat{G}_0^S a_\mu^{(1)}\hat{G}_0^P a_\rho^{(1)}sgn(z'-z'')\hat{G}_0^P,$$

after Fourier transform over x_s, x_g, and ν_g,

$$\begin{aligned}=()\left(\frac{1}{8\eta_g\nu_g^3}\right)\Bigg[&-\frac{1}{C+1}a_\mu^{(1)}(z)a_\rho^{(1)}(z)-\frac{1}{C+1}a_\mu^{(1)\prime}(z)\int\limits_{-\infty}^{z}dz'a_\rho^{(1)}(z')\\&+\frac{1}{2}a_\mu^{(1)}(z)a_\rho^{(1)}(z)+\frac{1}{2}\int\limits_{-\infty}^{z}dz'a_\mu^{(1)}(z')a_{\rho\,z}^{(1)}\left(\frac{(C+1)z-(C-1)z'}{2}\right)\Bigg],\end{aligned}$$

139

and for

$$()\hat{G}_0^S a_\mu^{(1)} \hat{G}_0^P a_\rho^{(1)} \delta(z' - z'') \hat{G}_0^P,$$

after Fourier transform over x_s, x_g, and ν_g,

$$= ()\frac{i}{8\eta_g \nu_g^2} \left[a_\mu^{(1)}(z) a_\rho^{(1)}(z) \right],$$

For SSP case, considering

$$()\hat{G}_0^S a_\mu^{(1)} \hat{G}_0^S a_\rho^{(1)} \hat{G}_0^P,$$

where "()" is the coefficient in terms of k_g, q_g and some constants. After Fourier transform over x_s, x_g, and ν_g, where Fourier transform over ν_g is to multiply

$$2\pi \frac{1}{2\pi} \int\limits_{-\infty}^{+\infty} d(\nu_g + \eta_g) e^{-i(\nu_g + \eta_g)z},$$

$$= () \left(\frac{1}{8\eta_g^2 \nu_g^2} \right) \left[-\frac{1}{2C} a_\mu^{(1)}(z) a_\rho^{(1)}(z) - \frac{1}{2C} \int\limits_{-\infty}^{z} dz' a_{\mu}^{(1)}{}_z \left(\frac{(C+1)z + (C-1)z'}{2C} \right) a_\rho^{(1)}(z') \right.$$

$$\left. -\frac{1}{C+1} a_\mu^{(1)}(z) a_\rho^{(1)}(z) - \frac{1}{C+1} a_\rho^{(1)\prime}(z) \int\limits_{-\infty}^{z} dz' a_\mu^{(1)}(z') \right],$$

where C satisfies $\eta_g = C\nu_g$. For

$$()\hat{G}_0^S a_\mu^{(1)} \hat{G}_0^S a_\rho^{(1)} sgn(z' - z'') \hat{G}_0^P,$$

after Fourier transform over x_s, x_g, and ν_g,

$$= () \left(\frac{1}{8\eta_g^2 \nu_g^2} \right) \left[-\frac{1}{2C} a_\mu^{(1)}(z) a_\rho^{(1)}(z) - \frac{1}{2C} \int\limits_{-\infty}^{z} dz' a_\mu^{(1)}{}_z \left(\frac{(C+1)z + (C-1)z'}{2C} \right) a_\rho^{(1)}(z') \right.$$

$$\left. + \frac{1}{C+1} a_\mu^{(1)}(z) a_\rho^{(1)}(z) + \frac{1}{C+1} a_\rho^{(1)\prime}(z) \int\limits_{-\infty}^{z} dz' a_\mu^{(1)}(z') \right],$$

and for

$$() \hat{G}_0^S a_\mu^{(1)} \hat{G}_0^S a_\rho^{(1)} \delta(z' - z'') \hat{G}_0^P,$$

after Fourier transform over x_s, x_g, and ν_g,

$$= () \frac{i}{8\eta_g^2 \nu_g} \left[a_\mu^{(1)}(z) a_\rho^{(1)}(z) \right],$$

For PPS case, considering

$$() \hat{G}_0^P a_\mu^{(1)} \hat{G}_0^P a_\rho^{(1)} \hat{G}_0^S,$$

where "()" is the coefficient in terms of k_g, q_g and some constants. After Fourier transform over x_s, x_g, and ν_g, where Fourier transform over ν_g is to multiply

$$2\pi \frac{1}{2\pi} \int\limits_{-\infty}^{+\infty} d(\nu_g + \eta_g) e^{-i(\nu_g + \eta_g)z},$$

$$= () \left(\frac{1}{8\eta_g \nu_g^3} \right) \left[-\frac{1}{2} a_\mu^{(1)}(z) a_\rho^{(1)}(z) - \frac{1}{2} \int\limits_{-\infty}^{z} dz' a_\mu^{(1)}{}_z \left(\frac{(C+1)z - (C-1)z'}{2} \right) a_\rho^{(1)}(z') \right.$$

$$\left. - \frac{1}{C+1} a_\mu^{(1)}(z) a_\rho^{(1)}(z) - \frac{1}{C+1} a_\rho^{(1)\prime}(z) \int\limits_{-\infty}^{z} dz' a_\mu^{(1)}(z') \right],$$

where C satisfies $\eta_g = C\nu_g$. For

$$()\hat{G}_0^P a_\mu^{(1)} \hat{G}_0^P a_\rho^{(1)} sgn(z' - z'')\hat{G}_0^S,$$

after Fourier transform over x_s, x_g, and ν_g,

$$=() \left(\frac{1}{8\eta_g\nu_g^3}\right) \left[-\frac{1}{2}a_\mu^{(1)}(z)a_\rho^{(1)}(z) - \frac{1}{2}\int\limits_{-\infty}^{z} dz' a_\mu^{(1)}{}_z \left(\frac{(C+1)z - (C-1)z'}{2}\right) a_\rho^{(1)}(z') \right.$$
$$\left. +\frac{1}{C+1}a_\mu^{(1)}(z)a_\rho^{(1)}(z) + \frac{1}{C+1}a_\rho^{(1)\prime}(z)\int\limits_{-\infty}^{z} dz' a_\mu^{(1)}(z') \right],$$

and for

$$()\hat{G}_0^P a_\mu^{(1)} \hat{G}_0^P a_\rho^{(1)} \delta(z' - z'')\hat{G}_0^S,$$

after Fourier transform over x_s, x_g, and ν_g,

$$= ()\frac{i}{8\eta_g\nu_g^2} \left[a_\mu^{(1)}(z)a_\rho^{(1)}(z)\right],$$

For PSS case, considering

$$()\hat{G}_0^P a_\mu^{(1)} \hat{G}_0^S a_\rho^{(1)} \hat{G}_0^S,$$

where "()" is the coefficient in terms of k_g, q_g and some constants. After Fourier transform over x_s, x_g, and ν_g, where Fourier transform over ν_g is to multiply

$$2\pi\frac{1}{2\pi}\int\limits_{-\infty}^{+\infty} d(\nu_g + \eta_g)e^{-i(\nu_g+\eta_g)z},$$

$$=() \left(\frac{1}{8\eta_g^2\nu_g^2}\right) \left[-\frac{1}{C+1}a_\mu^{(1)}(z)a_\rho^{(1)}(z) - \frac{1}{C+1}a_\mu^{(1)\prime}(z)\int\limits_{-\infty}^{z} dz' a_\rho^{(1)}(z') \right.$$

$$\left. -\frac{1}{2C}a_\mu^{(1)}(z)a_\rho^{(1)}(z) - \frac{1}{2C}\int\limits_{-\infty}^{z} dz' a_\mu^{(1)}(z')a_{\rho\ z}^{(1)}\left(\frac{(C+1)z+(C-1)z'}{2C}\right) \right],$$

where C satisfies $\eta_g = C\nu_g$. For

$$()\hat{G}_0^P a_\mu^{(1)}\hat{G}_0^S a_\rho^{(1)} sgn(z'-z'')\hat{G}_0^S,$$

after Fourier transform over x_s, x_g, and ν_g,

$$=() \left(\frac{1}{8\eta_g^2\nu_g^2}\right) \left[-\frac{1}{C+1}a_\mu^{(1)}(z)a_\rho^{(1)}(z) - \frac{1}{C+1}a_\mu^{(1)\prime}(z)\int\limits_{-\infty}^{z} dz' a_\rho^{(1)}(z') \right.$$

$$\left. +\frac{1}{2C}a_\mu^{(1)}(z)a_\rho^{(1)}(z) + \frac{1}{2C}\int\limits_{-\infty}^{z} dz' a_\mu^{(1)}(z')a_{\rho\ z}^{(1)}\left(\frac{(C+1)z+(C-1)z'}{2C}\right) \right],$$

and for

$$()\hat{G}_0^P a_\mu^{(1)}\hat{G}_0^S a_\rho^{(1)} \delta(z'-z'')\hat{G}_0^S,$$

after Fourier transform over x_s, x_g, and ν_g,

$$= () \frac{i}{8\eta_g^2\nu_g} \left[a_\mu^{(1)}(z)a_\rho^{(1)}(z) \right].$$

6 The coefficients before every linear quantity $(a_\gamma^{(1)}, a_\rho^{(1)}, a_\mu^{(1)})$ — different incidence angle θ

For P to P case, we have

$$k_g^{PP} = \frac{\omega}{\alpha_0} \sin \theta^{PP},$$

$$\nu_g^{PP} = \frac{\omega}{\alpha_0} \cos \theta^{PP}.$$

For S to P case,

$$k_g^{PS} = \frac{\omega}{\beta_0} \sin \theta^{PS},$$

$$\nu_g^{PS} = \frac{\omega}{\alpha_0} \sqrt{1 - \frac{\alpha_0^2}{\beta_0^2} \sin^2 \theta^{PS}},$$

$$\eta_g^{PS} = \frac{\omega}{\beta_0} \cos \theta^{PS}.$$

For P to S case,

$$k_g^{SP} = \frac{\omega}{\alpha_0} \sin \theta^{SP},$$

$$\nu_g^{SP} = \frac{\omega}{\alpha_0} \cos \theta^{SP},$$

$$\eta_g^{SP} = \frac{\omega}{\beta_0} \sqrt{1 - \frac{\beta_0^2}{\alpha_0^2} \sin^2 \theta^{SP}}.$$

For S to S case,

$$k_g^{SS} = \frac{\omega}{\beta_0} \sin \theta^{SS},$$

$$\eta_g^{SS} = \frac{\omega}{\beta_0} \cos \theta^{SS}.$$

Let the arguments of $a_\rho^{(1)}$ and $a_\mu^{(1)}$ in Eqs. (4.41), (4.42), (4.43) and (4.44) equal, we need

$$-2\nu_g^{PP} = -\nu_g^{PS} - \eta_g^{PS} = -\nu_g^{SP} - \eta_g^{SP} = -2\eta_g^{SS},$$

which leads to

$$2\frac{\omega}{\alpha_0}\cos\theta^{PP} = \frac{\omega}{\alpha_0}\sqrt{1 - \frac{\alpha_0^2}{\beta_0^2}\sin^2\theta^{PS}} + \frac{\omega}{\beta_0}\cos\theta^{PS} = \frac{\omega}{\alpha_0}\cos\theta^{SP} + \frac{\omega}{\beta_0}\sqrt{1 - \frac{\beta_0^2}{\alpha_0^2}\sin^2\theta^{SP}}$$

$$= 2\frac{\omega}{\beta_0}\cos\theta^{SS}.$$

From the expression above, given θ^{PP}, we can find the corresponding θ^{PS}, θ^{SP} and θ^{SS}.

$$\theta^{PS} = \cos^{-1}\left[\frac{4b^2\cos^2\theta^{PP} + 1 - b^2}{4b\cos\theta^{PP}}\right],$$

$$\theta^{SP} = \cos^{-1}\left[\frac{4b^2\cos^2\theta^{PP} - 1 + b^2}{4b^2\cos\theta^{PP}}\right],$$

$$\theta^{SS} = \cos^{-1}\left(b\cos\theta^{PP}\right),$$

where $b = \frac{\beta_0}{\alpha_0}$.

7 Expressing $a_R^{(1)}$ and $a_R^{(2)}$ in terms of $a_\gamma^{(1)}$, $a_\gamma^{(2)}$, $a_\mu^{(1)}$ and $a_\mu^{(2)}$

The following is the derivation of expressing $a_R^{(1)}$ and $a_R^{(2)}$ in terms of $a_\gamma^{(1)}$, $a_\gamma^{(2)}$, $a_\mu^{(1)}$ and $a_\mu^{(2)}$.

Since

$$a_\gamma = \frac{\gamma}{\gamma_0} - 1 = \frac{\rho\alpha^2}{\rho_0\alpha_0^2} - 1,$$

$$a_\mu = \frac{\mu}{\mu_0} - 1 = \frac{\rho\beta^2}{\rho_0\beta_0^2} - 1,$$

and

$$a_R = \frac{\alpha/\beta}{\alpha_0/\beta_0} - 1,$$

145

then we have

$$(a_R + 1)^2 = \frac{a_\gamma + 1}{a_\mu + 1},$$

then

$$a_R^2 + 2a_R + 1 = (a_\gamma + 1)(1 - a_\mu + a_\mu^2 - \cdots),$$

where the series expansion is valid for $|a_\mu| < 1$.

Expanding the relative changes, we have

$$a_\gamma = a_\gamma^{(1)} + a_\gamma^{(2)} + a_\gamma^{(3)} + \cdots,$$

$$a_\mu = a_\mu^{(1)} + a_\mu^{(2)} + a_\mu^{(3)} + \cdots,$$

$$a_R = a_R^{(1)} + a_R^{(2)} + a_R^{(3)} + \cdots,$$

then after substitutions, we obtain

$$a_R^{(1)} = \frac{1}{2}\left(a_\gamma^{(1)} - a_\mu^{(1)}\right),$$

$$a_R^{(2)} = \frac{1}{2}\left(a_\gamma^{(2)} - a_\mu^{(2)} + a_\mu^{(1)^2} - a_R^{(1)^2} - a_\gamma^{(1)}a_\mu^{(1)}\right).$$

C. TWO PARAMETER CASE: ELASTIC REDUCE TO ACOUSTIC

In the acoustic case, if we start directly with the pressure wave equation and choose θ as the free parameter, α and β as the two material property parameters as shown in Chapter 3, we arrive at the following equation for the second order (first term beyond linear) Eq. (3.12):

$$
\frac{1}{\cos^2\theta}\alpha_2(z) + (1 - \tan^2\theta)\beta_2(z)
$$
$$
= -\frac{1}{2\cos^4\theta}\alpha_1^2(z)
$$
$$
-\frac{1}{2}(1 + \tan^4\theta)\beta_1^2(z)
$$
$$
+\frac{\tan^2\theta}{\cos^2\theta}\alpha_1(z)\beta_1(z)
$$
$$
-\frac{1}{2\cos^4\theta}\alpha_1'(z)\int_0^z dz'[\alpha_1(z') - \beta_1(z')]
$$
$$
+\frac{1}{2}(\tan^4\theta - 1)\beta_1'(z)\int_0^z dz'[\alpha_1(z') - \beta_1(z')].
$$

But if we start with the displacement domain, as discussed in the elastic case (Chapter 4), letting μ_0, β_0, μ, and $\beta = 0$ and choosing θ as the free parameter, a_γ and a_ρ as the two material property parameters, what kind of solution for the second order would we get? In the following, we give the detailed derivations and show that the two results agree with each other.

According to Appendix B, we have the following forms for $\hat{V}_1^{PP}$, $\hat{V}_1^{PS}$ and $\hat{V}_1^{SP}$, respectively

$$\hat{V}_1^{PP} = -\nabla^2 a_\gamma^{(1)} - \frac{\omega^2}{\alpha_0^2} \left(a_\rho^{(1)} \partial_1^2 + \partial_2 a_\rho^{(1)} \partial_2\right) \frac{1}{\nabla^2} + 2\partial_1^2 a_{mu}^{(1)} + 2\partial_1^2 \nabla^2 a_{mu}^{(1)} \frac{1}{\nabla^2}$$
$$- 4\partial_1^2 \left(a_{mu}^{(1)} \partial_1^2 + \partial_2 a_{mu}^{(1)} \partial_2\right) \frac{1}{\nabla^2},$$

$$\hat{V}_1^{PS} = \frac{\alpha_0^2}{\beta_0^2} \left[\frac{\omega^2}{\alpha_0^2} \left(\partial_1 a_\rho^{(1)} \partial_2 - \partial_2 a_\rho^{(1)} \partial_1\right) + 2\partial_1 \partial_2 a_{mu}^{(1)} \left(\partial_2^2 - \partial_1^2\right) - 2\left(\partial_2^2 - \partial_1^2\right) a_{mu}^{(1)} \partial_2 \partial_1\right] \frac{1}{\nabla^2},$$

$$\hat{V}_1^{SP} = -\left[\frac{\omega^2}{\alpha_2^2} \left(\partial_1 a_\rho^{(1)} \partial_2 - \partial_2 a_\rho^{(1)} \partial_1\right) + 2\partial_1 \partial_2 a_{mu}^{(1)} \left(\partial_2^2 - \partial_1^2\right) - 2\left(\partial_2^2 - \partial_1^2\right) a_{mu}^{(1)} \partial_2 \partial_1\right] \frac{1}{\nabla^2},$$

For the first equation of the non-linear elastic inversion

$$\hat{G}_0^P \hat{V}_2^{PP} \hat{G}_0^P = -\hat{G}_0^P \hat{V}_1^{PP} \hat{G}_0^P \hat{V}_1^{PP} \hat{G}_0^P - \hat{G}_0^P \hat{V}_1^{PS} \hat{G}_0^S \hat{V}_1^{SP} \hat{G}_0^P, \qquad \text{(C.1)}$$

Left side: after Fourier transforming over x_s, x_g and ν_g, let $\beta, \beta_0 = 0$, we get

$$-\frac{1}{4}\frac{1}{\cos^2\theta} a_\gamma^{(2)}(z) - \frac{1}{4}(1 - \tan^2\theta) a_\rho^{(2)}(z).$$

Right side: the first term, $-\hat{G}_0^P \hat{V}_1^{PP} \hat{G}_0^P \hat{V}_1^{PP} \hat{G}_0^P$, let $\beta, \beta_0 = 0$, we get

$$\hat{V}_1^{PP} = -\nabla^2 a_\gamma^{(1)} - \frac{\omega^2}{\alpha_0^2} \left(a_\rho^{(1)} \partial_1^2 + \partial_2 a_\rho^{(1)} \partial_2\right) \frac{1}{\nabla^2},$$

then, in this case, we have

$$- \hat{G}_0^P \hat{V}_1^{PP} \hat{G}_0^P \hat{V}_1^{PP} \hat{G}_0^P$$
$$= -\hat{G}_0^P \left[-\nabla^2 a_\gamma^{(1)} - \frac{\omega^2}{\alpha_0^2} \left(a_\rho^{(1)} \partial_1^2 + \partial_2 a_\rho^{(1)} \partial_2\right) \frac{1}{\nabla^2}\right] \hat{G}_0^P$$
$$\times \left[-\nabla^2 a_\gamma^{(1)} - \frac{\omega^2}{\alpha_0^2} \left(a_\rho^{(1)} \partial_1^2 + \partial_2 a_\rho^{(1)} \partial_2\right) \frac{1}{\nabla^2}\right] \hat{G}_0^P$$
$$= -\hat{G}_0^P \left[-\nabla^2 a_\gamma^{(1)}\right] \hat{G}_0^P \left[-\nabla^2 a_\gamma^{(1)}\right] \hat{G}_0^P$$
$$- \hat{G}_0^P \left[-\nabla^2 a_\gamma^{(1)}\right] \hat{G}_0^P \left[-\frac{\omega^2}{\alpha_0^2} \left(a_\rho^{(1)} \partial_1^2 + \partial_2 a_\rho^{(1)} \partial_2\right) \frac{1}{\nabla^2}\right] \hat{G}_0^P$$

$$- \hat{G}_0^P \left[-\frac{\omega^2}{\alpha_0^2} \left(a_\rho^{(1)} \partial_1^2 + \partial_2 a_\rho^{(1)} \partial_2 \right) \frac{1}{\nabla^2} \right] \hat{G}_0^P \left[-\nabla^2 a_\gamma^{(1)} \right] \hat{G}_0^P$$

$$- \hat{G}_0^P \left[-\frac{\omega^2}{\alpha_0^2} \left(a_\rho^{(1)} \partial_1^2 + \partial_2 a_\rho^{(1)} \partial_2 \right) \frac{1}{\nabla^2} \right] \hat{G}_0^P \left[-\frac{\omega^2}{\alpha_0^2} \left(a_\rho^{(1)} \partial_1^2 + \partial_2 a_\rho^{(1)} \partial_2 \right) \frac{1}{\nabla^2} \right] \hat{G}_0^P$$

$$= term1 + term2 + term3 + term4.$$

Using some partial integrals, we replace all the ∂_1^2 as $-k_g^2$, and for $term1$

$$-\hat{G}_0^P \left[-\nabla^2 a_\gamma^{(1)} \right] \hat{G}_0^P \left[-\nabla^2 a_\gamma^{(1)} \right] \hat{G}_0^P, \tag{C.2}$$

replace the first ∇^2 as $-\frac{\omega^2}{\alpha_0^2}$, and the second ∇^2 as $-\frac{\omega^2}{\alpha_0^2} + 2i\nu_g \delta(z' - z'')$, then, written in integrals and after Fourier transforming over x_s and x_g, Eq. (C.2) becomes

$$- \frac{\omega^4}{\alpha_0^4} \left(\frac{i}{16\pi\nu_g^3} \right) \int\limits_{-\infty}^{+\infty} dz' \int\limits_{-\infty}^{+\infty} dz'' e^{i\nu_g z'} a_\gamma^{(1)}(z') e^{i\nu_g |z' - z''|} a_\gamma^{(1)}(z'') e^{i\nu_g z''}$$

$$+ 2i\nu_g \frac{\omega^2}{\alpha_0^2} \left(\frac{i}{16\pi\nu_g^3} \right) \int\limits_{-\infty}^{+\infty} dz' \int\limits_{-\infty}^{+\infty} dz'' e^{i\nu_g z'} a_\gamma^{(1)}(z') \delta(z' - z'') e^{i\nu_g |z' - z''|} a_\gamma^{(1)}(z'') e^{i\nu_g z''},$$

After Fourier transforming over ν_g, it becomes

$$\frac{1}{8\cos^4\theta} \left[a_\gamma^{(1)}(z) a_\gamma^{(1)}(z) + a_\gamma^{(1)\prime}(z) \int\limits_{-\infty}^{z} dz' a_\gamma^{(1)}(z') \right]$$

$$- \frac{1}{4\cos^2\theta} a_\gamma^{(1)}(z) a_\gamma^{(1)}(z).$$

Similarly, for $term2$

$$-\hat{G}_0^P \left[-\nabla^2 a_\gamma^{(1)} \right] \hat{G}_0^P \left[-\frac{\omega^2}{\alpha_0^2} \left(a_\rho^{(1)} \partial_1^2 + \partial_2 a_\rho^{(1)} \partial_2 \right) \frac{1}{\nabla^2} \right] \hat{G}_0^P,$$

we replace the ∇^2 as $-\frac{\omega^2}{\alpha_0^2}$, first ∂_2 as $-i\nu_g sgn(z'' - z')$, second ∂_2 as $i\nu_g$, and $\frac{1}{\nabla^2}$ as $-\frac{\alpha_0^2}{\omega^2}$,

then, written in integrals and after Fourier transforming over x_s and x_g, the $term2$ becomes

$$\frac{\omega^2}{\alpha_0^2} k_g^2 \left(\frac{i}{16\pi\nu_g^3} \right) \int\limits_{-\infty}^{+\infty} dz' \int\limits_{-\infty}^{+\infty} dz'' e^{i\nu_g z'} a_\gamma^{(1)}(z') e^{i\nu_g|z'-z''|} a_\rho^{(1)}(z'') e^{i\nu_g z''}$$

$$+ \frac{\omega^2}{\alpha_0^2} \nu_g^2 \left(\frac{i}{16\pi\nu_g^3} \right) \int\limits_{-\infty}^{+\infty} dz' \int\limits_{-\infty}^{+\infty} dz'' e^{i\nu_g z'} a_\gamma^{(1)}(z') sgn(z'-z'') e^{i\nu_g|z'-z''|} a_\rho^{(1)}(z'') e^{i\nu_g z''},$$

After Fourier transforming over ν_g, it becomes

$$-\frac{\tan^2\theta}{16\cos^2\theta} \left[2a_\gamma^{(1)}(z) a_\rho^{(1)}(z) + a_\gamma^{(1)\prime}(z) \int\limits_{-\infty}^{z} dz' a_\rho^{(1)}(z') + a_\rho^{(1)\prime}(z) \int\limits_{-\infty}^{z} dz' a_\gamma^{(1)}(z') \right]$$

$$-\frac{1}{16\cos^2\theta} \left[a_\gamma^{(1)\prime}(z) \int\limits_{-\infty}^{z} dz' a_\rho^{(1)}(z') - a_\rho^{(1)\prime}(z) \int\limits_{-\infty}^{z} dz' a_\gamma^{(1)}(z') \right].$$

For $term3$,

$$-\hat{G}_0^P \left[-\frac{\omega^2}{\alpha_0^2} \left(a_\rho^{(1)}\partial_1^2 + \partial_2 a_\rho^{(1)}\partial_2 \right) \frac{1}{\nabla^2} \right] \hat{G}_0^P \left[-\nabla^2 a_\gamma^{(1)} \right] \hat{G}_0^P$$

$$= -\hat{G}_0^P \left[\frac{\omega^2}{\alpha_0^2} \left(a_\rho^{(1)}\partial_1^2 + \partial_2 a_\rho^{(1)}\partial_2 \right) \right] \hat{G}_0^P \left[a_\gamma^{(1)} \right] \hat{G}_0^P,$$

after the first ∂_2 is replaced by $-i\nu_g$, and the second ∂_2 is replaced by $i\nu_g sgn(z'-z'')$, $term3$ leads to the same result as that of the $term2$. Therefore, after Fourier transforming over x_s, x_g and ν_g, $term3$ will be the same as $term2$

$$-\frac{\tan^2\theta}{16\cos^2\theta} \left[2a_\gamma^{(1)}(z) a_\rho^{(1)}(z) + a_\gamma^{(1)\prime}(z) \int\limits_{-\infty}^{z} dz' a_\rho^{(1)}(z') + a_\rho^{(1)\prime}(z) \int\limits_{-\infty}^{z} dz' a_\gamma^{(1)}(z') \right]$$

$$-\frac{1}{16\cos^2\theta} \left[a_\gamma^{(1)\prime}(z) \int\limits_{-\infty}^{z} dz' a_\rho^{(1)}(z') - a_\rho^{(1)\prime}(z) \int\limits_{-\infty}^{z} dz' a_\gamma^{(1)}(z') \right].$$

150

For *term4*,

$$-\hat{G}_0^P\left[-\frac{\omega^2}{\alpha_0^2}\left(a_\rho^{(1)}\partial_1^2+\partial_2 a_\rho^{(1)}\partial_2\right)\frac{1}{\nabla^2}\right]\hat{G}_0^P\left[-\frac{\omega^2}{\alpha_0^2}\left(a_\rho^{(1)}\partial_1^2+\partial_2 a_\rho^{(1)}\partial_2\right)\frac{1}{\nabla^2}\right]\hat{G}_0^P$$

$$=\hat{G}_0^P\left[\frac{\omega^2}{\alpha_0^2}\left(a_\rho^{(1)}\partial_1^2+\partial_2 a_\rho^{(1)}\partial_2\right)\frac{1}{\nabla^2}\right]\hat{G}_0^P\left(a_\rho^{(1)}\partial_1^2+\partial_2 a_\rho^{(1)}\partial_2\right)\hat{G}_0^P,$$

where

$$\frac{1}{\nabla'^2}\left[\frac{e^{i\nu_g|z'-z''|}}{\nu_g}e^{ik_g x'}\right]=-\frac{1}{\nu_g^2+k_g^2}\left[\frac{e^{i\nu_g|z'-z''|}}{\nu_g}-\frac{e^{-k_g|z'-z''|}}{ik_g}\right]e^{ik_g x'},$$

(please see the detail derivation in Appendix B about the $\frac{1}{\nabla^2}$ acting on the middle Green's causal function), where $\frac{1}{\nu_g^2+k_g^2}=\frac{\alpha_0^2}{\omega^2}$, then, after Fourier transforming over x_s and x_g, the *term4* becomes

$$-\left(\frac{i}{16\pi\nu_g^2}\right)\int_{-\infty}^{+\infty}dz'\int_{-\infty}^{+\infty}dz''e^{i\nu_g z'}\left[a_\rho^{(1)}(z')(-k_g^2)+\frac{\partial}{\partial z'}a_\rho^{(1)}(z')\frac{\partial}{\partial z'}\right]$$

$$\times\left[\frac{e^{i\nu_g|z'-z''|}}{\nu_g}-\frac{e^{-k_g|z'-z''|}}{ik_g}\right]\times\left[a_\rho^{(1)}(z'')(-k_g^2)+\frac{\partial}{\partial z''}a_\rho^{(1)}(z'')\frac{\partial}{\partial z''}\right]e^{i\nu_g z''}$$

$$=-k_g^4\left(\frac{i}{16\pi\nu_g^2}\right)\int_{-\infty}^{+\infty}dz'\int_{-\infty}^{+\infty}dz''e^{i\nu_g z'}a_\rho^{(1)}(z')\left[\frac{e^{i\nu_g|z'-z''|}}{\nu_g}-\frac{e^{-k_g|z'-z''|}}{ik_g}\right]a_\rho^{(1)}(z'')e^{i\nu_g z''}$$

$$+k_g^2\left(\frac{i}{16\pi\nu_g^2}\right)\int_{-\infty}^{+\infty}dz'\int_{-\infty}^{+\infty}dz''e^{i\nu_g z'}a_\rho^{(1)}(z')\left[\frac{e^{i\nu_g|z'-z''|}}{\nu_g}-\frac{e^{-k_g|z'-z''|}}{ik_g}\right]$$

$$\times\left[\frac{\partial}{\partial z''}a_\rho^{(1)}(z'')\frac{\partial}{\partial z''}\right]e^{i\nu_g z''}$$

$$+k_g^2\left(\frac{i}{16\pi\nu_g^2}\right)\int_{-\infty}^{+\infty}dz'\int_{-\infty}^{+\infty}dz''e^{i\nu_g z'}\left[\frac{\partial}{\partial z'}a_\rho^{(1)}(z')\frac{\partial}{\partial z'}\right]\times\left[\frac{e^{i\nu_g|z'-z''|}}{\nu_g}-\frac{e^{-k_g|z'-z''|}}{ik_g}\right]$$

$$\times a_\rho^{(1)}(z'')e^{i\nu_g z''}$$

$$-\left(\frac{i}{16\pi\nu_g^2}\right)\int_{-\infty}^{+\infty}dz'\int_{-\infty}^{+\infty}dz''e^{i\nu_g z'}\left[\frac{\partial}{\partial z'}a_\rho^{(1)}(z')\frac{\partial}{\partial z'}\right]\times\left[\frac{e^{i\nu_g|z'-z''|}}{\nu_g}-\frac{e^{-k_g|z'-z''|}}{ik_g}\right]$$

$$\times\left[\frac{\partial}{\partial z''}a_\rho^{(1)}(z'')\frac{\partial}{\partial z''}\right]e^{i\nu_g z''}$$

$$= - k_g^4 \left(\frac{i}{16\pi\nu_g^2} \right) \int\limits_{-\infty}^{+\infty} dz' \int\limits_{-\infty}^{+\infty} dz'' e^{i\nu_g z'} a_\rho^{(1)}(z') \left[\frac{e^{i\nu_g|z'-z''|}}{\nu_g} - \frac{e^{-k_g|z'-z''|}}{ik_g} \right] a_\rho^{(1)}(z'') e^{i\nu_g z''}$$

$$- \left(\frac{i}{16\pi\nu_g^2} \right) \int\limits_{-\infty}^{+\infty} dz' \int\limits_{-\infty}^{+\infty} dz'' e^{i\nu_g z'} \left[\frac{\partial}{\partial z'} a_\rho^{(1)}(z') \frac{\partial}{\partial z'} \right] \times \left[\frac{e^{i\nu_g|z'-z''|}}{\nu_g} - \frac{e^{-k_g|z'-z''|}}{ik_g} \right]$$

$$\times \left[\frac{\partial}{\partial z''} a_\rho^{(1)}(z'') \frac{\partial}{\partial z''} \right] e^{i\nu_g z''},$$

where

$$- \left(\frac{i}{16\pi\nu_g^2} \right) \int\limits_{-\infty}^{+\infty} dz' \int\limits_{-\infty}^{+\infty} dz'' e^{i\nu_g z'} \left[\frac{\partial}{\partial z'} a_\rho^{(1)}(z') \frac{\partial}{\partial z'} \right] \times \left[\frac{e^{i\nu_g|z'-z''|}}{\nu_g} - \frac{e^{-k_g|z'-z''|}}{ik_g} \right]$$

$$\times \left[\frac{\partial}{\partial z''} a_\rho^{(1)}(z'') \frac{\partial}{\partial z''} \right] e^{i\nu_g z''}$$

$$= - \left(\frac{i}{16\pi\nu_g^2} \right) \int\limits_{-\infty}^{+\infty} dz' \int\limits_{-\infty}^{+\infty} dz'' e^{i\nu_g z'} \left[-i\nu_g a_\rho^{(1)}(z') \right]$$

$$\times \left[i\nu_g sgn(z' - z'') \frac{e^{i\nu_g|z'-z''|}}{\nu_g} + k_g sgn(z' - z'') \frac{e^{-k_g|z'-z''|}}{ik_g} \right] \times \left[\frac{\partial}{\partial z''} a_\rho^{(1)}(z'') i\nu_g \right] e^{i\nu_g z''}$$

$$= - \nu_g^2 \left(\frac{i}{16\pi\nu_g^2} \right) \int\limits_{-\infty}^{+\infty} dz' \int\limits_{-\infty}^{+\infty} dz'' e^{i\nu_g z'} a_\rho^{(1)}(z')$$

$$\times \left[\left(2i\nu_g \delta(z' - z'') - \nu_g^2 \right) \frac{e^{i\nu_g|z'-z''|}}{\nu_g} + \left(2k_g \delta(z' - z'') - k_g^2 \right) \frac{e^{-k_g|z'-z''|}}{ik_g} \right] \times a_\rho^{(1)}(z'') e^{i\nu_g z''}$$

$$= - \nu_g^2 \left(\frac{i}{16\pi\nu_g^2} \right) \int\limits_{-\infty}^{+\infty} dz' \int\limits_{-\infty}^{+\infty} dz'' e^{i\nu_g z'} a_\rho^{(1)}(z') \left[-\nu_g^2 \frac{e^{i\nu_g|z'-z''|}}{\nu_g} - k_g^2 \frac{e^{-k_g|z'-z''|}}{ik_g} \right] a_\rho^{(1)}(z'') e^{i\nu_g z''}.$$

Then, $term4$ becomes

$$= - k_g^4 \left(\frac{i}{16\pi\nu_g^2} \right) \int\limits_{-\infty}^{+\infty} dz' \int\limits_{-\infty}^{+\infty} dz'' e^{i\nu_g z'} a_\rho^{(1)}(z') \left[\frac{e^{i\nu_g|z'-z''|}}{\nu_g} - \frac{e^{-k_g|z'-z''|}}{ik_g} \right] a_\rho^{(1)}(z'') e^{i\nu_g z''}$$

$$- \nu_g^2 \left(\frac{i}{16\pi\nu_g^2} \right) \int\limits_{-\infty}^{+\infty} dz' \int\limits_{-\infty}^{+\infty} dz'' e^{i\nu_g z'} a_\rho^{(1)}(z') \left[-\nu_g^2 \frac{e^{i\nu_g|z'-z''|}}{\nu_g} - k_g^2 \frac{e^{-k_g|z'-z''|}}{ik_g} \right] a_\rho^{(1)}(z'') e^{i\nu_g z''}$$

$$
=(\nu_g^4 - k_g^4)\left(\frac{i}{16\pi\nu_g^3}\right)\int\limits_{-\infty}^{+\infty} dz' \int\limits_{-\infty}^{+\infty} dz'' e^{i\nu_g z'} a_\rho^{(1)}(z') e^{i\nu_g|z'-z''|} a_\rho^{(1)}(z'') e^{i\nu_g z''}
$$

$$
+ (k_g^4 + \nu_g^2 k_g^2)\left(\frac{i}{16\pi\nu_g^2}\right)\int\limits_{-\infty}^{+\infty} dz' \int\limits_{-\infty}^{+\infty} dz'' e^{i\nu_g z'} a_\rho^{(1)}(z') \left[\frac{e^{-k_g|z'-z''|}}{ik_g}\right] a_\rho^{(1)}(z'') e^{i\nu_g z''}
$$

$$
= I_1 + I_2,
$$

where I_1 after Fourier transforming over ν_g becomes

$$
\widetilde{I}_1 = -\frac{1-\tan^2\theta}{8\cos^2\theta}\left[a_\rho^{(1)}(z)a_\rho^{(1)}(z) + a_\rho^{(1)'}(z)\int\limits_{-\infty}^{z} dz' a_\rho^{(1)}(z')\right].
$$

Considering the second term of the right hand side of Eq. (C.1)

$$
-\hat{G}_0^P \hat{V}_1^{PS} \hat{G}_0^S \hat{V}_1^{SP} \hat{G}_0^P
$$

$$
=\hat{G}_0^P \frac{\alpha_0^2}{\beta_0^2}\left[\frac{\omega^2}{\alpha_0^2}\left(\partial_1 a_\rho^{(1)} \partial_2 - \partial_2 a_\rho^{(1)} \partial_1\right) + 2\partial_1\partial_2 a_{mu}^{(1)}\left(\partial_2^2 - \partial_1^2\right) - 2\left(\partial_2^2 - \partial_1^2\right) a_{mu}^{(1)} \partial_2\partial_1\right]\frac{1}{\nabla^2}\hat{G}_0^S
$$

$$
\times\left[\frac{\omega^2}{\alpha_0^2}\left(\partial_1 a_\rho^{(1)} \partial_2 - \partial_2 a_\rho^{(1)} \partial_1\right) + 2\partial_1\partial_2 a_{mu}^{(1)}\left(\partial_2^2 - \partial_1^2\right) - 2\left(\partial_2^2 - \partial_1^2\right) a_{mu}^{(1)} \partial_2\partial_1\right]\frac{1}{\nabla^2}\hat{G}_0^P,
$$

where

$$
\frac{1}{\nabla'^2}\left[\frac{e^{i\eta_g|z'-z''|}}{\eta_g}e^{ik_g x'}\right] = -\frac{1}{\eta_g^2 + k_g^2}\left[\frac{e^{i\eta_g|z'-z''|}}{\eta_g} - \frac{e^{-k_g|z'-z''|}}{ik_g}\right]e^{ik_g x'},
$$

where $\frac{1}{\eta_g^2 + k_g^2} = \frac{\beta_0^2}{\omega^2}$.

Then, after Fourier transforming over x_s and x_g, the second term can be written as

$$
=\frac{\alpha_0^4}{\omega^4}\left(\frac{i}{16\pi\nu_g^2}\right)\int\limits_{-\infty}^{+\infty} dz' \int\limits_{-\infty}^{+\infty} dz'' e^{i\nu_g z'}\left[\frac{\omega^2}{\alpha_0^2}\left(ik_g a_\rho^{(1)} \partial_2 - \partial_2 a_\rho^{(1)} ik_g\right)\right.
$$

$$
\left. + 2\partial_1\partial_2 a_{mu}^{(1)}\left(\partial_2^2 - \partial_1^2\right) - 2\left(\partial_2^2 - \partial_1^2\right) a_{mu}^{(1)} \partial_2\partial_1\right] \times \left[\frac{e^{i\eta_g|z'-z''|}}{\eta_g} - \frac{e^{-k_g|z'-z''|}}{ik_g}\right]
$$

$$
\times\left[\frac{\omega^2}{\alpha_0^2}\left(ik_g a_\rho^{(1)} \partial_2 - \partial_2 a_\rho^{(1)} ik_g\right) + 2\partial_1\partial_2 a_{mu}^{(1)}\left(\partial_2^2 - \partial_1^2\right) - 2\left(\partial_2^2 - \partial_1^2\right) a_{mu}^{(1)} \partial_2\partial_1\right] e^{i\nu_g z''}
$$

For acoustic case, let $\beta, \beta_0 = 0$, and ignore terms with $\hat{G}_0^S$, the second term reduces to

$$\frac{\alpha_0^4}{\omega^4}\left(\frac{i}{16\pi\nu_g^2}\right)\int\limits_{-\infty}^{+\infty}dz'\int\limits_{-\infty}^{+\infty}dz''e^{i\nu_g z'}\frac{\omega^2}{\alpha_0^2}\left(ik_g a_\rho^{(1)}(z')\frac{\partial}{\partial z'} - \frac{\partial}{\partial z'}a_\rho^{(1)}(z')ik_g\right)\left[-\frac{e^{-k_g|z'-z''|}}{ik_g}\right]$$

$$\times \frac{\omega^2}{\alpha_0^2}\left(ik_g a_\rho^{(1)}(z'')\frac{\partial}{\partial z''} - \frac{\partial}{\partial z''}a_\rho^{(1)}(z'')ik_g\right)e^{i\nu_g z''}$$

$$=k_g^2\left(\frac{i}{16\pi\nu_g^2}\right)\int\limits_{-\infty}^{+\infty}dz'\int\limits_{-\infty}^{+\infty}dz''e^{i\nu_g z'}\left(a_\rho^{(1)}(z')\frac{\partial}{\partial z'} - \frac{\partial}{\partial z'}a_\rho^{(1)}(z')\right)\left[\frac{e^{-k_g|z'-z''|}}{ik_g}\right]$$

$$\times \left(a_\rho^{(1)}(z'')\frac{\partial}{\partial z''} - \frac{\partial}{\partial z''}a_\rho^{(1)}(z'')\right)e^{i\nu_g z''}$$

$$=k_g^2\left(\frac{i}{16\pi\nu_g^2}\right)\int\limits_{-\infty}^{+\infty}dz'\int\limits_{-\infty}^{+\infty}dz''e^{i\nu_g z'}\left(a_\rho^{(1)}(z')\frac{\partial}{\partial z'}\right)\left[\frac{e^{-k_g|z'-z''|}}{ik_g}\right]\times\left(a_\rho^{(1)}(z'')\frac{\partial}{\partial z''}\right)e^{i\nu_g z''}$$

$$- k_g^2\left(\frac{i}{16\pi\nu_g^2}\right)\int\limits_{-\infty}^{+\infty}dz'\int\limits_{-\infty}^{+\infty}dz''e^{i\nu_g z'}\left(a_\rho^{(1)}(z')\frac{\partial}{\partial z'}\right)\left[\frac{e^{-k_g|z'-z''|}}{ik_g}\right]\times\left(\frac{\partial}{\partial z''}a_\rho^{(1)}(z'')\right)e^{i\nu_g z''}$$

$$- k_g^2\left(\frac{i}{16\pi\nu_g^2}\right)\int\limits_{-\infty}^{+\infty}dz'\int\limits_{-\infty}^{+\infty}dz''e^{i\nu_g z'}\left(\frac{\partial}{\partial z'}a_\rho^{(1)}(z')\right)\left[\frac{e^{-k_g|z'-z''|}}{ik_g}\right]\times\left(a_\rho^{(1)}(z'')\frac{\partial}{\partial z''}\right)e^{i\nu_g z''}$$

$$+ k_g^2\left(\frac{i}{16\pi\nu_g^2}\right)\int\limits_{-\infty}^{+\infty}dz'\int\limits_{-\infty}^{+\infty}dz''e^{i\nu_g z'}\left(\frac{\partial}{\partial z'}a_\rho^{(1)}(z')\right)\left[\frac{e^{-k_g|z'-z''|}}{ik_g}\right]\times\left(\frac{\partial}{\partial z''}a_\rho^{(1)}(z'')\right)e^{i\nu_g z''}$$

$$=- k_g^2\left(\frac{i}{16\pi\nu_g^2}\right)\int\limits_{-\infty}^{+\infty}dz'\int\limits_{-\infty}^{+\infty}dz''e^{i\nu_g z'}\left(a_\rho^{(1)}(z')\frac{\partial}{\partial z'}\right)\left[\frac{e^{-k_g|z'-z''|}}{ik_g}\right]\times\left(\frac{\partial}{\partial z''}a_\rho^{(1)}(z'')\right)e^{i\nu_g z''}$$

$$- k_g^2\left(\frac{i}{16\pi\nu_g^2}\right)\int\limits_{-\infty}^{+\infty}dz'\int\limits_{-\infty}^{+\infty}dz''e^{i\nu_g z'}\left(\frac{\partial}{\partial z'}a_\rho^{(1)}(z')\right)\left[\frac{e^{-k_g|z'-z''|}}{ik_g}\right]\times\left(a_\rho^{(1)}(z'')\frac{\partial}{\partial z''}\right)e^{i\nu_g z''}$$

$$=- k_g^2\left(\frac{i}{16\pi\nu_g^2}\right)\int\limits_{-\infty}^{+\infty}dz'\int\limits_{-\infty}^{+\infty}dz''e^{i\nu_g z'}a_\rho^{(1)}(z')\left[-2k_g\delta(z'-z'') + k_g^2\right]\left[\frac{e^{-k_g|z'-z''|}}{ik_g}\right]a_\rho^{(1)}(z'')e^{i\nu_g z''}$$

$$- k_g^2\nu_g^2\left(\frac{i}{16\pi\nu_g^2}\right)\int\limits_{-\infty}^{+\infty}dz'\int\limits_{-\infty}^{+\infty}dz''e^{i\nu_g z'}a_\rho^{(1)}(z')\left[\frac{e^{-k_g|z'-z''|}}{ik_g}\right]a_\rho^{(1)}(z'')e^{i\nu_g z''}$$

$$=2k_g^3\left(\frac{i}{16\pi\nu_g^2}\right)\int\limits_{-\infty}^{+\infty}dz'\int\limits_{-\infty}^{+\infty}dz''e^{i\nu_g z'}a_\rho^{(1)}(z')\delta(z'-z'')\left[\frac{e^{-k_g|z'-z''|}}{ik_g}\right]a_\rho^{(1)}(z'')e^{i\nu_g z''}$$

$$- k_g^2(k_g^2 + \nu_g^2) \left(\frac{i}{16\pi\nu_g^2} \right) \int\limits_{-\infty}^{+\infty} dz' \int\limits_{-\infty}^{+\infty} dz'' e^{i\nu_g z'} a_\rho^{(1)}(z') \left[\frac{e^{-k_g|z'-z''|}}{ik_g} \right] a_\rho^{(1)}(z'') e^{i\nu_g z''}$$

$$= I_3 + I_4,$$

where $I_4 = -I_2$, and I_3, after Fourier transforming over ν_g, we have

$$\widetilde{I_3} = \frac{\tan^2\theta}{4} a_\rho^{(1)}(z) a_\rho^{(1)}(z).$$

PS. When working on the second term, after $\frac{1}{\nabla^2}$ acts on the middle $\hat{G}_0^S$, then ignore terms with β, β_0 and $\hat{G}_0^S$, then do the partial integration for further detail.

Then, the right hand side of Eq. (C.1) is (after Fourier transforming over x_s, x_g and ν_g)

$$\frac{1}{8\cos^4\theta} \left[a_\gamma^{(1)}(z) a_\gamma^{(1)}(z) + a_\gamma^{(1)\prime}(z) \int\limits_{-\infty}^{z} dz' a_\gamma^{(1)}(z') \right]$$

$$- \frac{1}{4\cos^2\theta} a_\gamma^{(1)}(z) a_\gamma^{(1)}(z)$$

$$- 2\frac{\tan^2\theta}{16\cos^2\theta} \left[2a_\gamma^{(1)}(z) a_\rho^{(1)}(z) + a_\gamma^{(1)\prime}(z) \int\limits_{-\infty}^{z} dz' a_\rho^{(1)}(z') + a_\rho^{(1)\prime}(z) \int\limits_{-\infty}^{z} dz' a_\gamma^{(1)}(z') \right]$$

$$- 2\frac{1}{16\cos^2\theta} \left[a_\gamma^{(1)\prime}(z) \int\limits_{-\infty}^{z} dz' a_\rho^{(1)}(z') - a_\rho^{(1)\prime}(z) \int\limits_{-\infty}^{z} dz' a_\gamma^{(1)}(z') \right]$$

$$+ \frac{\tan^2\theta}{4} a_\rho^{(1)}(z) a_\rho^{(1)}(z)$$

$$= \frac{1}{8}(\tan^4\theta - 1) a_\gamma^{(1)}(z) a_\gamma^{(1)}(z) - \frac{\tan^2\theta}{4\cos^2\theta} a_\gamma^{(1)}(z) a_\rho^{(1)}(z) + \frac{1}{8} \left(\frac{1}{\cos^4\theta} - 2 \right) a_\rho^{(1)}(z) a_\rho^{(1)}(z)$$

$$+ \frac{1}{8\cos^4\theta} a_\gamma^{(1)\prime}(z) \int\limits_{-\infty}^{z} dz' \left[a_\gamma^{(1)}(z') - a_\rho^{(1)}(z') \right]$$

$$+ \frac{1}{8}(1 - \tan^4\theta) a_\rho^{(1)\prime}(z) \int\limits_{-\infty}^{z} dz' \left[a_\gamma^{(1)}(z') - a_\rho^{(1)}(z') \right].$$

Hence, for acoustic case, choosing a_γ and a_ρ as the two material property parameters, after

left side = right side, we get

$$
\frac{1}{\cos^2\theta}a_\gamma^{(2)}(z) + (1-\tan^2\theta)a_\rho^{(2)}(z)
$$
$$
= -\frac{1}{2}(\tan^4\theta - 1)a_\gamma^{(1)^2}(z)
$$
$$
-\frac{1}{2}\left(\frac{1}{\cos^4\theta} - 2\right)a_\rho^{(1)^2}(z)
$$
$$
+\frac{\tan^2\theta}{\cos^2\theta}a_\gamma^{(1)}(z)a_\rho^{(1)}(z)
$$
$$
-\frac{1}{2\cos^4\theta}a_\gamma^{(1)'}(z)\int_0^z dz'[a_\gamma^{(1)}(z') - a_\rho^{(1)}(z')]
$$
$$
+\frac{1}{2}(\tan^4\theta - 1)a_\rho^{(1)'}(z)\int_0^z dz'[a_\gamma^{(1)}(z') - a_\rho^{(1)}(z')], \tag{C.3}
$$

where the definition of θ is the same as that of Eq. (3.12), $a_\gamma^{(1)'} = \frac{da_\gamma^{(1)}}{dz}$ and $a_\rho^{(1)'} = \frac{da_\rho^{(1)}}{dz}$.

Next, we will show that the two results Eqs. (3.12) and (C.3) agree with each other.

Since $\alpha = 1 - \frac{\gamma_0}{\gamma}$, then

$$
a_\gamma = \frac{\gamma}{\gamma_0} - 1 = \frac{\alpha}{1-\alpha} = \alpha + \alpha^2 + \alpha^3 + \cdots,
$$

where the series expansion is valid for $|\alpha| < 1$, and then we have

$$
a_\gamma^{(1)} = \alpha_1,
$$

$$
a_\gamma^{(2)} = \alpha_2 + \alpha_1^2,
$$

$$
\vdots
$$

Similarly, since $\beta = 1 - \frac{\rho_0}{\rho}$, then

$$
a_\rho = \frac{\rho}{\rho_0} - 1 = \frac{\beta}{1-\beta} = \beta + \beta^2 + \beta^3 + \cdots,
$$

where the series expansion is valid for $|\beta| < 1$, and then we have

$$a_\rho^{(1)} = \beta_1,$$

$$a_\rho^{(2)} = \beta_2 + \beta_1^2,$$

$$\vdots$$

Then, after substitutions, Eq. (C.3) becomes

$$\frac{1}{\cos^2\theta}\alpha_2(z) + (1 - \tan^2\theta)\beta_2(z)$$

$$= -\frac{1}{2\cos^4\theta}\alpha_1^2(z)$$

$$-\frac{1}{2}(1 + \tan^4\theta)\beta_1^2(z)$$

$$+\frac{\tan^2\theta}{\cos^2\theta}\alpha_1(z)\beta_1(z)$$

$$-\frac{1}{2\cos^4\theta}\alpha_1'(z)\int_0^z dz'[\alpha_1(z') - \beta_1(z')]$$

$$+\frac{1}{2}(\tan^4\theta - 1)\beta_1'(z)\int_0^z dz'[\alpha_1(z') - \beta_1(z')],$$

which is Eq. (3.12) exactly. Therefore Eq. (3.12) and Eq. (C.3) agree with each other.